Comparative Studies of the Biosynthetic Gene Clusters for Anthraquinone-Fused Enediynes Shedding Light into the Tailoring Steps of Tiancimycin Biosynthesis

Xiaohui Yan,[†,∥] Jian-Jun Chen, [†,∥] Ajeeth Adhikari,[†] Christiana N. Teijaro,[†] Huiming Ge,[†] Ivana Crnovcic,[†] Chin-Yuan Chang,[†] Thibault Annaval, [†] Dong Yang, [†] Christoph Rader,[⊥] and Ben Shen*[,†,‡,§]

[†]Department of Chemistry, [‡]Department of Molecular Medicine, [§]Natural Products Library Initiative at the Scripps Research Institute, and [⊥]Department of Immunology and Microbiology, The Scripps Research Institute, Jupiter, Florida 33458, United States

*To whom correspondence should be addressed: The Scripps Research Institute, 130 Scripps Way, #3A1, Jupiter, FL 33458; Tel: (561)228-2456. Email: shenb@scripps.edu

Supplemental Information (SI)

General Experimental Procedures. All ^{1}H, ^{13}C, and 2D NMR (^{1}H–^{1}H COSY, ^{1}H–^{13}C HSQC, ^{1}H–^{13}C HMBC, ^{1}H–^{1}H ROESY) spectra were collected on a Bruker Avance III Ultrashield 700 at 700 MHz for ^{1}H and 175 MHz for ^{13}C nuclei. MPLC separation Optical Rotations were measured using an AUTOPOL IV automatic polarimeter (Rudolph Research Analytic). UV spectra were measured with a NanoDrop 2000C spectrophotometer (Thermo Scientific). IR spectra were obtained using a Spectrum One FT-IR spectrophotometer (PerkinElmer). MPLC separation was carried out on a Biotage Isolera One equipped with a Biotage SNAP Cartridge KP-C18-HS column (30 g). Semipreparative HPLC was performed on a Varian liquid chromatography system equipped with a YMC-pack ODS-A column (250 mm × 10 mm, 5 μm), unless specified otherwise. Sephadex column chromatography was conducted using Sephadex™ LH-20 (GE Healthcare). LC-MS was performed on an Agilent 1260 Infinity LC system coupled to an Agilent 6230 TOF (HR-ESI) equipped with a Poroshell 120 EC-C18 column (Agilent, 50 mm × 4.6 mm, 2.7 μm). Electrophoresis was carried out using a Bio-Rad Power Pac 300.

Bacterial Strains, Plasmids, and Chemicals. The bacterial strains, plasmids, and PCR primers used in this study are listed in Tables S1–S3, respectively. PCR primers were synthesized by Sigma-Aldrich. High-fidelity DNA polymerase (Q5), restriction endonucleases, and T4 DNA ligase were purchase from NEB. DNA sequencing was conducted by Eton Bioscience. For Southern hybridization, the DIG-High Prime DNA Labeling and Detection Starter Kits I and II were used (Roche Diagnostics Corp.), and the Southern hybridization was performed by following the protocols suggested by the manufacturer.

Culture Conditions. *E. coli* strains containing plasmids or cosmids were cultured in lysogeny broth (LB) with appropriate antibiotic.[S1] *S.* sp. CB03234 wild-type strain and it mutants were grown on solid GYM *Streptomyces* medium (glucose 4 g/L, yeast extract 4 g/L, malt extract 10 g/L, $CaCO_3$ 2 g/L, agar 12 g/L, pH 7.2) for sporulation and on solid ISP4 medium for intergeneric conjugation.[S2] For the fermentation, fresh spores of *S.* sp. CB03234 and it mutant strains were inoculated into tryptic soy broth (TSB) seed medium and cultured for 36–48 h at 28 °C and 250 rpm, then the seed culture was inoculated (5% v/v) into the production medium (yeast extract 10 g/L, malt extract 10 g/L, maltose 10 g/L, $CuSO_4$•$5H_2O$ 10 mg/L, NaI 5 mg/L, adjusted to pH 7.2) and cultured at 28 °C and 250 rpm for five to seven days. For small-scale production, the fermentation was performed in 250-mL baffled flasks containing 50 mL production medium; for large-scale production, the fermentation was performed in 2-L baffled flasks containing 500 mL production medium.

Inactivation of *tnmE6* in *S.* sp CB03234 to Afford the Δ*tnmE6* Mutant SB20019. Gene replacement of *tnmE6* was carried out as previously described.[S2,S3] Briefly, pBS20001, a cosmid containing a partial *tnm* gene cluster, was transformed into *E. coli* BW25113/pIJ790.[S4] The *tnmE6* gene was replaced with the kanamycin resistance cassette from pJTU4659 using λRED-mediated PCR-targeting strategy in *E. coli* BW25113/pIJ790[S4] harboring pBS20001, to afford pBS20022 (i.e., pBS20001 *tnmE6*::*aphA*). The genotype of the pBS20022 was confirmed by PCR using primers KD-tnmE6F and KD-tnmE6R. Then pBS20022 was introduced into *S.* sp. CB03234 wild-type strain by intergeneric conjugation using the same protocol as previously reported.[S2,S3] Double crossover with the kanamycin-resistant and apramycin-sensitive phenotype was selected, to afford the *S.* sp. CB03234 Δ*tnmE6* mutant strain, SB20019. The genotype of SB20019 was confirmed by PCR using primers KD-tnmE6F and KD-tnmE6R, and by Southern analysis (Figure S2).

Inactivation of *tnmL* in *S*. sp CB03234 to Afford the Δ*tnmL* Mutant SB20020. Gene replacement of *tnmL* was carried out as previously described.[S2,S3] Briefly, pBS20002, a cosmid containing a partial *tnm* gene cluster, was transformed into *E. coli* BW25113/pIJ790.[S4] The *tnmL* gene was replaced with the kanamycin resistance cassette from pJTU4659 using λRED-mediated PCR-targeting strategy in *E. coli* BW25113/pIJ790[S4] harboring pBS20002, to afford pBS20023 (i.e., pBS20002 *tnmL*::*aphA*). The genotype of the pBS20023 was confirmed by PCR using primers KD-tnmLF and KD-tnmLR. Then pBS20023 was introduced into *S.* sp. CB03234 wild-type strain by intergeneric conjugation using the same protocol as previously reported.[S2,S3] Double crossover with the kanamycin-resistant and apramycin-sensitive phenotype was selected, to afford the *S*. sp. CB03234 Δ*tnmL* mutant strain, SB20020. The genotype of SB20020 was confirmed by PCR using primers KD-tnmLF and KD-tnmLR, and by Southern analysis (Figure S3).

Inactivation of *tnmQ* in *S*. sp CB03234 to Afford the Δ*tnmQ* Mutant SB20021. Gene replacement of *tnmQ* was carried out as previously described.[S2,S3] Briefly, pBS20003, a cosmid containing a partial *tnm* gene cluster, was transformed into *E. coli* BW25113/pIJ790.[S4] The *tnmQ* gene was replaced with the kanamycin resistance cassette from pJTU4659 using λRED-mediated PCR-targeting strategy in *E. coli* BW25113/pIJ790[S4] harboring pBS20003, to afford pBS20023 (i.e., pBS20003 *tnmQ*::*aphA*). The genotype of the pBS20023 was confirmed by PCR using primers KD-tnmQF and KD-tnmQR. Then pBS20023 was introduced into *S.* sp. CB03234 wild-type strain by intergeneric conjugation using the same protocol as previously reported.[S2,S3] Double crossover with the kanamycin-resistant and apramycin-sensitive phenotype was selected, to afford the *S*. sp. CB03234 Δ*tnmQ* mutant strain, SB20021. The genotype of SB20021 was confirmed by PCR using primers KD-tnmQF and KD-tnmQR, and by Southern analysis (Figure S4).

Generation of the *tnmH* Complementation Mutant Strain SB20022. To complement the *tnmH* gene in SB20002 (i.e., *S*. sp. CB03234 Δ*tnmH* mutant stain), the *tnmH* gene was amplified using primers GE-tnmHF and GE-tnmHR, digested with *Spe*I and *Eco*RI, then inserted into pBS21003, to afford pBS20025, in which the expression of tnmH is under the control of *kasO** promoter. Sequence of the inserted gene was confirmed by Sanger sequencing. Then pBS20025 was introduced into SB20002 by intergeneric conjugation[S2], to afford SB20022.

Generation of the *tnmL* Complementation Mutant Strain SB20023. To complement the *tnmL* gene in SB20020 (i.e., *S*. sp. CB03234 Δ*tnmL* mutant strain), the *tnmL* gene was amplified using primers GE-tnmLF and GE-tnmLR, digested with *Spe*I and *Eco*RI, then inserted into pBS21003, to afford pBS20026, in which the expression of tnmL is under the control of *kasO** promoter. Sequence of the inserted gene was confirmed by Sanger sequencing. Then pBS20026 was introduced into SB20020 by intergeneric conjugation, to afford SB20023.

Analysis of Production Profiles of the *S*. sp. CB03234 Wild-type and Mutant Strains. After small-scale fermentations, each culture was centrifuged, the supernatant was extracted with EtOAC, and the cell palette was extracted with CH_3COCH_3. Then the extracts were combined, dried in vacuum, and dissolved in CH_3OH. The CH_3OH was used directly for LC-MS analysis. Chromatography for LC-MS was performed using a linear gradient of CH_3CN in H_2O with 0.1% formic acid (0–18 min, 5–100%) at a flow rate of 0.4 mL min^{-1}. To perform the time course of TNM congeners production in the *S*. sp. CB03234 wild-type and mutant strains, the fermentation was carried out for seven days, with three flasks taken every 24 h and extracted three times with

equal volume of EtOAC. Then the crude extracts were dried, dissolved in MeOH, and analyzed with LC-MS using the conditions described above.

Isolation and Structural Elucidation of TNM Congeners from *S*. sp. CB03234 Wild-type Strain. For a large-scale fermentation (14 L) of the *S.* sp. CB03234 wild-type and mutant strains, twenty-eight 2.0 L baffled flasks, each containing 500 mL of production medium, were inoculated with 50 mL of seed culture and incubated for five to seven days. After fermentation, 20 g of Diaion HP-20 resin was added into the broth and stirred overnight. The resin and the cell pellets were harvested by centrifugation, washed by deionized H_2O, and extracted three times with ca. 1 L MeOH. The MeOH extract was concentrated under reduced pressure, then suspended in 1 L deionized H_2O and washed three times with EtOAc (ca. 700 mL each time). The organic solvent was evaporated under vacuum to yield the crude extract, and the resulting oil was loaded onto a Biotage SNAP Cartridge KP-C18-HS column (30 g) and fractionated by MPLC with a linear gradient of 5% MeOH in H_2O to 90% MeOH in H_2O at a flow rate of 20 mL min^{-1}.

For the *S.* sp. CB03234 wild-type strain, the MPLC fractions were analyzed by TLC and pooled to obtain seven fractions (Fr01–Fr07). HPLC analysis showed that the TNM congeners were in Fr04–Fr06. Fr05 was fractionated by semi-preparative reverse-phase HPLC using MeCN/H_2O (32/68) as the mobile phase, and the two major fractions were respectively chromatographed over Sephadex LH-20 column and eluted with MeOH, to afford pure **1** (7.2 mg) and **6** (2.3 mg). Fr06 was fractionated by reverse-phase semi-preparative HPLC eluted with MeCN/H_2O (35/65) to afford TNM B (0.2 mg). Fr04 was fractionated by semi-preparative reverse-phase HPLC eluted with CH_3CN/H_2O (27/73), to give purified **11** (0.3 mg), **8** (2.7 mg), **9** (1.8 mg), **10** (0.5 mg), **7** (0.9 mg), **15** (0.1 mg), **13** (0.1 mg), and **14** (0.2 mg). All semi-preparative reverse-phase HPLC was carried out at a flow rate of 3 mL min^{-1}.

For the Δ*tnmL* mutant strain SB20020, the MPLC fractions were analyzed by TLC and pooled to obtain seven fractions (Fr01–Fr07). HPLC analysis showed that the TNM congeners were in Fr04–Fr06. Fr06 was separated by semi-preparative HPLC using MeCN/H_2O (35/65) as the mobile phase, to afford **13** (1.9 mg) and **12** (2.3 mg). Fr05 was separated by semi-preparative HPLC using MeCN/H_2O (32/68) as the mobile, to afford **15** (1.2 mg), **16** (0.6 mg), and **14** (0.8 mg). Fr04 was separated by semi-preparative HPLC using MeCN/H_2O (30/70) as the mobile phase to afford **19** (6.5 mg), **18** (9.5 mg), and **17** (2.8 mg).

For the Δ*tnmH* mutant strain SB20002, the MPLC fractions were analyzed by TLC and pooled to obtain six fractions (Fr01–Fr06). HPLC analysis showed that the TNM congeners were in Fr03–Fr04. Fr04 was purified by semi-preparative HPLC, with an Agilent Eclipse Plus Phenyl-Hexyl column (250 mm × 9.4 mm, 5 μm) using MeOH/H_2O (70/30) as the mobile phase, to afford **5** (4.1 mg) and **20** (1.2 mg). Fr03 was purified by semi-preparative HPLC using MeCN/H_2O (27/73) as the mobile phase to afford **24** (2.2 mg), **22** (1.5 mg), **21** (0.6 mg), **23** (0.3 mg), and **25** (1.2 mg).

Physicochemical Properties of the Isolated TNM Congeners.

TNM D (**6**): purple powder; $[\alpha]_D^{25}$ + 400.0 (C = 0.002, CH_3OH); UV (CH_3OH) λ_{max} (logε) 242 (4.10), 261 (4.09), 286 (shoulder), 408 (3.16), 544 (3.78), 581 (4.06) nm; IR (neat) 3377, 2924, 2352, 2115, 1992, 1739, 1597, 1559, 1492, 1454, 1373, 1238, 1133, 1012 cm^{-1}; HR-ESI-MS

(positive ion) at *m/z* 574.1349 (calcd $[M + H]^+$ for molecular formula $C_{30}H_{23}NO_{11}$ *m/z* = 574.1344).

7: Blue powder; $[\alpha]_D^{25}$ + 400.0 (C = 0.001, CH_3OH); UV (CH_3OH) λ_{max} (logε) 242 (4.37), 280 (shoulder), 412 (3.36), 531 (shoulder), 563 (4.15), 603 (4.16) nm; IR (neat) 3431, 1590, 1558, 1457, 1374, 1243, 1064, 1010, 949, 811cm^{-1}; HR-ESI-MS (positive ion) at *m/z* 522.1403 (calcd $[M + H]^+$ for molecular formula $C_{27}H_{23}NO_{10}$ *m/z* = 522.1395).

8: Blue powder; $[\alpha]_D^{25}$ + 300.0 (C = 0.001, CH_3OH); UV (CH_3OH) λ_{max} (logε) 242 (4.20), 257 (shoulder), 412 (3.19), 523 (shoulder), 561 (4.02), 601 (4.02) nm; IR (neat) 3344, 1634, 1511, 1461, 1375, 1282, 1061, 1015 cm^{-1}; HR-ESI-MS (positive ion) at *m/z* 506.1454 (calcd $[M + H]^+$ for molecular formula $C_{27}H_{23}NO_9$ *m/z* = 506.1446).

9: Blue powder; $[\alpha]_D^{25}$ + 300.0 (C = 0.001, CH_3OH); UV (CH_3OH) λ_{max} (logε) 242 (4.31), 254 (shoulder), 413 (3.28), 523 (shoulder), 560 (4.10), 603 (4.12) nm; IR (neat) 3369, 2920, 2849, 1640, 1590, 1562, 1509, 1460, 1375, 1280, 1250, 1059, 1013 cm^{-1}; HR-ESI-MS (positive ion) at *m/z* 490.1498 (calcd $[M + H]^+$ for molecular formula $C_{27}H_{23}NO_8$ *m/z* = 490.1496).

10: Purple powder; $[\alpha]_D^{25}$ + 1200 (C = 0.0005, CH_3OH); UV (CH_3OH) λ_{max} (logε) 240 (4.18), 268 (4.44), 388 (shoulder), 519 (shoulder), 553 (4.17), 591 (4.10) nm; IR (neat) 3439, 2923, 1785, 1618, 1581, 1501, 1455, 1366, 1338, 1256, 1096, 1070, 1009, 764 cm^{-1}; HR-ESI-MS (positive ion) at *m/z* 5466.1394 (calcd $[M + H]^+$ for molecular formula $C_{29}H_{23}NO_{10}$ *m/z* = 546.1395).

11: Purple powder; $[\alpha]_D^{25}$ + 800.0 (C = 0.0005, CH_3OH); UV (CH_3OH) λ_{max} (logε) 240 (3.94), 269 (4.24), 400 (3.09), 516 (shoulder), 548 (3.92), 590 (3.90) nm; IR (neat) 3370, 2924, 2854, 1784, 1580, 1500, 1455, 1380, 1347, 1259, 1103, 1062, 1010, 731 cm^{-1}; HR-ESI-MS (positive ion) at *m/z* 530.1450 (calcd $[M + H]^+$ for molecular formula $C_{29}H_{23}NO_9$ *m/z* = 530.1446).

TNM B (**12**): Red powder; $[\alpha]_D^{25}$ + 900.0 (C = 0.002, CH_3OH); UV (CH_3OH) λ_{max} (logε) 215 (4.14), 257 (4.13), 323 (shoulder), 533 (3.48) nm; IR (neat) 3343, 2945, 2834, 2328, 2117, 1996, 1715, 1623, 1587, 1480, 1351, 1232, 1019 cm^{-1}; HR-ESI-MS (positive ion) at *m/z* 494.1239 (calcd $[M + H]^+$ for molecular formula $C_{29}H_{19}NO_7$ *m/z* = 494.1234).

TNM E (**13**): Red powder; $[\alpha]_D^{25}$ + 2500 (C = 0.002, CH_3OH); UV (CH_3OH) λ_{max} (logε) 257 (4.45), 286 (shoulder), 323 (shoulder), 538 (3.92), 573 (3.81) nm; IR (neat) 3372, 2925, 2854, 2328, 2118, 1995, 1738, 1621, 1586, 1566, 1484, 1353, 1272, 1235, 1199, 1093, 1075, 1011, 727 cm^{-1}; HR-ESI-MS (positive ion) at *m/z* 528.1290 (calcd $[M + H]^+$ for molecular formula $C_{29}H_{21}NO_9$ *m/z* = 528.1289).

14: Purple powder; $[\alpha]_D^{25}$ + 400.0 (C = 0.0003, CH_3OH); UV (CH_3OH) λ_{max} (logε) 252 (4.15), 320 (4.71), 523 (3.54), 558 (3.75), 595 (3.70) nm; IR (neat) 3419, 2925, 1712, 1615, 1585, 1490, 1437, 1242, 1172, 1055, 729 cm^{-1}; HR-ESI-MS (positive ion) at *m/z* 514.1500 (calcd $[M + H]^+$ for molecular formula $C_{29}H_{23}NO_8$ *m/z* = 514.1496).

15: Purple powder; $[\alpha]_D^{25}$ + 800.0 (C = 0.0003, CH_3OH); UV (CH_3OH) λ_{max} (logε) 252 (4.24), 320 (3.46), 523 (shoulder), 556 (3.82), 595 (3.78) nm; IR (neat) 3461, 2926, 1712, 1615, 1585, 1499, 1436, 1350, 1267, 1214, 1174, 1052, 1026, 729 cm^{-1}; HR-ESI-MS (positive ion) at *m/z* 498.1555 (calcd $[M + H]^+$ for molecular formula $C_{29}H_{23}NO_7$ *m/z* = 498.1547).

16: Purple powder; $[\alpha]_D^{25}$ + 700.0 (C = 0.001, CH_3OH); UV (CH_3OH) λ_{max} (logε) 254 (4.24), 287 (shoulder), 320 (shoulder), 558 (3.71), 593 (3.63) nm; IR (neat) 3419, 2925, 1677, 1587, 1450, 1259, 727 cm^{-1}; HR-ESI-MS (positive ion) at *m*/*z* 466.1288 (calcd $[M + H]^+$ for molecular formula $C_{28}H_{19}NO_6$ *m*/*z* = 466.1285).

17: Blue powder; $[\alpha]_D^{25}$ + 400.0 (C = 0.001, CH_3OH); UV (CH_3OH) λ_{max} (logε) 254 (4.40), 284 (shoulder), 320 (shoulder), 521 (shoulder), 560 (3.99), 596 (3.94) nm; IR (neat) 3399, 1785, 1614, 1584, 1499, 1471, 1251, 1104, 1064, 1029, 957, 729 cm^{-1}; HR-ESI-MS (positive ion) at *m*/*z* 532.1240 (calcd $[M + H]^+$ for molecular formula $C_{28}H_{21}NO_{10}$ *m*/*z* = 532.1238).

18: Blue powder; $[\alpha]_D^{25}$ + 1000 (C = 0.001, CH_3OH); UV (CH_3OH) λ_{max} (logε) 254 (4.57), 320 (shoulder), 520 (shoulder), 554 (4.15), 595 (4.12) nm; IR (neat) 3419, 1785, 1615, 1584, 1500, 1254, 1165, 1105, 1074, 1046, 1029, 1004, 754, 740 cm^{-1}; HR-ESI-MS (positive ion) at *m*/*z* 516.1287 (calcd $[M + H]^+$ for molecular formula $C_{28}H_{21}NO_9$ *m*/*z* = 516.1289).

19: Purple powder; $[\alpha]_D^{25}$ + 600.0 (C = 0.001, CH_3OH); UV (CH_3OH) λ_{max} (logε) 254 (4.37), 320 (shoulder), 521 (shoulder), 556 (3.94), 596 (3.91) nm; IR (neat) 9293, 2925, 1775, 1586, 1500, 1262, 1166, 1107, 1072, 1009, 728 cm^{-1}; HR-ESI-MS (positive ion) at *m*/*z* 500.1339 (calcd $[M + H]^+$ for molecular formula $C_{28}H_{21}NO_8$ *m*/*z* = 500.1340).

TNM F (**20**): Red powder; $[\alpha]_D^{25}$ + 2200 (C = 0.002, CH_3OH); UV (CH_3OH) λ_{max} (logε) 239 (4.15), 272 (4.33), 400 (3.33), 533 (3.91), 565 (3.80) nm; IR (neat) 3275, 2954, 2846, 2360, 1991, 1636, 1583, 1450, 1359, 1326, 1264, 1204, 1113, 1072, 1014 cm^{-1}; HR-ESI-MS (positive ion) at *m*/*z* 544.1239 (calcd $[M + H]^+$ for molecular formula $C_{29}H_{21}NO_{10}$ *m*/*z* = 544.1238).

21: Purple powder; $[\alpha]_D^{25}$ + 500.0 (C = 0.001, CH_3OH); UV (CH_3OH) λ_{max} (logε) 239 (3.81), 269 (3.95), 308 (shoulder), 400 (2.87), 520 (shoulder), 548 (3.65), 585 (3.62) nm; IR (neat) 3247, 2924, 2854, 1784, 1558, 1503, 1251, 1210, 1164, 1096, 1071, 981, 739 cm^{-1}; HR-ESI-MS (positive ion) at *m*/*z* 532.1233 (calcd $[M + H]^+$ for molecular formula $C_{28}H_{21}NO_{10}$ *m*/*z* = 532.1238).

22: Blue powder; $[\alpha]_D^{25}$ + 600.0 (C = 0.001, CH_3OH); UV (CH_3OH) λ_{max} (logε) 242 (4.34), 257 (shoulder), 423 (3.27), 523 (shoulder), 558 (4.12), 600 (4.11) nm; IR (neat) 3406, 1785, 1562, 1504, 1456, 1250, 1140, 1100, 977, 742 cm^{-1}; HR-ESI-MS (positive ion) at *m*/*z* 548.1189 (calcd $[M + H]^+$ for molecular formula $C_{28}H_{21}NO_{11}$ *m*/*z* = 548.1187).

23: Purple powder; $[\alpha]_D^{25}$ + 1400 (C = 0.001, CH_3OH); UV (CH_3OH) λ_{max} (logε) 240 (4.09), 269 (4.26), 306 (shoulder), 393 (3.28), 514 (shoulder), 548 (3.98), 586 (3.95) nm; IR (neat) 3418, 2923, 1783, 1578, 1500, 1348, 1259, 1165, 1103, 1064, 1009, 942, 764, 732 cm^{-1}; HR-ESI-MS (positive ion) at *m*/*z* 516.1285 (calcd $[M + H]^+$ for molecular formula $C_{28}H_{21}NO_9$ *m*/*z* = 516.1289).

24: Blue powder; $[\alpha]_D^{25}$ + 200.0 (C = 0.001, CH_3OH); UV (CH_3OH) λ_{max} (logε) 242 (4.06), 251 (shoulder), 294 (shoulder), 423 (3.05), 523 (shoulder), 556 (3.91), 600 (3.92) nm; IR (neat) 3365, 2853, 1782, 1560, 1504, 1454, 1253, 1161, 1101, 1055, 1024, 1006, 926, 758, 726 cm^{-1}; HR-ESI-MS (positive ion) at *m*/*z* 532.1241 (calcd $[M + H]^+$ for molecular formula $C_{28}H_{21}NO_{10}$ *m*/*z* = 532.1238).

25: Blue powder; $[\alpha]_D^{25}$ + 200.0 (C = 0.001, CH_3OH); UV (CH_3OH) λ_{max} (logε) 242 (4.34), 256 (shoulder), 280 (3.99), 425 (3.35), 526 (shoulder), 560 (4.18), 600 (4.18) nm; IR (neat) 3362,

1786, 1597, 1504, 1249, 1037, 960, 760 cm^{-1}; HR-ESI-MS (positive ion) at *m*/*z* 564.1141 (calcd $[M + H]^+$ for molecular formula $C_{28}H_{21}NO_{12}$ *m*/*z* = 564.1137).

Cytotoxicity Assay of the Enediyne Compounds Isolated in this Study. The IC_{50}s of the TNM congeners against different human cancer cell lines, including melanoma (SK-MEL-5), breast (MDA-MB-231 and SKBR-3), central nervous system (SF-295), and non-small cell lung cancer (NCI-H226), were determined using the Cell-Titer 96 Aqueous One Solution Proliferation Assay (MTS) kit (Promega), according to the protocol suggested by the manufacturer. Briefly, suspended cultures of different cancer cell lines were diluted to a concentration of 5×10^4 cells mL^{-1} in RPMI 1640 medium supplemented with 10% fetal bovine serum, 100 μg mL^{-1} of streptomycin, and 100 unit mL^{-1} of penicillin. The suspended cultures were dispensed into 96-well plates (100 μL per well), and the plates were incubated for 24 h at 37 °C in an atmosphere of 5% CO_2, 95% air, and 100% humidity. The original medium was then removed, and 100 μL of fresh medium was added, followed by adding serial dilutions of drugs (1 μL in DMSO with final concentration ranging from 0 to 1000 nM). Plates were incubated for 72 h. Finally, 20 μL of CellTiter 96® AQueous One Solution Reagent was added to the plates and incubation continued at 37 °C in a humidified, 5% CO_2 atmosphere for 30 to 60 min. The absorbance at 490 nm was recorded using an ELISA plate reader. Each point represents the mean ± SD of three replicates, and the IC_{50} was determined by computerized curve fitting using GraphPad Prism (Table 1).

Table S1. Plasmids and cosmids used in this study

Plasmid	Description	Source (Reference)
pJTU4659	Plasmid containing kanamycin resistance cassette; used as template for λRED-mediated PCR targeting.	S5
pBS21003	pSET152-based integrative plasmid containing a constitutive *kasO*□ promoter for *Streptomyces* spp.; used for gene complementation; apramycin resistance	S6
pBS20001	Cosmid 4G2 from CB03234 cosmid library, containing partial *tnm* gene cluster	S3
pBS20002	Cosmid 11A1 from CB03234 cosmid library, containing partial *tnm* gene cluster	S3
pBS20003	Cosmid 4C3 from CB03234 cosmid library, containing partial *tnm* gene cluster	S3
pBS20022	pBS20001 with *tnmE6* replaced by kanamycin resistance gene cassette by PCR targeting (i.e., Δ*tnmE6*)	This study
pBS20023	pBS20002 with *tnmL* replaced by kanamycin resistance gene cassette by PCR targeting (i.e., Δ*tnmL*)	This study
pBS20024	pBS20001 with *tnmQ* replaced by kanamycin resistance gene cassette by PCR targeting (i.e., Δ*tnmQ*)	This study
pBS20025	pBS21003 with the *tnmH* gene inserted into the *Spe*I and *Eco*RI sites, for *tnmH* gene complementation	This study
pBS20026	pBS21003 with the *tnmL* gene inserted into the *Spe*I and *Eco*RI sites, for *tnmL* gene complementation	This study

Table S2. Bacterial strains used in this study

Strain/plasmid	Genotype and description	Source (Reference)
Escherichia coli		
DH5*α*	Host for DNA cloning	Life Technologies
XL1-Blue MRF	Host for cosmid library construction	Fisher Scientific
BW25113/pIJ790	Host for λRED-mediated PCR targeting	S4
ET12567/pUZ8002	Methylation-deficient host for intergeneric conjugation	S7
***Streptomyces* sp.**		
CB03234	Wild-type TNM A producer	S3
SB20002	The Δ*tnmH* mutant strain of CB03234	S3
SB20019	The Δ*tnmE6* mutant strain of CB03234	This study
SB20020	The Δ*tnmL* mutant strain of CB03234	This study
SB20021	The Δ*tnmQ* mutant strain of CB03234	This study
SB20022	Mutant strain SB20002 harboring plasmid pBS20025 expressing *tnmH*, under the control of the *kasO** promoter, for *tnmH* complementation	This study
SB20023	Mutant strain SB20020 harboring plasmid pBS20026 expressing *tnmL*, under the control of the *kasO** promoter, for *tnmL* complementation	This study

Table S3. Primers used in this study

Primer	Nucleotide Sequence (5′-3′)	Function
tnmE6-RedETF	ACCCGCCCGCCGTCGGACCATCCACCTGGGGGAGAGA TGATTCCGGGGATCCGTCGACC	PCR targeting for replacement of *tnmE6*
tnmE6-RedETR	TCGCTCTACGGTTGCGTGTCCACGCGGGCCACAGCTT CATGTAGGCTGGAGCTGCTTC	PCR targeting for replacement of *tnmE6*
KD-tnmE6F	GAATCGCTCTACGGTTGCGTGT	PCR confirmation
KD-tnmE6R	GTCTGGTTCGACCGTGACACC	PCR confirmation
tnmL-RedETF	CGATGGTTCCGACGGTCTAGTCAGGAGGTACGTGTCA TGATTCCGGGGATCCGTCGACC	PCR targeting for replacement of *tnmL*
tnmL-RedETF	CGATGGTTCCGACGGTCTAGTCAGGAGGTACGTGTCA TGATTCCGGGGATCCGTCGACC	PCR targeting for replacement of *tnmL*
KD-tnmLF	GCTCCGATGGTTCCGACGGTCTAG	PCR confirmation
KD-tnmLR	CCTCGGCTGACCACGCCGTAC	PCR confirmation
tnmQ-RedETF	CCTCGGGGTCGCGGCGGTGTCCGCGATCAGCTGCGAT CAATTCCGGGGATCCGTCGACC	PCR targeting for replacement of *tnmQ*
tnmQ-RedETR	AGTTCCTGCTCCTCCAGCCGTCCCGCTGACACCGCCAT GTGTAGGCTGGAGCTGCTTC	PCR targeting for replacement of *tnmQ*
KD-tnmQF	CTGCCGTGAGGACAGGTGC	PCR confirmation
KD-tnmQR	CAACGAGTTCCTGCTCCTCCAG	PCR confirmation
GE-tnmHF	GGACTAGTCCACCGTGCTGTACGC (SpeI)	Gene complementation
GE-tnmHR	CGGAATTCGACCGCATGGAACCCGAG (EcoRI)	Gene complementation
GE-tnmLF	GGACTAGTAGGAGGTACGTGTCATGGCC (SpeI)	Gene complementation
GE-tnmLR	CGGAATTCCTCGTCACGAGGCCGCTCAC (EcoRI)	Gene complementation
SH-tnmE6F	GACAGATTCTCGTGCCCGTCG	Southern probe
SH-tnmE6R	TGTGGCCGTGGAACGGCAG	Southern probe
SH-tnmLF	GCAACTACCCGTTCCTGGG	Southern probe
SH-tnmLR	GACCGTCGGAACCATCGG	Southern probe
SH-tnmQF	GTTCGTGAAGTTCGCCCAGATCG	Southern probe
SH-tnmQR	TGTCCAGGCCCTCCACGAAG	Southern probe

Table S4. NMR Spectroscopic Data (700 MHz, acetone-d_6) for TNM B (**12**), C (**5**), D (**6**), E (**13**), and F (**20**)

	TNM B **(12)**		TNM C (**5**)*		TNM D **(6)**		TNM E (**13**)		TNM F (**20**)	
Position	δ_C, type	δ_H (*J* in Hz)	δ_C	δ_H (*J* in Hz)	δ_C	δ_H (*J* in Hz)	δ_C	δ_H (*J* in Hz)	δ_C	δ_H (*J* in Hz)
1		10.14, brs		9.90, brs		9.91, brs		10.15, d (4.4)		10.08, brs
2	143.7, C		145.0, C		144.9, C		144.3, C		144.2, C	
3	111.7, C		110.5, C		110.7, C		110.9, C		111.3, C	
4	187.6, C		188.5, C		188.5, C		187.4, C		186.4, C	
5	132.8, C		117.6, C		117.0, C		135.0, C		111.4, C	
6	126.9, CH	8.34, d (1.3)	150.9, C		152.8, C		126.2, CH	8.33, dd (8.4, 1.4)	120.6, CH	7.72, d (2.8)
7	133.6, CH	7.92, td (7.6, 1.4)	152.8, C		154.5, C		133.3, CH	7.90, td (7.5, 1.4)	155.7, C	
8	134.8, CH	7.96, td (7.6, 1.4)	120.1, CH	7.27, d (8.2)	115.8, CH	7.41, t (9.1)	134.6, CH	7.94, td (7.5, 1.4)	112.6, CH	7.31, d (8.2, 2.8)
9	126.3, CH	8.33, d (1.3)	120.3, CH	7.81, d (8.2)	119.7, CH	7.85, t (8.9)	126.7, CH	8.33, dd (8.4, 1.4)	129.2, CH	8.21, d (8.2)
10	130.2, C		124.4, C		124.7, C		132.8, C		125.4, C	
11	183.2, C		185.7, C		185.8, C		182.9, C		182.9, C	
12	113.3, C		112.4, C		112.5, C		112.9, C		112.3, C	
13	156.0, C		156.2, C		156.2, C		155.5, C		163.4, C	
14	130.3, CH	8.65, s	132.4, CH	8.70, s	132.3, CH	8.71, s	131.1, CH	8.72, s	135.7, CH	8.68, s
15	134.8, C		135.8, C		136.0, C		136.7, C		137.5, C	
16	66.9, C		67.8, C		67.3, C		67.3, C		67.3, C	
17	65.6, CH	5.06, brs	64.1, CH	6.27, brs	64.0, CH	6.31, s	64.0, CH	6.31, s	64.1, CH	6.29, d (5.1)
18	100.1, C		102.3, C		102.2, C		102.2, C		102.2, C	
19	91.0, C		91.7, C		91.8, C		91.7, C		91.7, C	
20	123.8, CH	6.14, d (10.0)	124.1, CH	6.06, d (10.0)	124.1, CH	6.07, d (9.9)	124.0, CH	6.05, d (9.8)	123.7, CH	6.03, d (10.0)
21	123.3, CH	6.00, d (10.0)	122.7, CH	5.94, d (10.0)	122.7, CH	5.96, d (9.9)	122.7, CH	5.94, d (9.8)	122.6, CH	5.94, d (10.0)
22	89.0, C		89.3, C		89.2, C		89.1, C		89.1, C	
23	97.8, C		97.6, C		97.5, C		97.7, C		97.7, C	
24	46.3, CH	4.99, d (4.4)	44.7, CH	5.41, d (4.9)	44.7, CH	5.43, d (3.8)	44.6, CH	5.39, d (4.7)	44.5, CH	5.36, d (4.3)
25	75.8, C		79.1, C		79.1, C		79.1, C		79.1, C	
26	148.3, C		76.5, C		76.5, C		76.5, C		76.5, C	
27	16.4, CH_3	2.43, d (1.4)	24.9, CH_3	1.66, s	24.9, CH_3	1.67, s	24.9, CH_3	1.67, s	24.8, CH_3	1.66, s
28	121.2, CH	6.55, d (1.4)	75.1, CH	4.42, s	75.2, CH	4.44, s	75.2, CH	4.44, s	75.2, CH	4.45, s
29	165.8, C		172.8, C		173.0, C		173.0, C		172.8, C	
6-OH				13.42, brs		13.41, brs				
13-OH		13.26, brs		13.68, brs		13.62, brs		13.27, brs		13.42, brs
7-OMe					55.8, CH_3	4.02, s				
29-OMe	50.7, CH_3	3.72, s	51.7, CH_3	3.76, s	51.7, CH_3	3.79, s	51.7, CH_3	3.79, s	51.7, CH_3	3.79, s

[a] Assignments are based on COSY, HSQC, HMBC, and ROESY correlations. (See Figure S7 for summary of key correlations)
*TNM C (**5**) has been isolated previously[S3]

Table S5. NMR Spectroscopic Data (700 MHz, acetone-d_6) for Compounds **7**–**11**

	7		**8**		**9**		**10**		**11**	
Position	δ_C, type	δ_H (*J* in Hz)	δ_C	δ_H (*J* in Hz)	δ_C	δ_H (*J* in Hz)	δ_C	δ_H (*J* in Hz)	δ_C, type	δ_H (*J* in Hz)
1		10.65, d (4.2)		10.52, brs		10.56, d (4.9)		10.80, d (5.0)		10.84, d (4.9)
2	145.4, C		144.6, C		144.7, C		143.1, C		143.1, C	
3	106.8, C		106.5, C		106.5, C		107.8, C		108.0, C	
4	186.1, C		185.9, C		185.5, C		180.9, C		180.9, C	
5	117.5, C		117.3, C		117.0, C		137.6, C		137.5, C	
6	152.3, C		152.1, C		151.8, C		109.7, CH	7.70, d (2.7)	109.7, CH	7.71, d (2.8)
7	154.2, C		153.8, C		153.6, C		164.7, C		164.7, C	
8	115.2, CH	7.34, d (8.4)	115.1, CH	7.32-7.38, m	115.0, CH	7.28, d (7.7)	119.3, CH	7.33, dd (8.6, 2.7)	119.3, CH	7.33, dd (8.4, 2.8)
9	119.0, CH	7.79, d (8.4)	119.1, CH	7.72, d (7.7)	119.1, CH	7.66, d (8.4)	128.7, CH	8.22, d (8.6)	128.6, CH	8.22, d (8.4)
10	124.9, C		124.7, C		124.5, C		126.0, C		126.5, C	
11	185.2, C		185.1, C		184.9, C		186.1, C		186.1, C	
12	111.9, C		111.8, C		111.6, C		112.4, C		112.3, C	
13	157.2, C		157.1, C		156.8, C		156.2, C		156.0, C	
14	131.9, CH	7.78, s	131.7, CH	7.77, s	132.9, CH	7.19, s	130.1, CH	7.77, s	131.4, CH	7.29, s
15	140.7, C		140.4, C		135.7, C		139.7, C		134.5, C	
16	77.3, C		77.6, C		48.6, CH	3.41, dd (6.3, 2.1)	76.9, CH		47.4, CH	3.74, dd (5.6, 2.8)
17	74.8, CH	5.09, d (7.0)	75.1, CH	5.10, brs	69.9, CH	5.14, dd (7.0, 6.3)	74.2, CH	5.62, d (5.6)	69.9, CH	5.67, dd (7.0, 5.6)
18	137.8, C		137.0, C		137.4, C		135.9, C		136.1, C	
19	118.5, CH	7.07, d (7.7)	128.8, CH	7.61, t (6.7)	129.1, CH	7.67, d (7.7)	126.6, CH	7.51, d (7.7)	126.5, CH	7.53, d (7.7)
20	128.4, CH	7.08, t (7.7)	128.3, CH	7.35, t (7.0)	128.3, CH	7.41, t (7.7)	126.9, CH	7.20, t (7.7)	126.8, CH	7.18, t (7.7)
21	114.0, CH	6.81, d (7.7)	127.8, CH	7.32-7.38, m	127.9, CH	7.31, t (7.7)	128.1, CH	7.25, t (7.7)	128.0, CH	7.25, t (7.7)
22	154.0, C		127.7, CH	7.60, d (7.0)	127.8, CH	7.67, d (7.7)	127.1, CH	7.46, d (7.7)	127.3, CH	7.46, d (7.7)
23	123.9, C		136.4, C		136.9, C		138.0, C		138.4, C	
24	51.1, CH	5.56, d (5.6)	57.5, CH	5.27, d (4.5)	55.3, CH	5.06, dd (4.9, 2.1)	55.8, CH	5.47, d (5.6)	53.2, CH	5.34, dd (5.6, 2.8)
25	72.3, C		72.5, C		70.6, C		79.8, C		78.5, C	
26	67.1, CH	3.88, q (6.3)	67.2, CH	3.86, d (5.8)	66.5, CH	3.76, q (6.3)	83.0, C		80.5, C	
27	19.8, CH_3	1.57, d (6.3)	19.7, CH_3	1.57, d (5.8)	16.6, CH_3	1.40, d (6.3)	18.5, CH_3	1.70, s	15.5, CH_3	1.58, s
28							75.2, CH	4.89, s	74.6, CH	5.03, s
29							172.6, C		172.3, C	
6-OH				13.51, brs		13.35, brs				13.67, brs
13-OH				13.96, brs		14.00, brs		13.60, brs	55.4, CH_3	4.02, s
7-OMe			55.6, CH_3	3.99, s	55.6, CH_3	4.00, s	55.4, CH_3	4.01, s		

[a] Assignments are based on COSY, HSQC, HMBC, and ROESY correlations. (See Figure S8 for summary of key correlations)

Table S6. NMR Spectroscopic Data (700 MHz, acetone-d_6) for Compounds **14** and **15**

	14		**15**	
Position	δ_C	δ_H (*J* in Hz)	δ_C	δ_H (*J* in Hz)
1		10.85, brs		10.94, s
2	144.6, C		143.5, C	
3	106.5, C		107.5, C	
4	185.9, C		186.9, C	
5	117.3, C		116.9, C	
6	152.1, CH	8.29, dd (12.9, 7.7)	151.8, CH	8.28, dd (7.7, 1.4)
7	153.8, CH	7.85, dt (7.7, 1.4)	153.6, CH	7.83, dt (7.7, 1.4)
8	115.1, CH	7.90, dt (7.7, 1.4)	115.0, CH	7.88, dt (7.7, 1.4)
9	119.1, CH	8.30, dd (7.7, 1.4)	119.1, CH	8.30, dd (14.1, 6.9)
10	124.7, C		124.5, C	
11	185.1, C		184.9, C	
12	111.8, C		111.6, C	
13	157.1, C		156.8, C	
14	131.7, CH	7.87, s	132.9, C	7.71, s
15	140.4, C		135.7, C	
16	77.6, C		49.1, CH	3.82, s
17	75.1, CH	3.97, d (1.4)	70.6, CH	4.93, d (10.7)
18	137.0, C		137.4, C	
19	128.8, CH	7.53, d (7.7)	129.1, CH	7.54, dd (7.7, 1.4)
20	128.3, CH	7.24, dt (7.7, 1.4)	128.3, CH	7.22, dt (7.7, 1.4)
21	127.8, CH	7.32, dt (7.7, 1.4)	127.9, CH	7.32, dt (7.7, 1.4)
22	127.7, CH	7.67, d (7.7)	127.8, CH	7.60, d (7.7)
23	136.4, C		136.9, C	
24	57.5, CH	5.10, d (5.1)	55.7, CH	5.10, d (5.1)
25	72.5, C		70.9, C	
26	67.2, C		66.5, C	
27	19.7, CH_3	2.49, s	13.1, CH_3	2.43, s
28				
29				
13-OH		13.52, brs		13.63, brs
7-OMe				
29-OMe	50.3 CH_3	3.57, s	50.4 CH_3	3.58, s

[a] Assignments are based on COSY, HSQC, HMBC, and ROESY correlations. (See Figure S9 for summary of key correlations)

Table S7. NMR Spectroscopic Data (700 MHz, acetone-d_6) for Compounds **17**–**19** and **21**

	17		**18**		**19**		**21**	
Position	δ_C, type	δ_H (*J* in Hz)	δ_C	δ_H (*J* in Hz)	δ_C	δ_H (*J* in Hz)	δ_C	δ_H (*J* in Hz)
1		10.91, brs		10.79, d (4.9)		10.87, d (4.2)		10.75, brs
2	143.9, C		142.9, C		143.1, C		142.9, C	
3	107.7, C		107.5, C		107.7, C		107.8, C	
4	186.9, C		186.9, C		187.0, C		181.2, C	
5	132.7, C		132.6, C		132.6, C		137.8, C	
6	125.9, CH	8.26, m	125.9, CH	8.19, dd (7.8, 0.8)	125.9, CH	8.27, dd (7.7, 1.4)	111.9, CH	7.66, d (2.8)
7	132.6, CH	7.80, dt (8.4, 1.4)	132.6, CH	7.73, dt (7.5, 1.2)	132.6, CH	7.80, dt (7.7, 1.4)	163.3, C	
8	134.2, CH	7.85, dt (8.4, 1.4)	134.2, CH	7.78, dt (7.7, 1.2)	134.2, CH	7.85, dt (7.7, 1.4)	120.2, CH	7.24, d (8.4)
9	126.4, CH	8.26, m	126.3, CH	8.21, dd (7.8, 0.8)	126.4, CH	8.26, dd (7.7, 1.4)	129.0, CH	8.16, d (8.4)
10	135.3, C		135.2, C		135.2, C		125.1, C	
11	181.1, C		181.2, C		181.2, C		186.1, C	
12	112.8, C		112.8, C		112.6, C		112.5, C	
13	156.3, C		156.3, C		156.2, C		155.5, C	
14	129.9, CH	7.80, s	129.8, CH	7.79, s	131.2, CH	7.31, s	130.0, CH	7.76, s
15	140.5, C		140.3, C		135.3, C		139.4, C	
16	76.7, C		76.9, C		47.5, CH	3.76, dd (5.3, 2.2)	76.9, C	
17	74.1, CH	5.62, s	74.2, CH	5.63, s	69.9, CH	5.68, t (5.8)	74.2, CH	5.62, d (5.6)
18	137.4, C		138.1, C		136.0, C		135.9, C	
19	117.6, CH	7.01, m	126.6, CH	7.52, d (7.7)	126.5, CH	7.54, d (7.7)	126.6, CH	7.51, d (7.7)
20	127.5, CH	7.00, m	126.9, CH	7.20, t (7.7)	126.9, CH	7.18, t (7.4)	126.8, CH	7.20, t (7.7)
21	113.8, CH	6.75, dd (6.6, 2.1)	128.2, CH	7.26, t (7.7)	128.0, CH	7.25, t (7.4)	128.1, CH	7.24, t (7.7)
22	152.7, C		127.2, CH	7.48, d (7.7)	127.4, CH	7.47, d (7.7)	127.2, CH	7.46, d (7.7)
23	125.0, C		135.8, C		138.4, C		138.0, C	
24	50.0, CH	5.59, d (4.9)	55.8, CH	5.48, d (4.9)	53.2, CH	5.35, dd (5.1, 2.3)	55.8, CH	5.45, d (3.8)
25	79.7, C		79.8, C		78.5, C		79.7, C	
26	82.8, C		82.9, C		80.5, C		83.1, C	
27	18.5, CH_3	1.73, s	18.5, CH_3	1.71, s	15.5, CH_3	1.58, s	18.5, CH_3	1.69, s
28	75.0, CH	4.98, s	75.1, CH	4.93, s	74.6, CH	5.04, s	75.2, CH	4.87, s
29	172.5, C		172.6, C		172.3, C		172.6, C	
13-OH		13.70, brs		13.48, brs		13.58, br		13.65, brs

[a] Assignments are based on COSY, HSQC, HMBC, and ROESY correlations. (See Figure S10 for summary of key correlations)

Table S7 Cont. NMR Spectroscopic Data (700 MHz, acetone-d_6) for Compounds **22**–**25**

	22		**23**		**24**		**25**	
Position	δ_C, type	δ_H (*J* in Hz)	δ_C	δ_H (*J* in Hz)	δ_C	δ_H (*J* in Hz)	δ_C	δ_H (*J* in Hz)
1		10.52, brs		10.79, brs		10.57, brs		10.61, brs
2	143.5, C		143.0, C		143.9, C		144.7, C	
3	107.3, C		108.1, C		107.4, C		107.3, C	
4	186.7, C		181.2, C		186.5, C		186.5, C	
5	117.9, C		137.7, C		117.8, C		117.8, C	
6	149.7, C		111.9, CH	7.66, brs	149.9, C		150.0, C	
7	152.0, C		163.1, C		152.1, C		152.3, C	
8	119.5, CH	7.74, d (8.3)	120.1, CH	7.24, d (8.4)	119.5, CH	7.20, d (7.7)	119.9, CH	7.20, d (8.3)
9	119.8, CH	7.25, m	129.0, CH	8.17, d (8.5)	119.7, CH	7.73, d (8.2)	119.5, CH	7.74, d (8.3)
10	124.4, C		125.2, C		124.3, C		124.3, C	
11	185.4, C		186.2, C		185.4, C		185.3, C	
12	112.3, C		112.3, C		112.1, C		112.2, C	
13	156.3, C		155.9, C		156.7, C		156.9, C	
14	131.2, CH	7.79, s	131.4, CH	7.27, s	132.7, CH	7.31, s	131.5, CH	7.80, s
15	139.4, C		134.3, C		134.4, C		139.9, C	
16	76.8, C		47.4, CH	3.73, d (3.5)	47.4, CH	3.76, d (4.2)	76.8, C	
17	74.0, CH	5.61, brs	69.9, CH	5.66, dd (4.9, 5.6)	69.8, CH	5.67, d (4.9)	74.0, CH	5.62, s
18	137.7, C		136.1, C		138.1, C		137.5, C	
19	126.7, CH	7.53, d (7.7)	126.5, CH	7.53, d (7.6)	126.6, CH	7.55, d (7.7)	117.7, CH	7.02, d (4.9)
20	127.0, CH	7.27, t (7.4)	126.8, CH	7.17, t (7.7)	128.0, CH	7.26, t (7.7)	113.9, CH	6.77, t (4.6)
21	128.2, CH	7.25, m	127.9, CH	7.24, t (7.7)	127.0, CH	7.20, t (7.7)	127.7, CH	7.02, d (4.9)
22	127.2, CH	7.47, d (7.7)	127.4, CH	7.46, d (7.6)	127.4, CH	7.48, d (7.7)	152.8, C	
23	135.8, C		138.4, C		136.1, C		124.7, C	
24	55.9, CH	5.52, brs	53.2, CH	5.33, d (3.5)	53.4, CH	5.40, brs	50.2, CH	5.66, d (4.9)
25	79.7, C		78.5, C		78.5, C		82.8, C	
26	82.7, C		80.5, C		80.5, C		79.7, C	
27	18.3, CH_3	1.71, s	15.5, CH_3	1.58, s	15.5, CH_3	1.58, s	18.5, CH_3	1.71, s
28	75.0, CH	5.13, s	74.6, CH	5.01, s	74.5, CH	5.03, s	75.1, CH	4.93, s
29	172.4, C		172.3, C		172.2, C		172.5, C	
6-OH						12.33, brs		
13-OH		13.90, brs		13.72, brs		12.90, brs		13.96, brs

[a] Assignments are based on COSY, HSQC, HMBC, and ROESY correlations. (See Figure S10 for summary of key correlations)

Table S8. NMR Spectroscopic Data (700 MHz, acetone-d_6) for Compound **16**

		16
Position	δ_C	δ_H (*J* in Hz)
1		10.72, s
2	142.3, C	
3	109.2, C	
4	181.8, C	
5	132.6, C	
6	126.1, CH	8.28, dd (7.7, 1.4)
7	133.0, CH	7.85, dt (7.7, 1.4)
8	134.4, CH	7.90, dt (7.7, 1.4)
9	126.5, CH	8.30, dd (7.7, 1.4)
10	135.0, C	
11	187.1, C	
12	113.3, C	
13	156.7, C	
14	126.4, CH	7.77, s
15	143.6, C	
16	75.7, C	
17	73.8, CH	3.97, d (1.4)
18	131.8, C	
19	128.6, CH	7.14, dd (7.7, 1.4)
20	128.0, CH	7.15, dt (7.7, 1.4)
21	128.7, CH	7.27, dt (7.7, 1.4)
22	129.7, CH	7.60, d (7.7)
23	138.0, C	
24	57.2, CH	5.16, d (4.9)
25	71.0, C	
26	66.4, C	
27	17.5, CH_3	2.16, d (1.4)
28	124.0, CH	5.69, m
29	195.2, C	
13-OH		13.42, brs

[a] Assignments are based on COSY, HSQC, HMBC, and ROESY correlations. (See Figure S11 for summary of key correlations)

Figure S1. Comparative analysis of anthraquinone-fused enediyne biosynthesis. Biosynthetic gene clusters of the four anthraquinone-fused enediynes, TNM A (**1**), UCM (**2**), YPM (**3**), and DYN (**4**) containing 32, 28, 34, and 45 genes, respectively. Comparison of the two smallest gene clusters, *tnm* and *ucm*, lead to the identification of four *tnm* genes, *tnmE6*, *tnmH*, *tnmL*, and *tnmQ*, which are inactivated in this study and highlighted in red with a black box. The *tnmE6*, *tnmH*, and *tnmQ* genes are unique to the *tnm* gene cluster, while *tnmL* has one homolog, *ypmL*, in the *ypm* gene cluster. Complete annotation of the four gene clusters and comparison of their predicted functions have been published previously.[S8,S9]

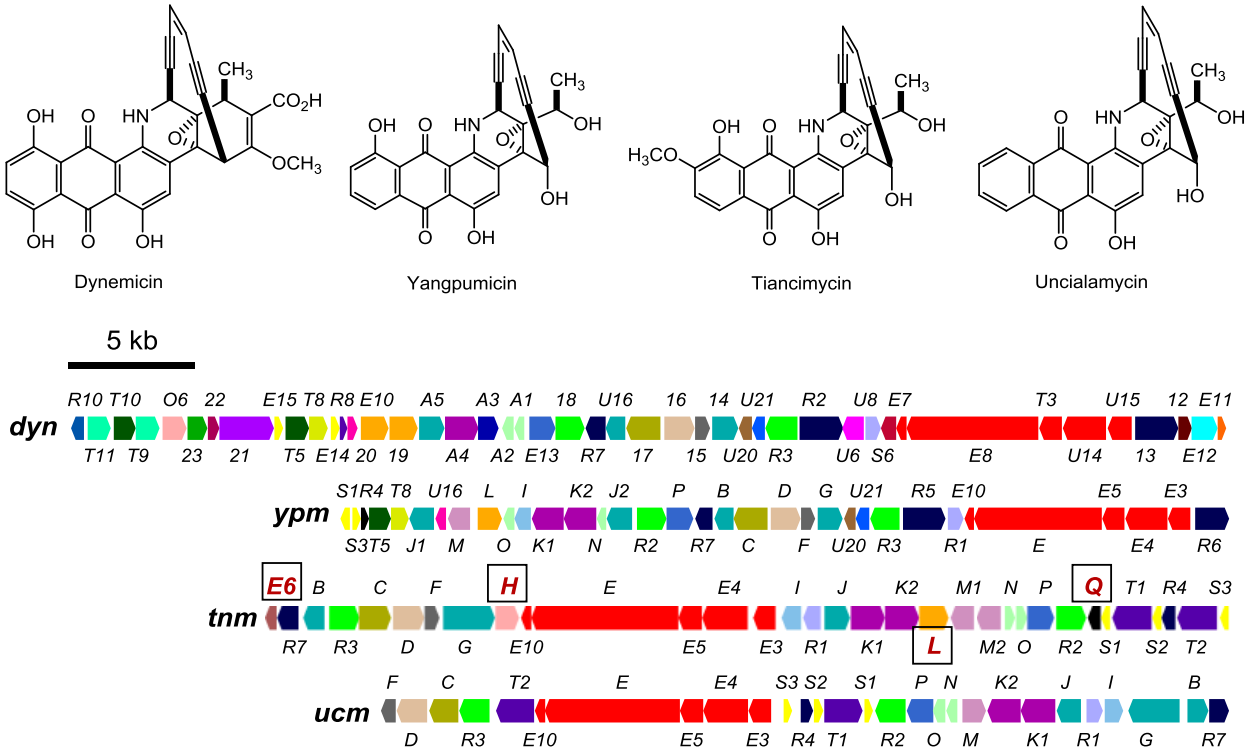

Figure S2. Inactivation of *tnmE6* by gene replacement. (A) Construction of the *tnmE6* gene replacement mutant and restriction map of *S.* sp. CB03234 wild-type and SB20019 mutant strains. N, *Nco*I; Apr^S, apramycin sensitive; Kana^S, kanamycin sensitive; Apr^R, apramycin resistant; Kana^R, kanamycin resistant. (B) Southern analysis of the genomic DNAs isolated from *S.* sp. CB03234 wild-type and SB20019 mutant strains digested with *Nco*I and hybridized with a 0.6 kb PCR-amplified probe. Lane 1, DNA Molecular Weight Marker VII (Roche); lane 2, SB20019 Δ*tnmE6* mutant; lane 3, *S.* sp. CB03234 wild-type.

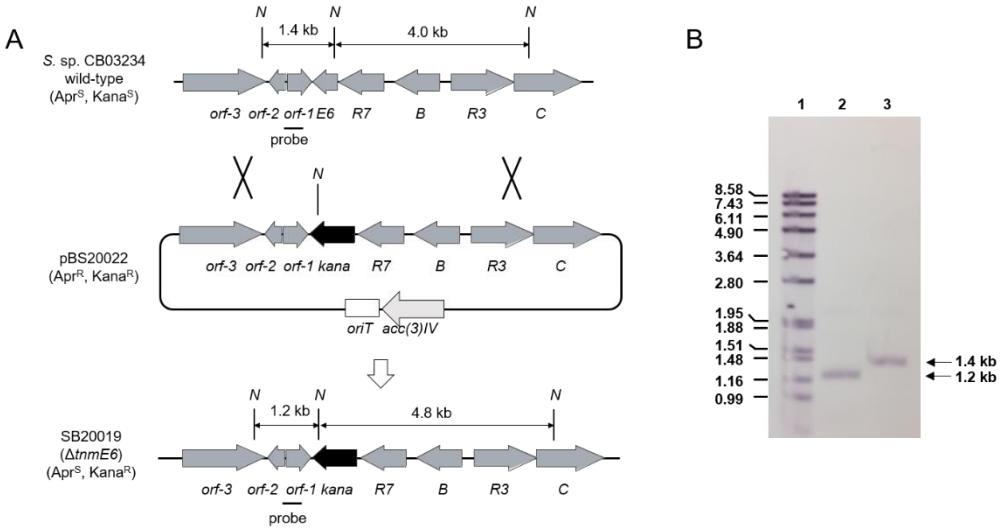

Figure S3. Inactivation of *tnmL* by gene replacement. (A) Construction of the *tnmL* gene replacement mutant and restriction map of *S.* sp. CB03234 wild-type and SB20020 mutant strains. S, *Sph*I; Apr^S, apramycin sensitive; Kana^S, kanamycin sensitive; Apr^R, apramycin resistant; Kana^R, kanamycin resistant. (B) Southern analysis of the genomic DNAs isolated from *S.* sp. CB03234 wild-type and SB20020 mutant strains digested with *Sph*I and hybridized with a 0.6 kb PCR-amplified probe. Lane 1, DNA Molecular Weight Marker VII (Roche); lane 2, SB20020 Δ*tnmL* mutant; lane 3, *S.* sp. CB03234 wild-type.

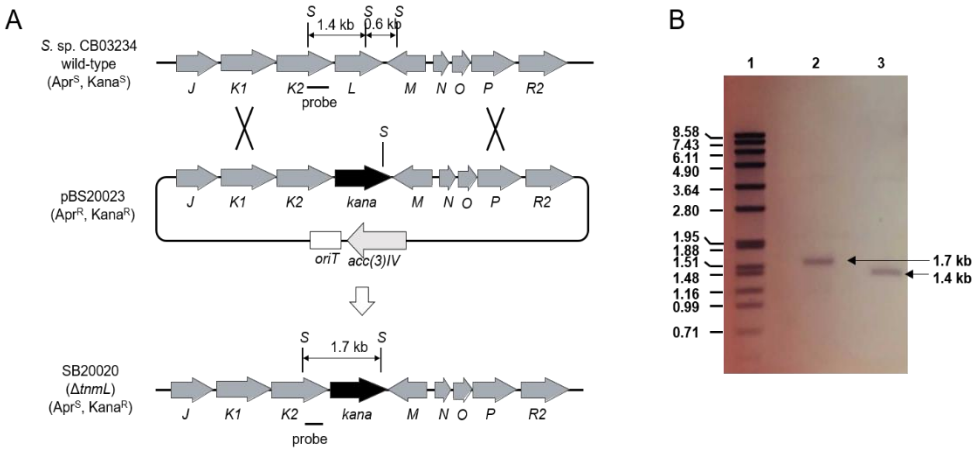

Figure S4. Inactivation of *tnmQ* by gene replacement. (A) Construction of the *tnmQ* gene replacement mutant and restriction map of *S.* sp. CB03234 wild-type and SB20021 mutant strains. S, *Sph*I; Apr^S, apramycin sensitive; Kana^S, kanamycin sensitive; Apr^R, apramycin resistant; Kana^R, kanamycin resistant. (B) Southern analysis of the genomic DNAs isolated from *S.* sp. CB03234 wild-type and SB20021 mutant strains digested with *Sph*I and hybridized with a 0.6 kb PCR-amplified probe. Lane 1, DNA Molecular Weight Marker VII (Roche); lane 2, *S.* sp. CB03234 wild-type; lane 3, SB20021 Δ*tnmQ* mutant.

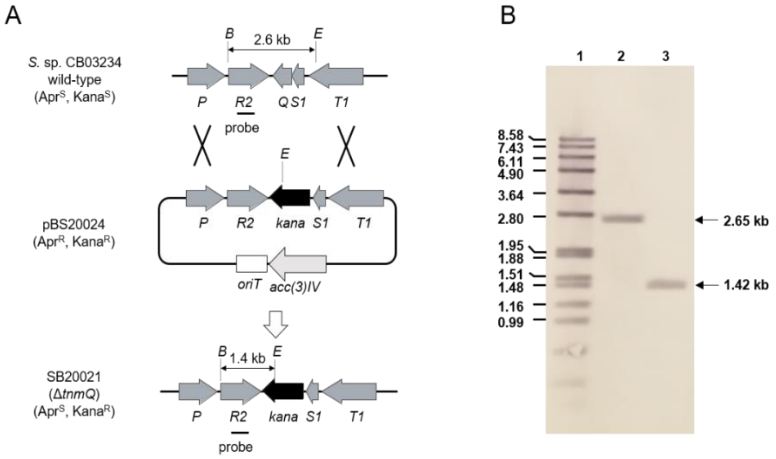

Figure S5. Time course of TNM congeners production in *S.* sp. CB03234 wild-type strain. The numbers above the peaks correspond to the TNM congeners isolated from the wild-type strain.

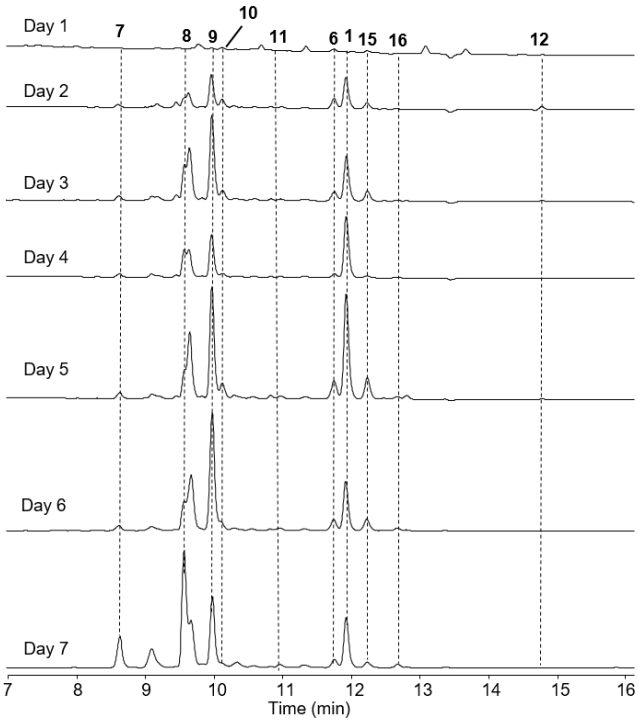

Figure S6. Time course of TNM congeners production in the Δ*tnmL* mutant SB20020. The numbers above the peaks correspond to the TNM congeners isolated from SB20020.

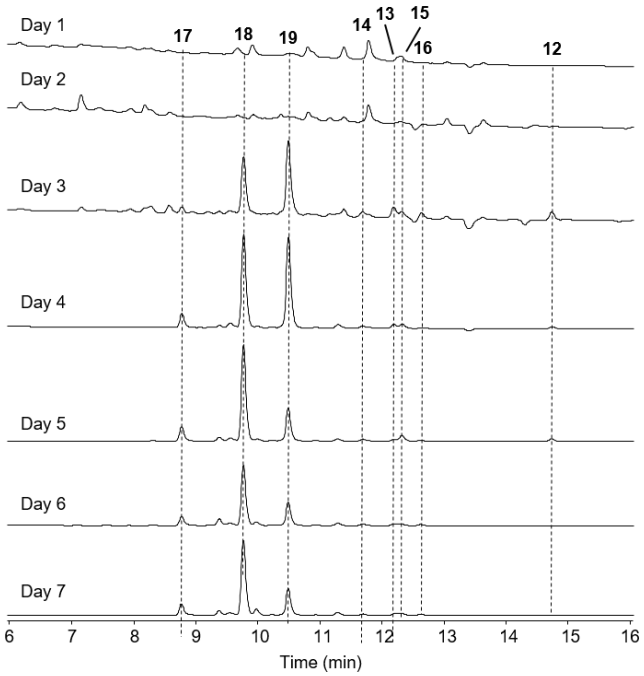

Figure S7. Time course of TNM congeners production in the Δ*tnmH* mutant SB20002. The numbers above the peaks correspond to the TNM congeners isolated from SB20002.

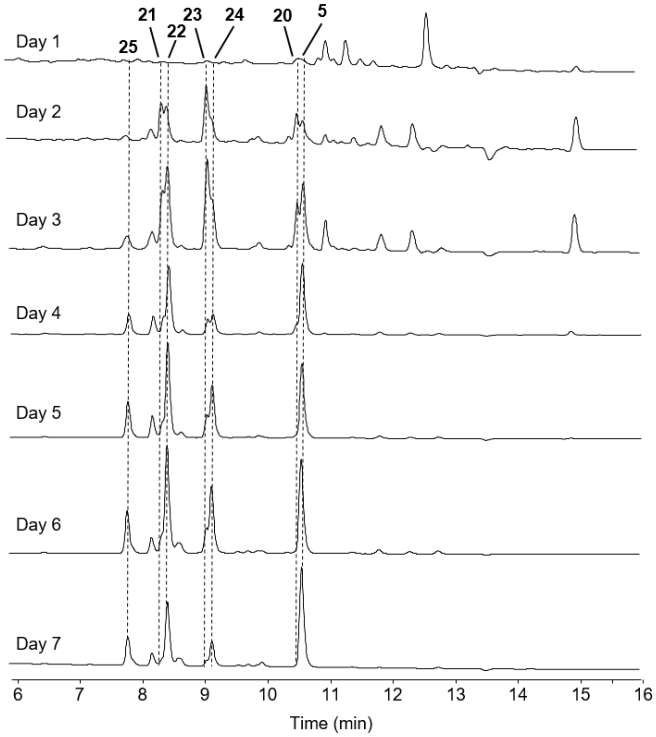

Figure S8. Key 2D NMR correlations supporting the structural elucidation of TNM B (**12**), C (**5**), D (**6**), E (**13**), and F (**20**). (A) ^{1}H-^{1}H COSY and HMBC correlations for TNM B B (**12**), C (**5**), D (**6**), E (**13**), and F (**20**), (B) ROSEY correlations using TNM C (**5**) as a model for TNM C (**5**), D (**6**), E (**13**), and F (**20**), and (C) Crystal structure of TNM C (**5**) in complex with TnmS3 PDB accession code 6BBX.[S4]

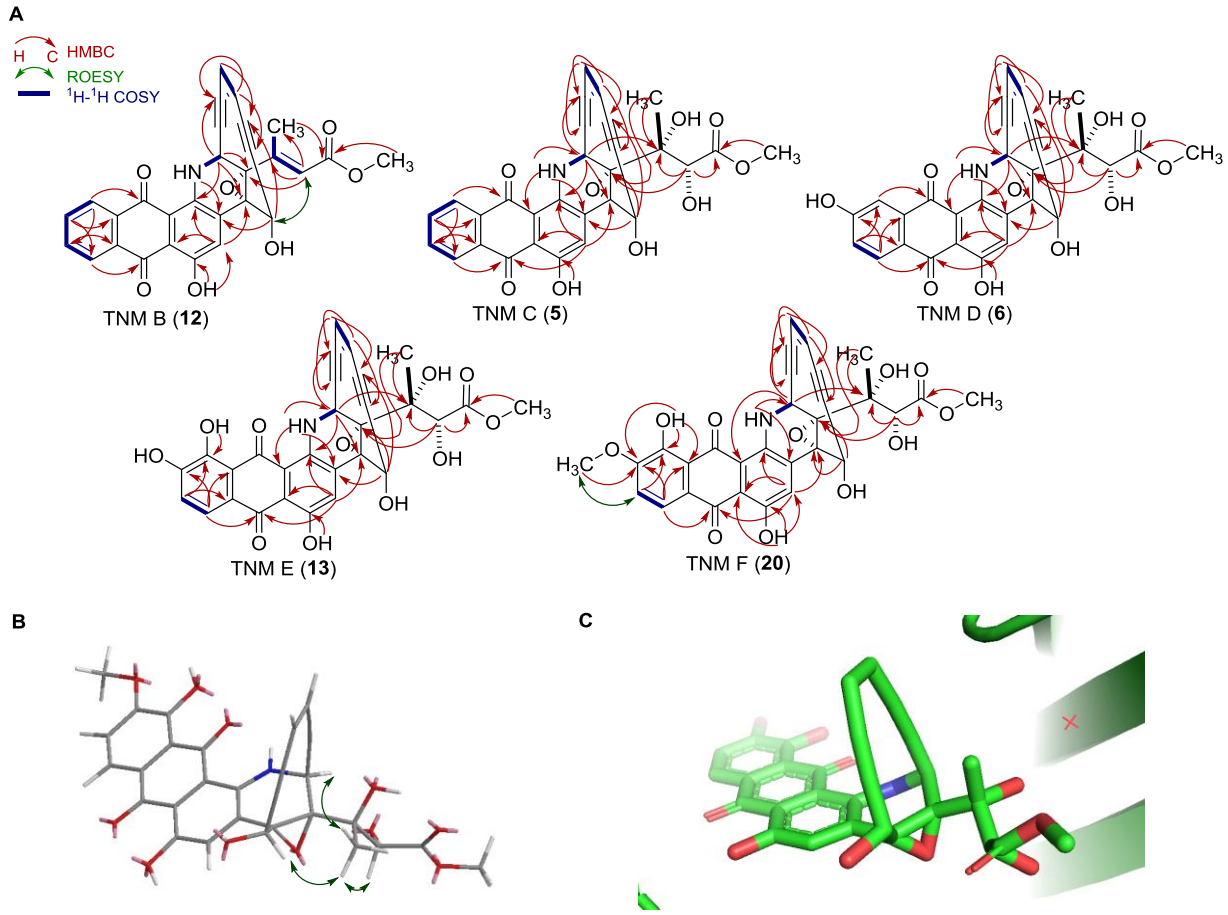

Figure S9. Key 2D NMR correlations supporting the structural elucidation of cyclized TNM compounds **7**-**9** with no side chain.

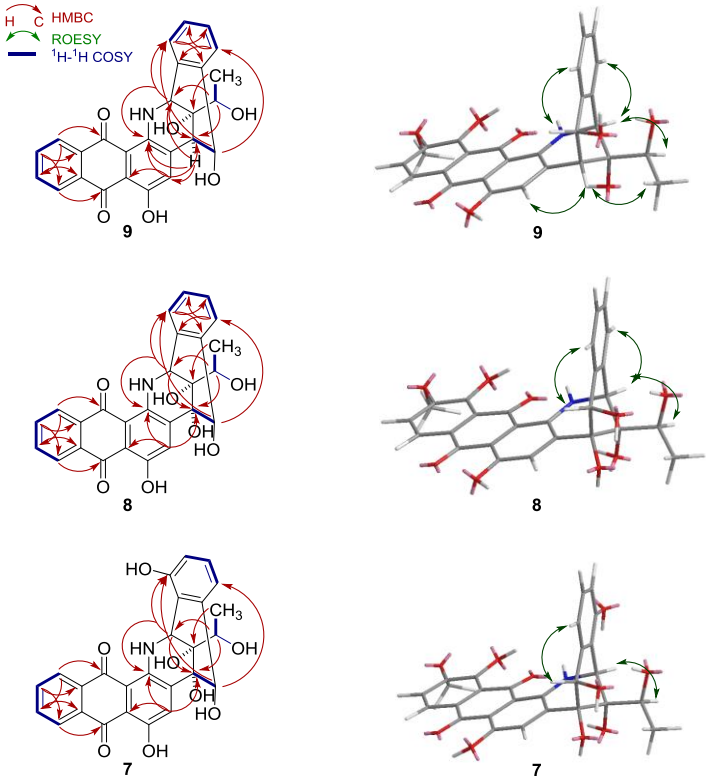

Figure S10. Key 2D NMR correlations supporting the structural elucidation of cyclized TNM compounds **14** and **15** with α,β-unsaturated methyl ester side chain.

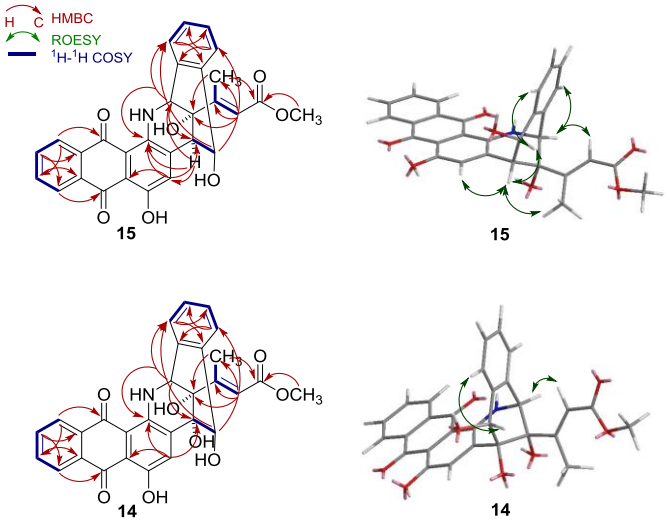

Figure S11. Key 2D NMR correlations supporting the structural elucidation of cyclized TNM compounds **10**, **11**, **17**-**19**, and **21**-**25** containing the lactone ring. Anthraquinone ^{1}H-^{1}H COSY and HMBC correlations of the cyclized compounds match the parent enediyne (Figure S8) with the corresponding oxidation patterns of the A-ring.

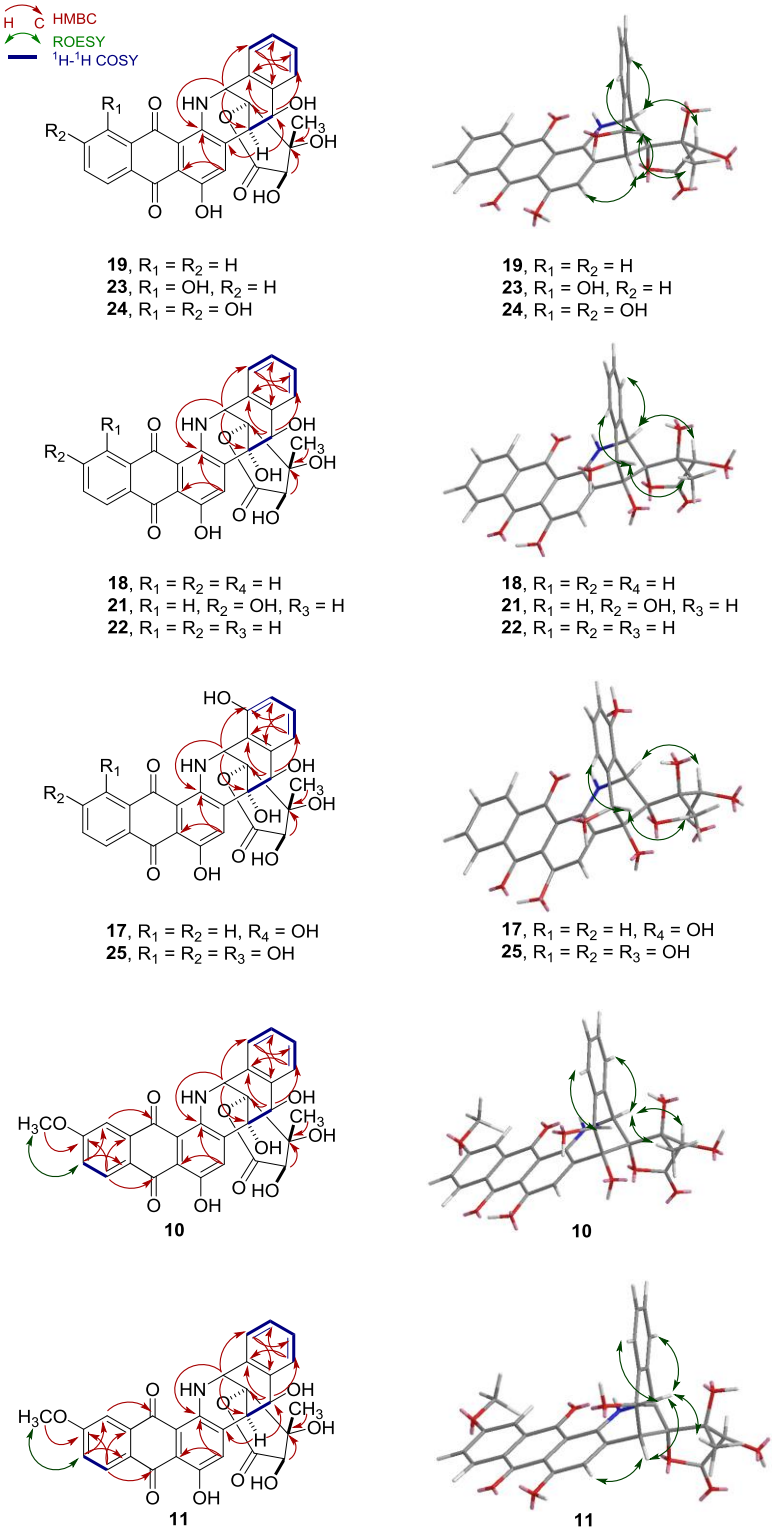

Figure S12. Key 2D NMR correlations supporting the structural elucidation of compound **16**

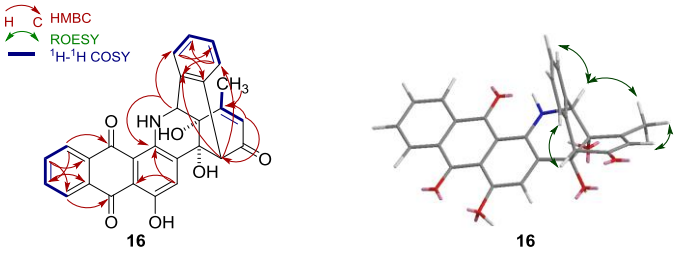

Figure S13. Formation of **7-9** from TNM A (**1**) isolated from CB03234 WT[S10-S12]

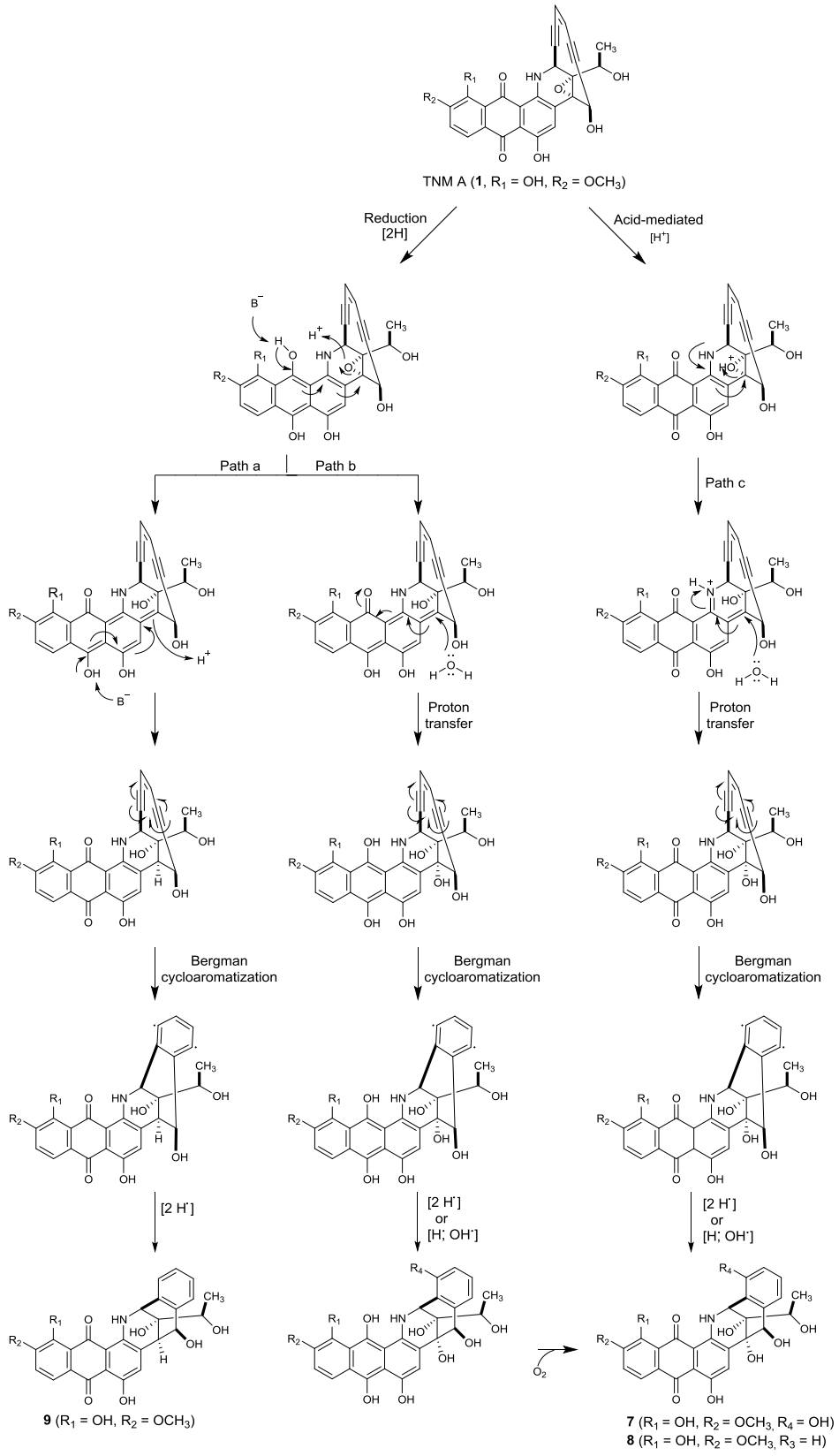

Figure S14. Formation of compounds **14** and **15** from TNM B (**12**) isolated from SB20023[S10-S12]

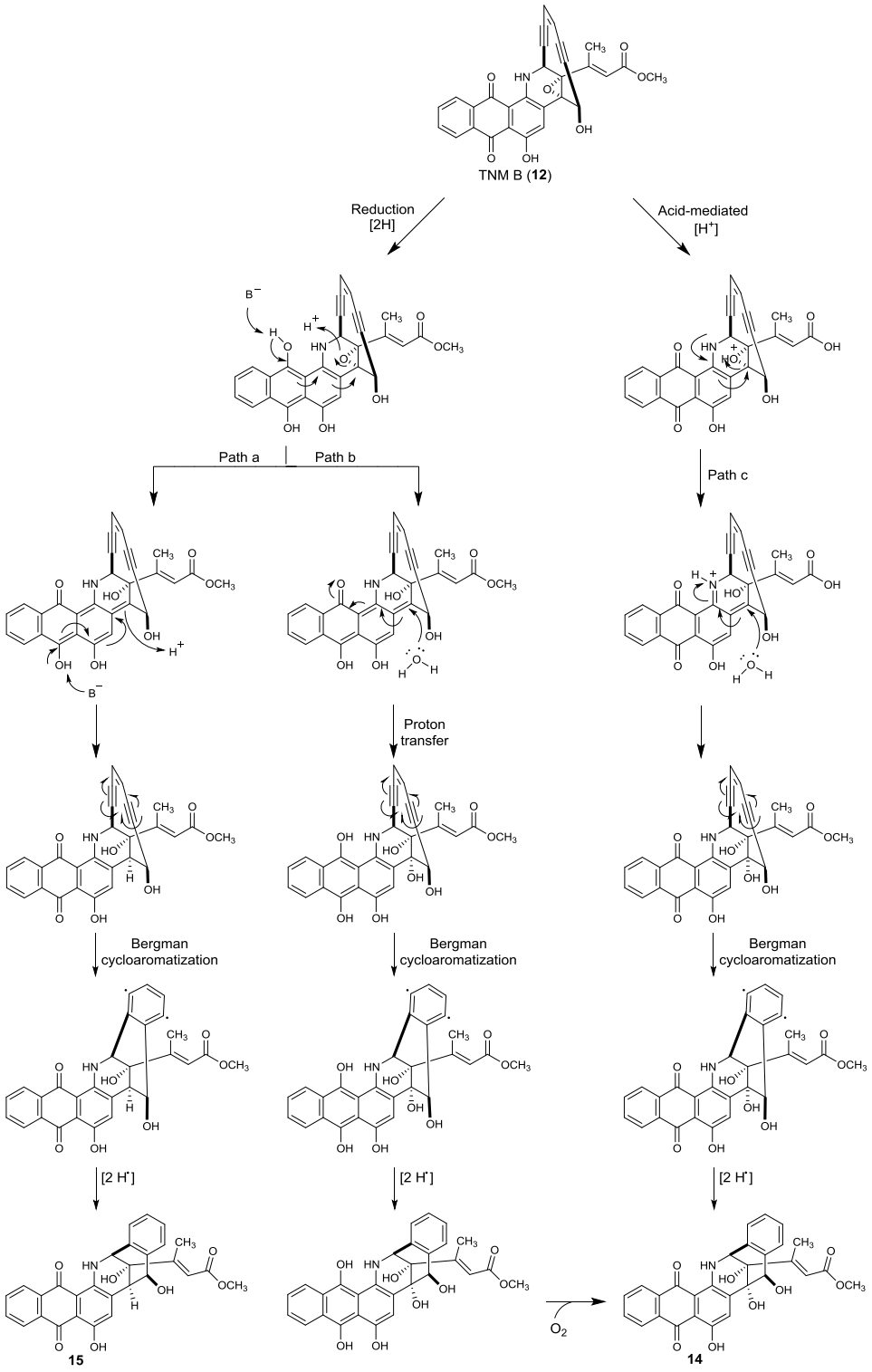

Figure S15. Formation of compounds **17**-**19** from TNM E (**13**), **21** and **23**-**24** from TNM F (**20**), **22** and **25** from TNM C (**5**), and formation of **10** and **11** from the corresponding enediyne that was not isolated [S10-S12]

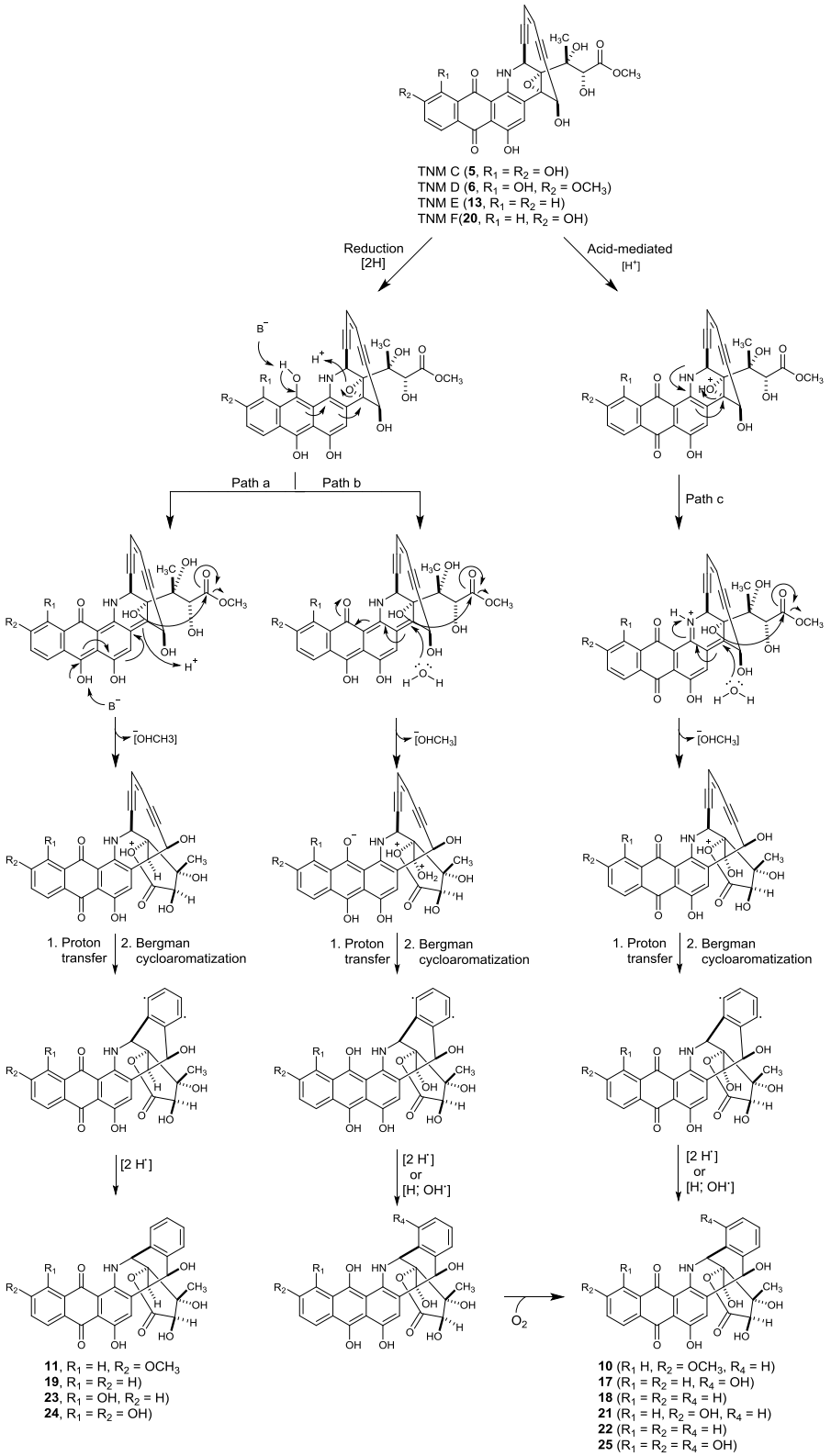

Figures S16. Formation of compound **16** from the corresponding enediyne **26** that was not isolated[S10-S12]

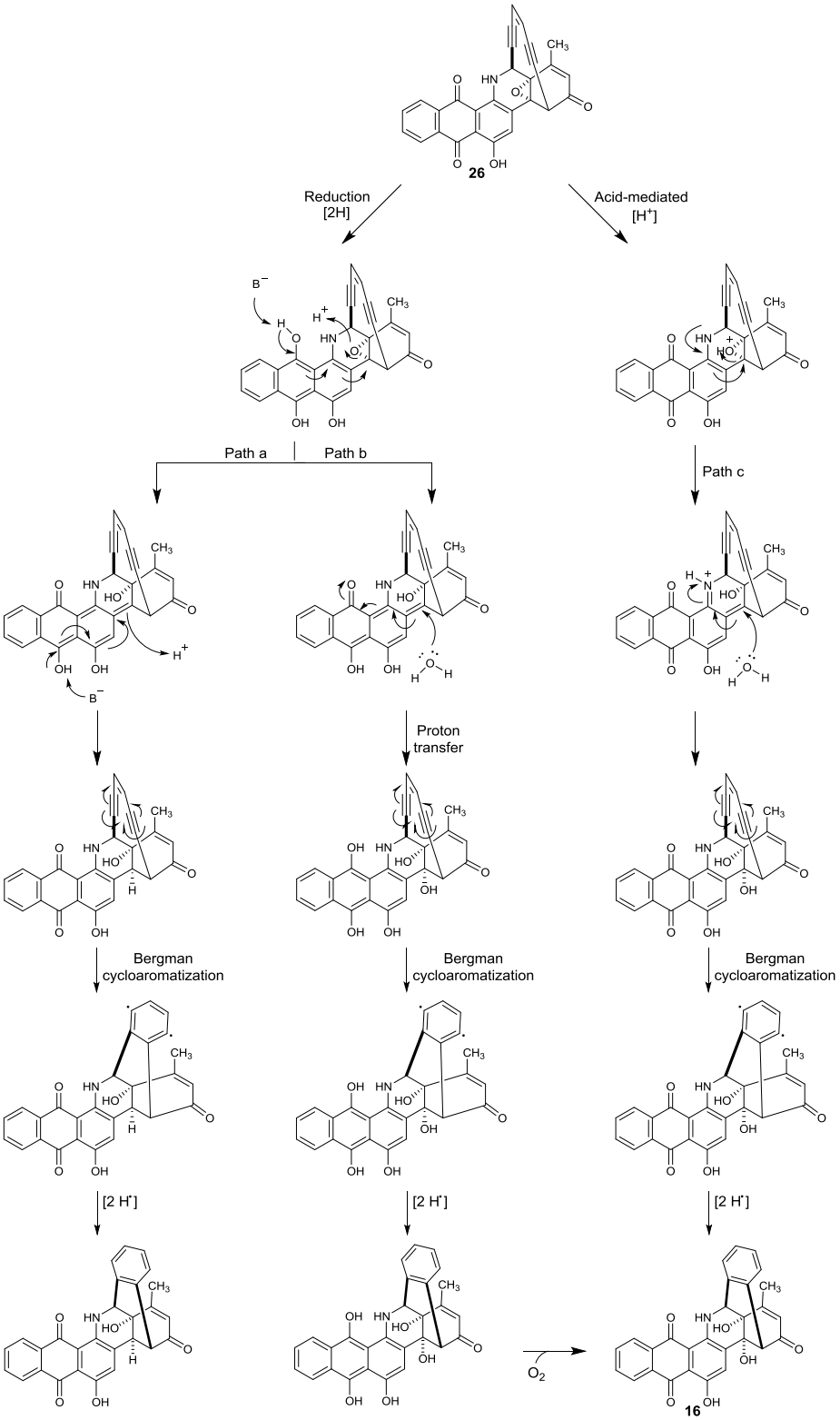

Figure S17. HR-ESI-MS analysis of TNM D (**6**)

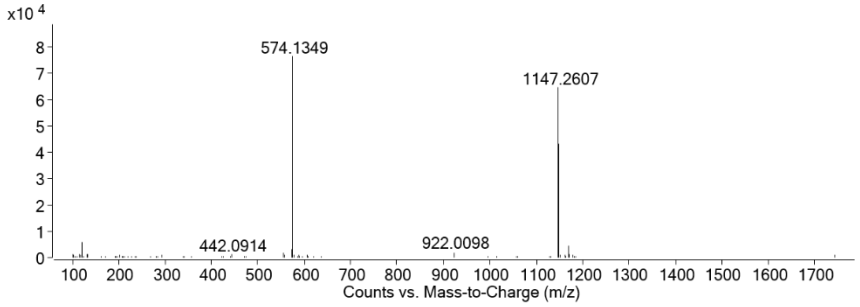

Figure S18. ^{1}H NMR Spectrum of TNM D (**6**) (700 MHz, acetone-d_6)

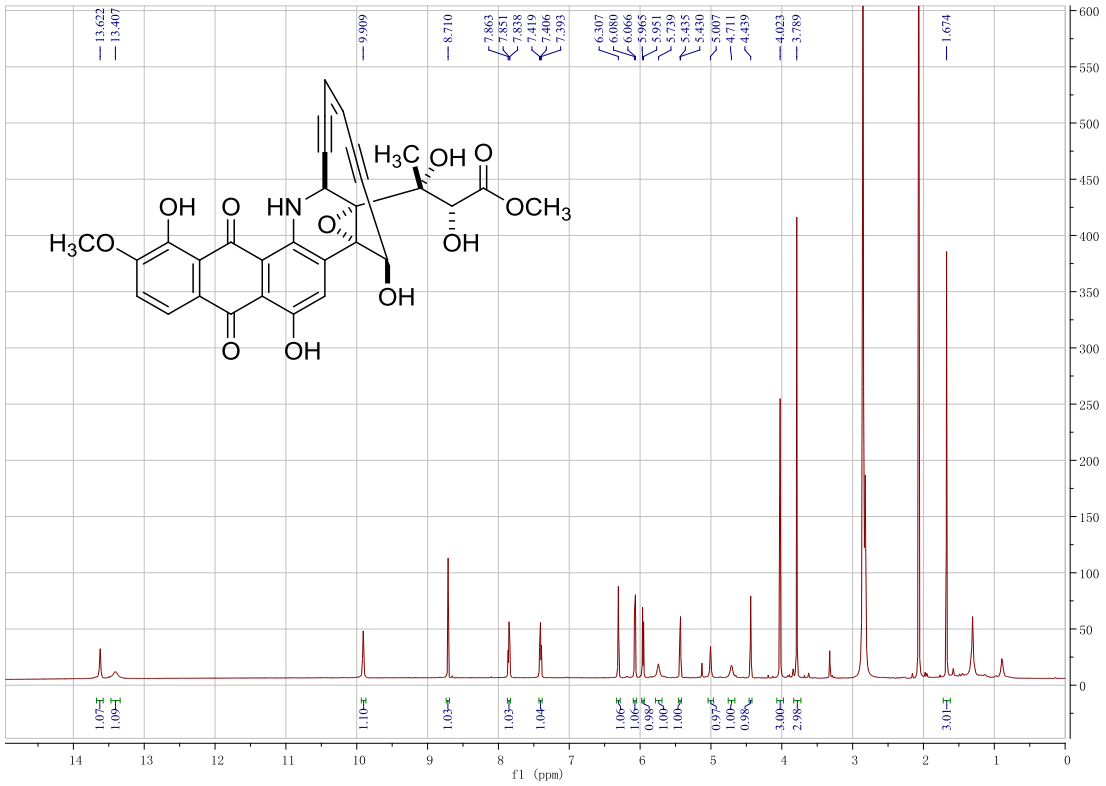

Figure S19. ^{13}C NMR spectrum of TNM D (**6**) (176 MHz, acetone-d_6)

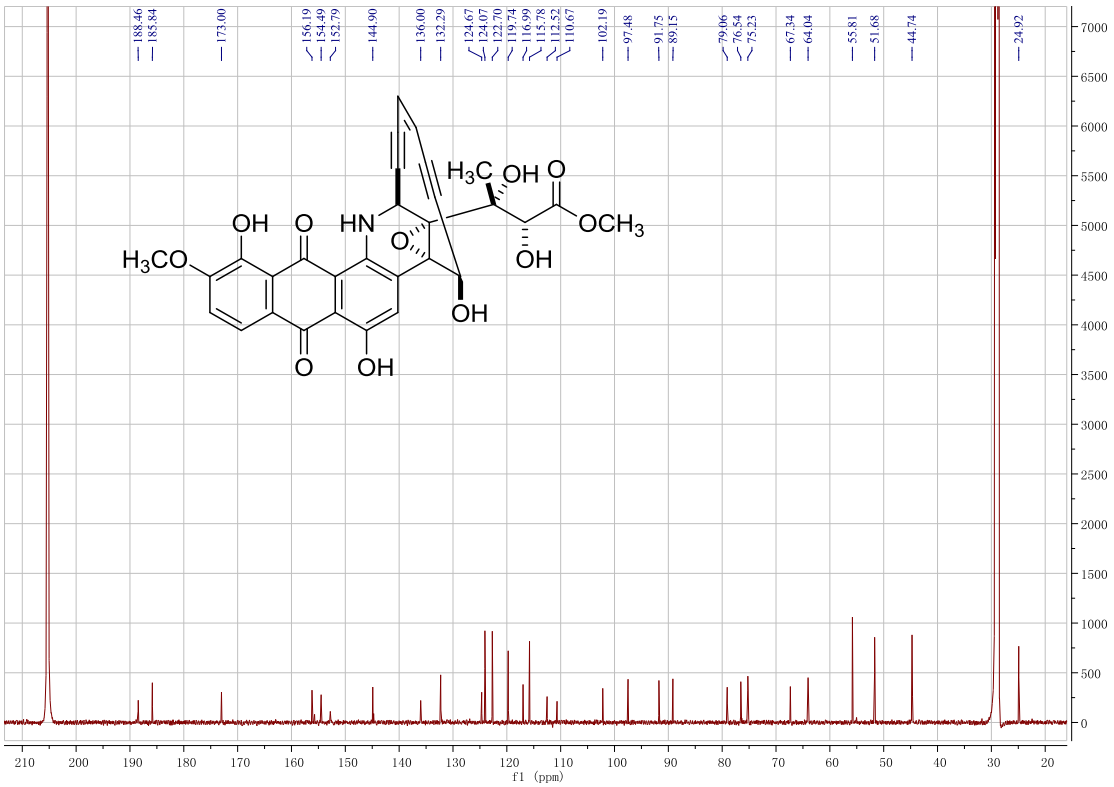

Figure S20. ^{1}H-^{1}H COSY spectrum of TNM D (**6**) (acetone-d_6)

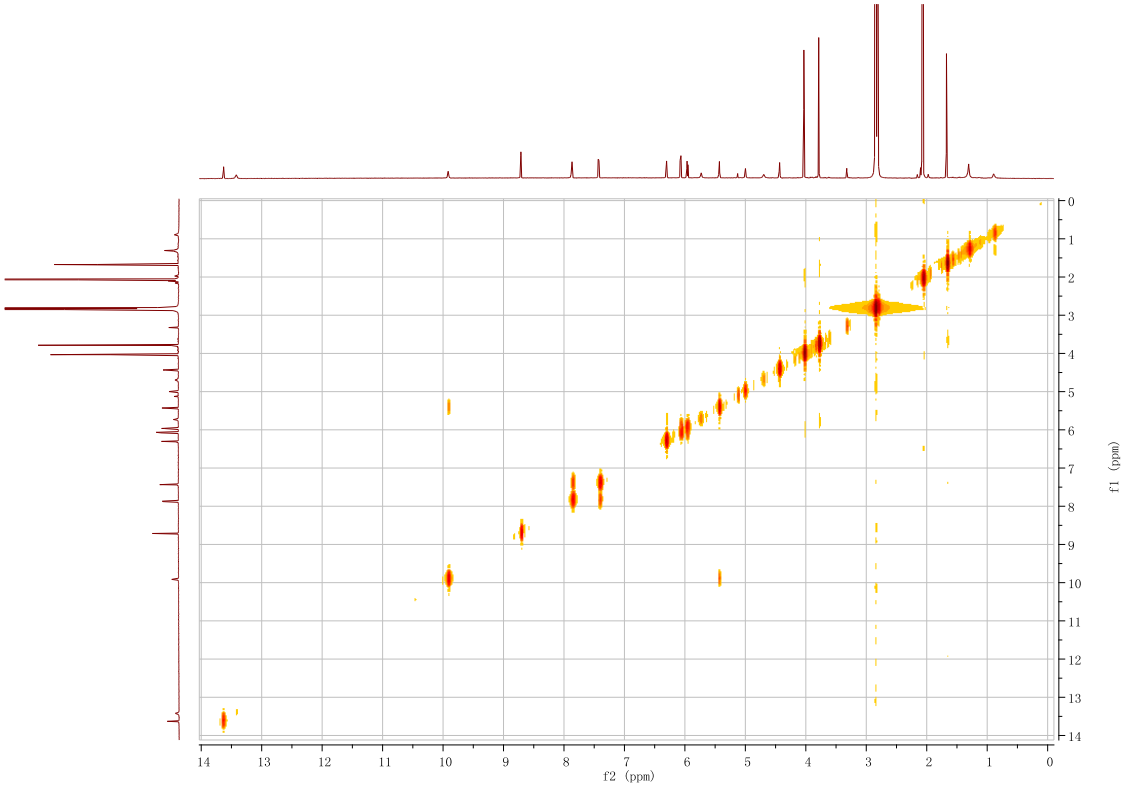

Figure S21. $^{1}H–^{13}C$ HSQC spectrum of TNM D (**6**) (acetone-d_6)

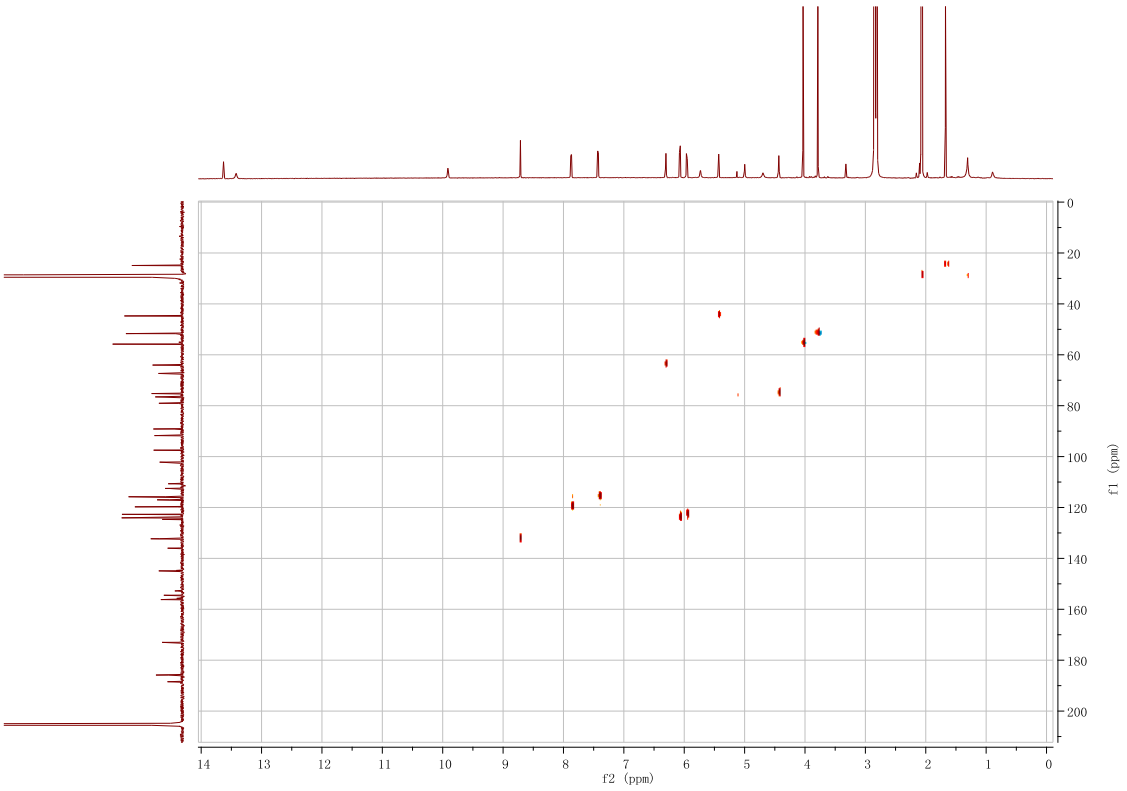

Figure S22. $^{1}H–^{13}C$ HMBC spectrum of TNM D (**6**) (acetone-d_6)

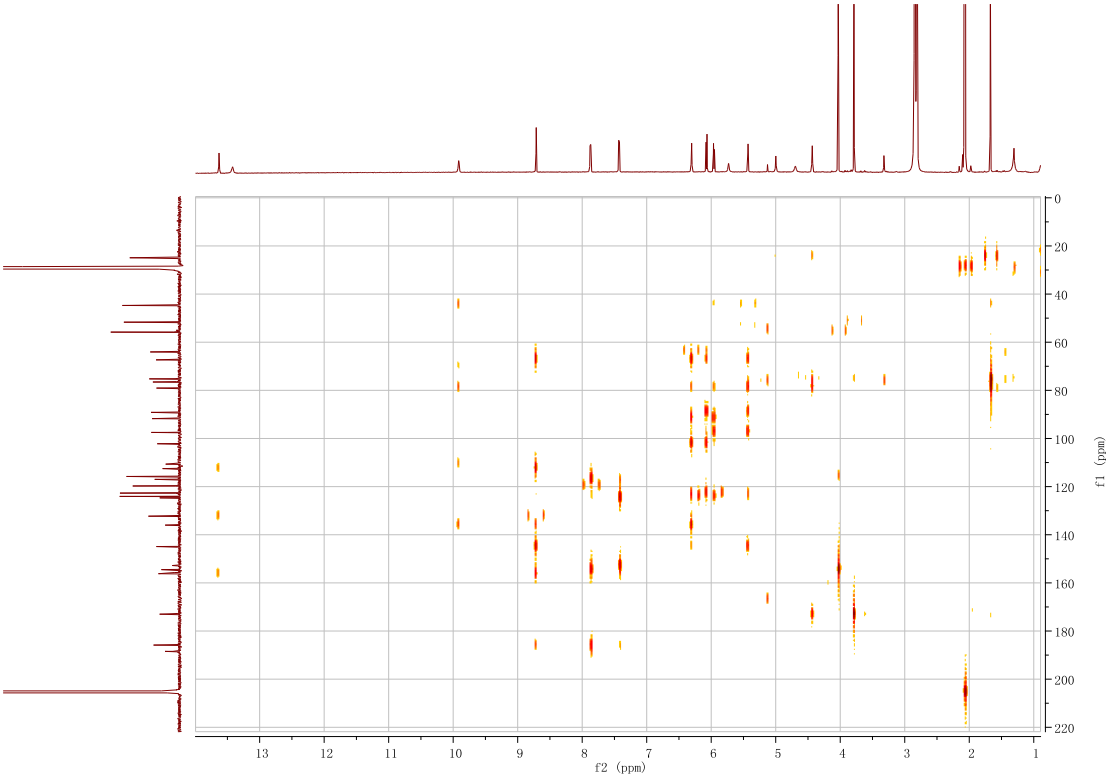

Figure S23. ^{1}H-^{1}H ROESY spectrum of TNM D (**6**) (acetone-d_6)

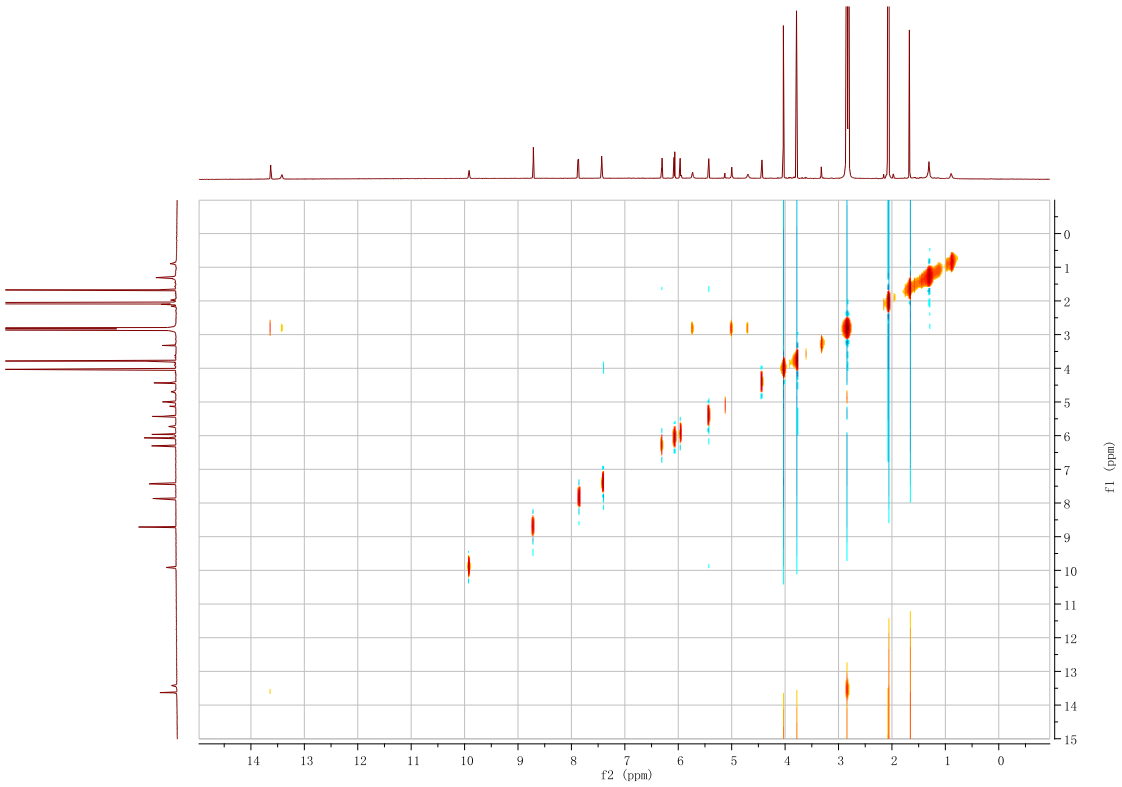

Figure S24. HR-ESI-MS spectrum of **7**

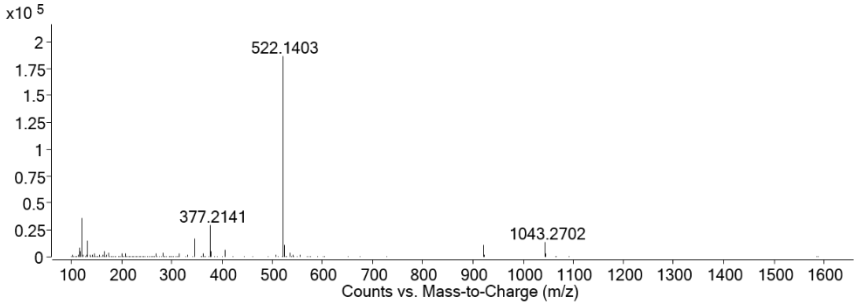

Figure S25. ^{1}H NMR Spectrum of **7** (700 MHz, acetone-d_6)

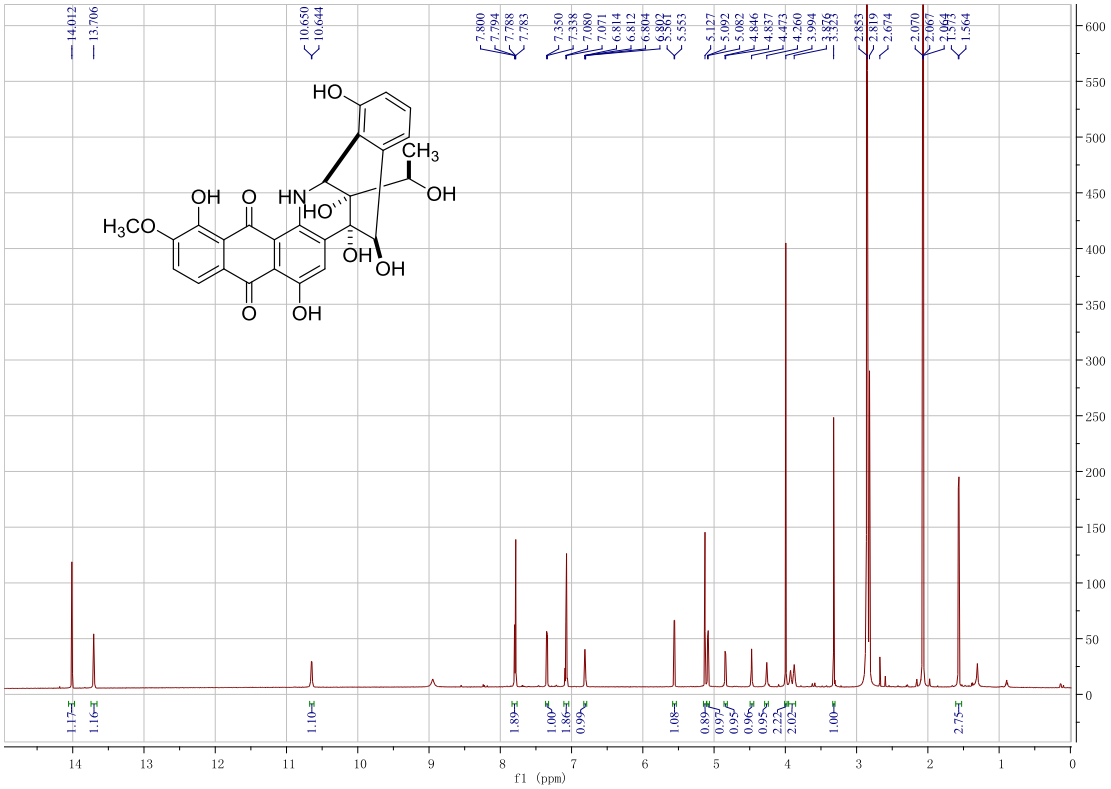

Figure S26. ^{13}C NMR spectrum of **7** (176 MHz, acetone-d_6)

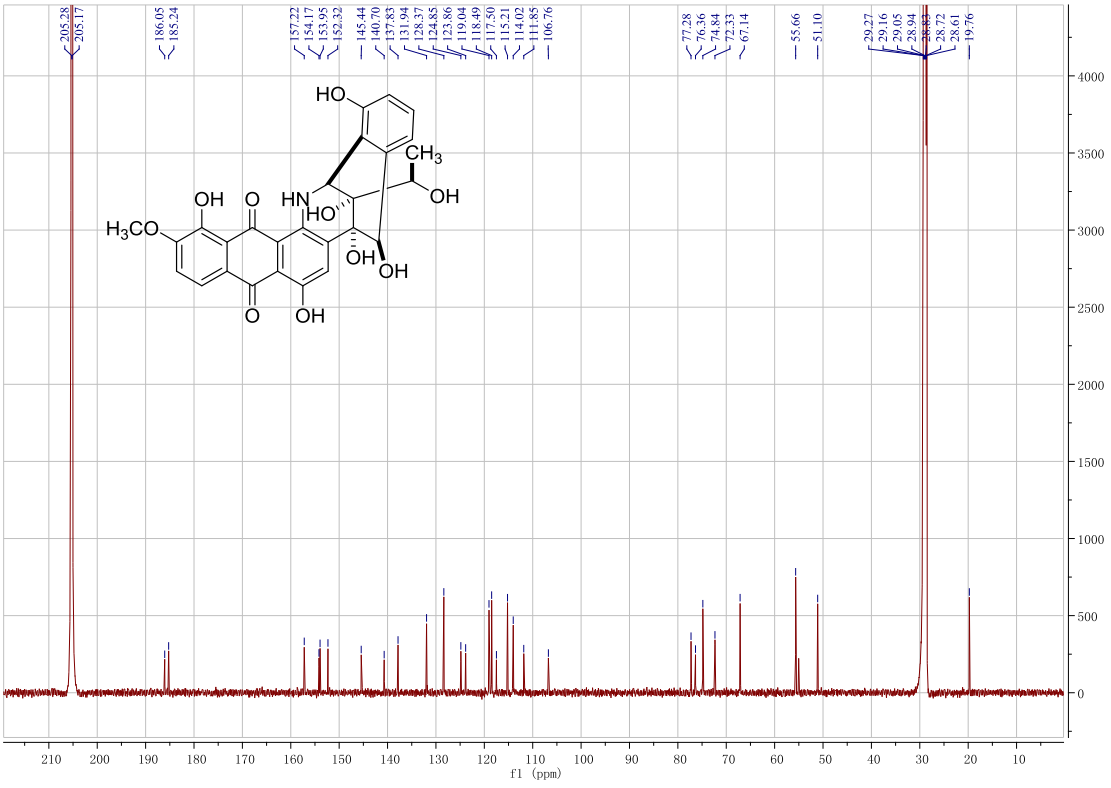

Figure S27. ^{1}H-^{1}H COSY spectrum of **7** (acetone-d_6)

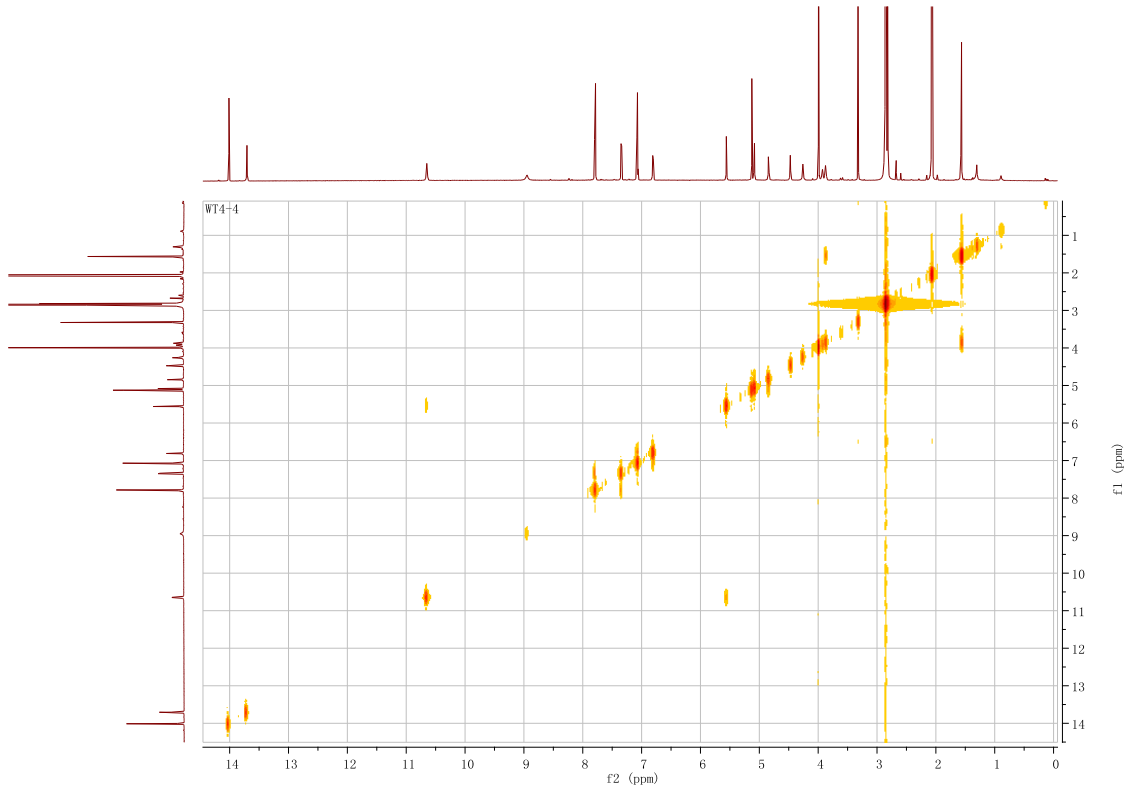

Figure S28. ^{1}H–^{13}C HSQC spectrum of **7** (acetone-d_6)

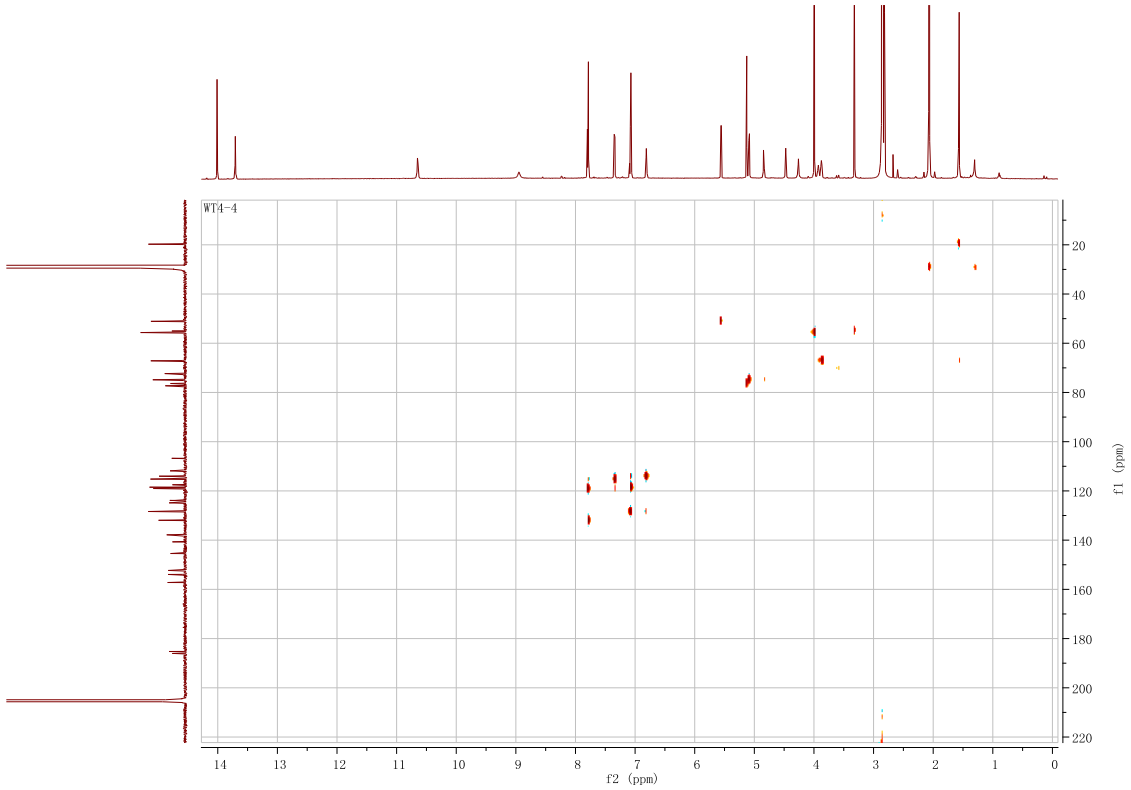

Figure S29. ^{1}H–^{13}C HMBC spectrum of **7** (acetone-d_6)

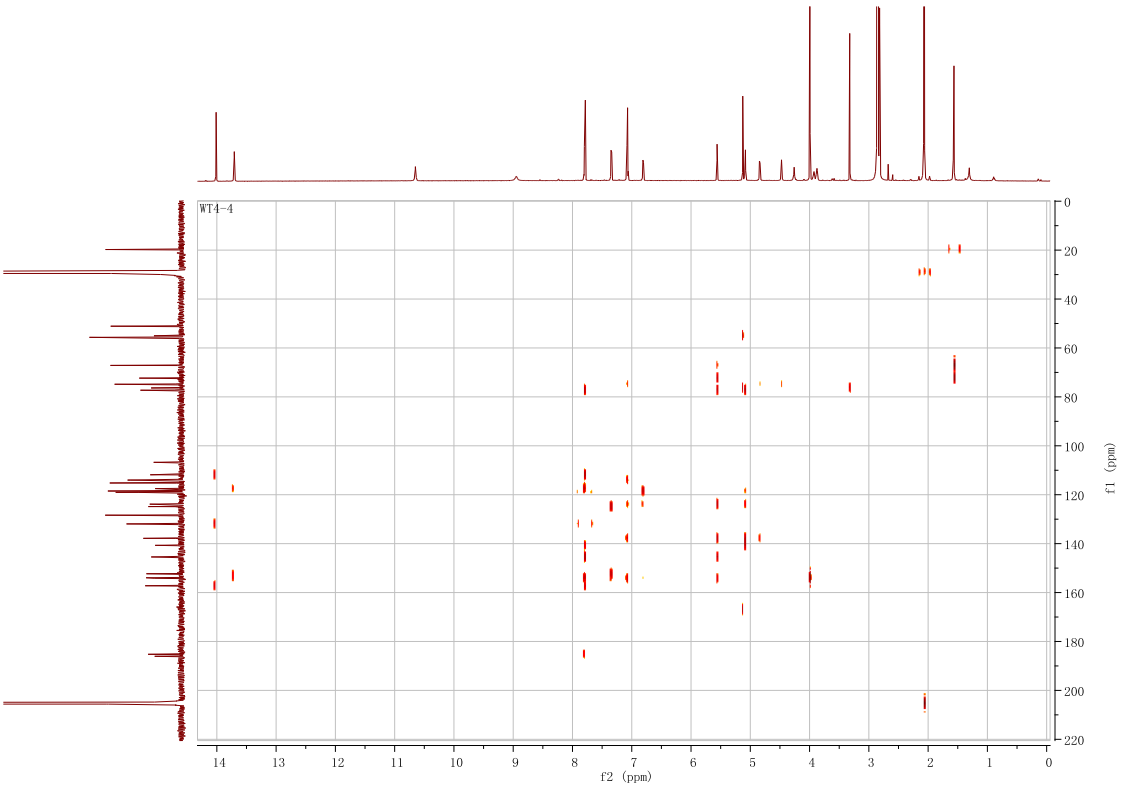

Figure S30. ^{1}H-^{1}H ROESY spectrum of **7** (acetone-d_6)

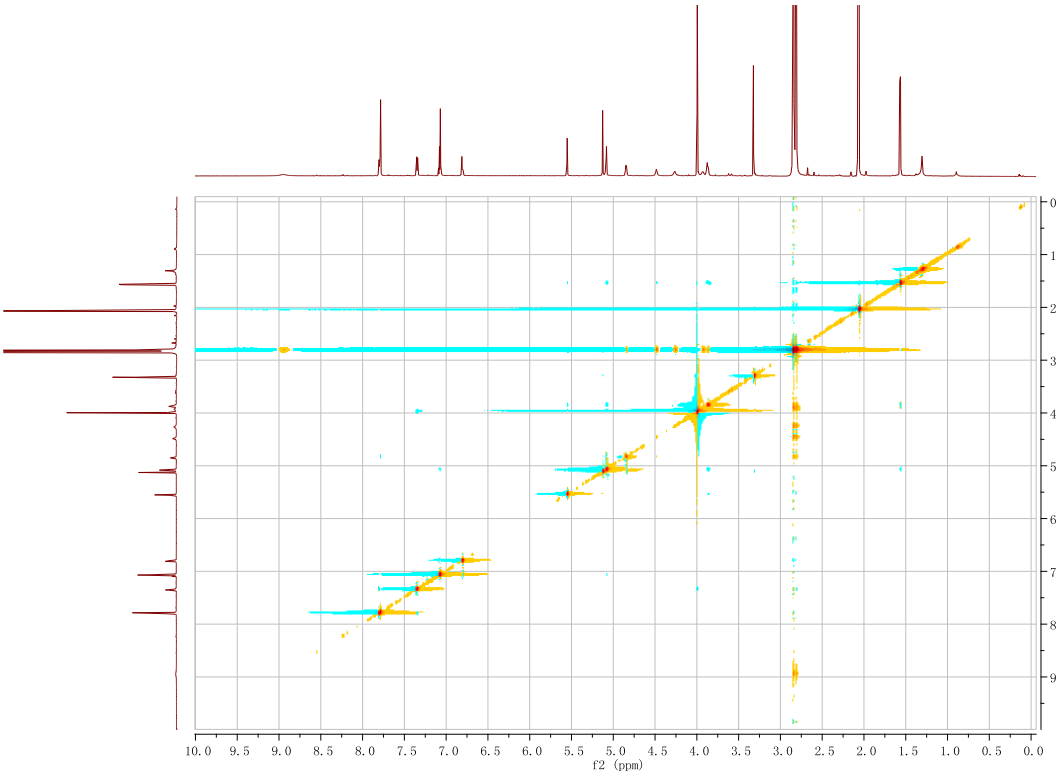

Figure S31. HR-ESI-MS spectrum of **8**

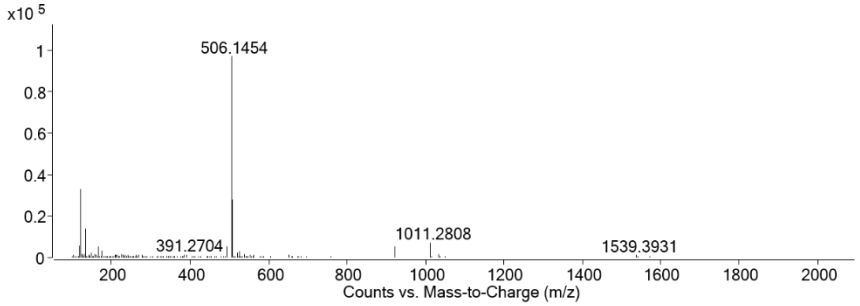

Figure S32. ^{1}H NMR Spectrum of **8** (700 MHz, acetone-d_6)

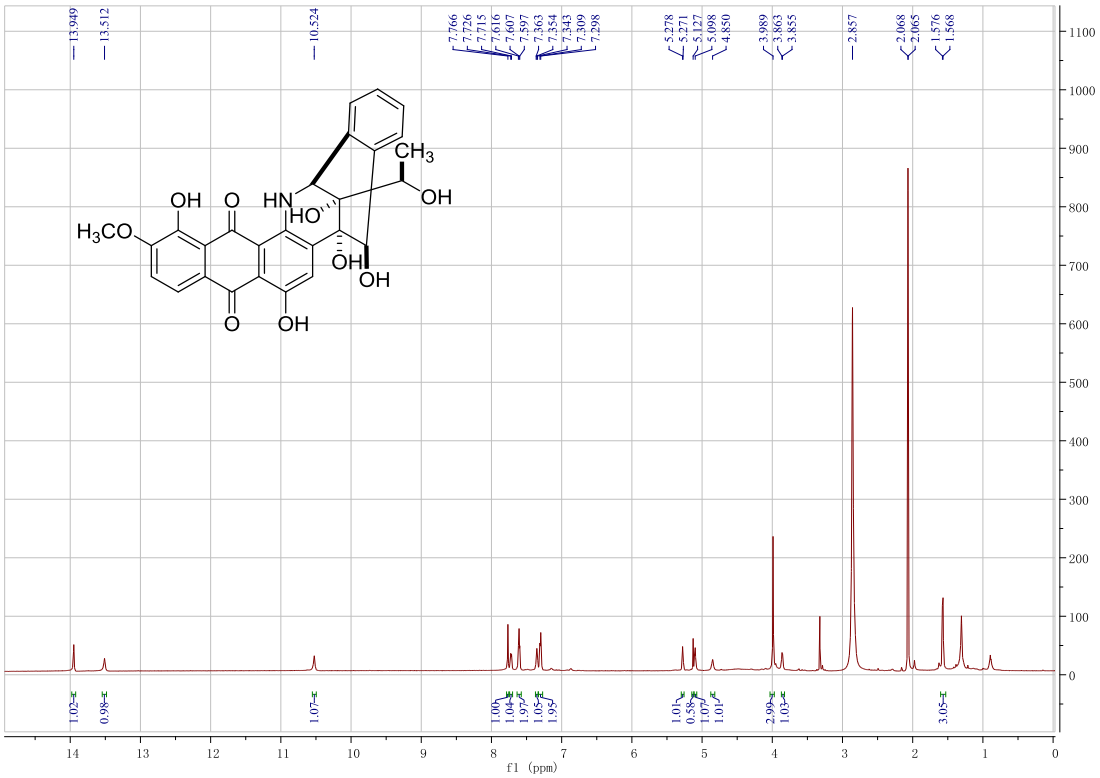

Figure S33. ^{13}C NMR spectrum of **8** (176 MHz, acetone-d_6)

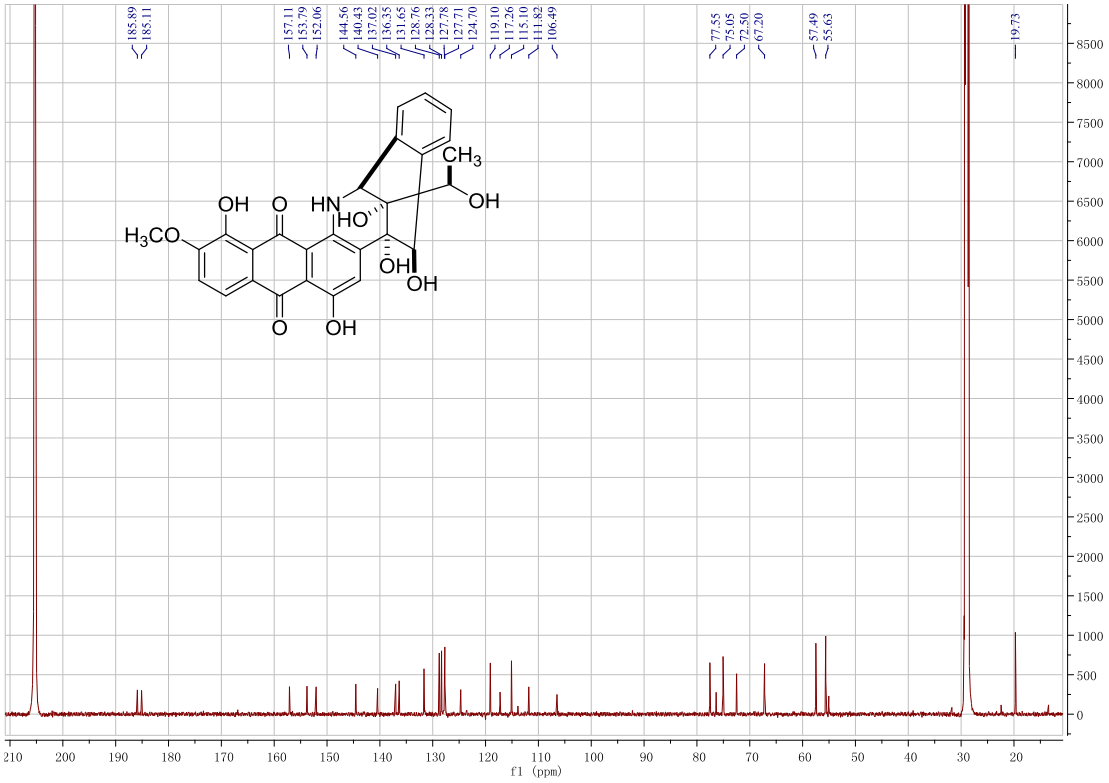

Figure S34. ^{1}H-^{1}H COSY spectrum of **8** (acetone-d_6)

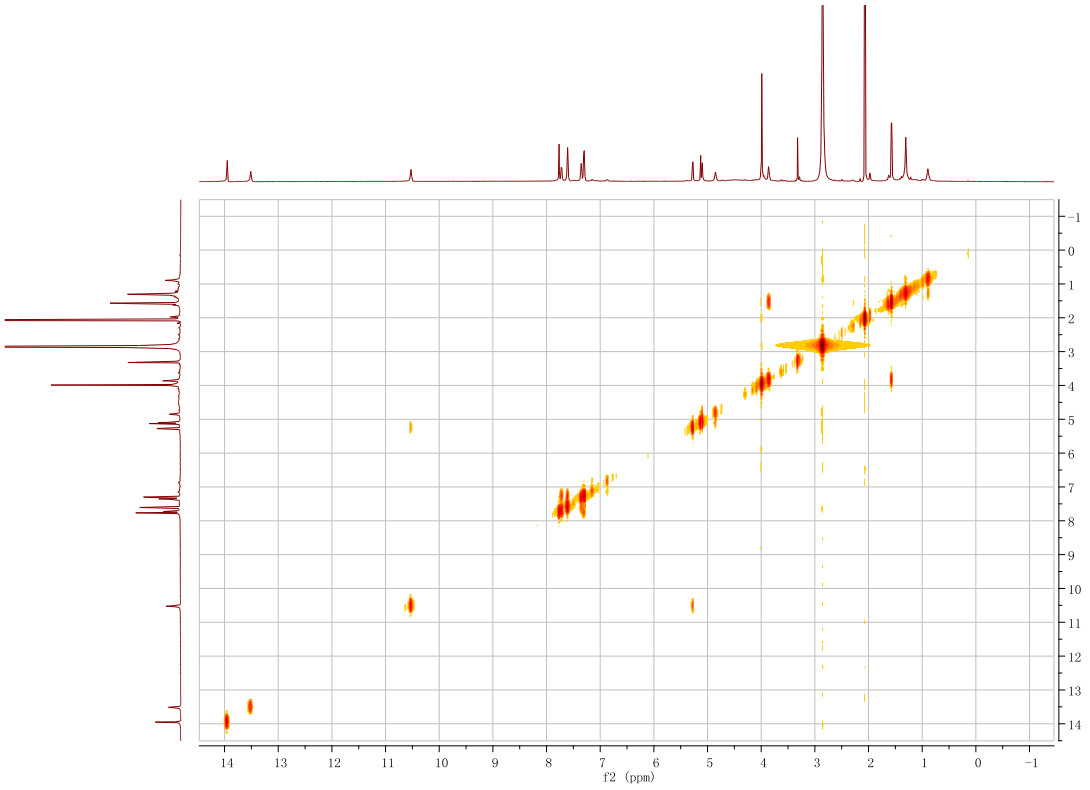

Figure S35. $^{1}H–^{13}C$ HSQC spectrum of **8** (acetone-d_6)

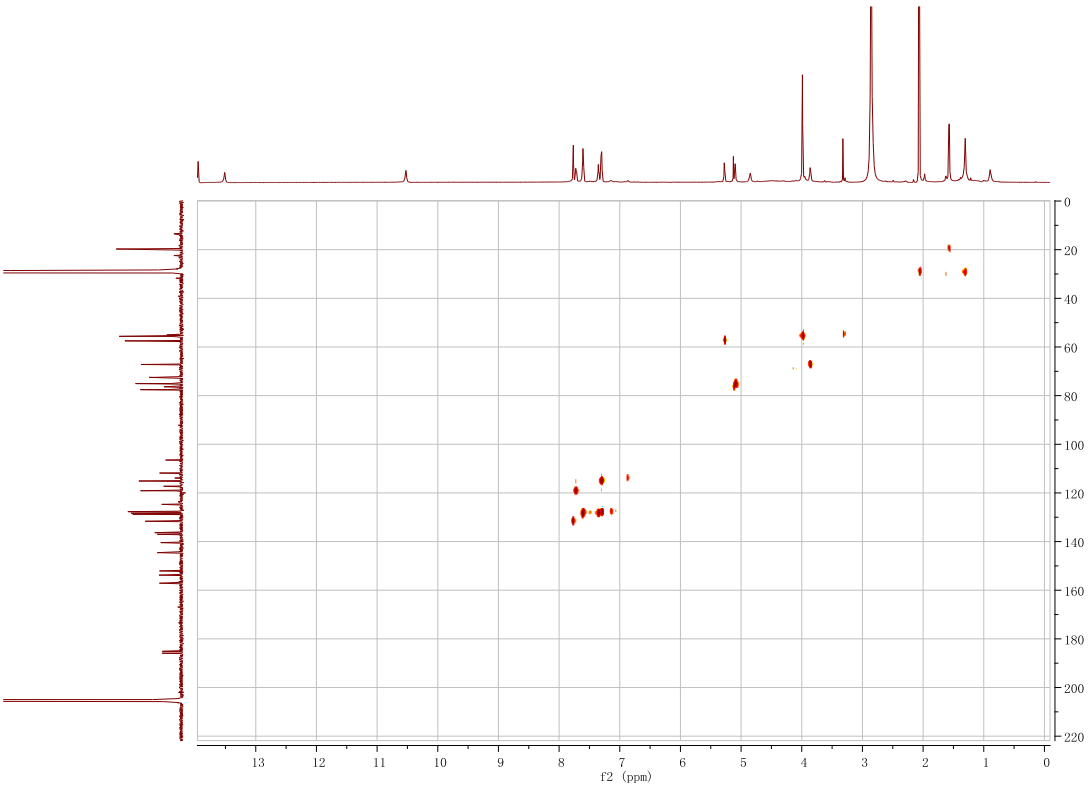

Figure S36. $^{1}H–^{13}C$ HMBC spectrum of **8** (acetone-d_6)

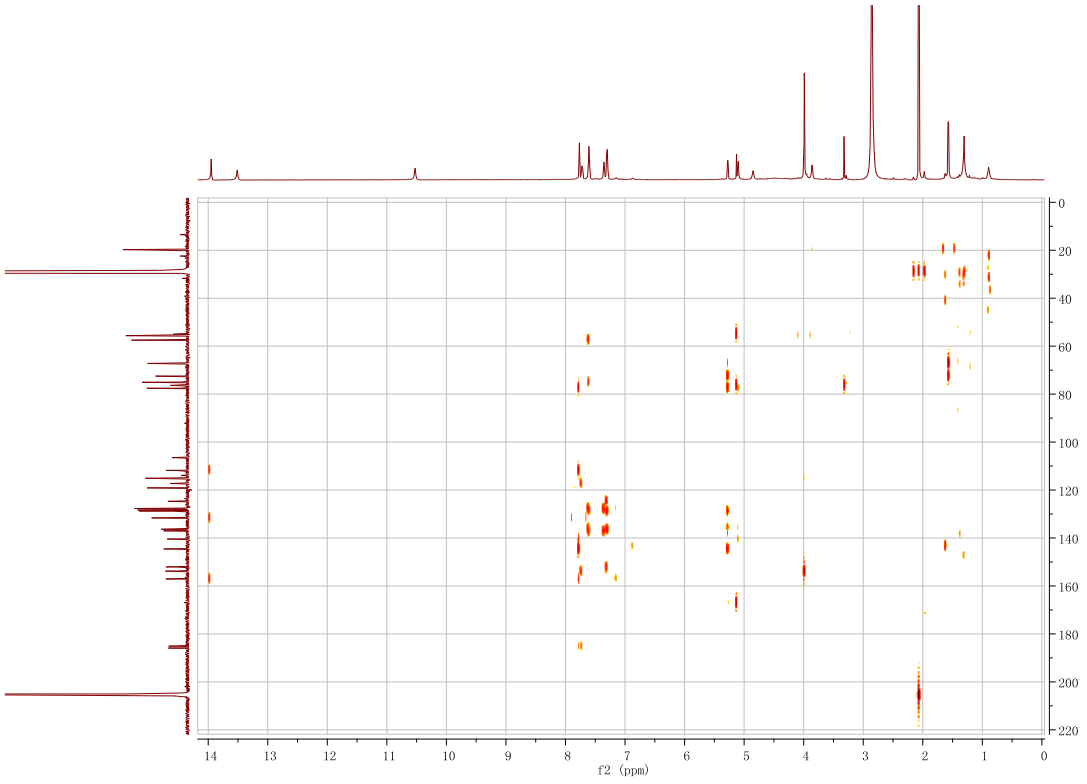

Figure S37. ^{1}H-^{1}H ROESY spectrum of **8** (acetone-d_6)

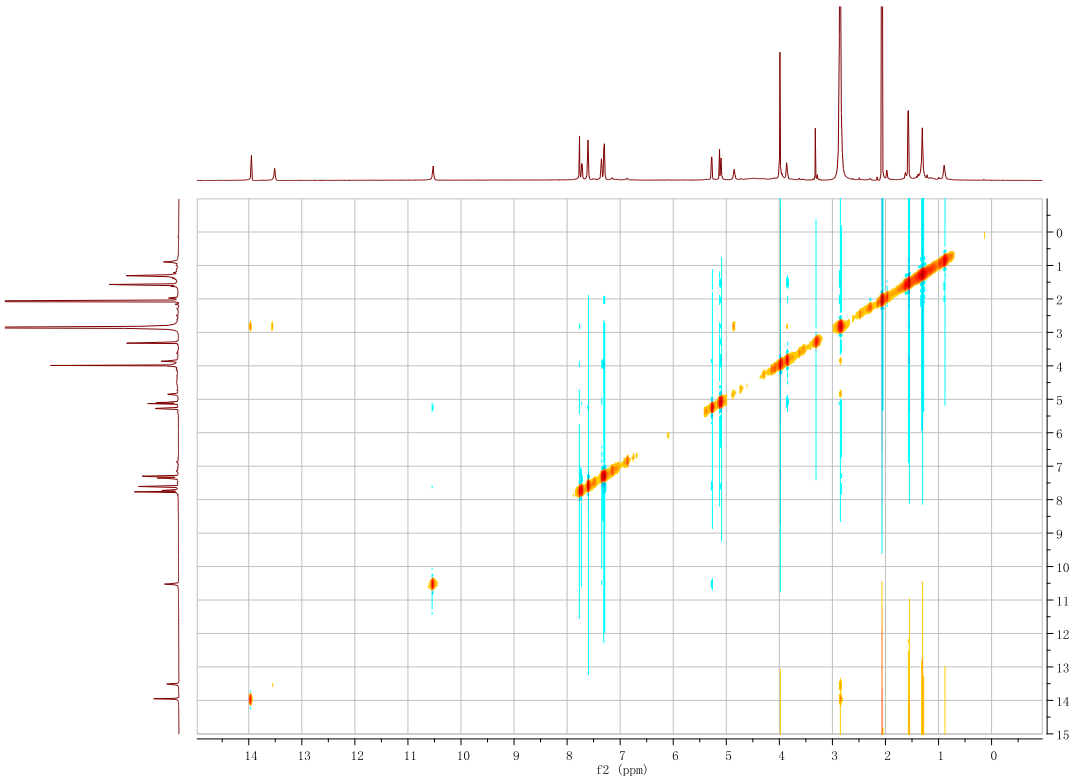

Figure S38. HR-ESI-MS spectrum of **9**

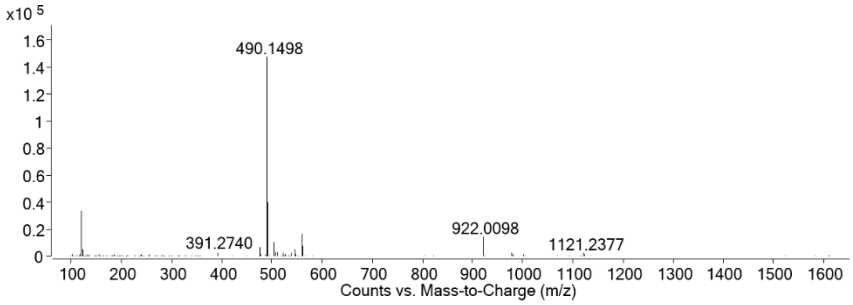

Figure S39. ^{1}H NMR Spectrum of **9** (700 MHz, acetone-d_6)

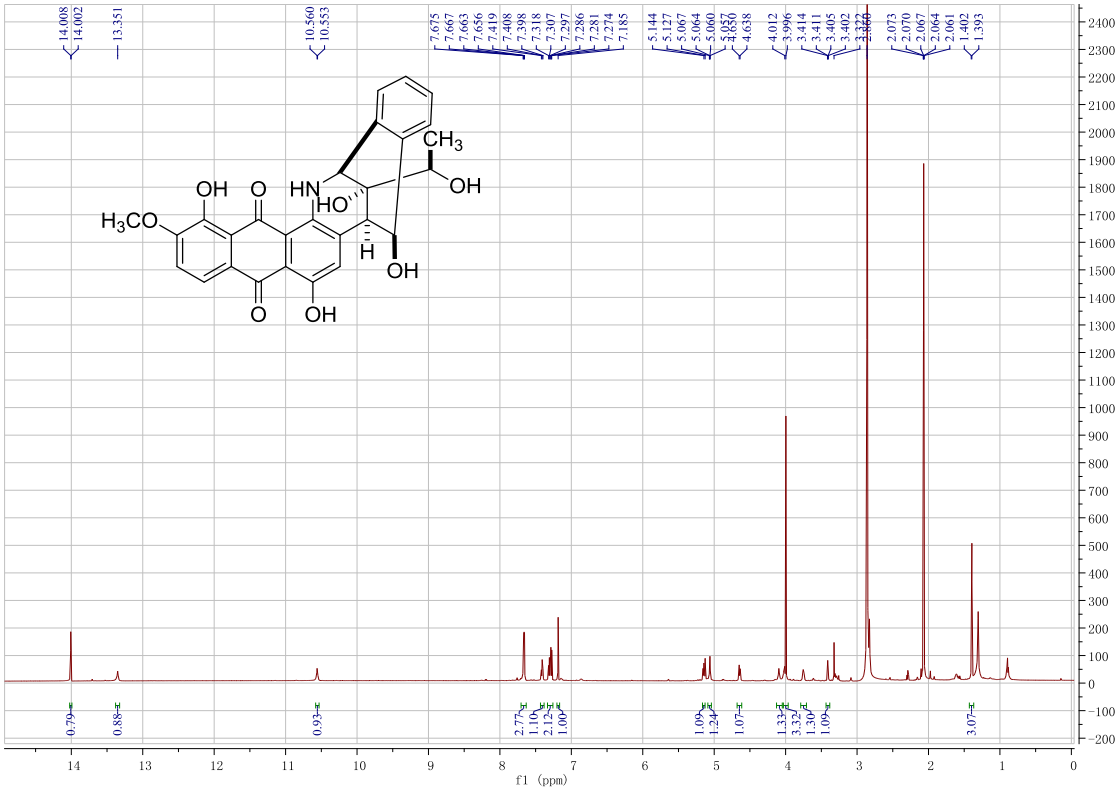

Figure S40. ^{13}C NMR spectrum of **9** (176 MHz, acetone-d_6)

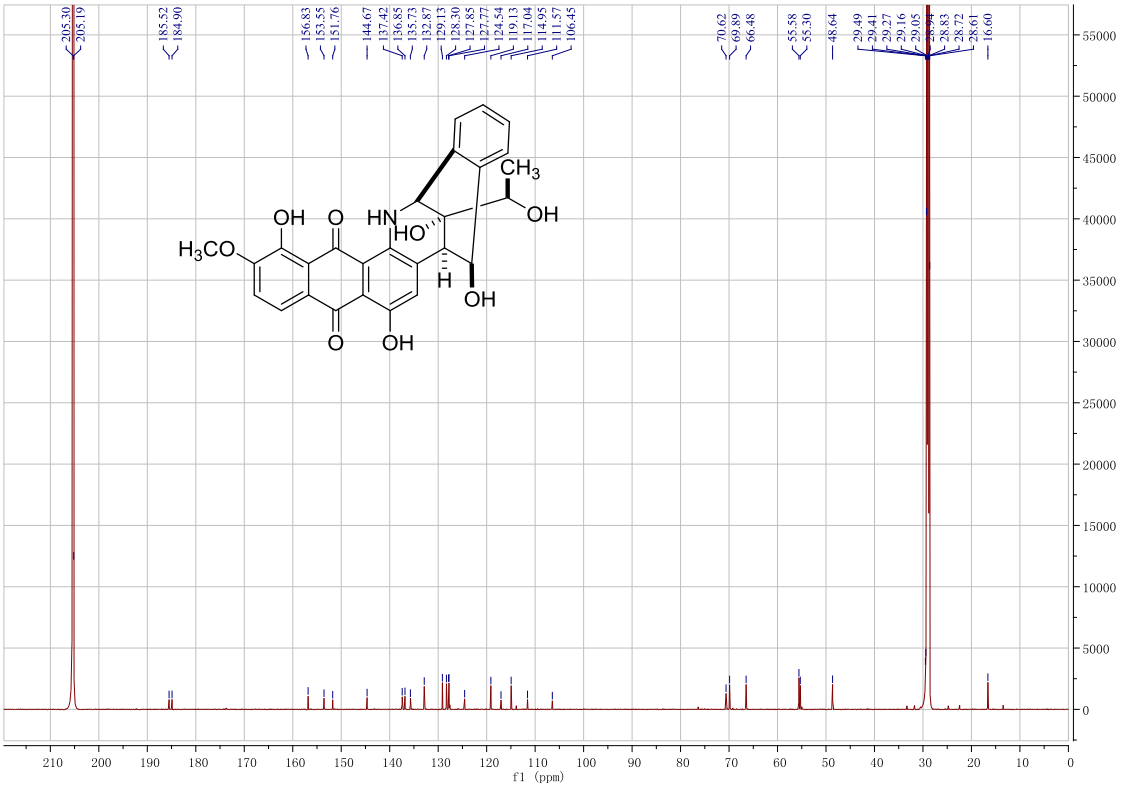

Figure S41. ^{1}H-^{1}H COSY spectrum of **9** (acetone-d_6)

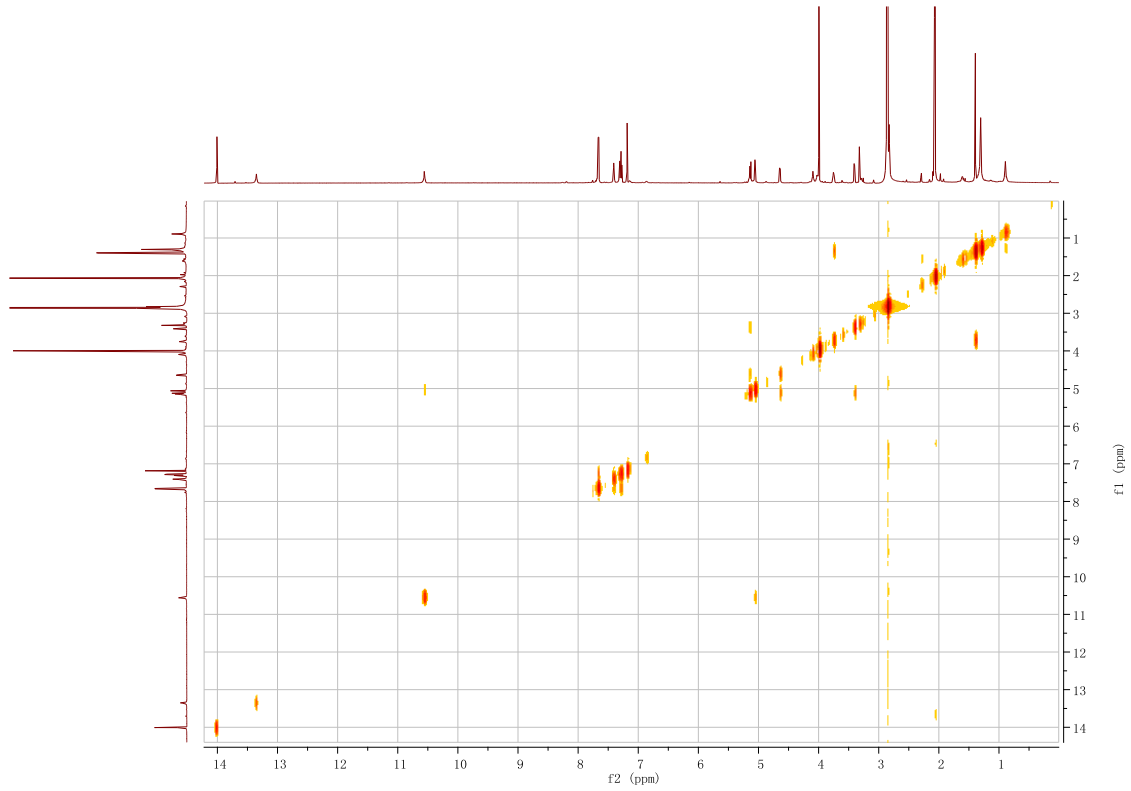

Figure S42. ^{1}H–^{13}C HSQC spectrum of **9** (acetone-d_6)

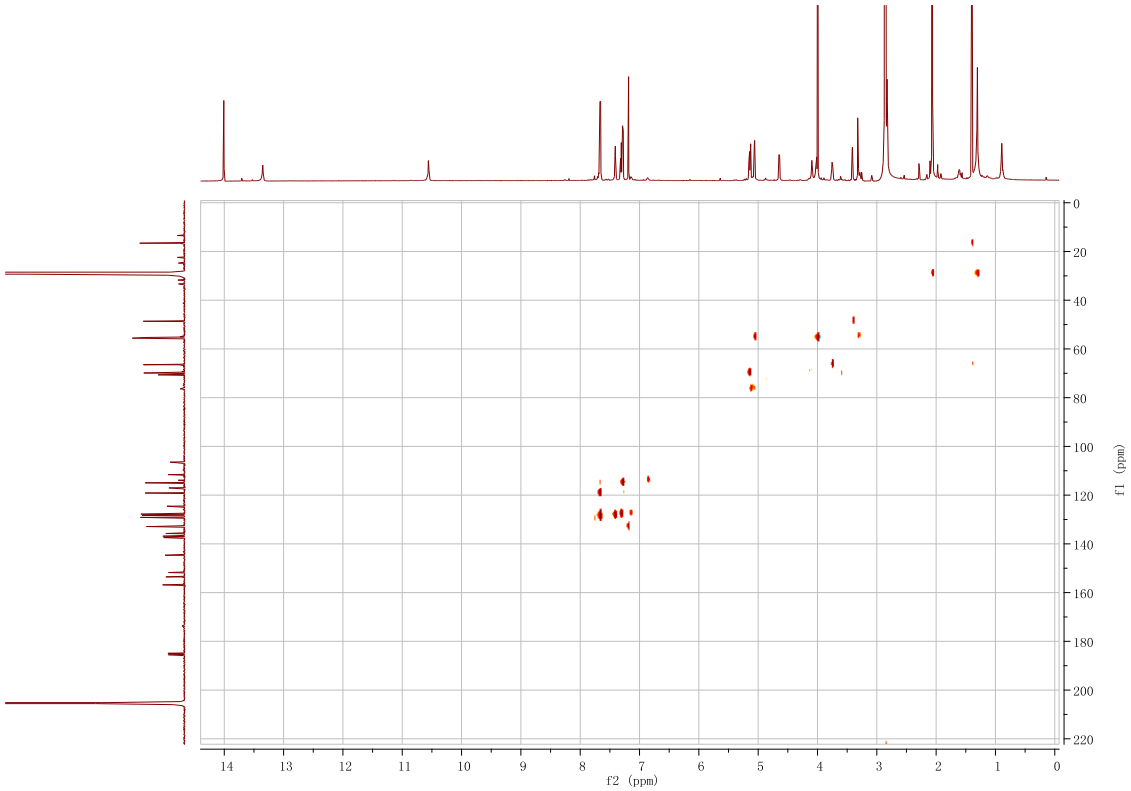

Figure S43. ^{1}H–^{13}C HMBC spectrum of **9** (acetone-d_6)

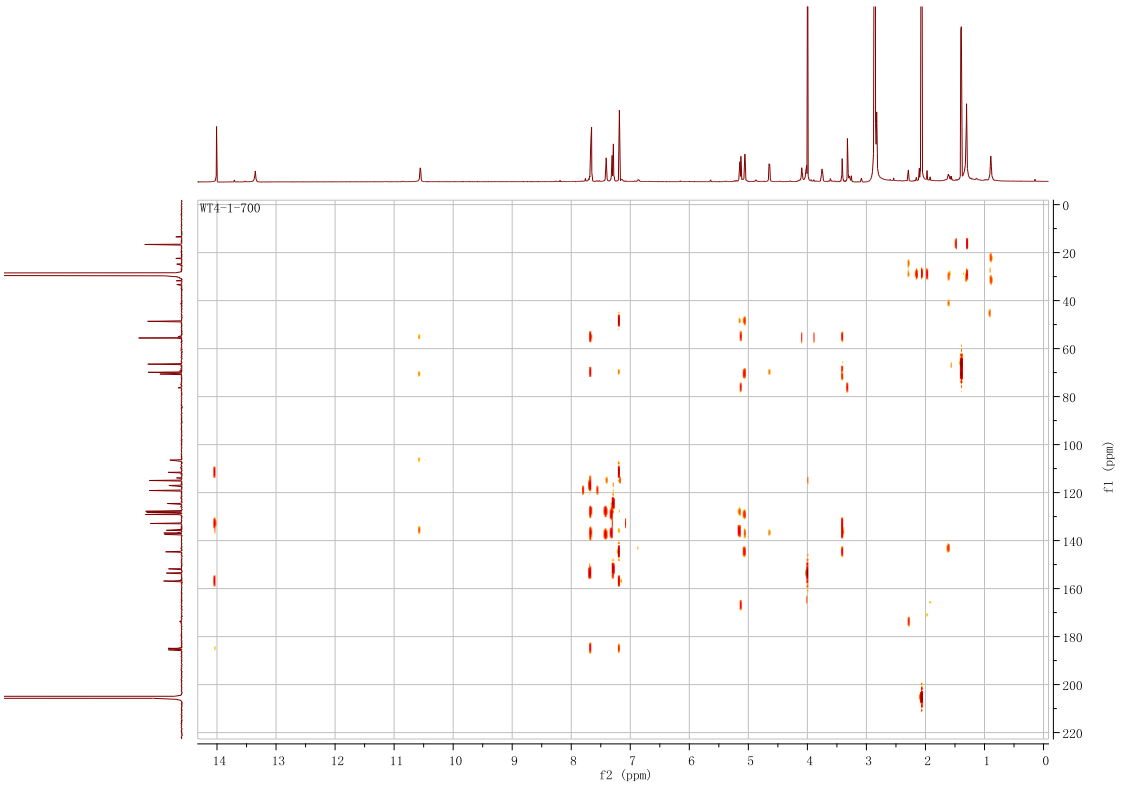

Figure S44. ^{1}H-^{1}H ROESY spectrum of **9** (acetone-d_6)

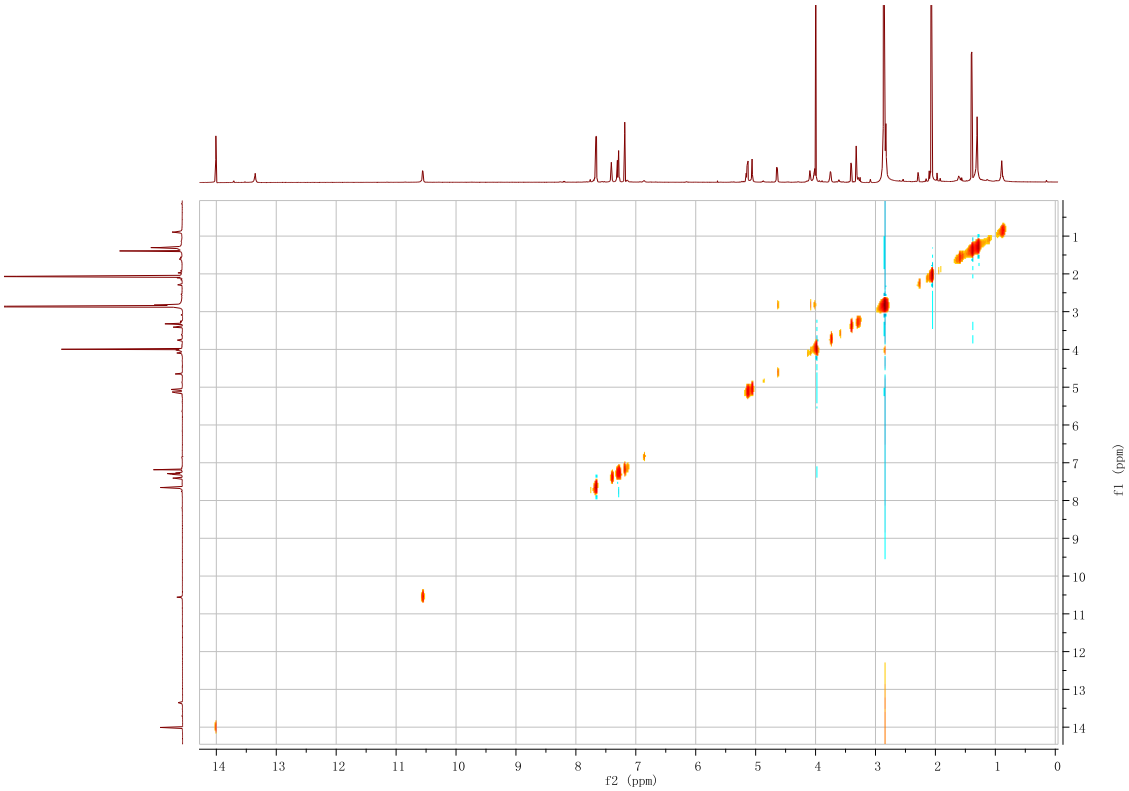

Figure S45. HR-ESI-MS spectrum of **10**

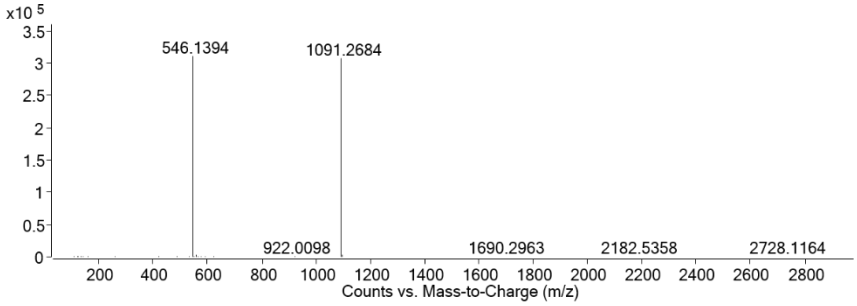

Figure S46. ^{1}H NMR Spectrum of **10** (700 MHz, acetone-d_6)

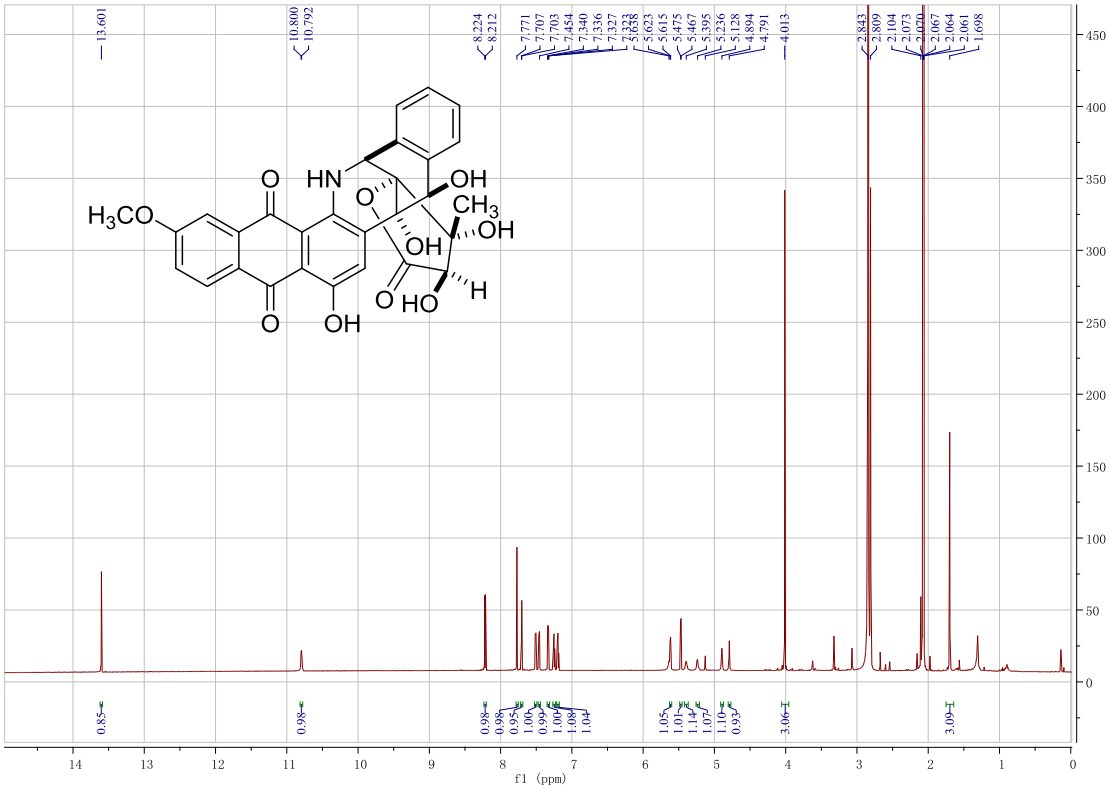

Figure S47. ^{13}C NMR spectrum of **10** (176 MHz, acetone-d_6)

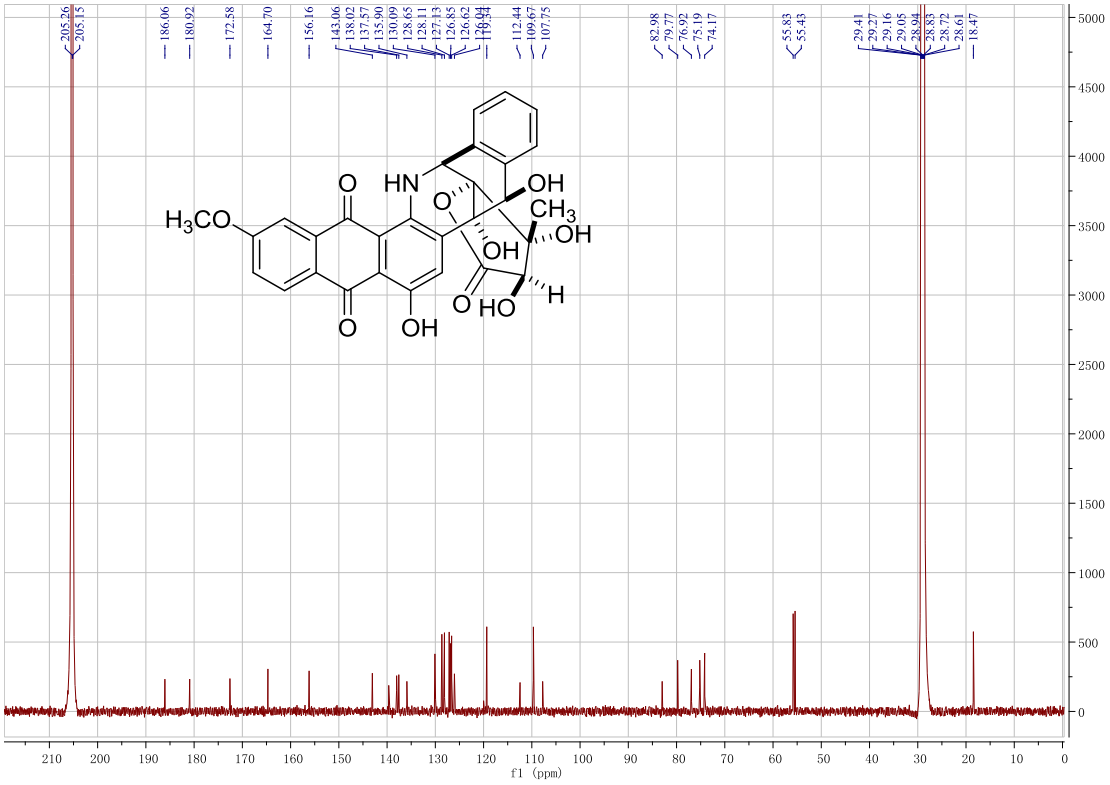

Figure S48. ^{1}H-^{1}H COSY spectrum of **10** (acetone-d_6)

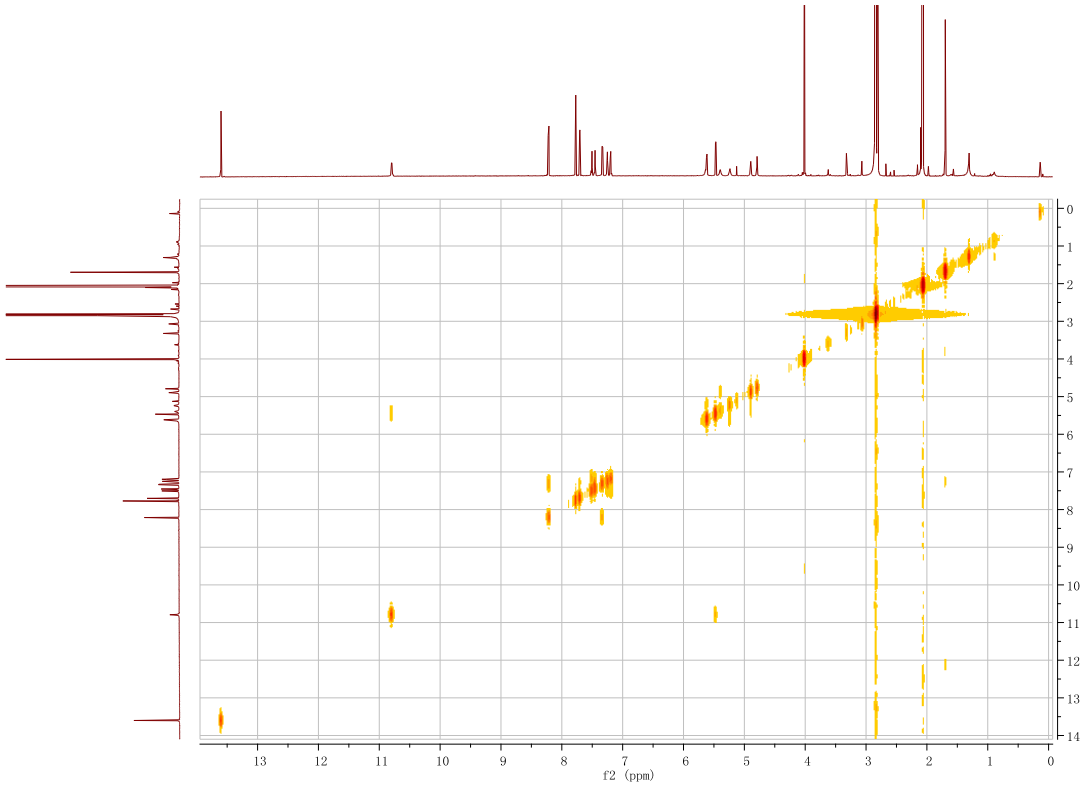

Figure S49. $^{1}H–^{13}C$ HSQC spectrum of **10** (acetone-d_6)

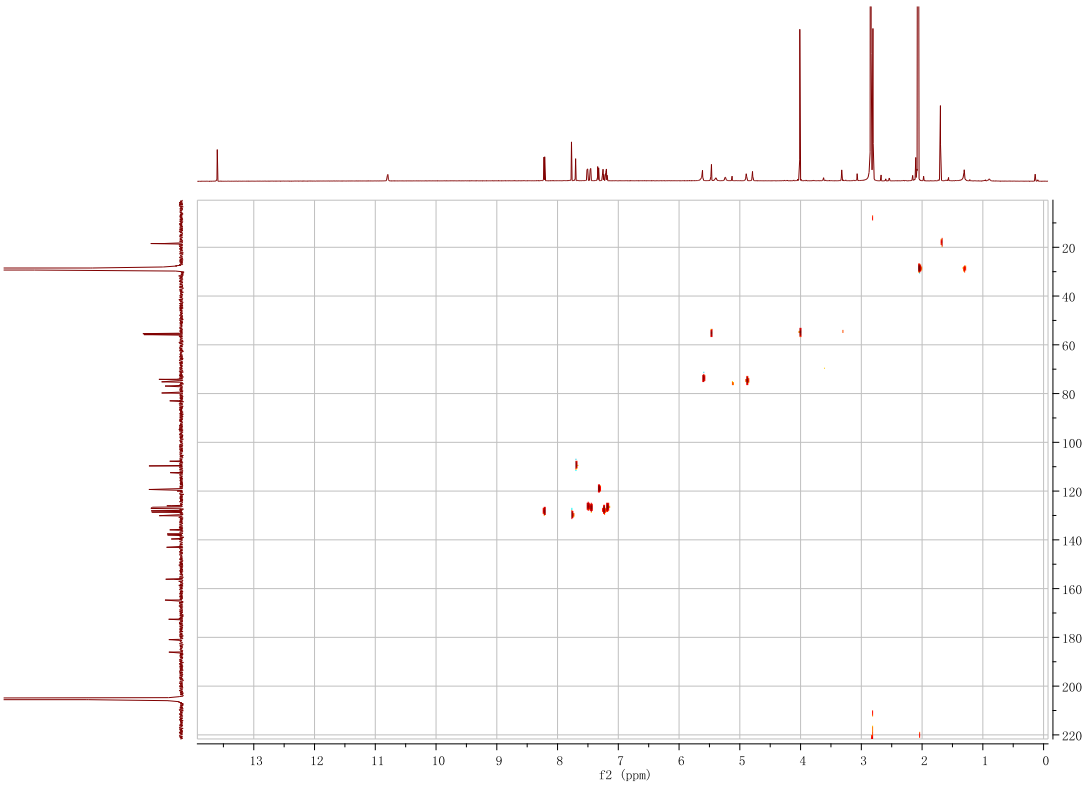

Figure S50. $^{1}H–^{13}C$ HMBC spectrum of **10** (acetone-d_6)

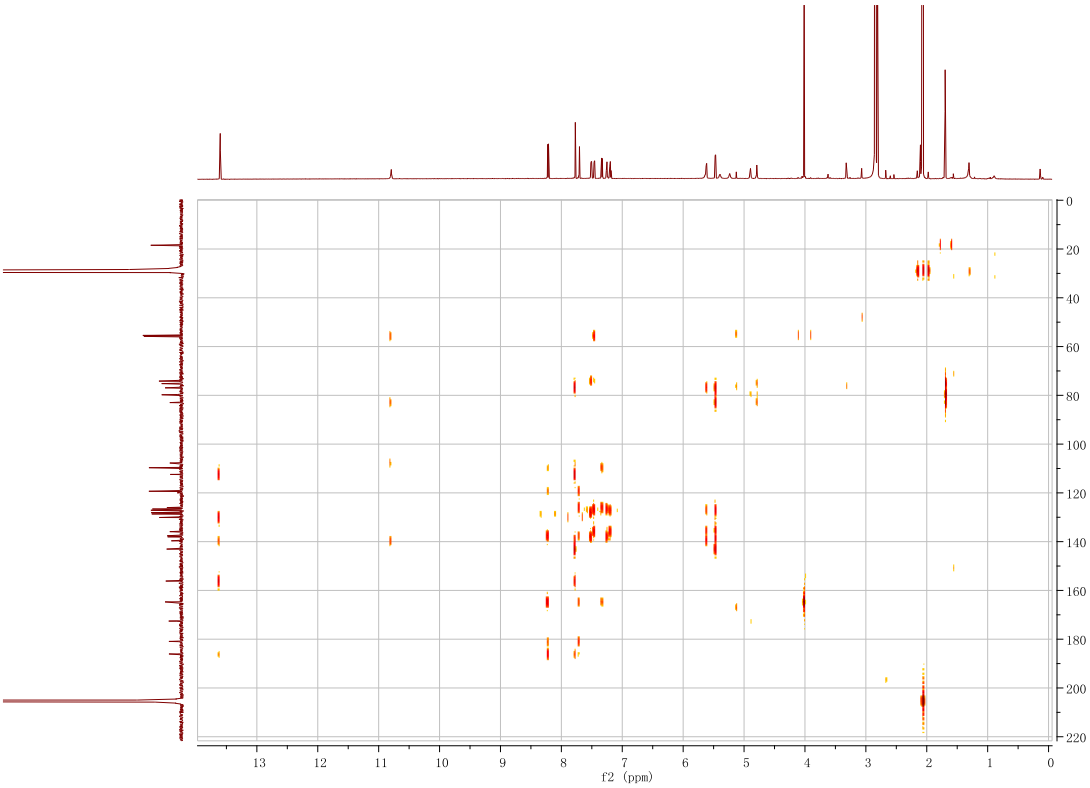

Figure S51. ^{1}H-^{1}H ROESY spectrum of **10** (acetone-d_6)

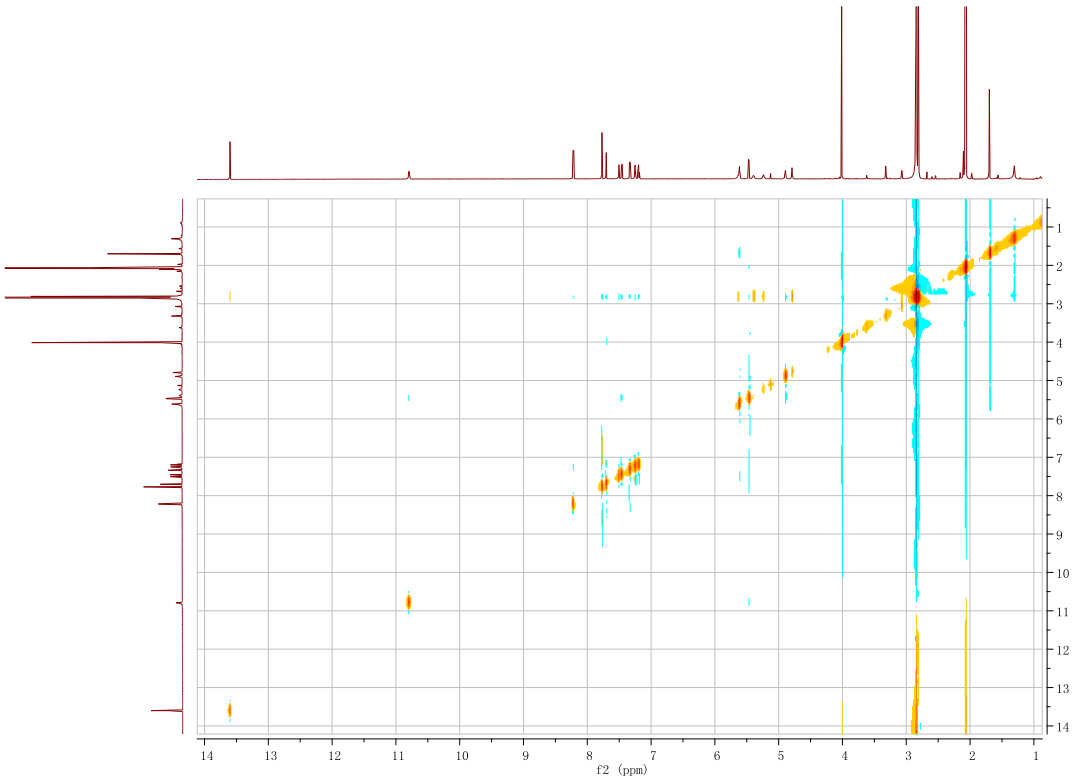

Figure S52. HR-ESI-MS spectrum of **11**

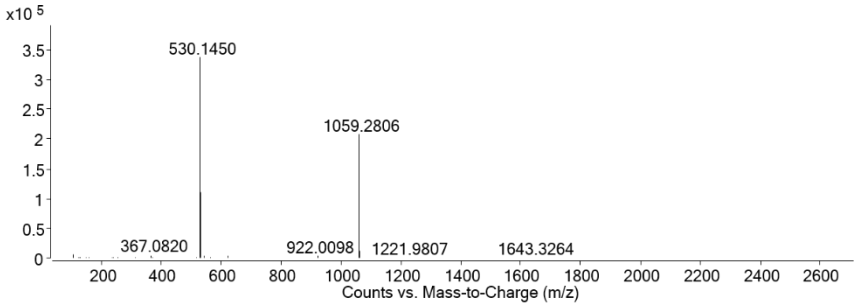

Figure S53. ^{1}H NMR Spectrum of **11** (700 MHz, acetone-d_6)

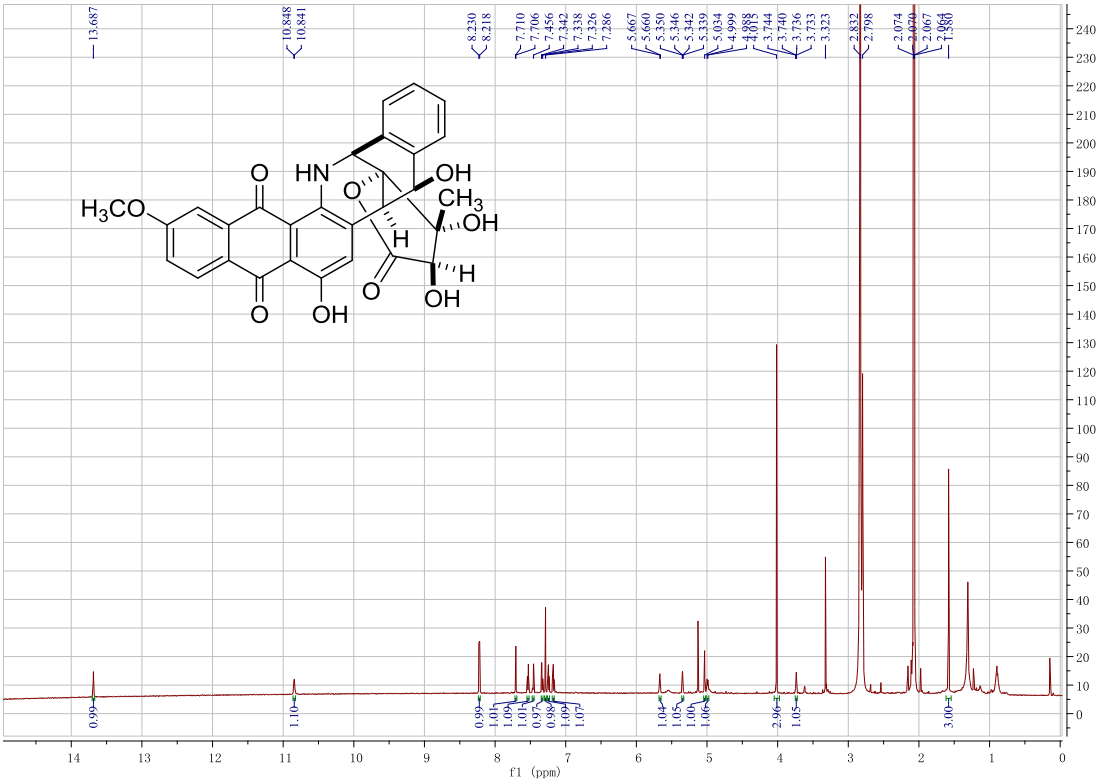

Figure S54. ^{13}C NMR spectrum of **11** (176 MHz, acetone-d_6)

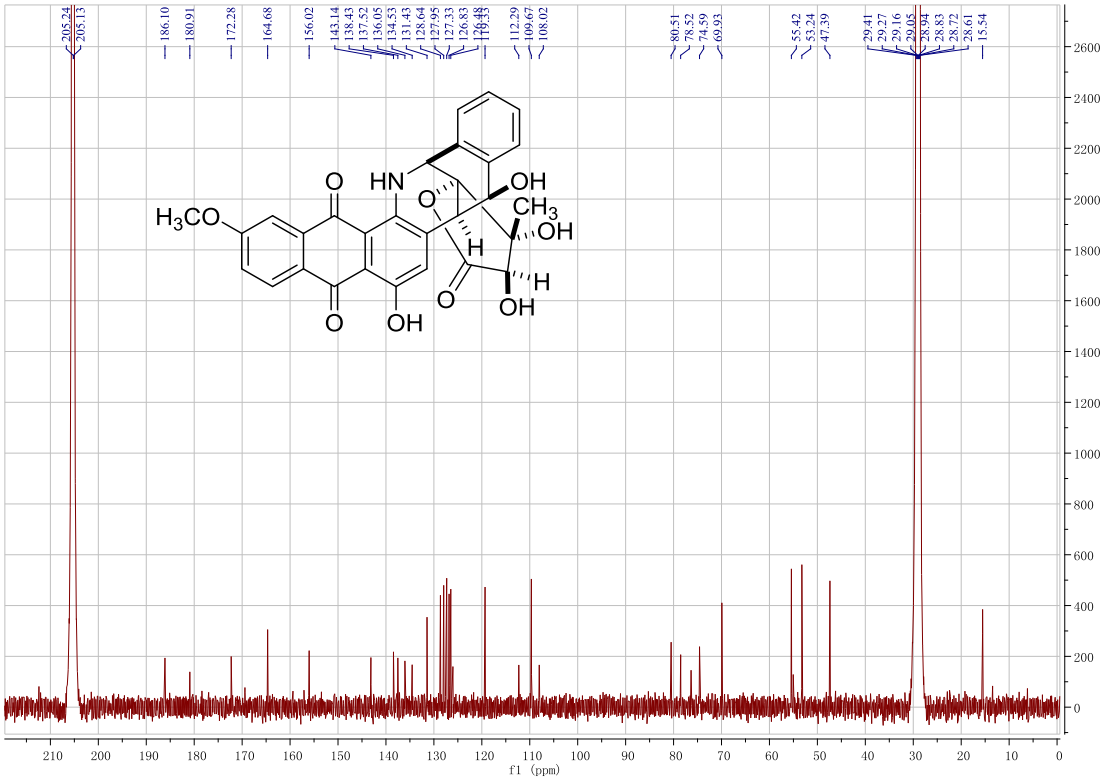

Figure S55. ^{1}H-^{1}H COSY spectrum of **11** (acetone-d_6)

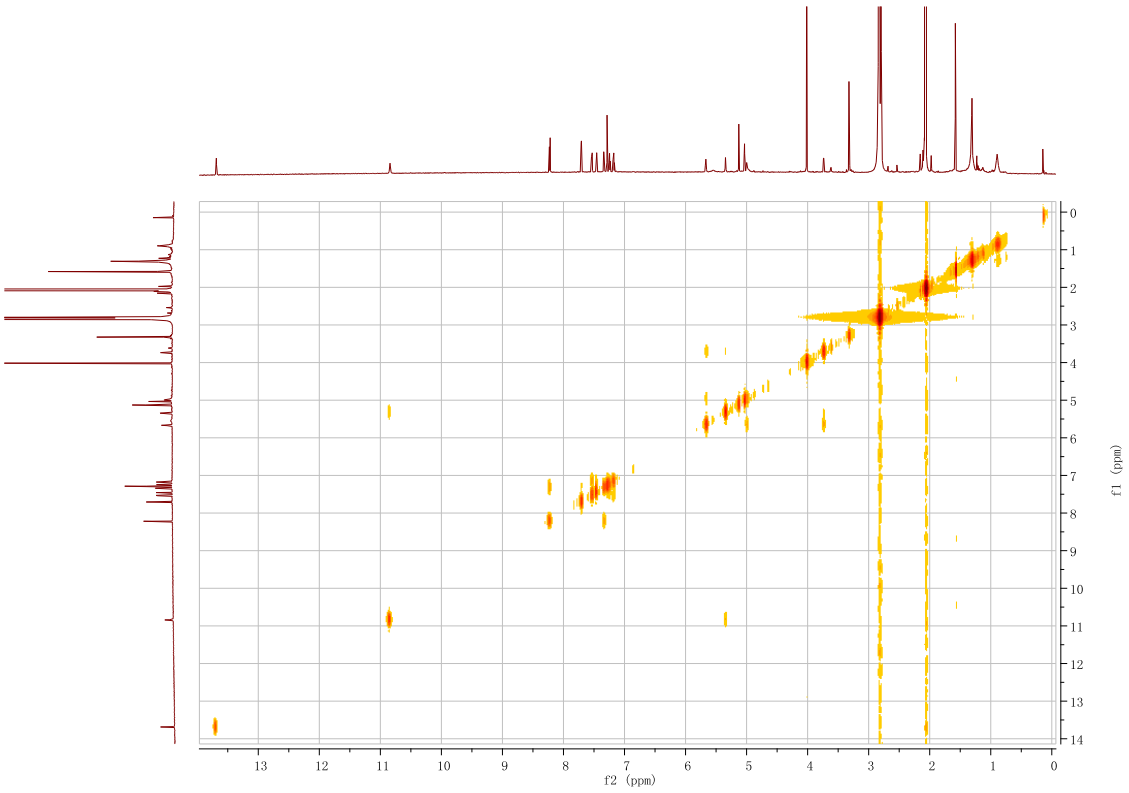

Figure S56. ^{1}H–^{13}C HSQC spectrum of **11** (acetone-d_6)

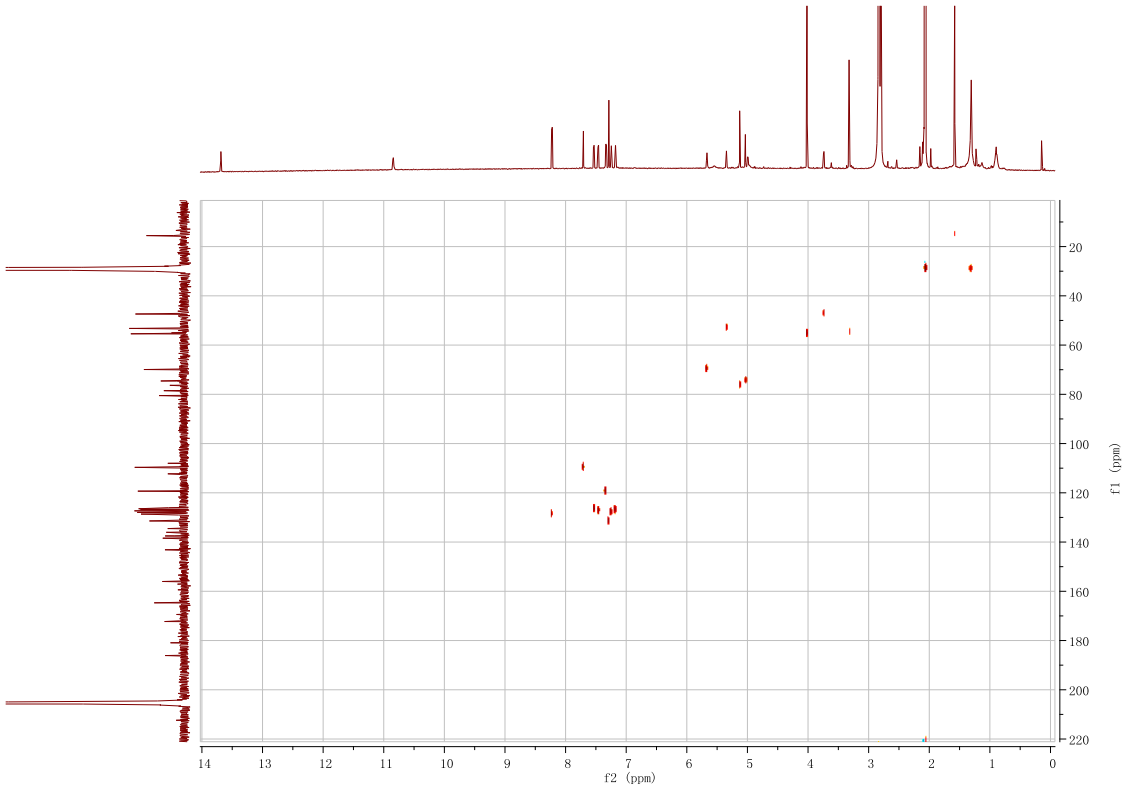

Figure S57. ^{1}H–^{13}C HMBC spectrum of **11** (acetone-d_6)

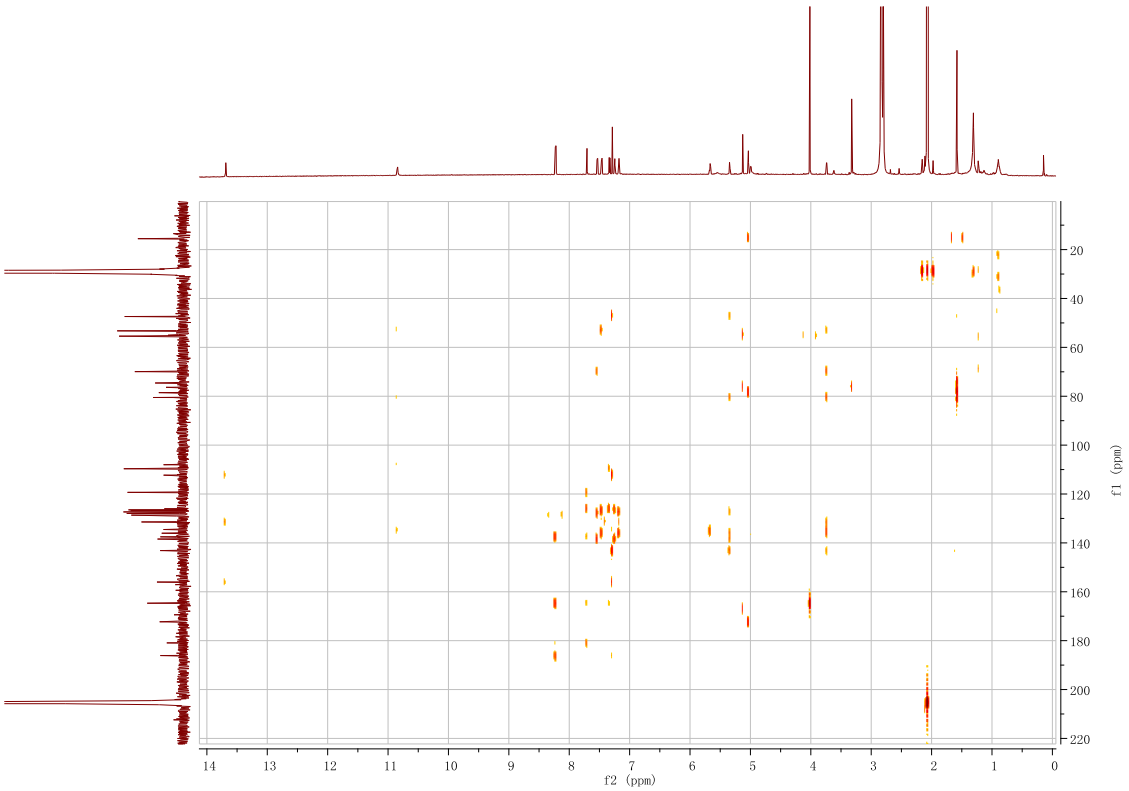

Figure S58. ^{1}H-^{1}H ROESY spectrum of **11** (acetone-d_6)

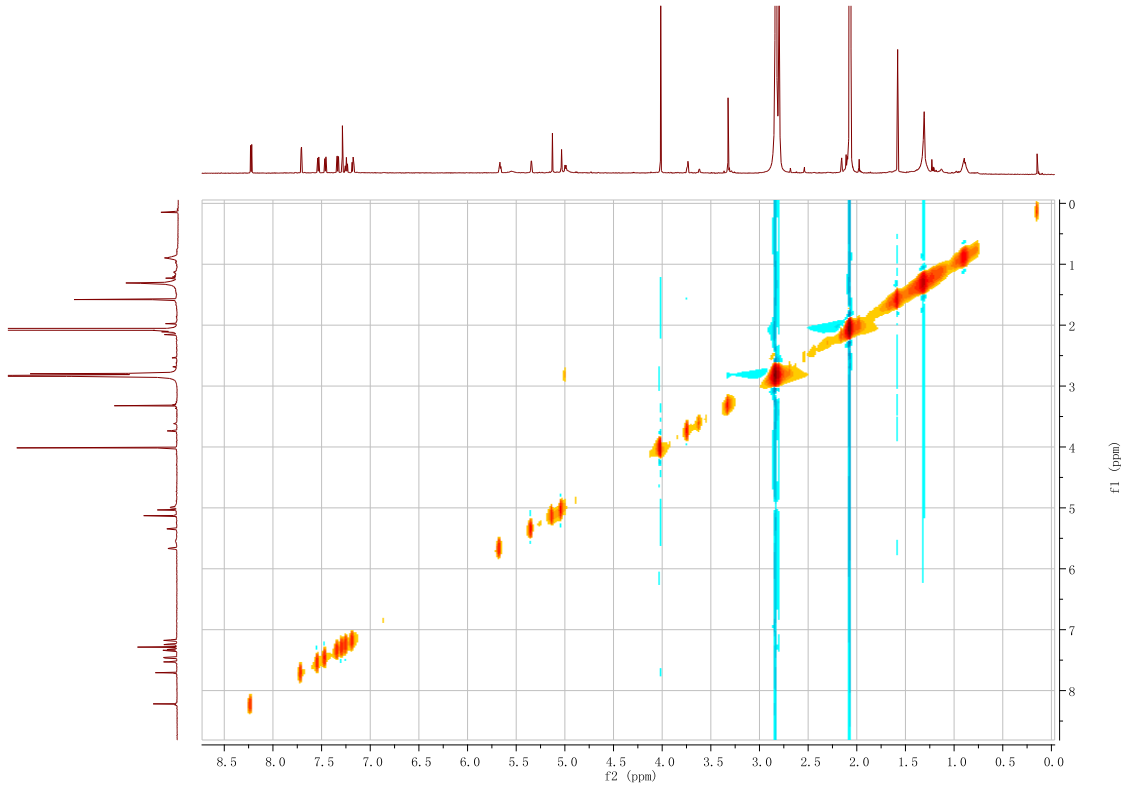

Figure S59. HR-ESI-MS spectrum of TNM B (**12**)

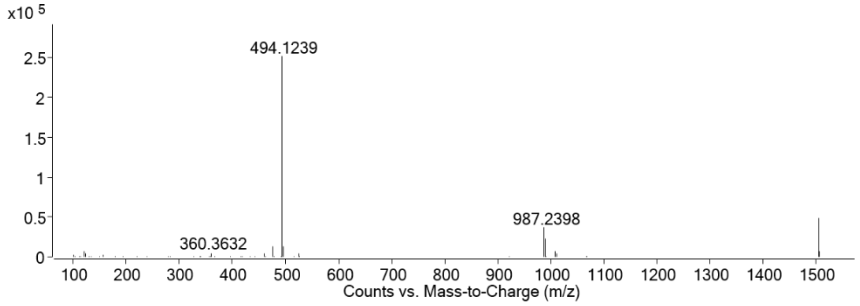

Figure S60. ^{1}H NMR Spectrum of TNM B (**12**) (700 MHz, acetone-d_6)

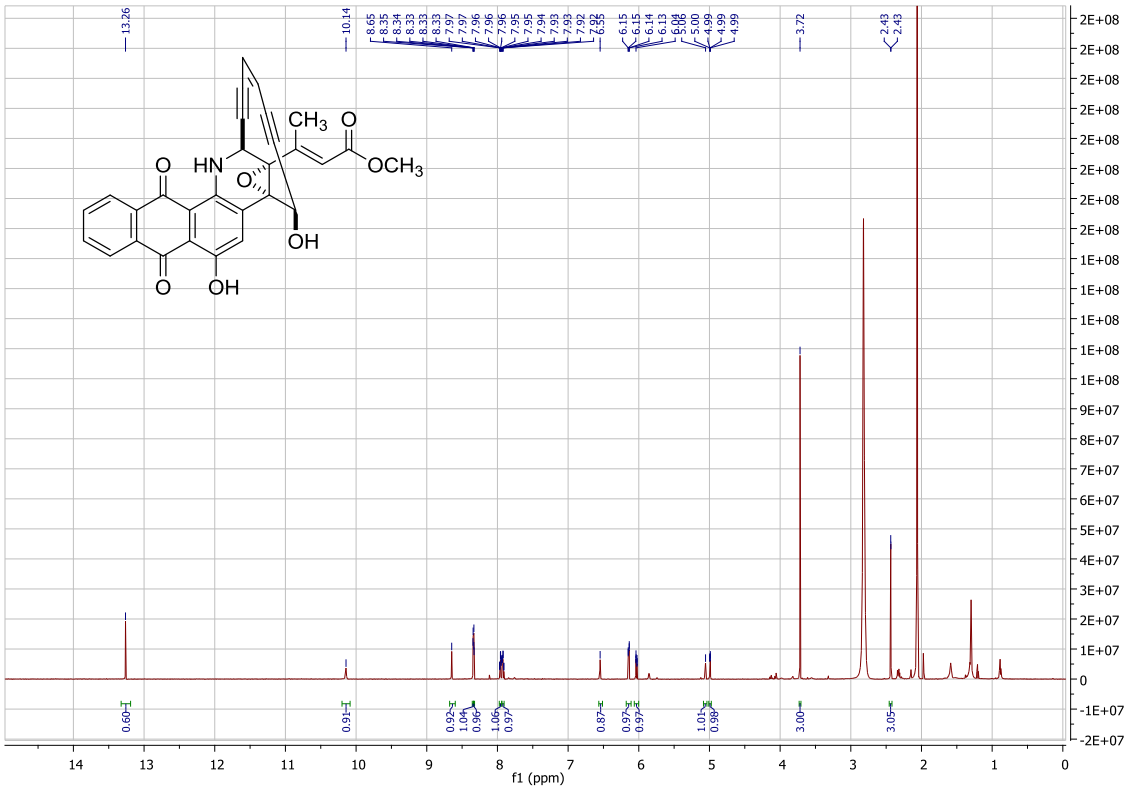

Figure S61. ^{13}C NMR spectrum of TNM B (**12**) (176 MHz, acetone-d_6)

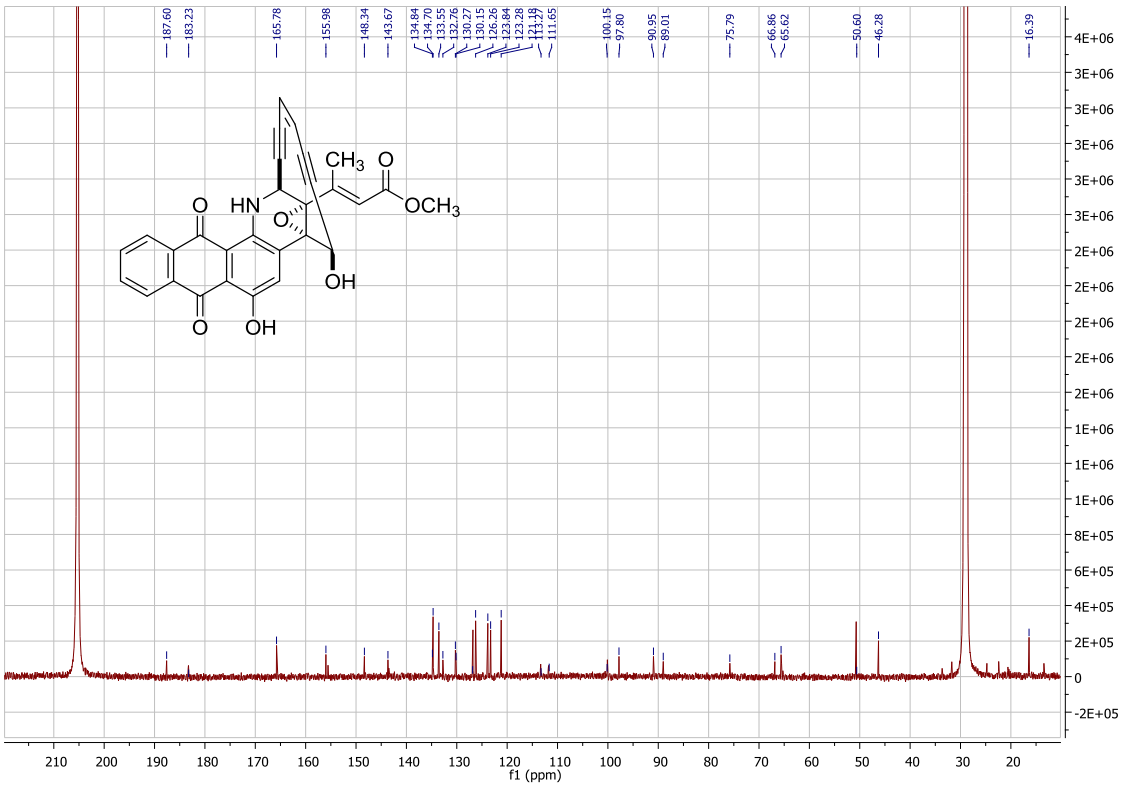

Figure S62. ^{1}H-^{1}H COSY spectrum of TNM B (**12**) (acetone-d_6)

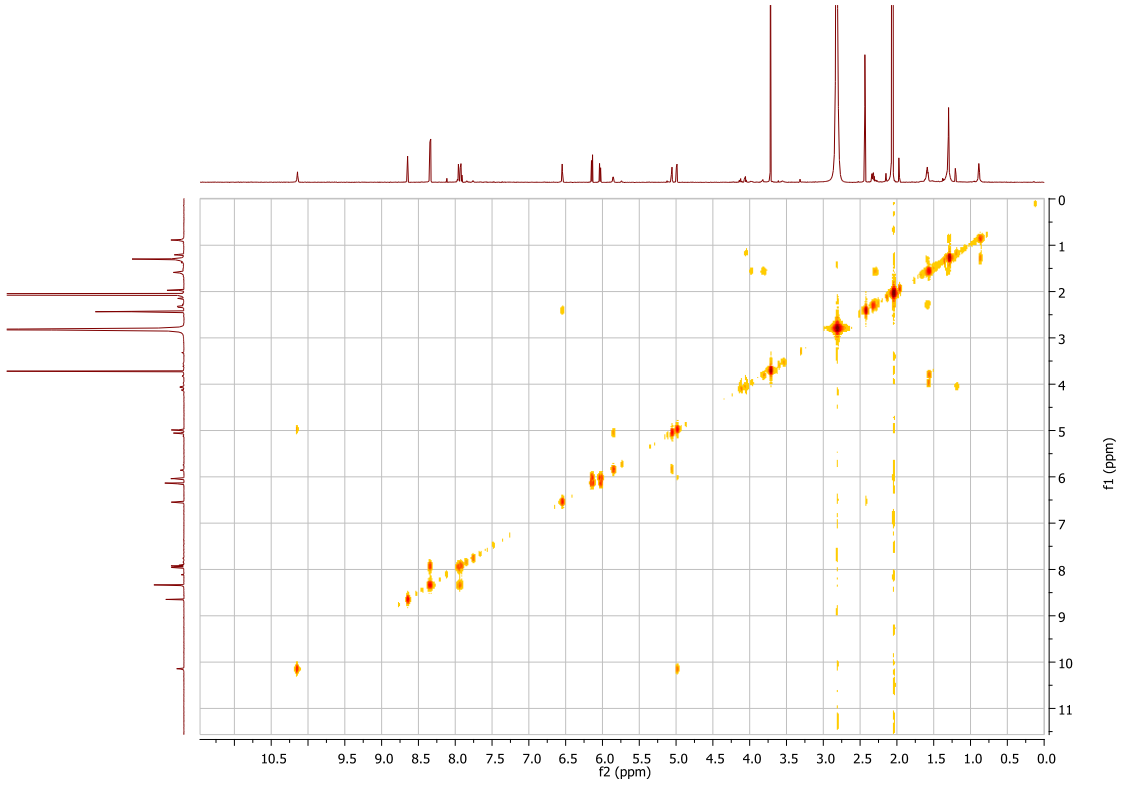

Figure S63. $^{1}H–^{13}C$ HSQC spectrum of TNM B (**12**) (acetone-d_6)

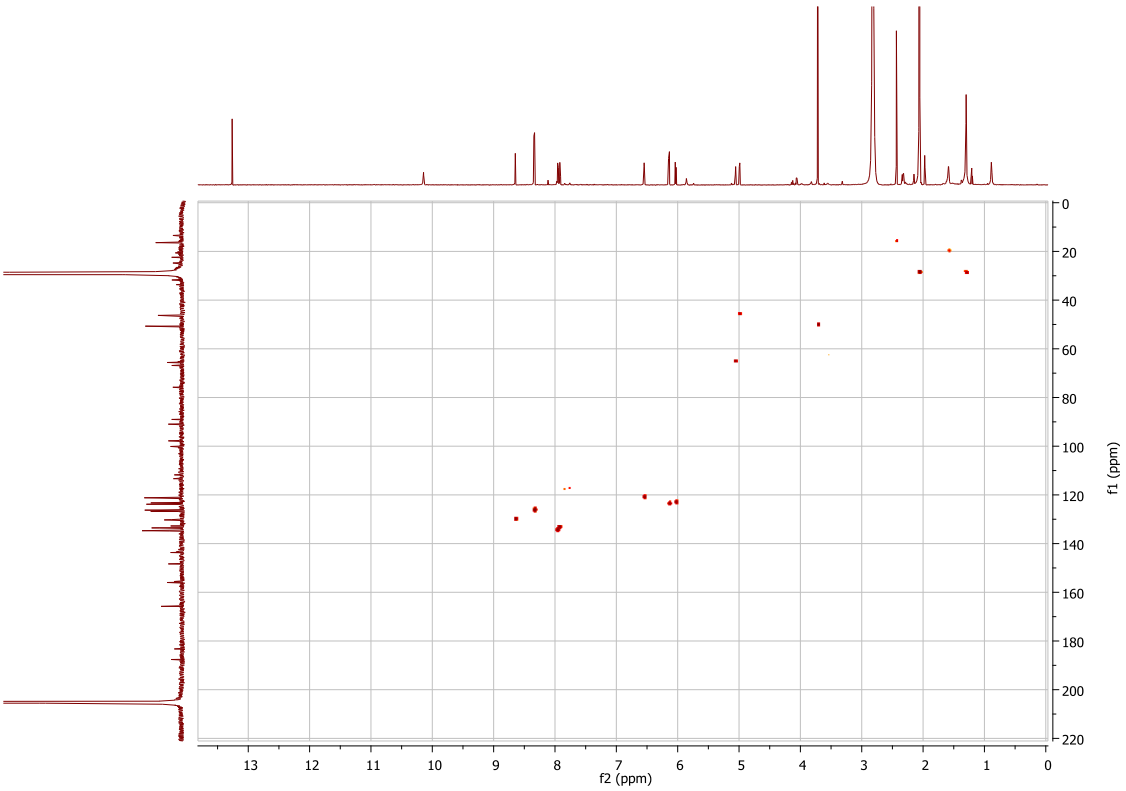

Figure S64. $^{1}H–^{13}C$ HMBC spectrum of TNM B (**12**) (acetone-d_6)

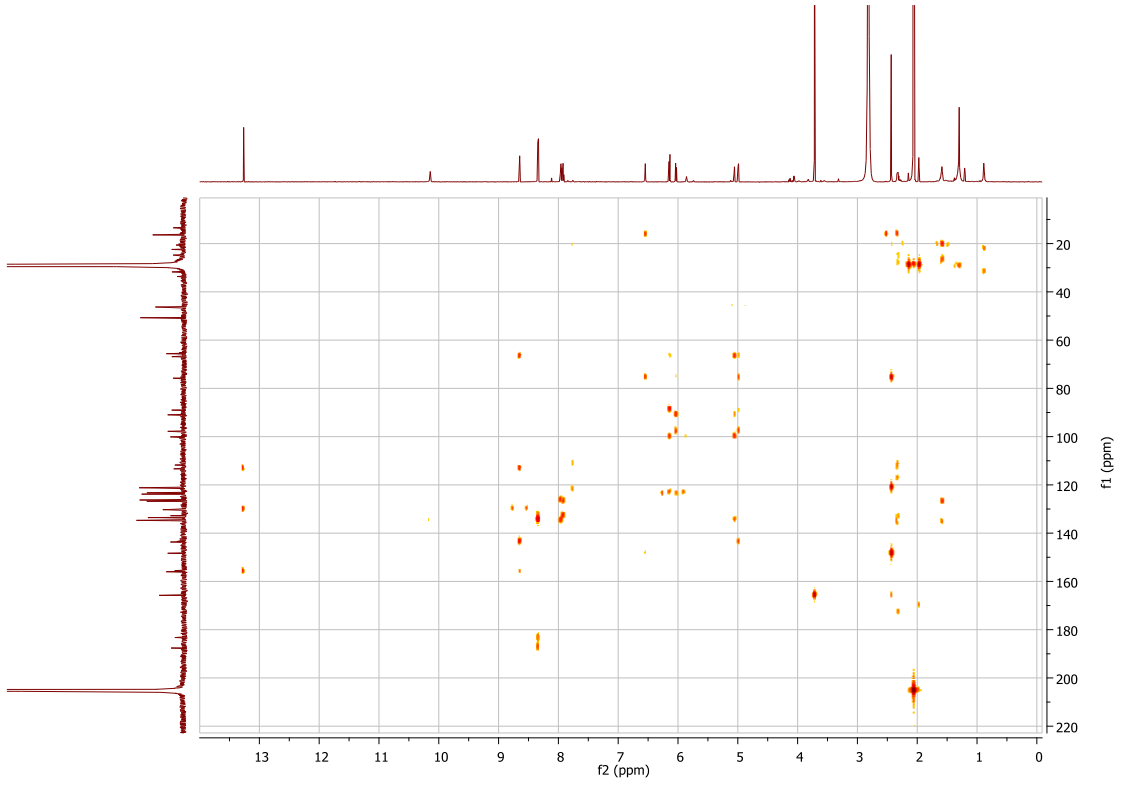

Figure S65. ^{1}H-^{1}H ROESY spectrum of TNM B (**12**) (acetone-d_6)

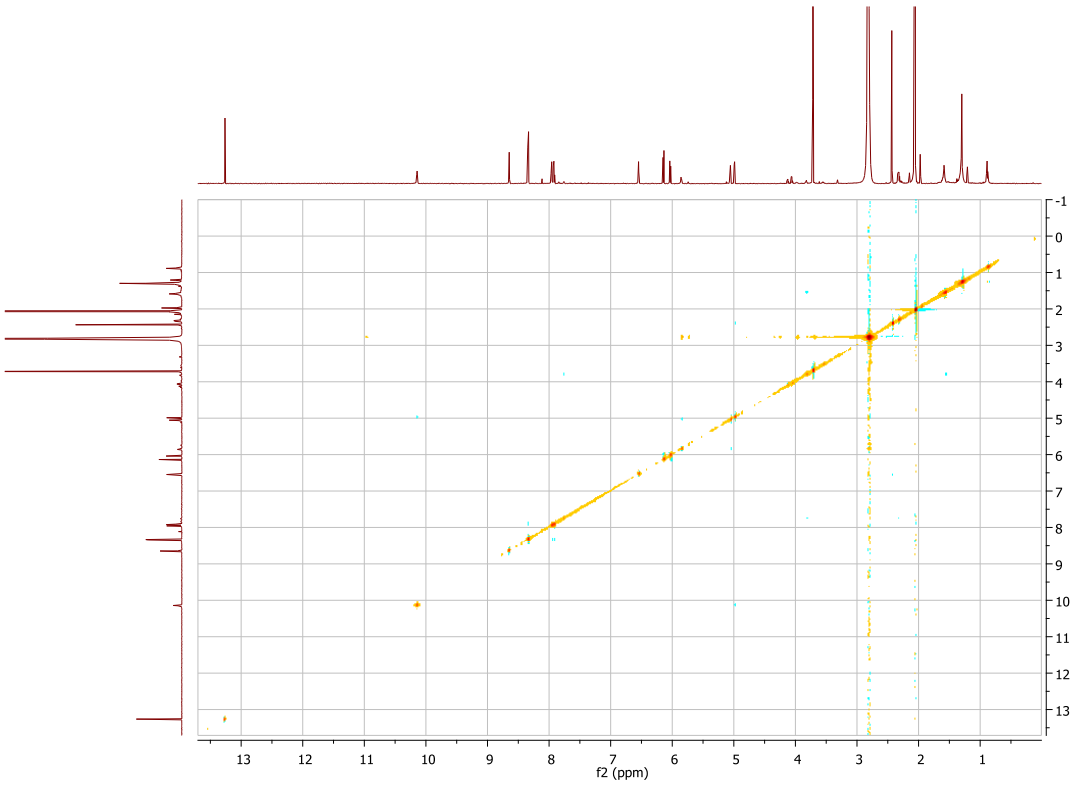

Figure S66. HR-ESI-MS spectrum of TNM E (**13**)

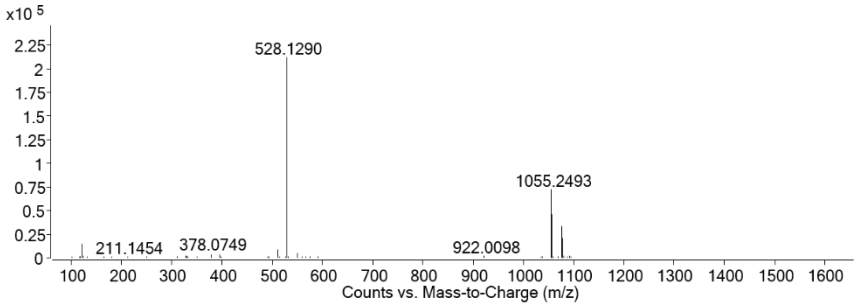

Figure S67. ^{1}H NMR Spectrum of TNM E (**13**) (700 MHz, acetone-d_6)

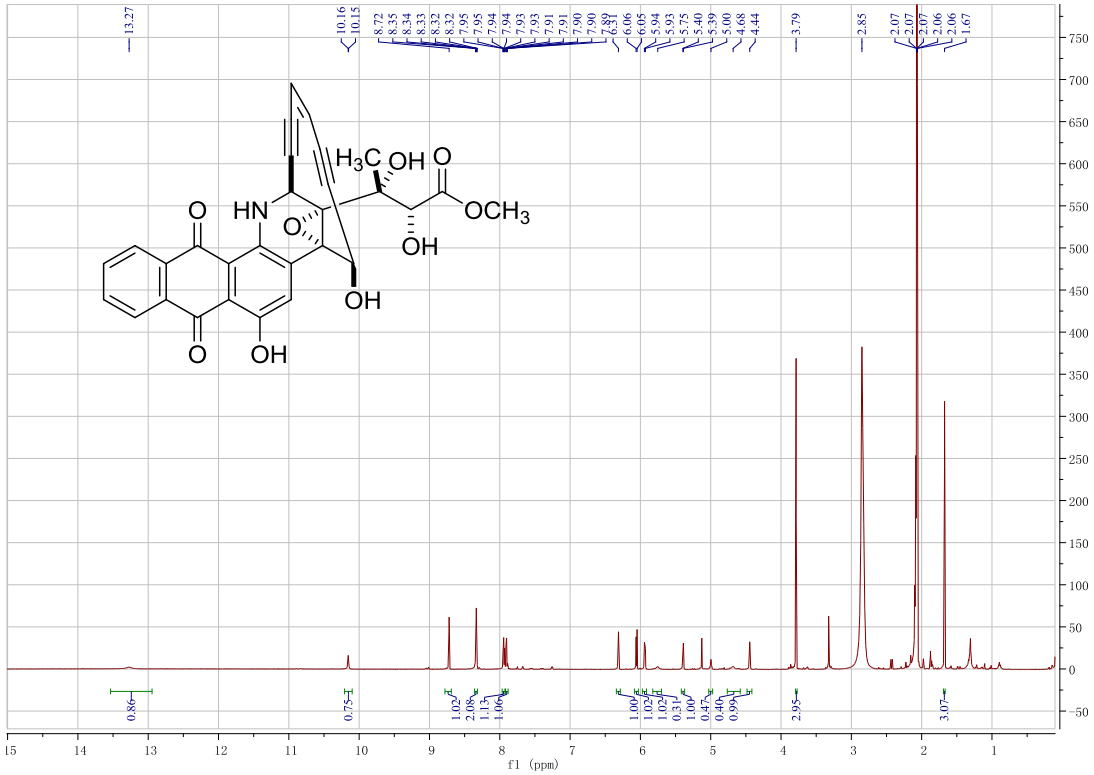

Figure S68. ^{13}C NMR spectrum of TNM E (**13**) (176 MHz, acetone-d_6)

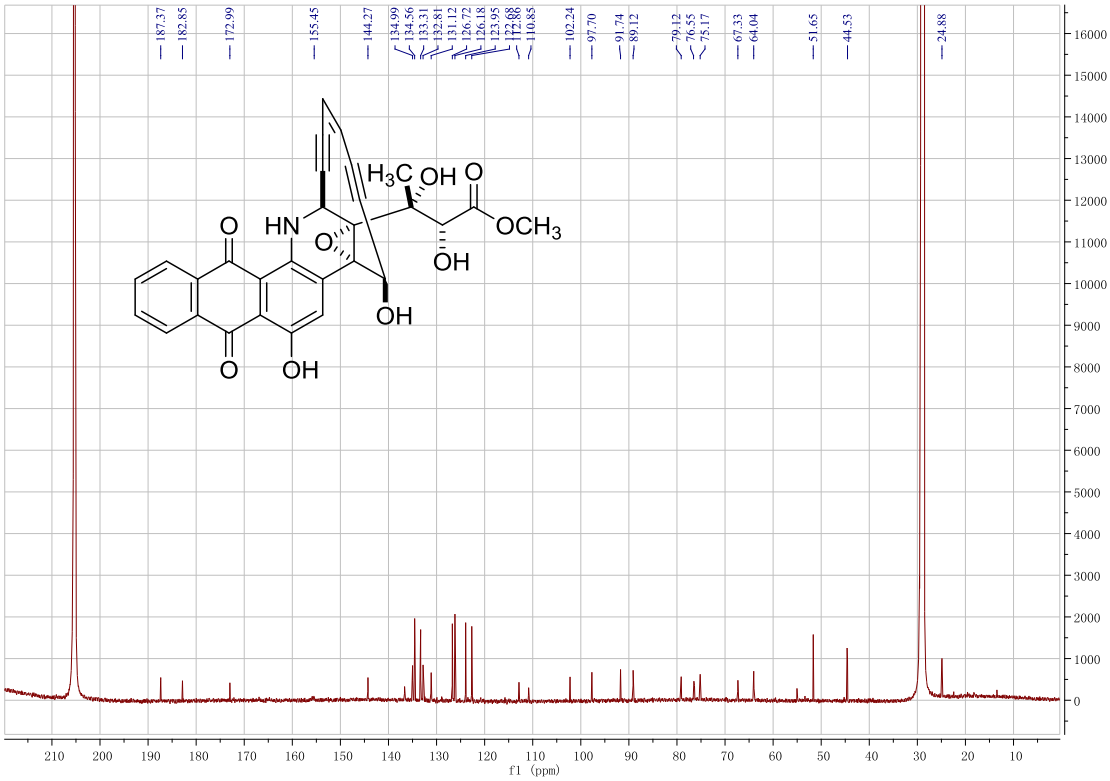

Figure S69. ^{1}H-^{1}H COSY spectrum of TNM E (**13**) (acetone-d_6)

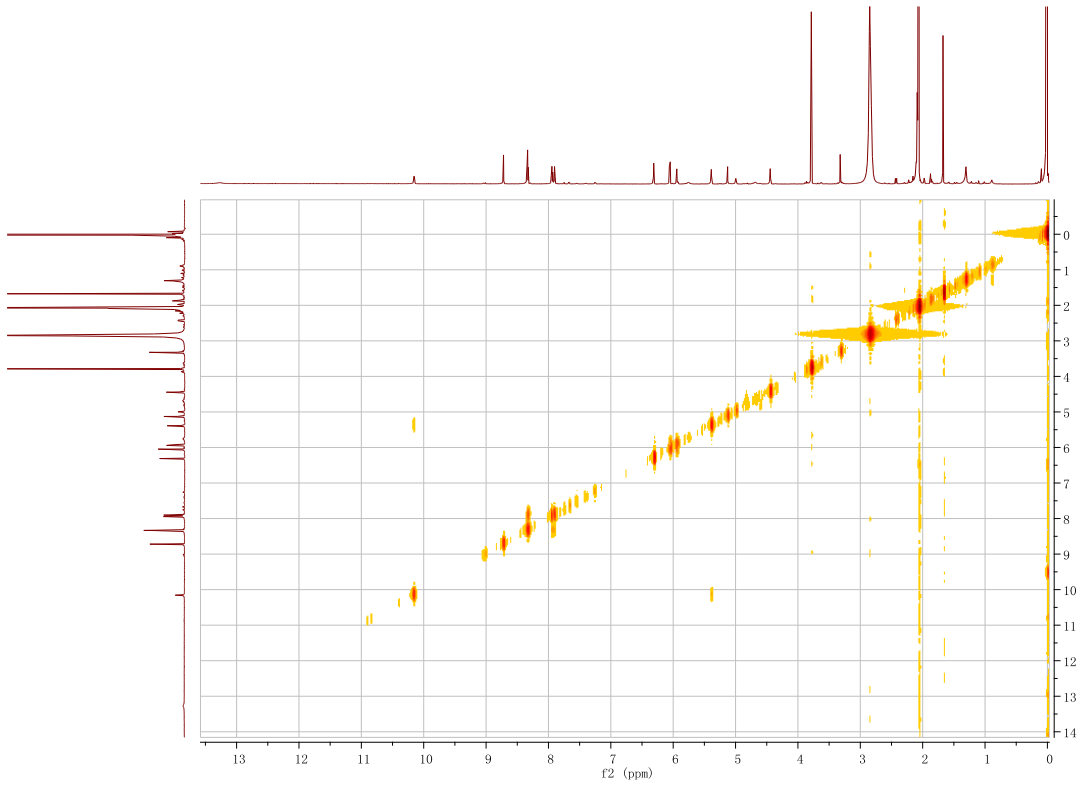

Figure S70. ^{1}H–^{13}C HSQC spectrum of TNM E (**13**) (acetone-d_6)

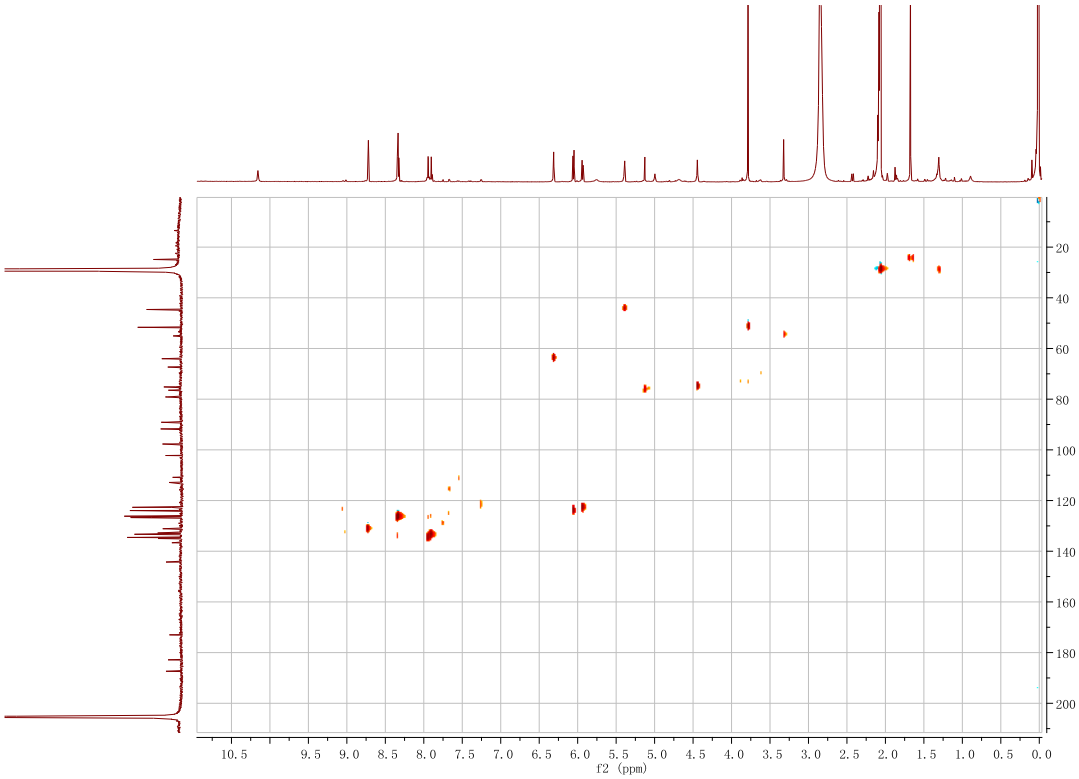

Figure S71. ^{1}H–^{13}C HMBC spectrum of TNM E (**13**) (acetone-d_6)

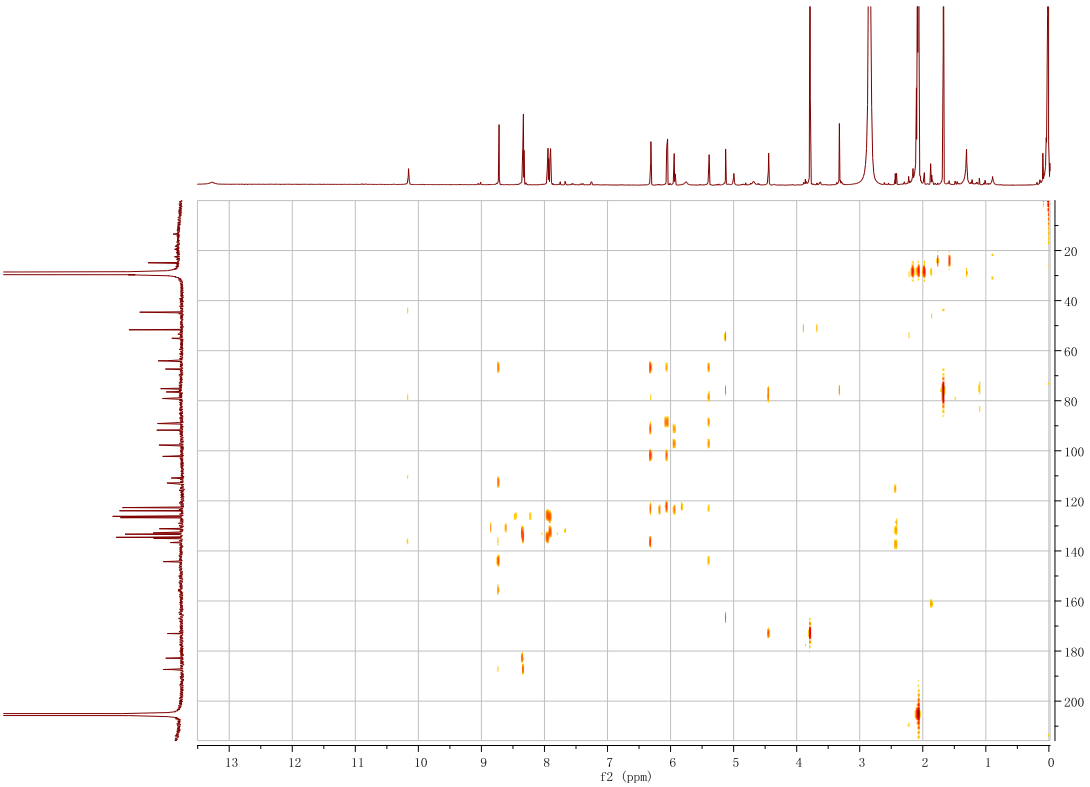

Figure S72. ^{1}H-^{1}H ROESY spectrum of TNM E (**13**) (acetone-d_6)

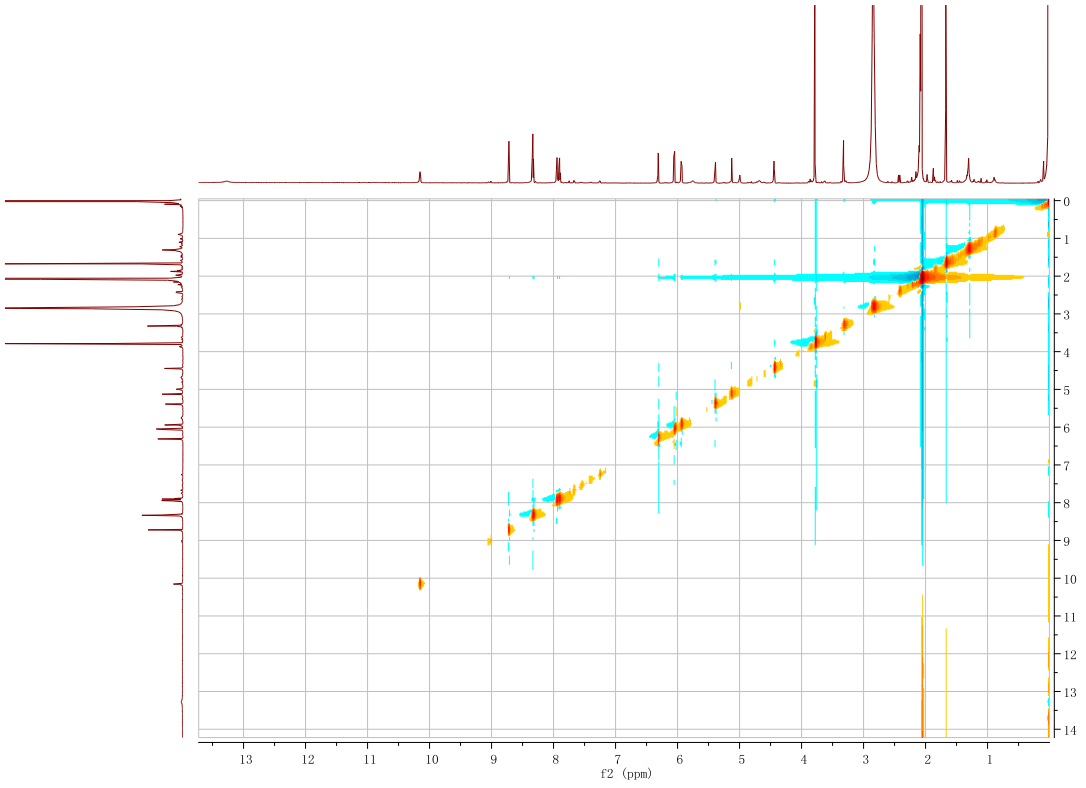

Figure S73. HR-ESI-MS spectrum of **14**

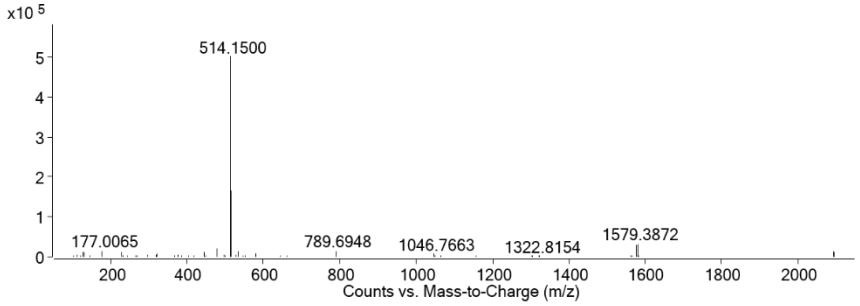

Figure S74. ^{1}H NMR Spectrum of **14** (700 MHz, acetone-d_6)

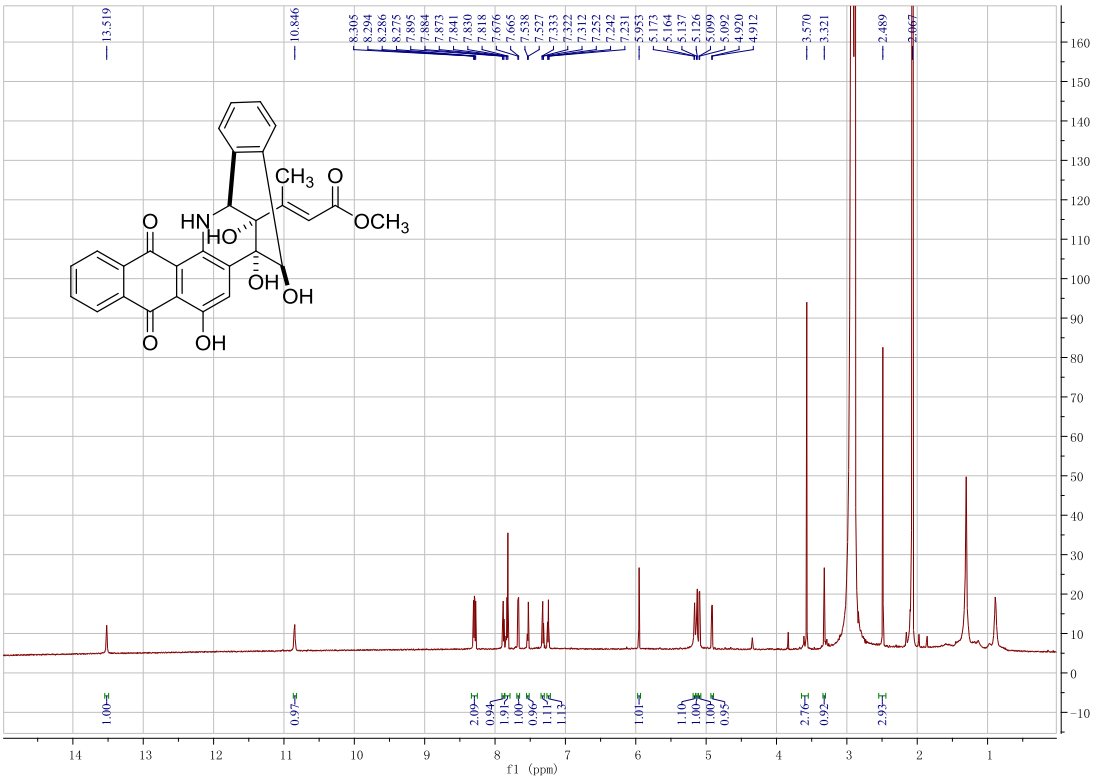

Figure S75. ^{13}C NMR spectrum of **14** (176 MHz, acetone-d_6)

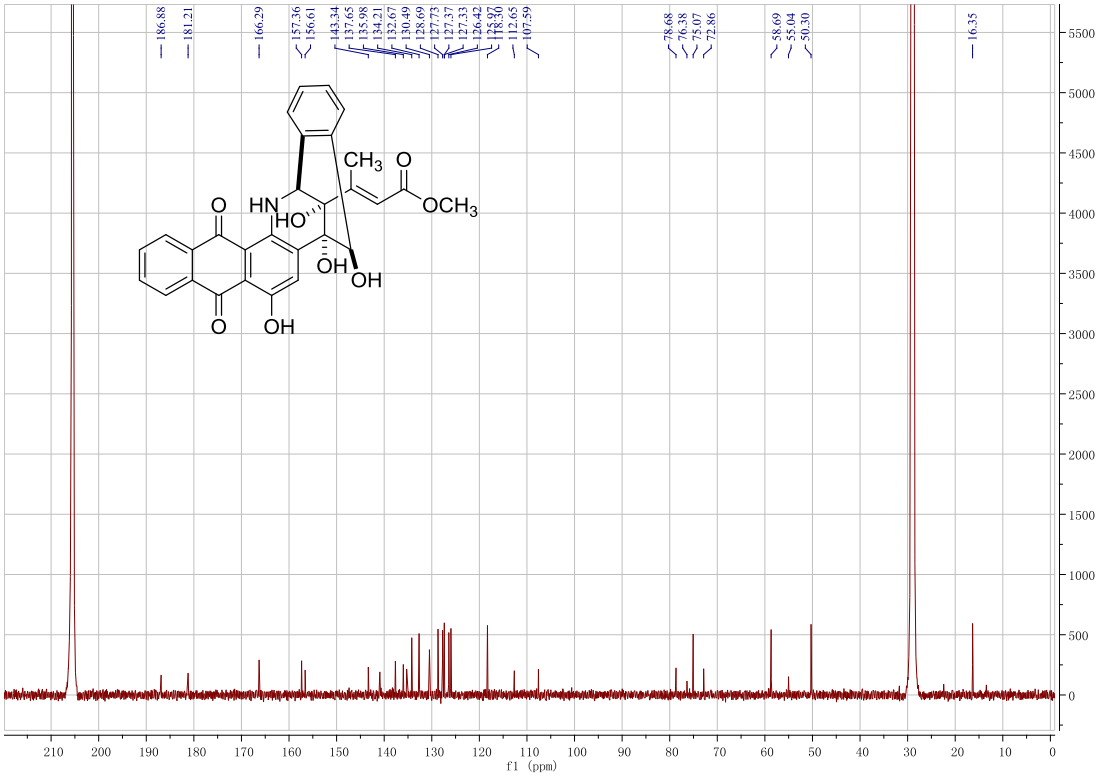

Figure S76. ^{1}H-^{1}H COSY spectrum of **14** (acetone-d_6)

Figure S77. $^{1}H–^{13}C$ HSQC spectrum of **14** (acetone-d_6)

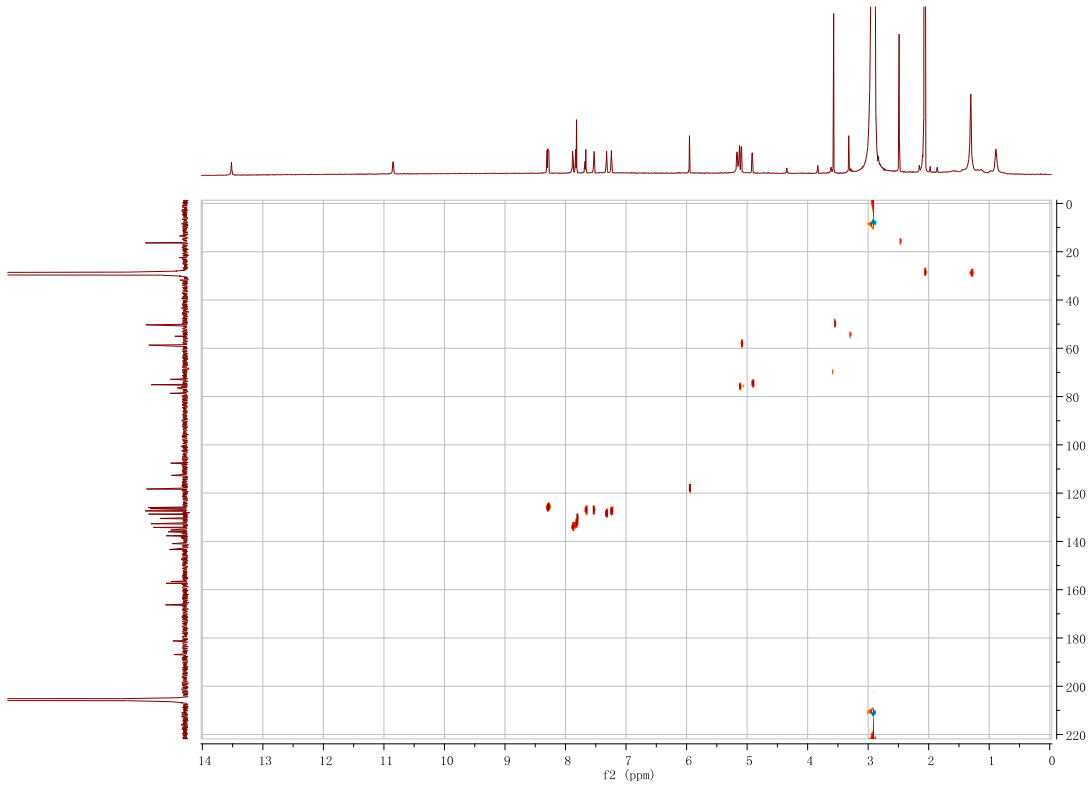

Figure S78. $^{1}H–^{13}C$ HMBC spectrum of **14** (acetone-d_6)

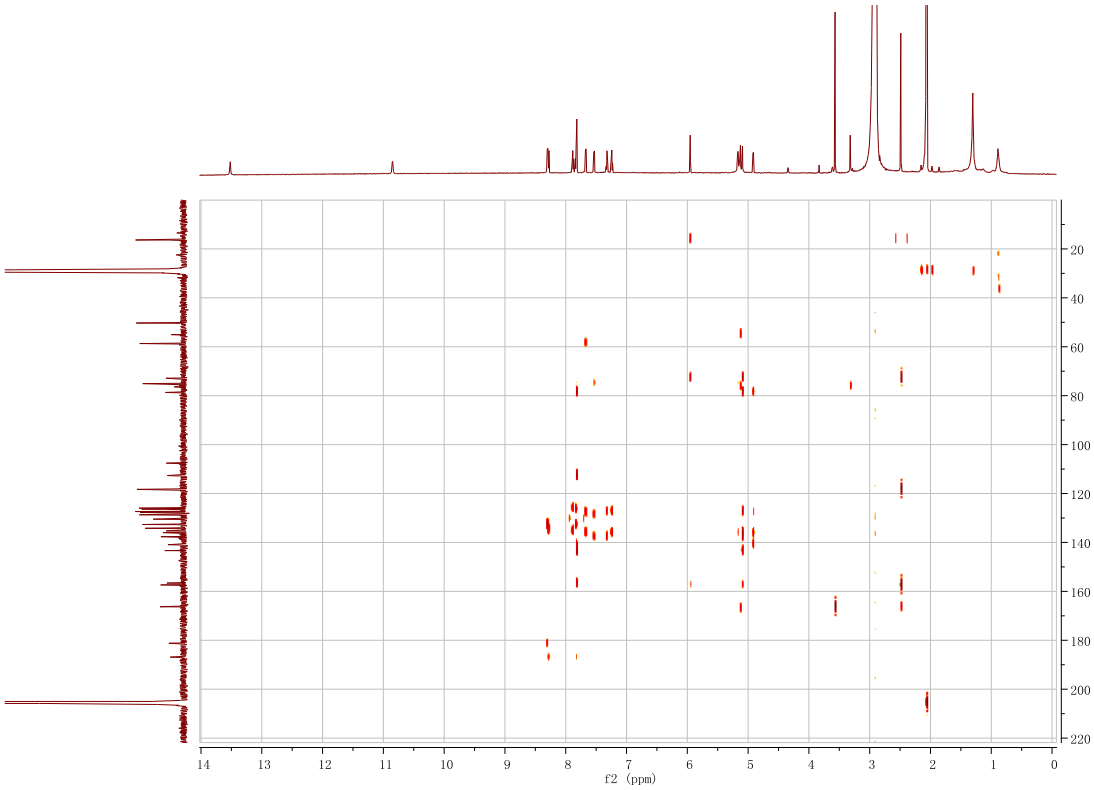

Figure S79. ^{1}H-^{1}H ROESY spectrum of **14** (acetone-d_6)

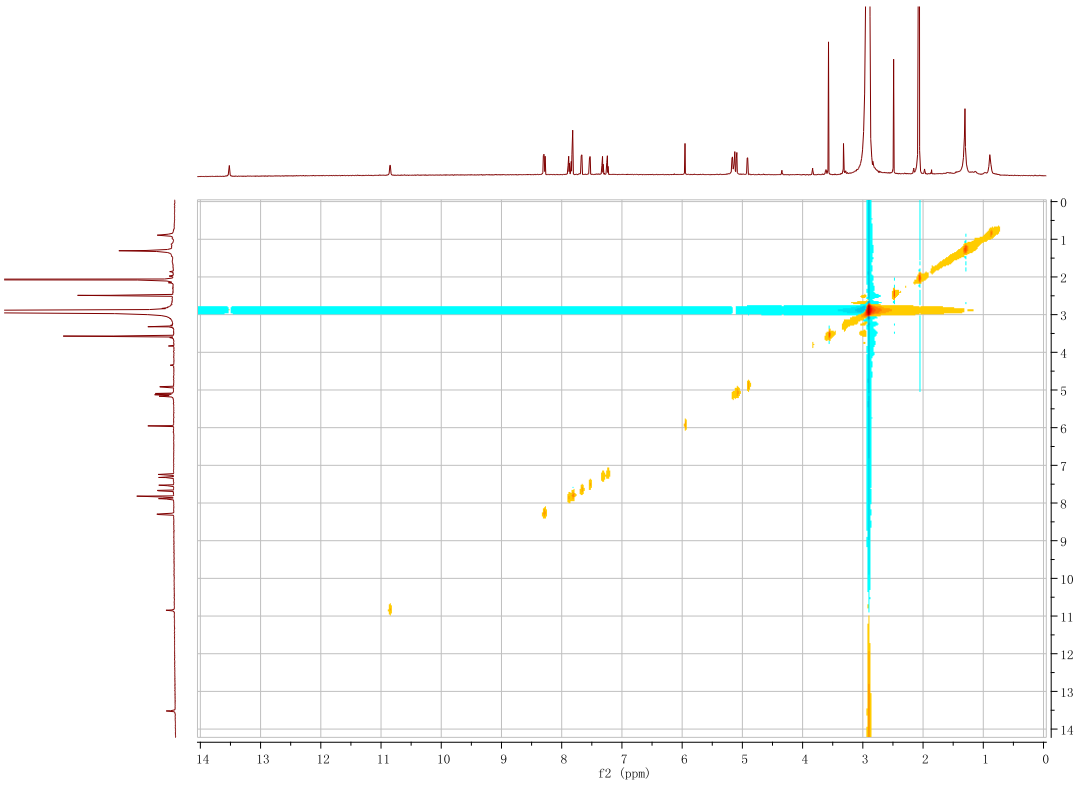

Figure S80. HR-ESI-MS spectrum of **15**

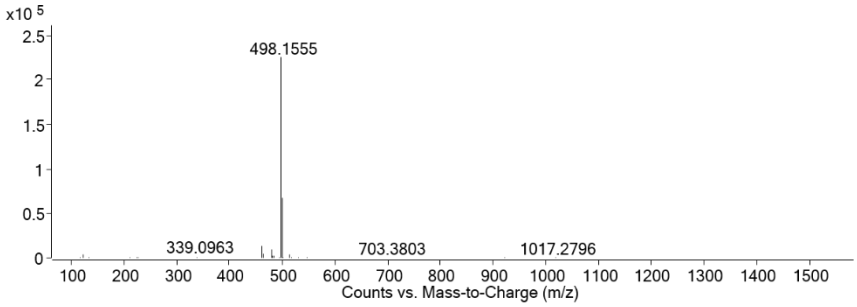

Figure S81. ^{1}H NMR Spectrum of **15** (700 MHz, acetone-d_6)

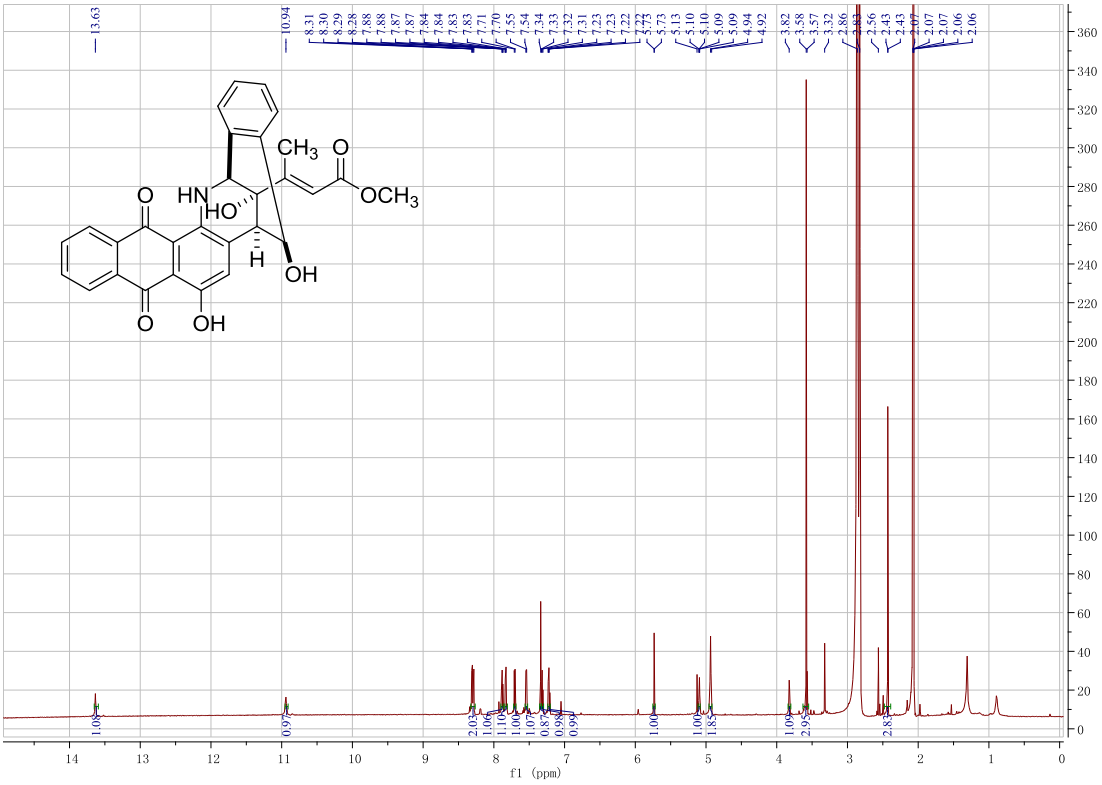

Figure S82. ^{13}C NMR spectrum of **15** (176 MHz, acetone-d_6)

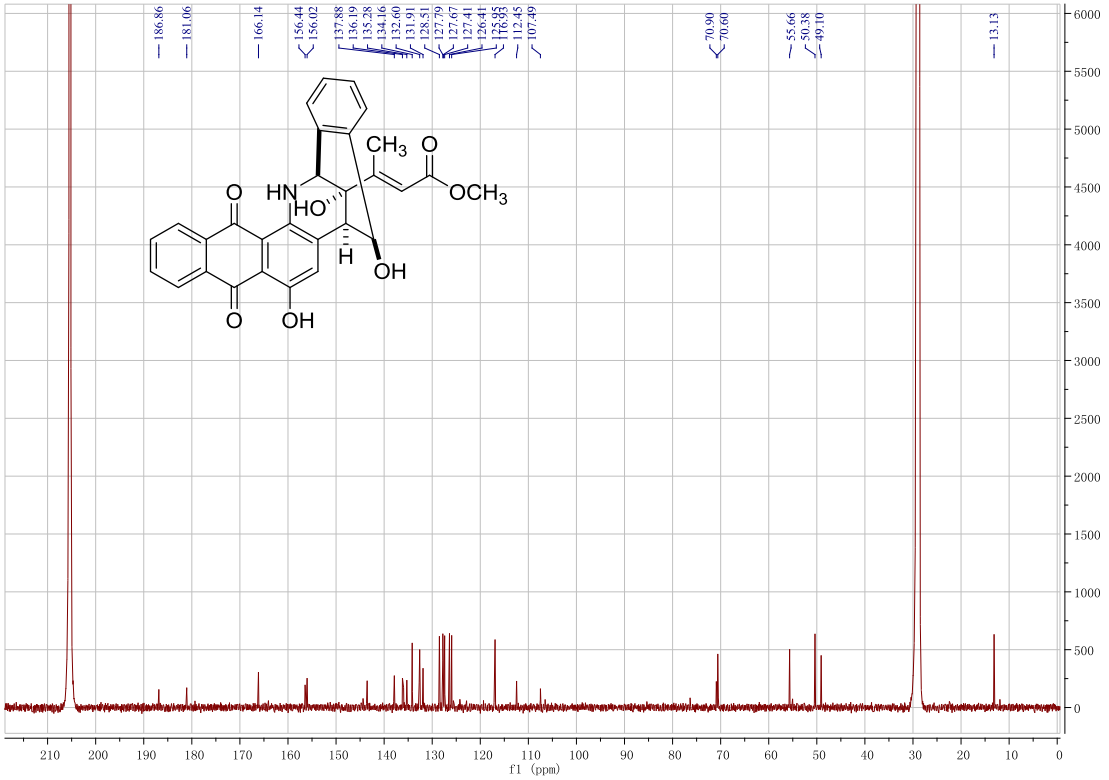

Figure S83. ^{1}H-^{1}H COSY spectrum of **15** (acetone-d_6)

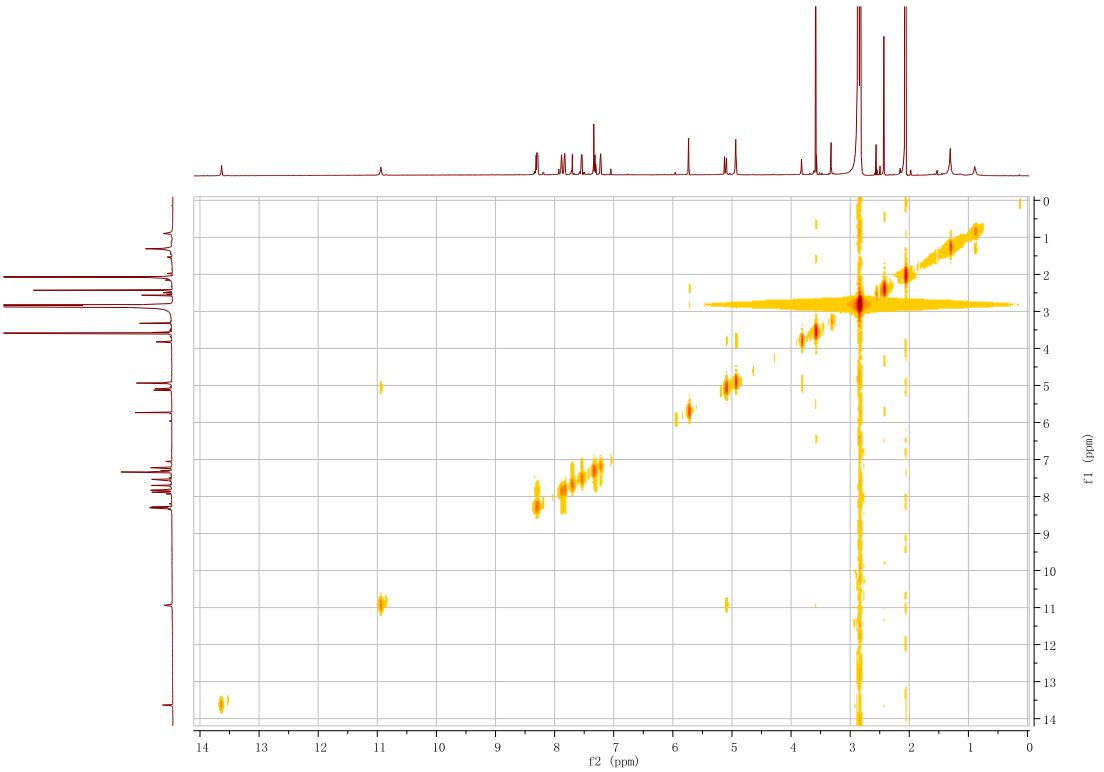

Figure S84. ^{1}H–^{13}C HSQC spectrum of **15** (acetone-d_6)

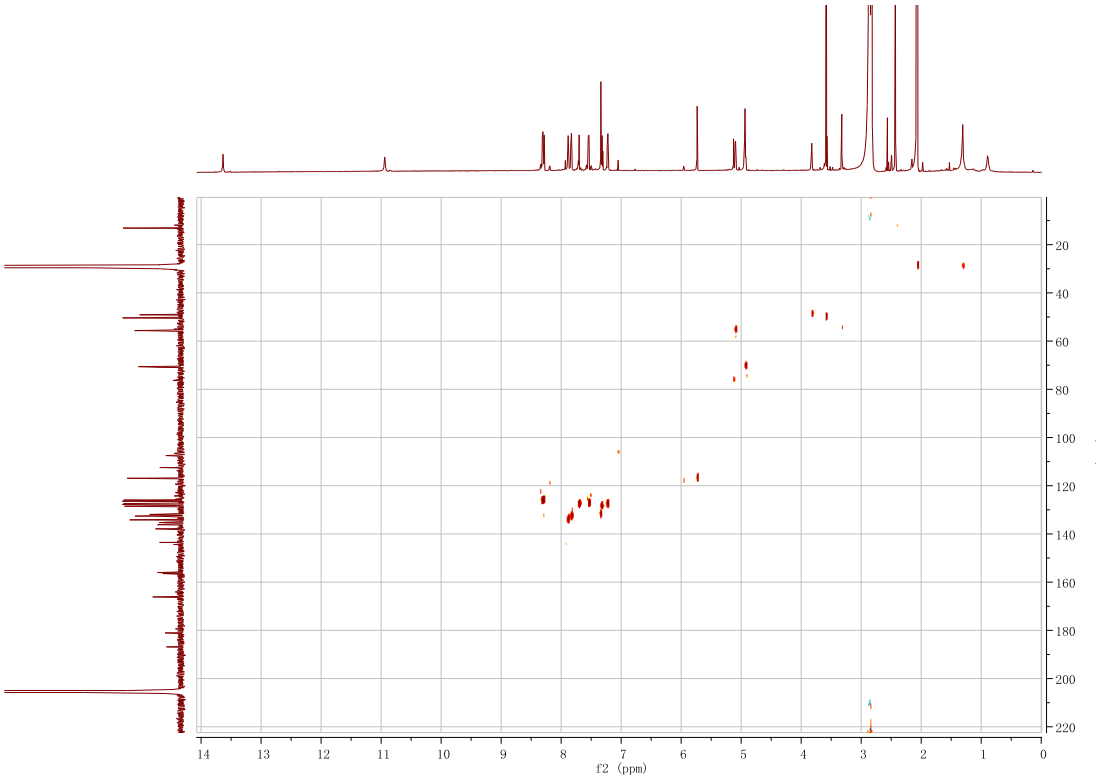

Figure S85. $^{1}H–^{13}C$ HMBC spectrum of **15** (acetone-d_6)

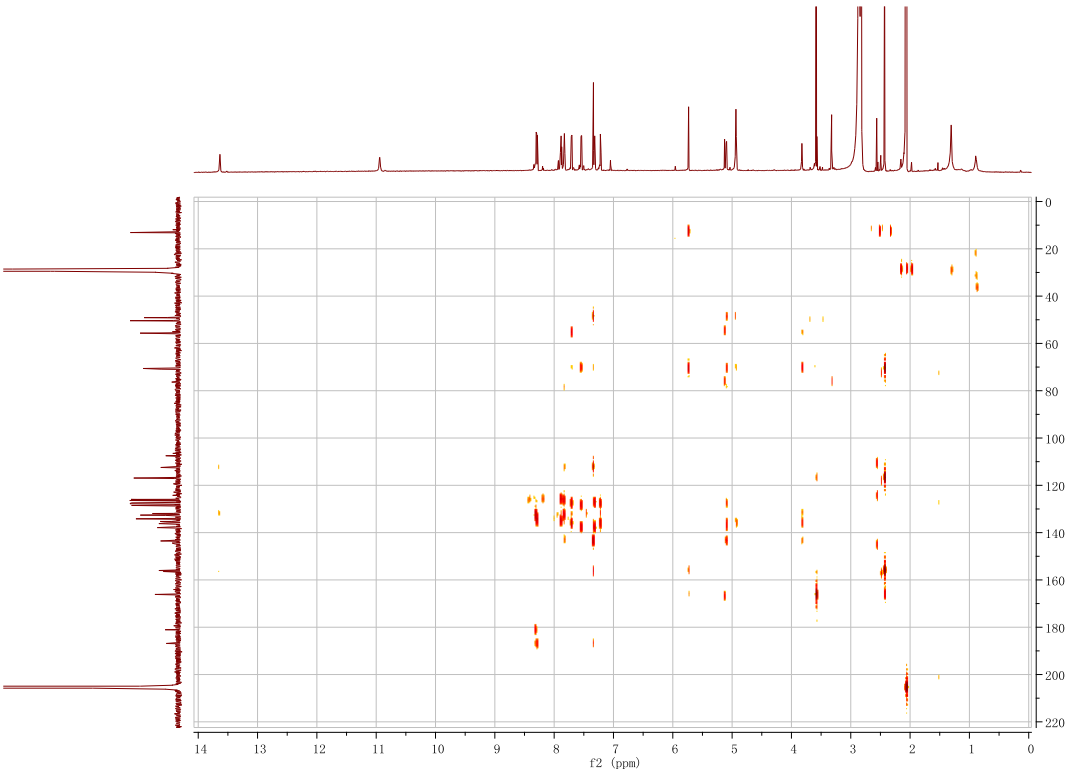

Figure S86. ^{1}H-^{1}H ROESY spectrum of **15** (acetone-d_6)

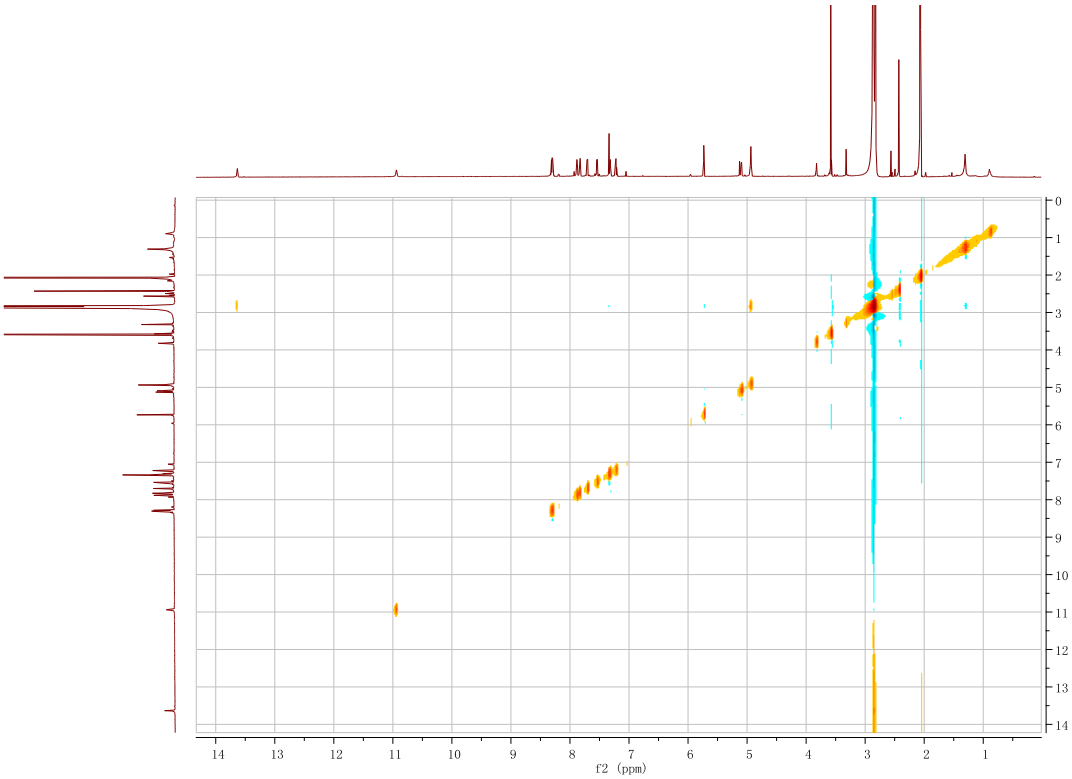

Figure S87. HR-ESI-MS spectrum of **16**

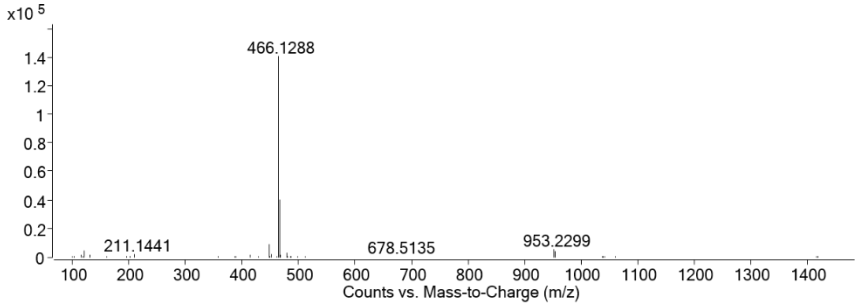

Figure S88. ^{1}H NMR Spectrum of **16** (700 MHz, acetone-d_6)

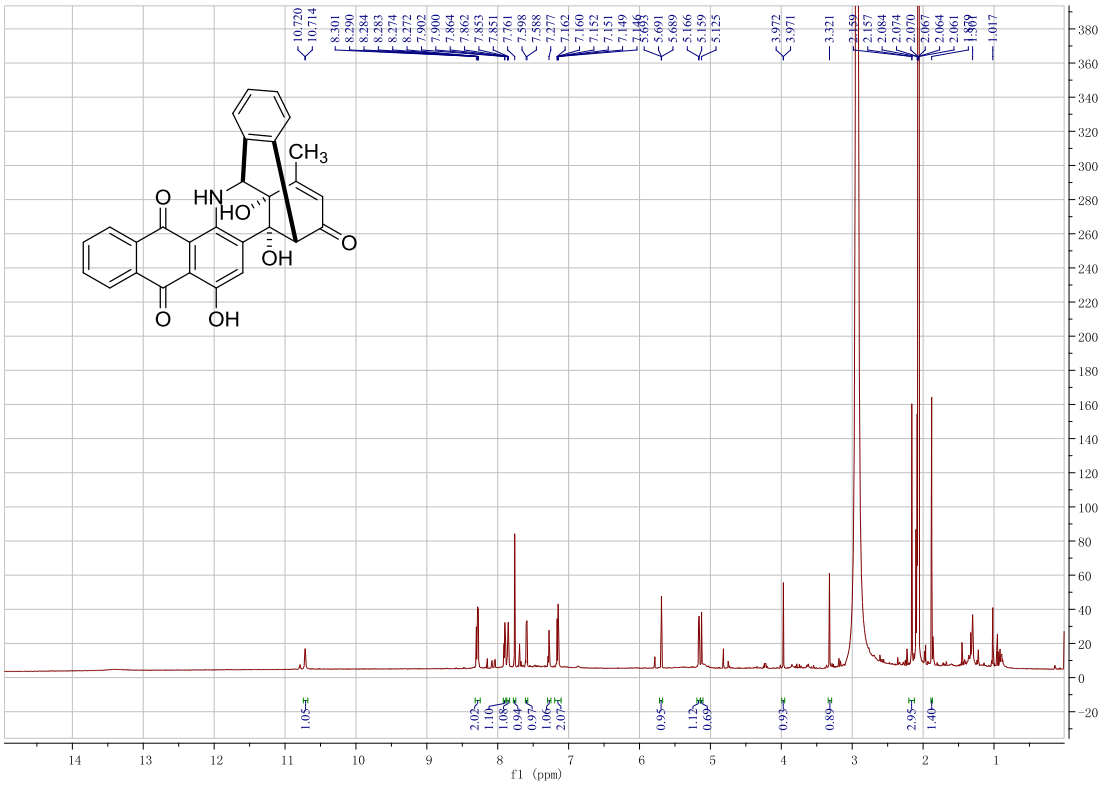

Figure S89. ^{13}C NMR spectrum of **16** (176 MHz, acetone-d_6)

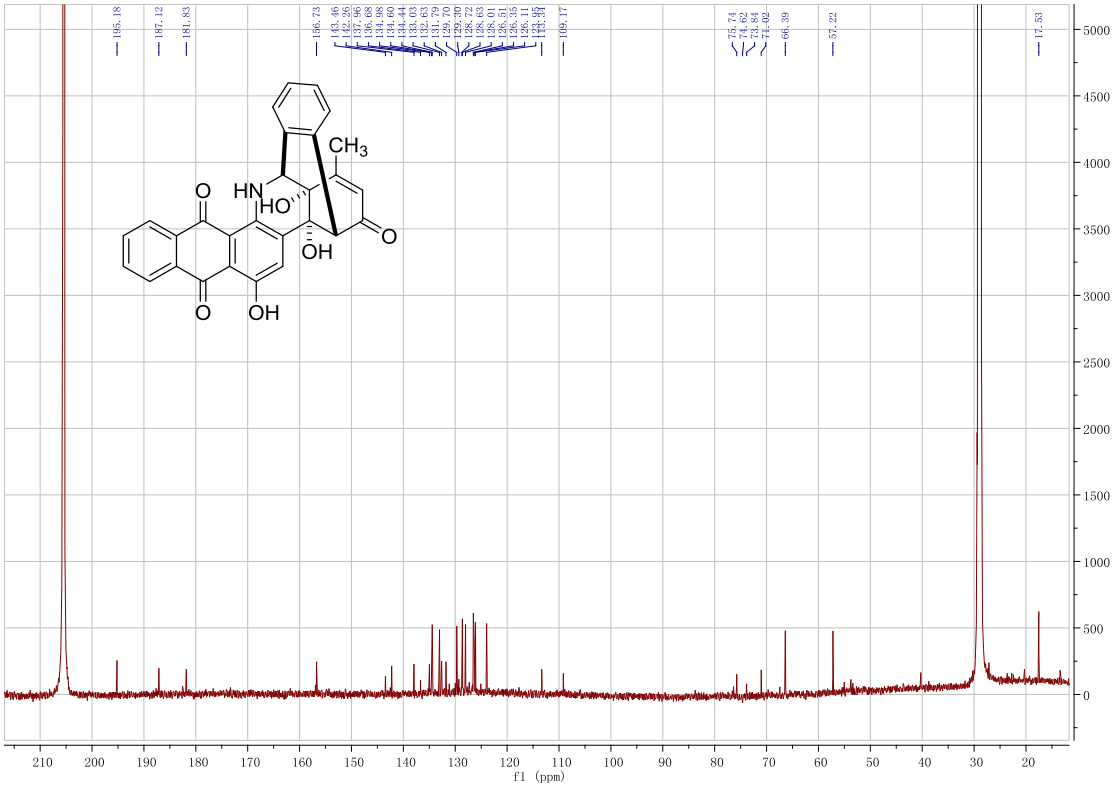

Figure S90. ^{1}H-^{1}H COSY spectrum of **16** (acetone-d_6)

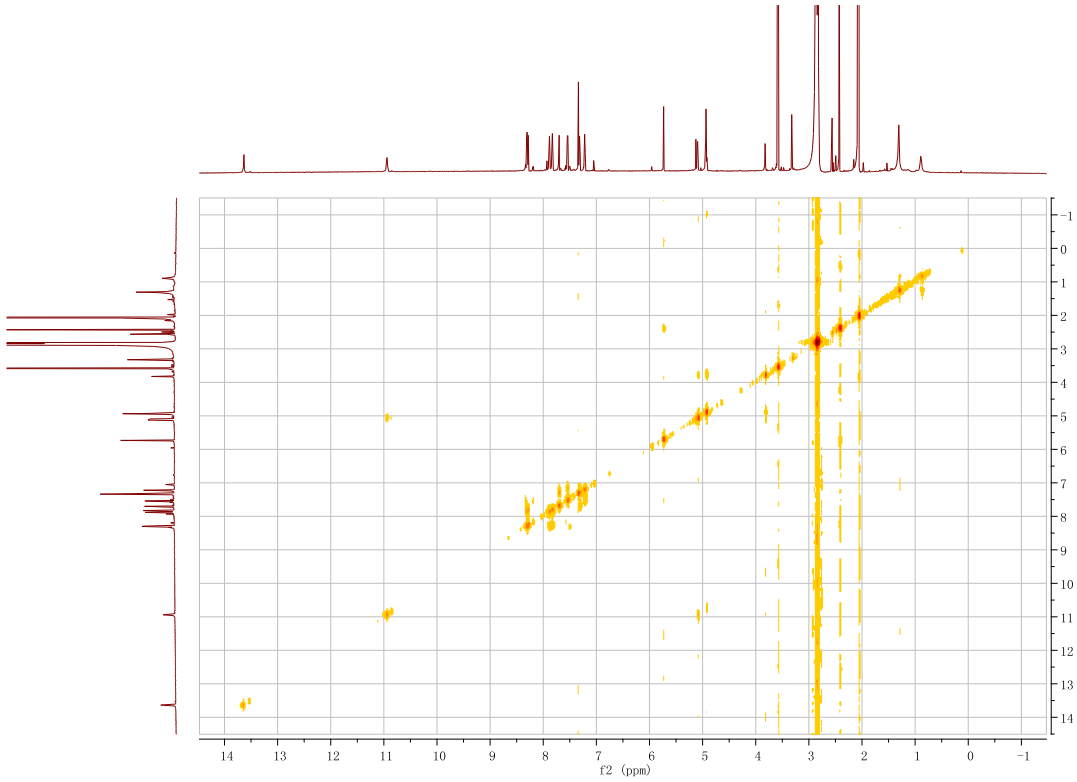

Figure S91. $^{1}H–^{13}C$ HSQC spectrum of **16** (acetone-d_6)

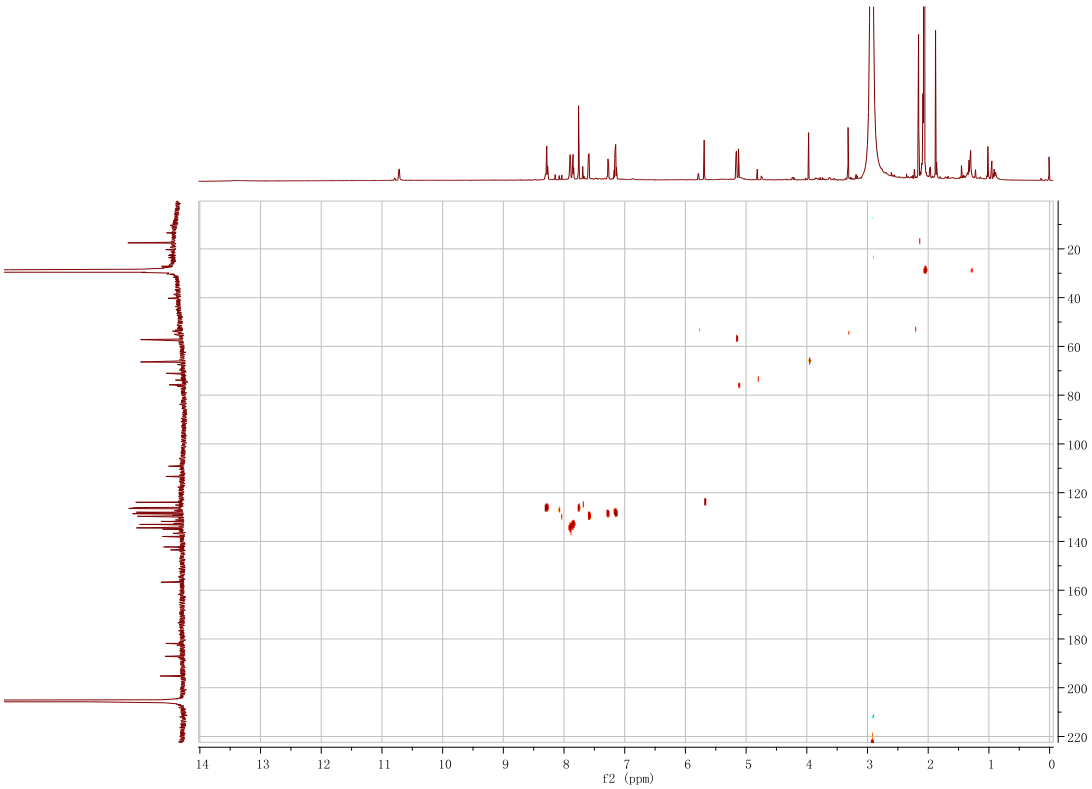

Figure S92. $^{1}H–^{13}C$ HMBC spectrum of **16** (acetone-d_6)

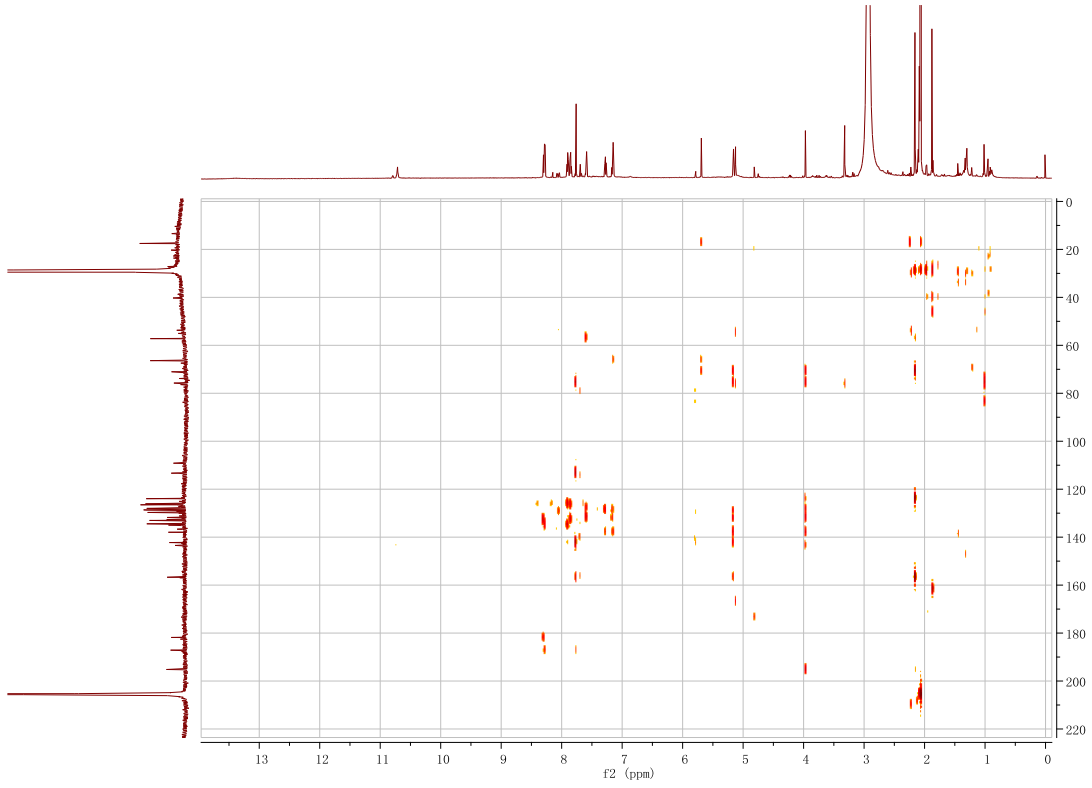

Figure S93. ^{1}H-^{1}H ROESY spectrum of **16** (acetone-d_6)

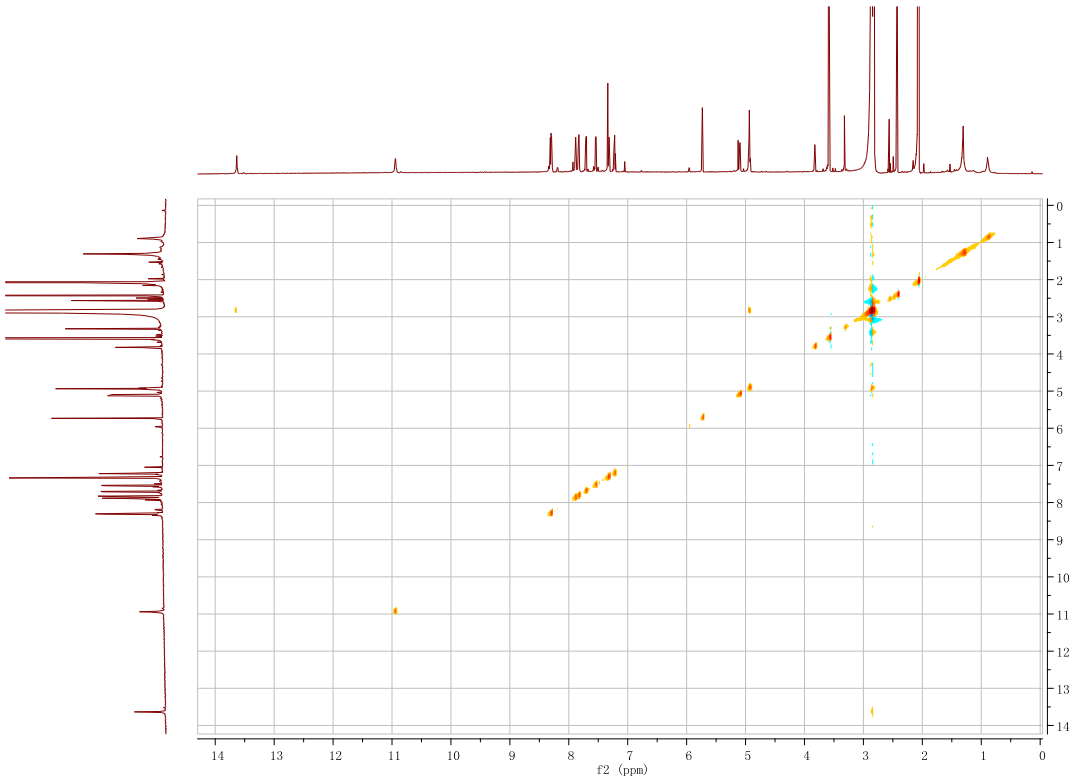

Figure S94. HR-ESI-MS spectrum of **17**

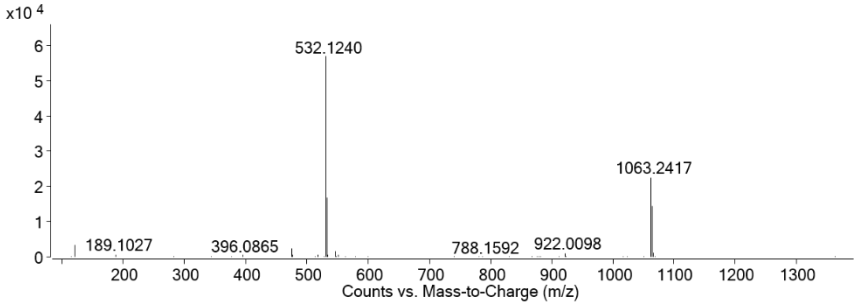

Figure S95. ^{1}H NMR Spectrum of **17** (700 MHz, acetone-d_6)

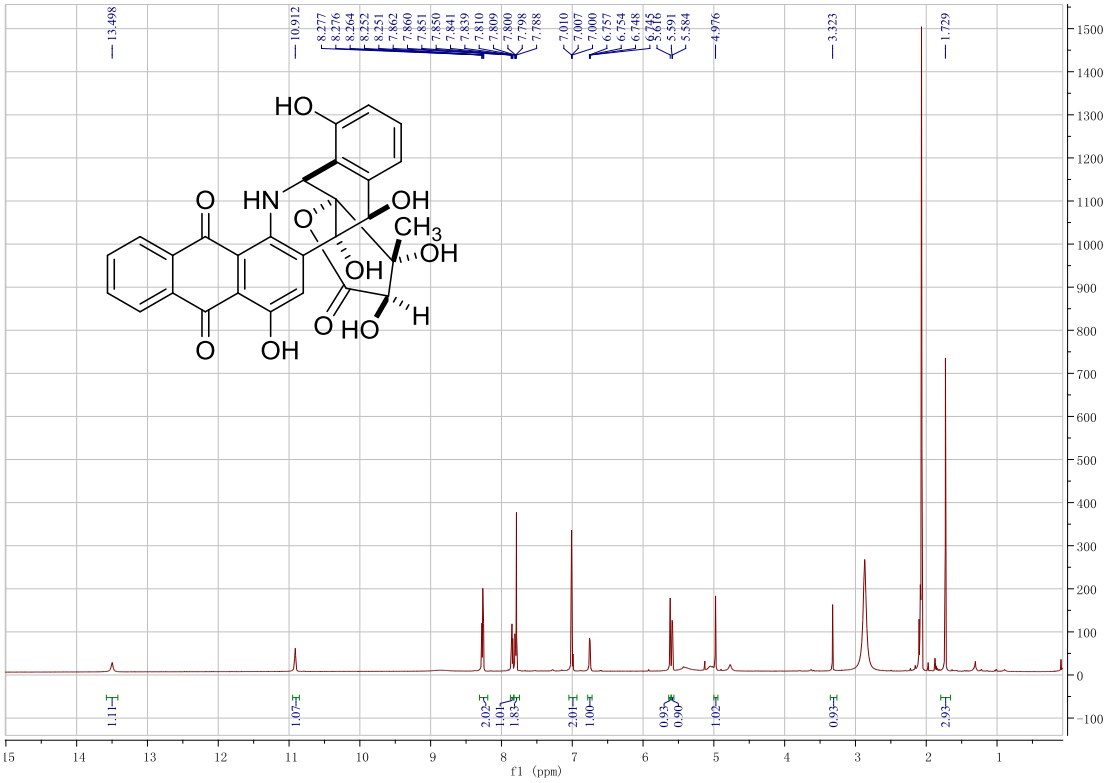

Figure S96. ^{13}C NMR spectrum of **17** (176 MHz, acetone-d_6)

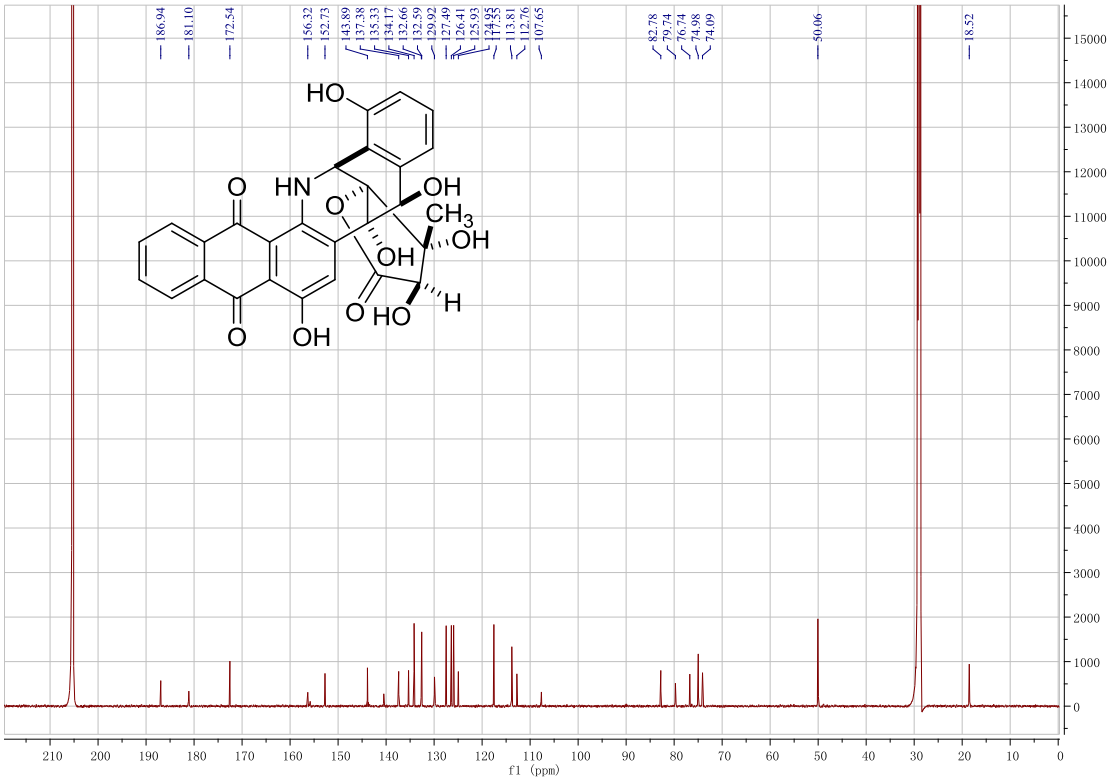

Figure S97. ^{1}H-^{1}H COSY spectrum of **17** (acetone-d_6)

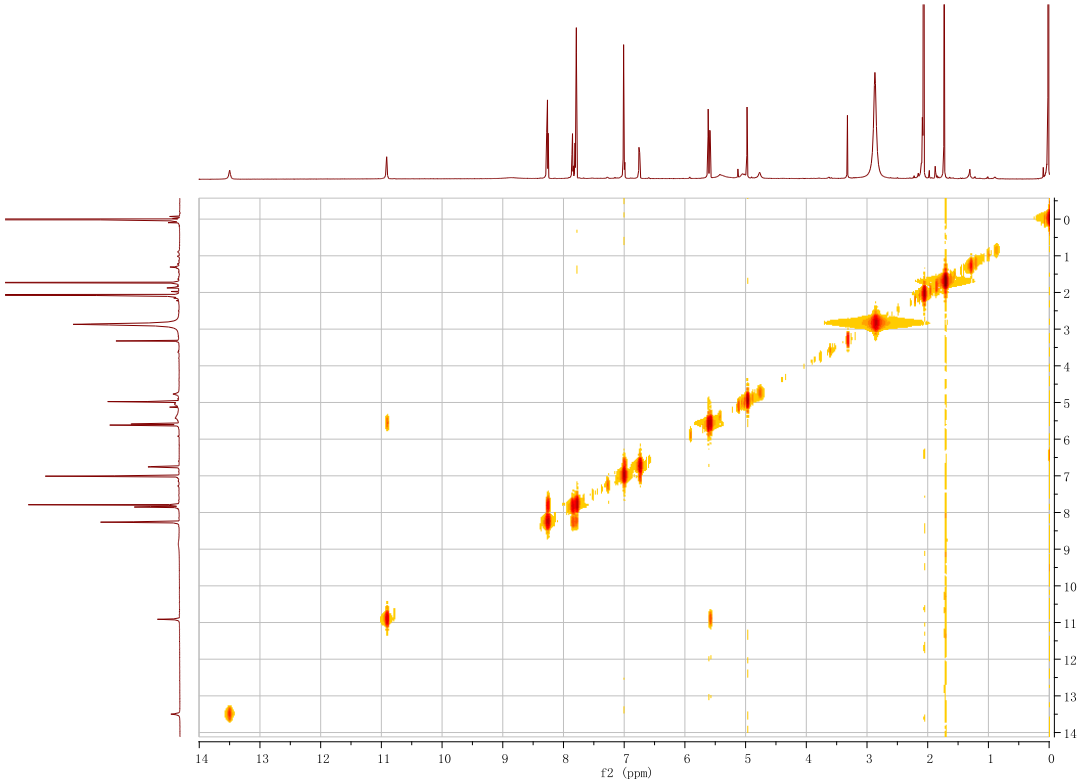

Figure S98. ^{1}H–^{13}C HSQC spectrum of **17** (acetone-d_6)

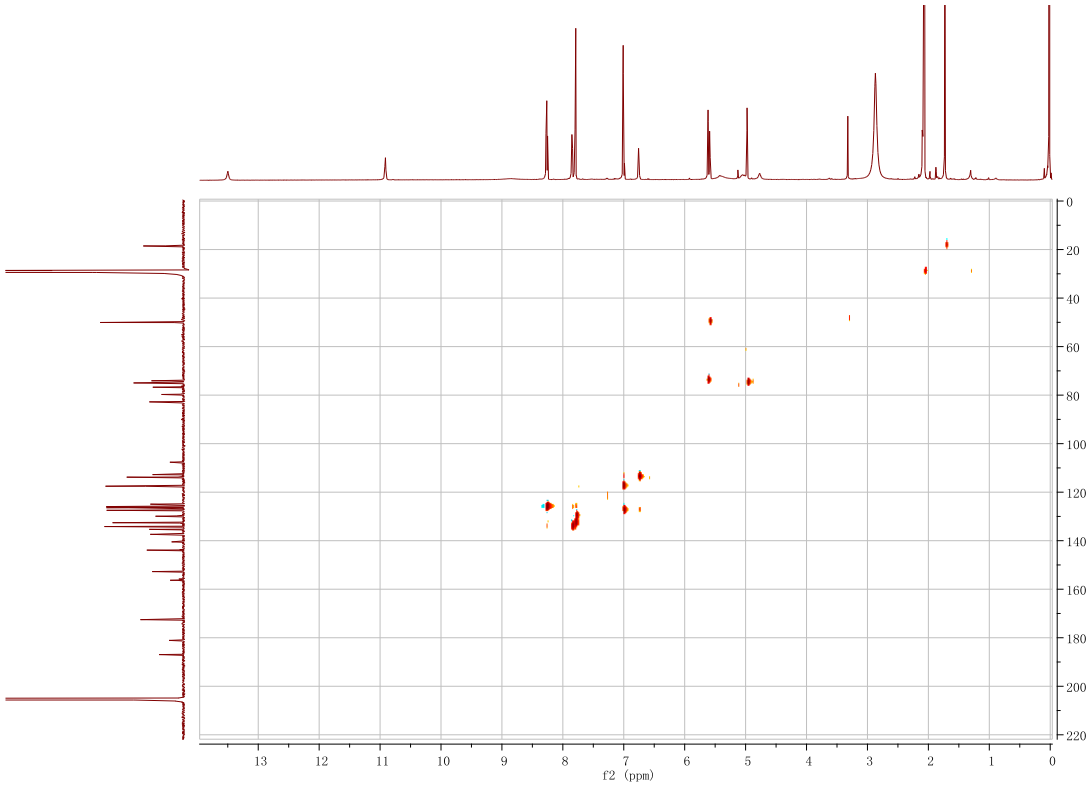

Figure S99. $^{1}H–^{13}C$ HMBC spectrum of **17** (acetone-d_6)

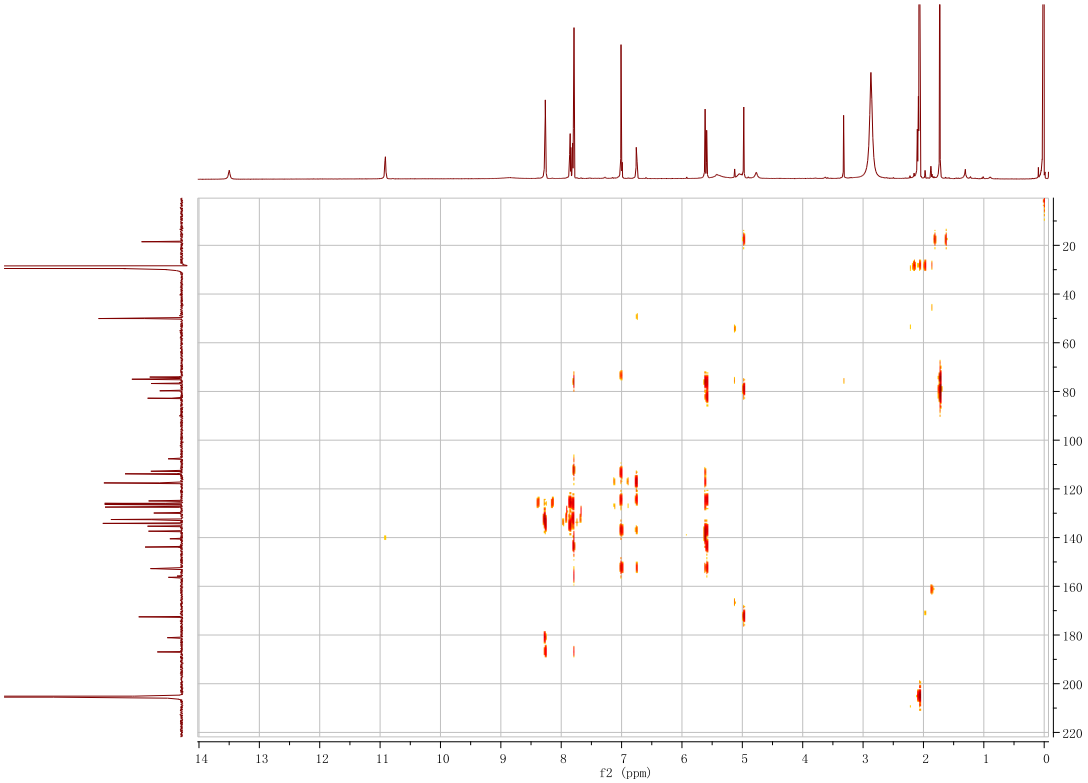

Figure S100. ^{1}H-^{1}H ROESY spectrum of **17** (acetone-d_6)

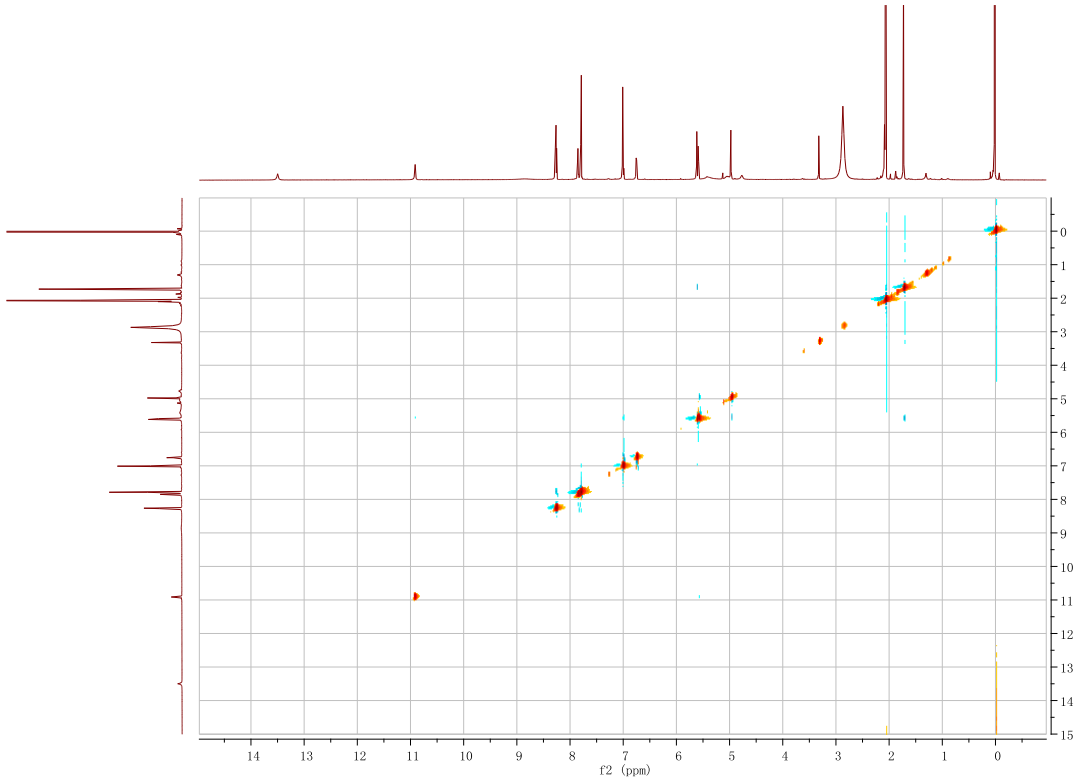

Figure S101. HR-ESI-MS spectrum of **18**

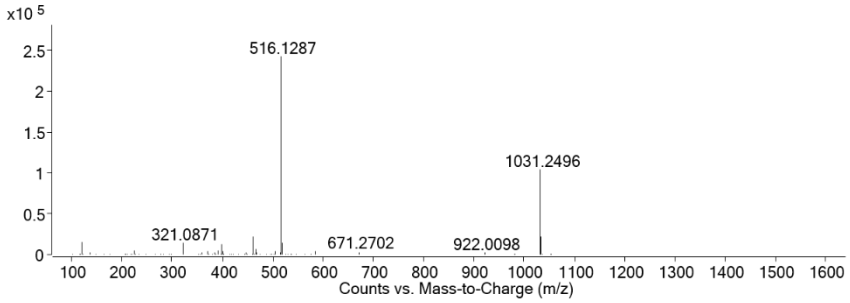

Figure S102. ^{1}H NMR Spectrum of **18** (700 MHz, acetone-d_6)

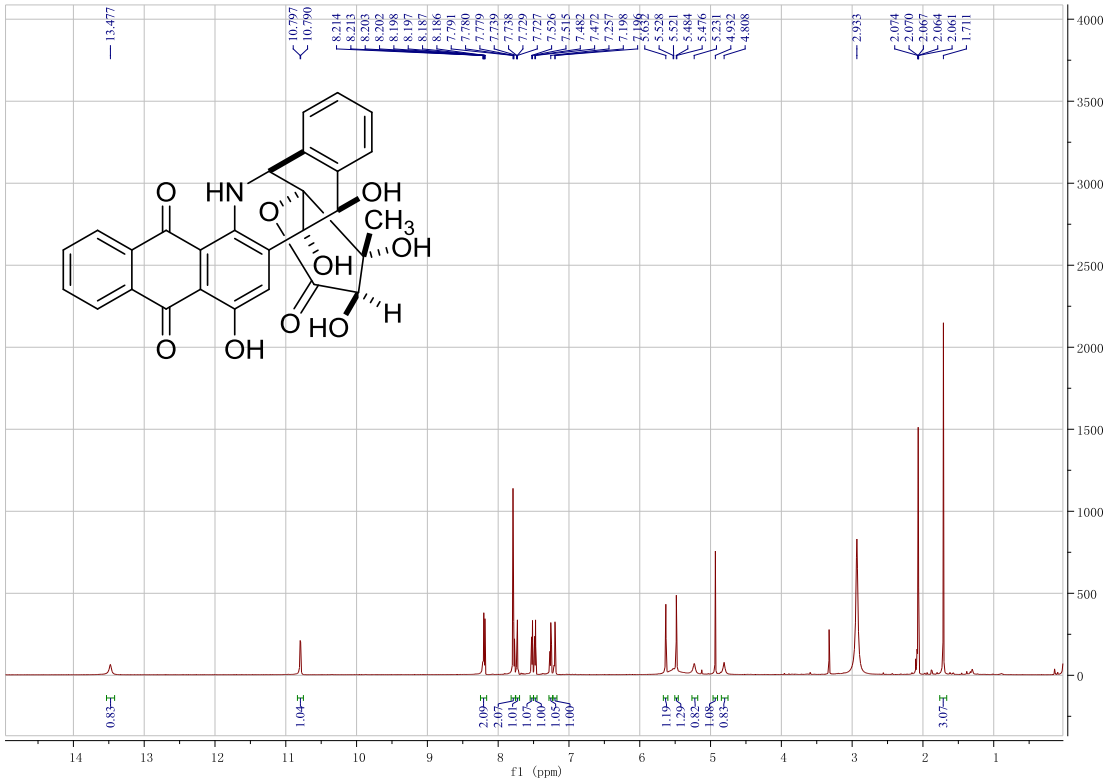

Figure S103. ^{13}C NMR spectrum of **18** (176 MHz, acetone-d_6)

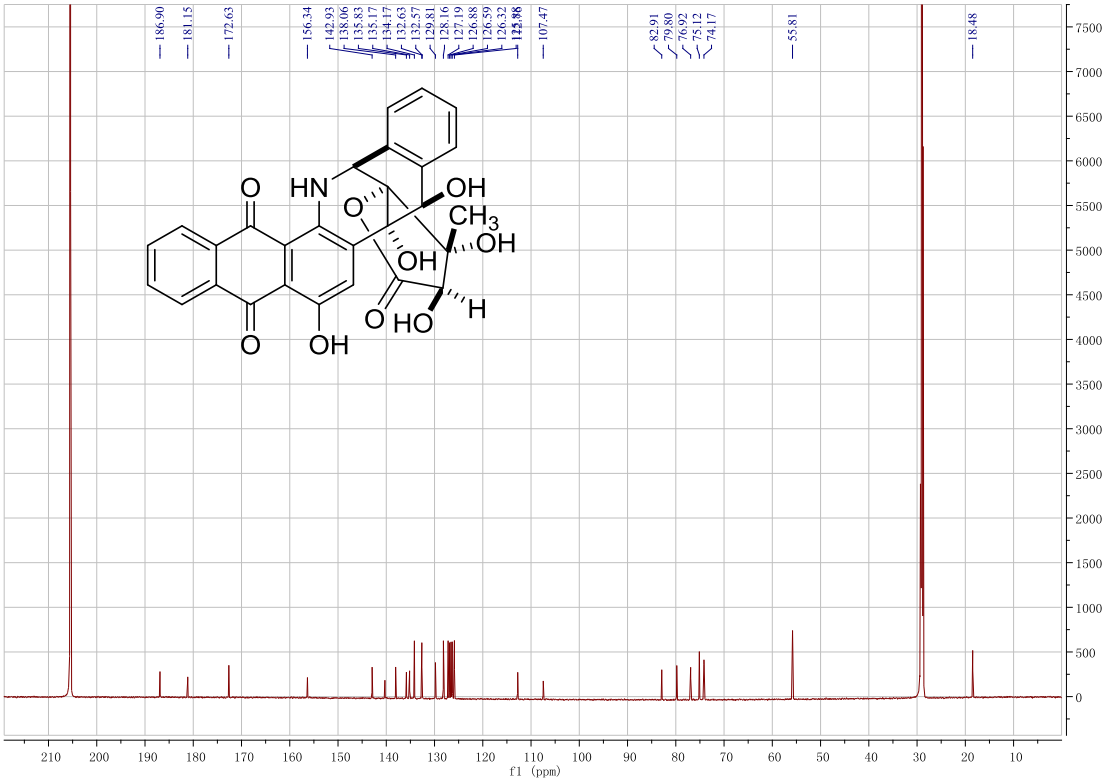

Figure S104. ^{1}H-^{1}H COSY spectrum of **18** (acetone-d_6)

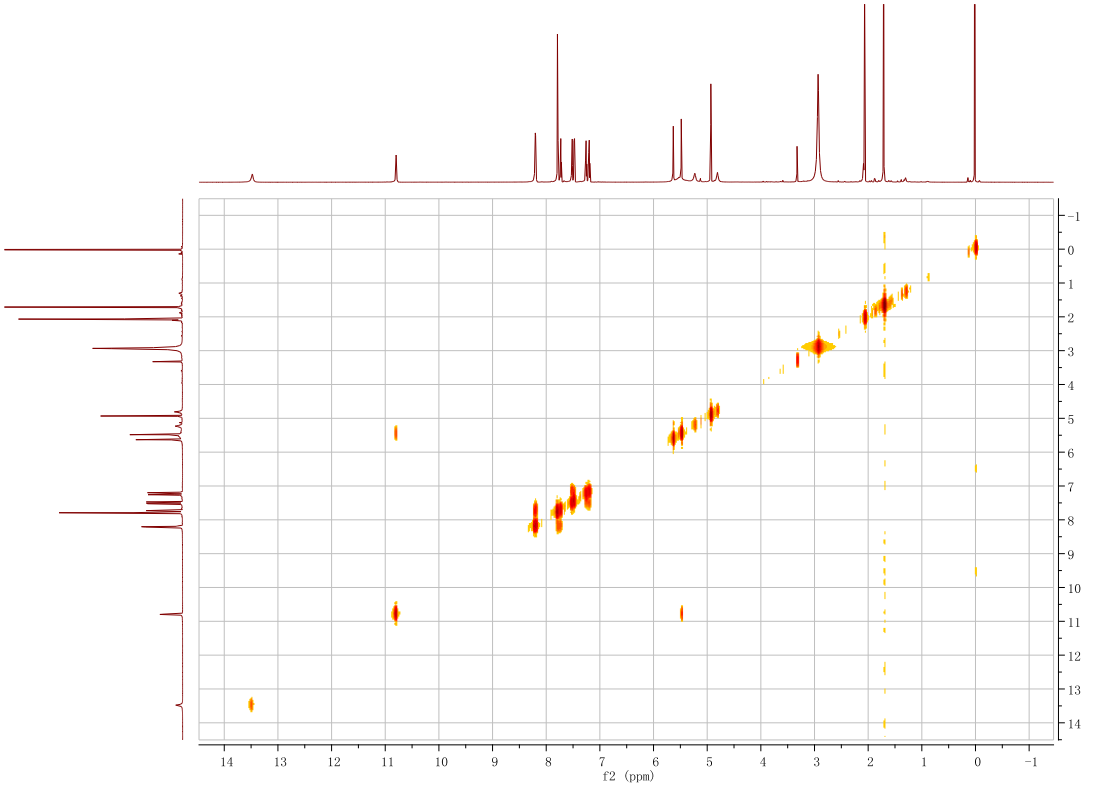

Figure S105. $^{1}H–^{13}C$ HSQC spectrum of **18** (acetone-d_6)

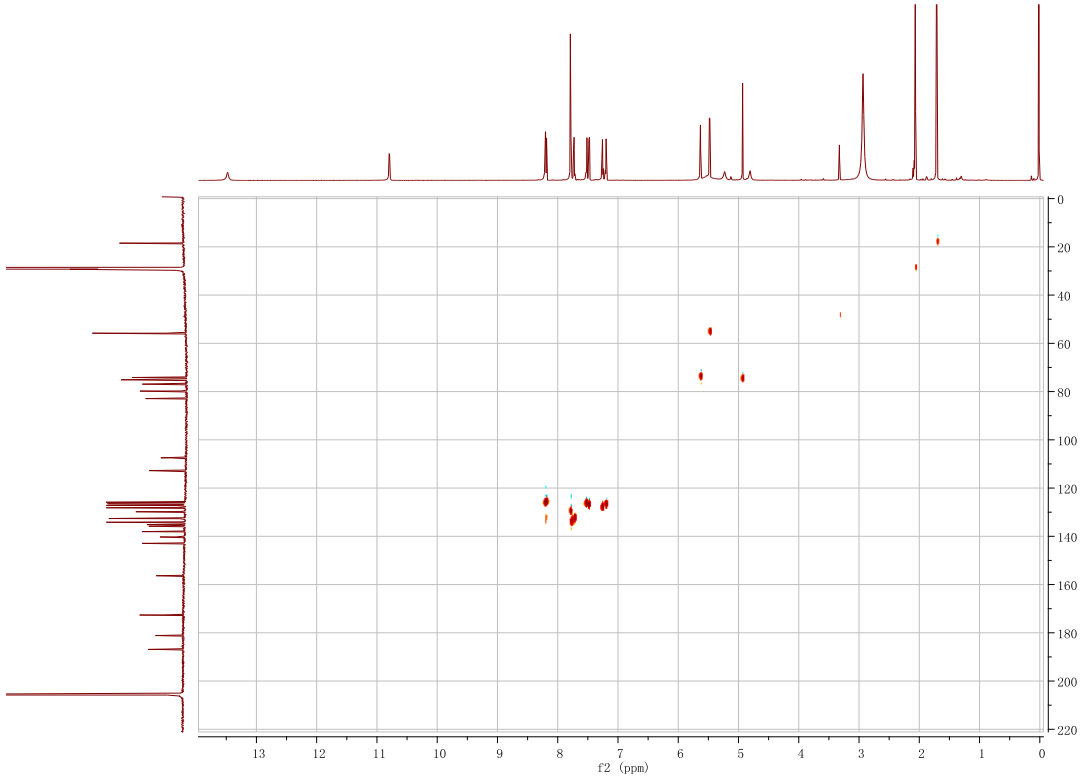

Figure S106. $^{1}H–^{13}C$ HMBC spectrum of **18** (acetone-d_6)

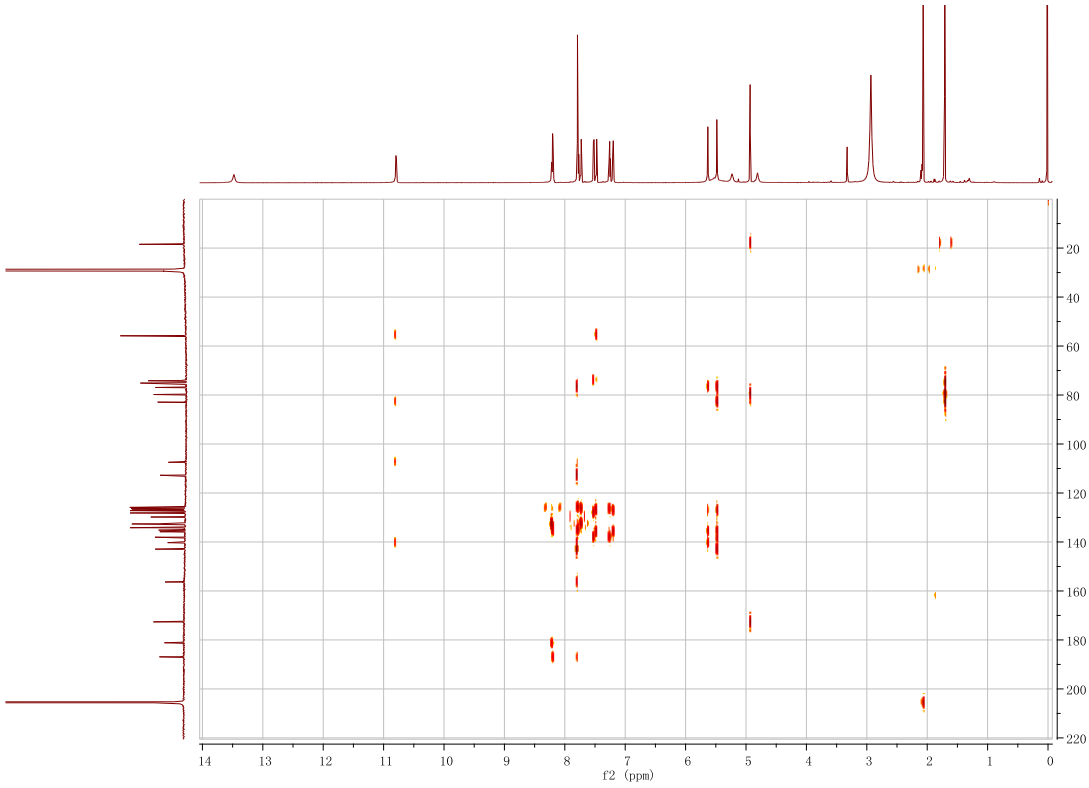

Figure S107. ^{1}H-^{1}H ROESY spectrum of **18** (acetone-d_6)

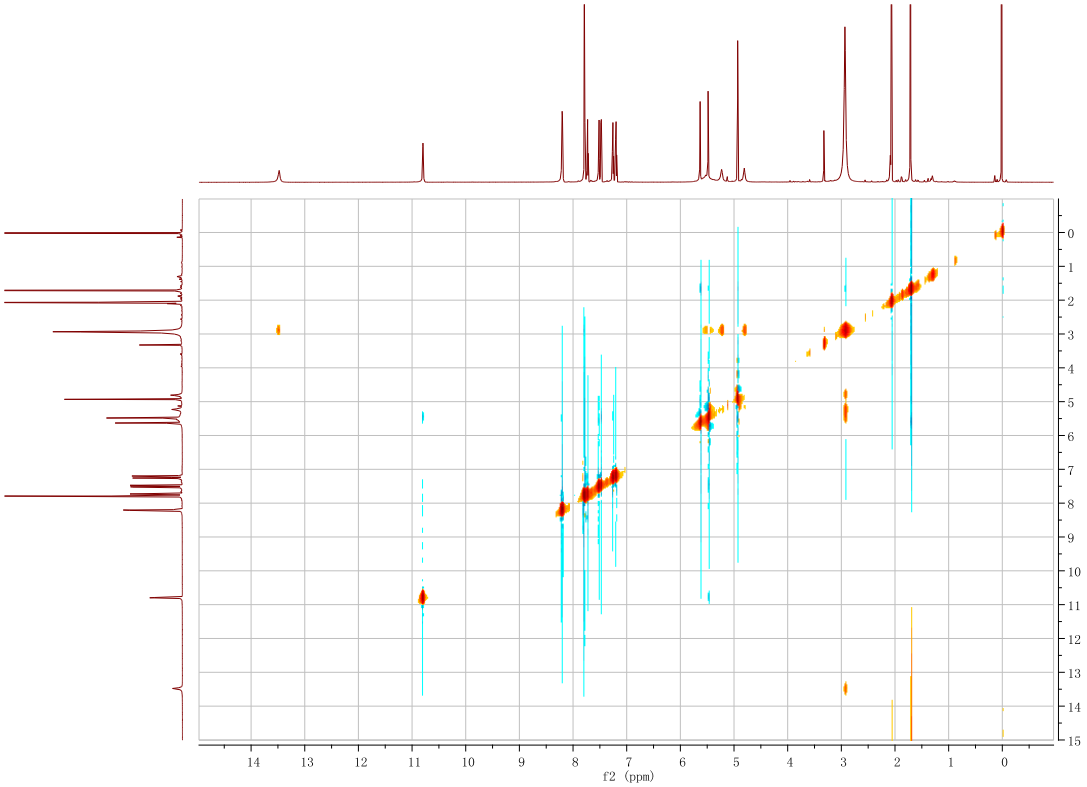

Figure S108. HR-ESI-MS spectrum of **19**

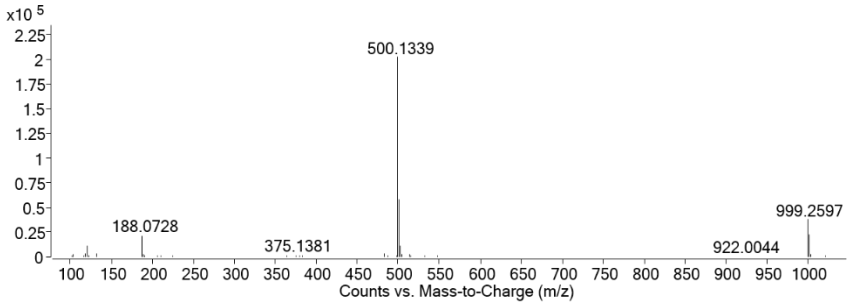

Figure S109. ^{1}H NMR Spectrum of **19** (700 MHz, acetone-d_6)

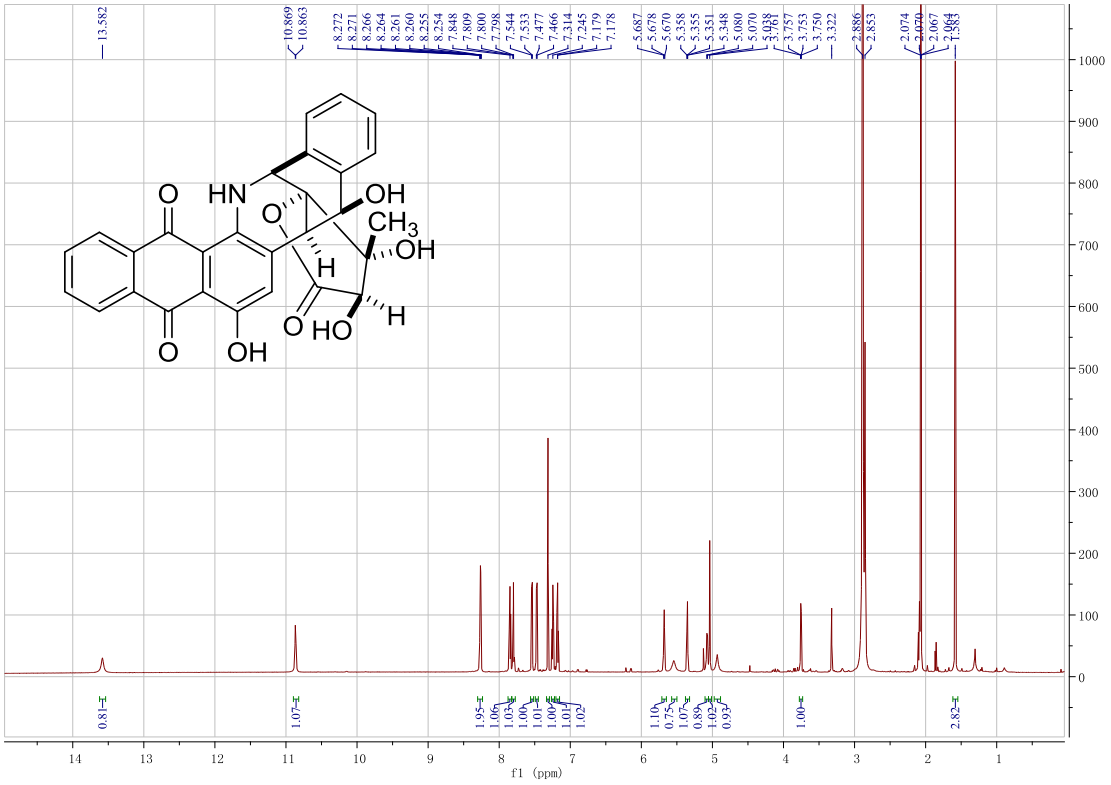

Figure S110. ^{13}C NMR spectrum of **19** (176 MHz, acetone-d_6)

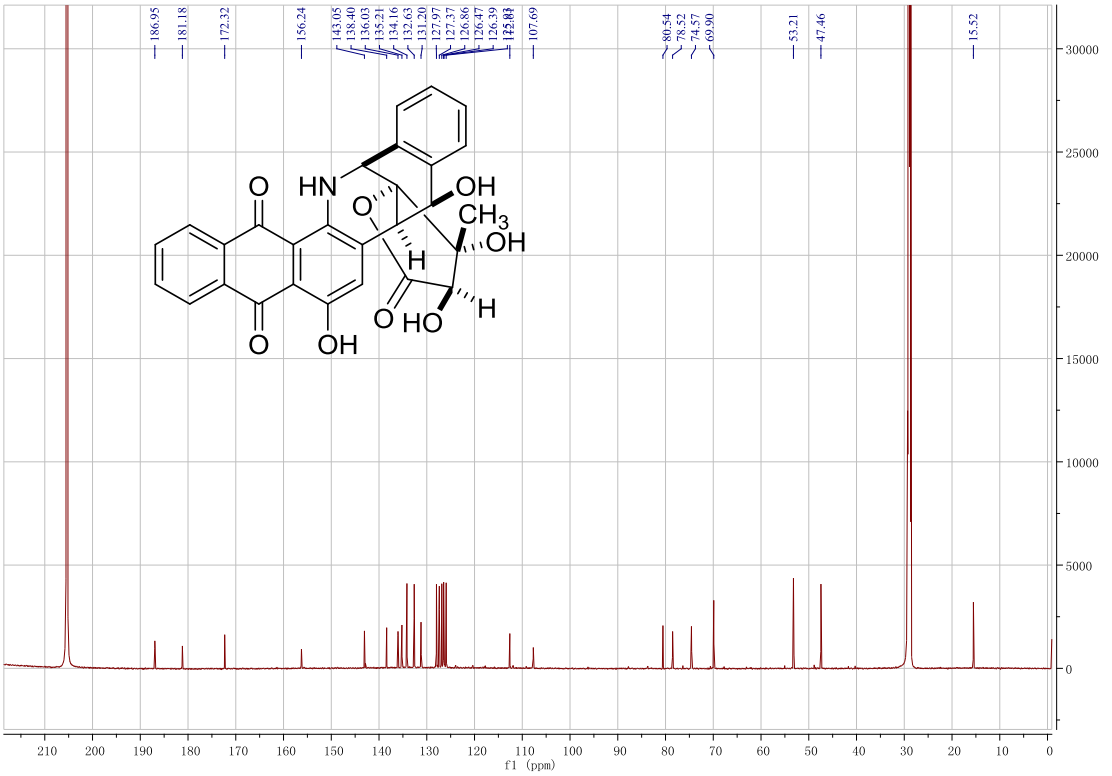

Figure S111. ^{1}H-^{1}H COSY spectrum of **19** (acetone-d_6)

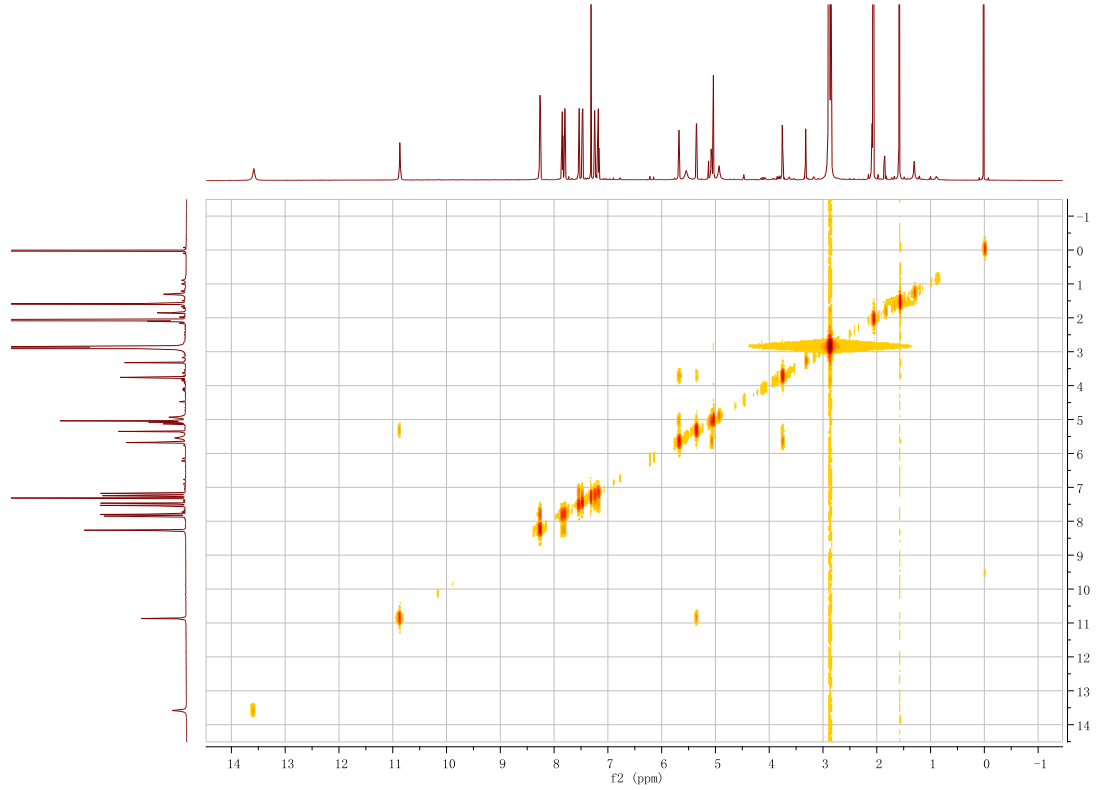

Figure S112. ^{1}H–^{13}C HSQC spectrum of **19** (acetone-d_6)

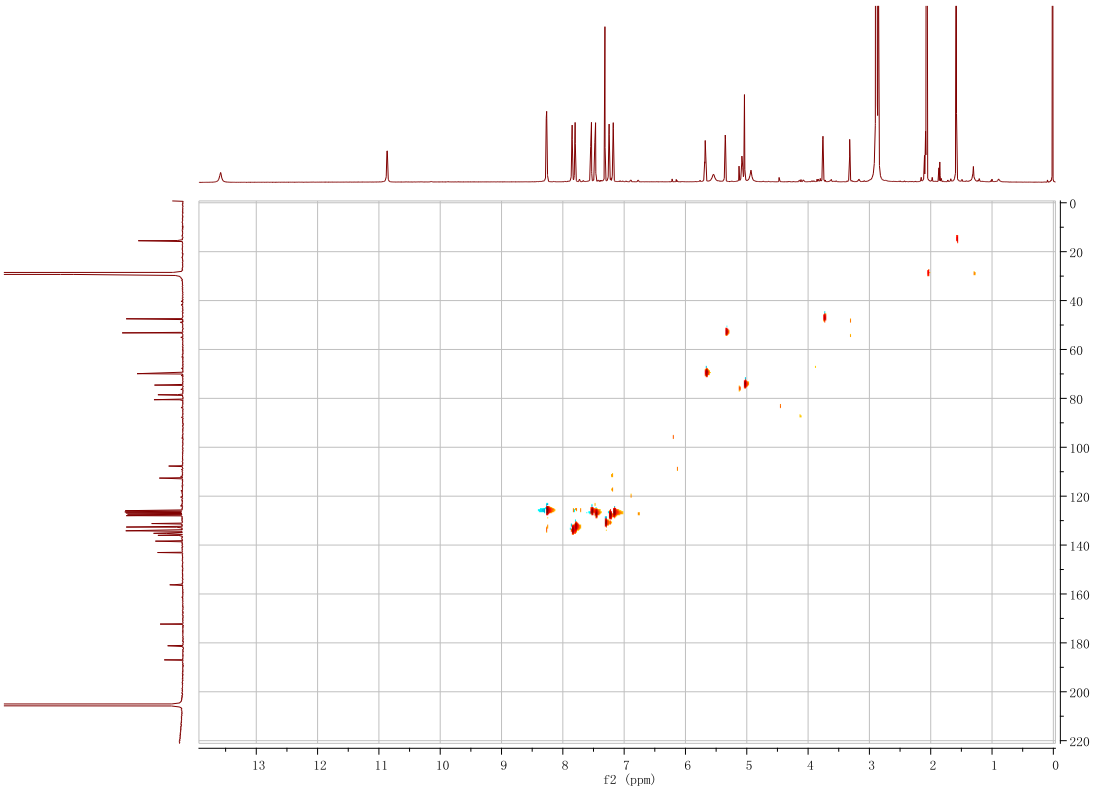

Figure S113. ^{1}H–^{13}C HMBC spectrum of **19** (acetone-d_6)

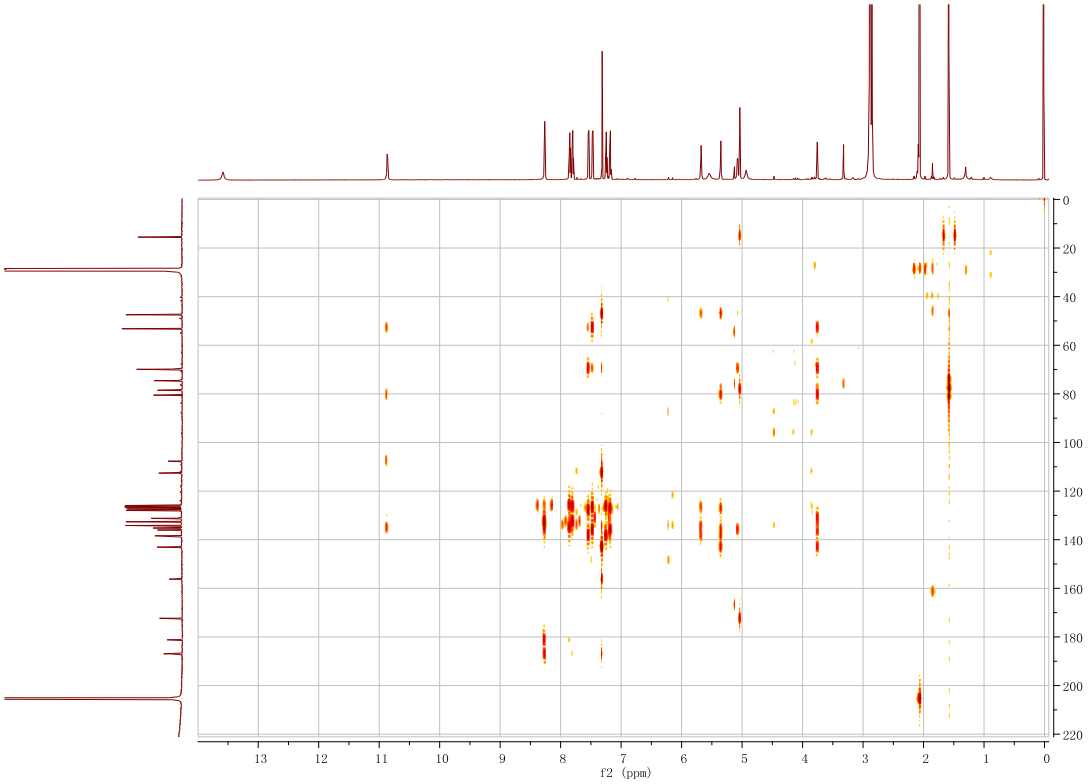

Figure S114. ^{1}H-^{1}H ROESY spectrum of **19** (acetone-d_6)

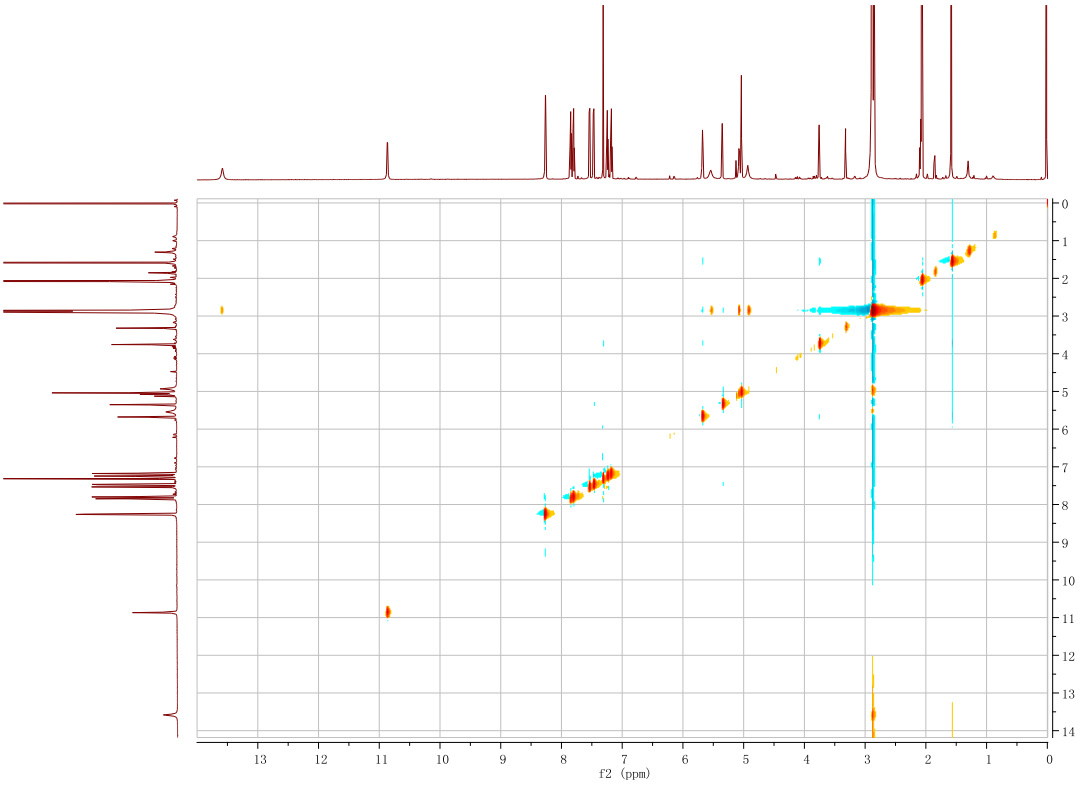

Figure S115. HR-ESI-MS spectrum of TNM F (**20**)

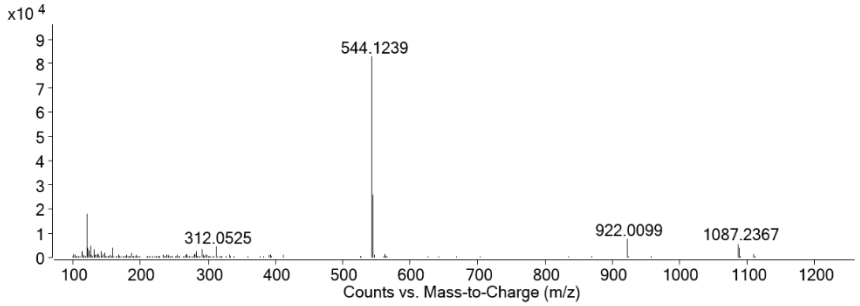

Figure S116. ^{1}H NMR Spectrum of TNM F (**20**) (700 MHz, acetone-d_6)

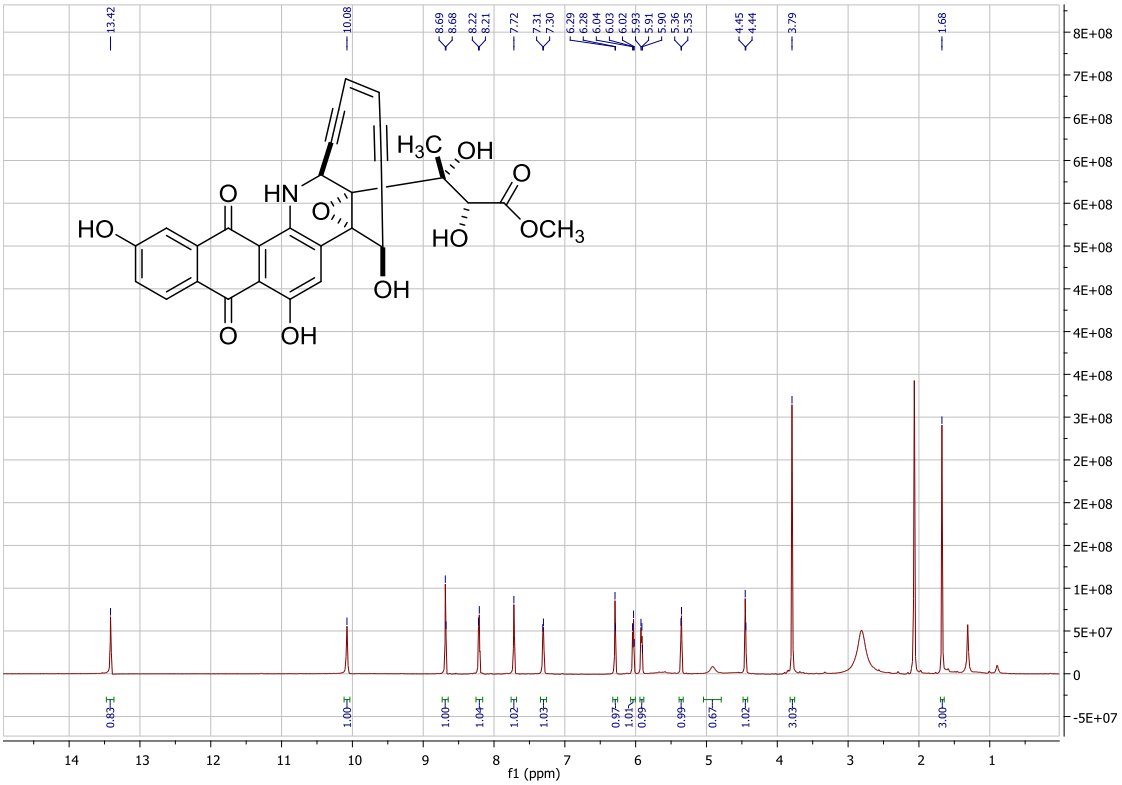

Figure S117. ^{13}C NMR spectrum of TNM F (**20**) (176 MHz, acetone-d_6)

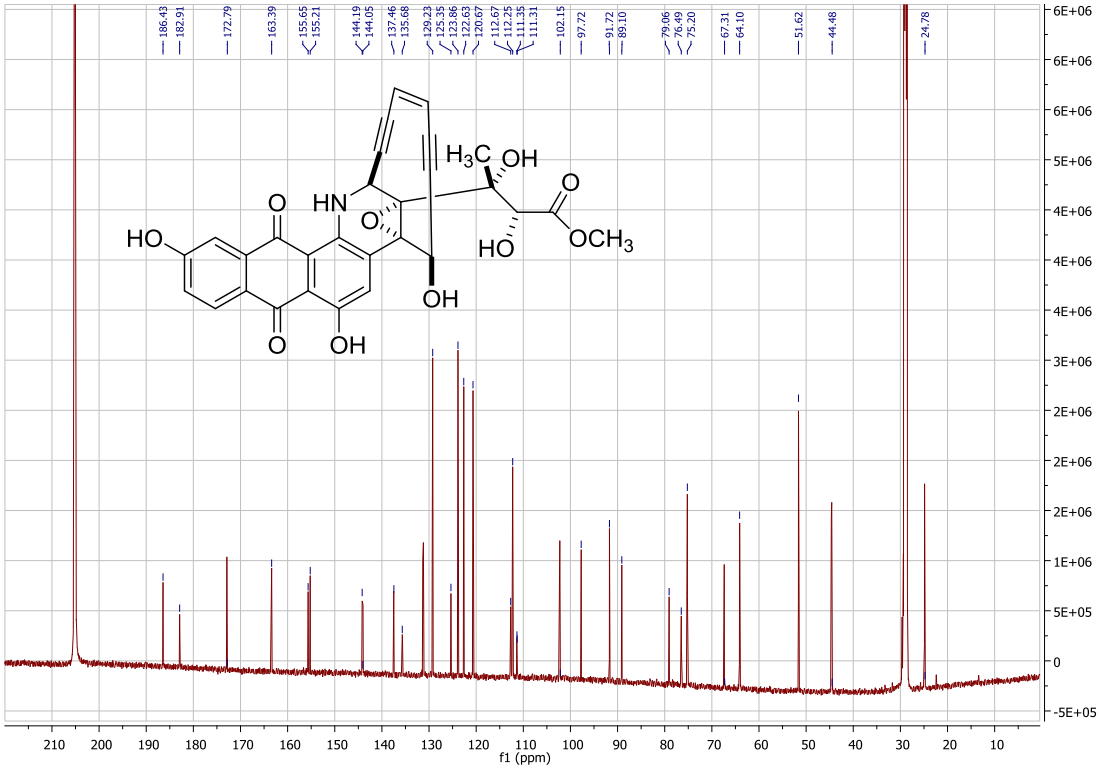

Figure S118. ^{1}H-^{1}H COSY spectrum of TNM F (**20**) (acetone-d_6)

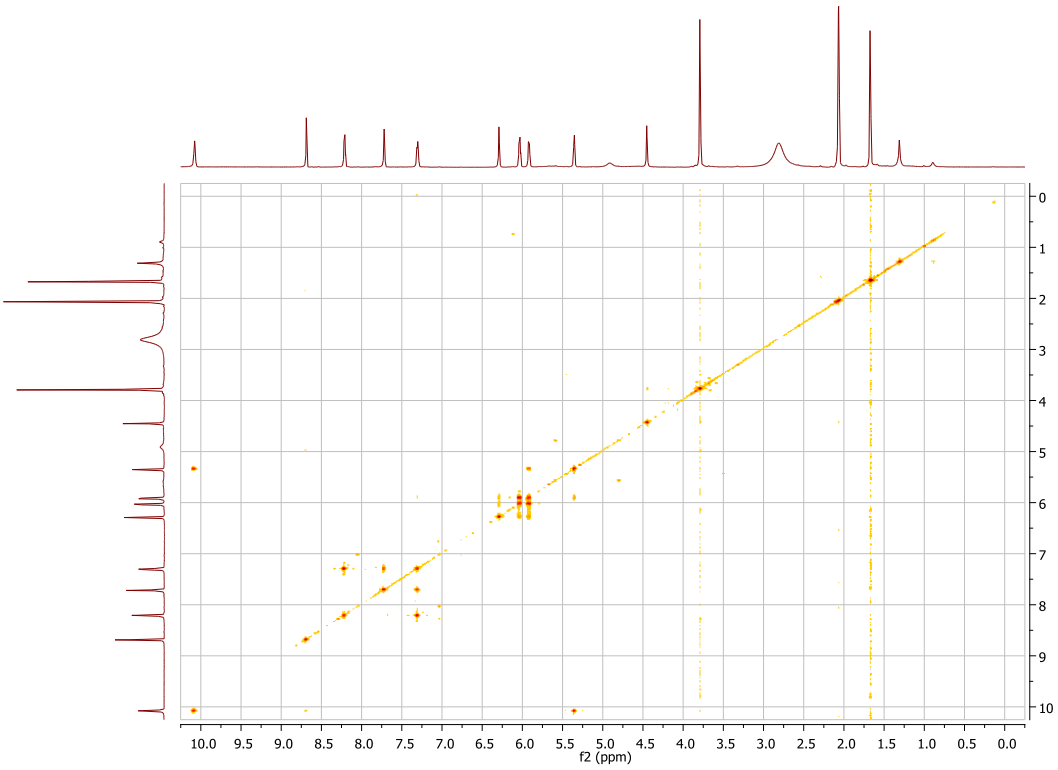

Figure S119. $^{1}H–^{13}C$ HSQC spectrum of TNM F (**20**) (acetone-d_6)

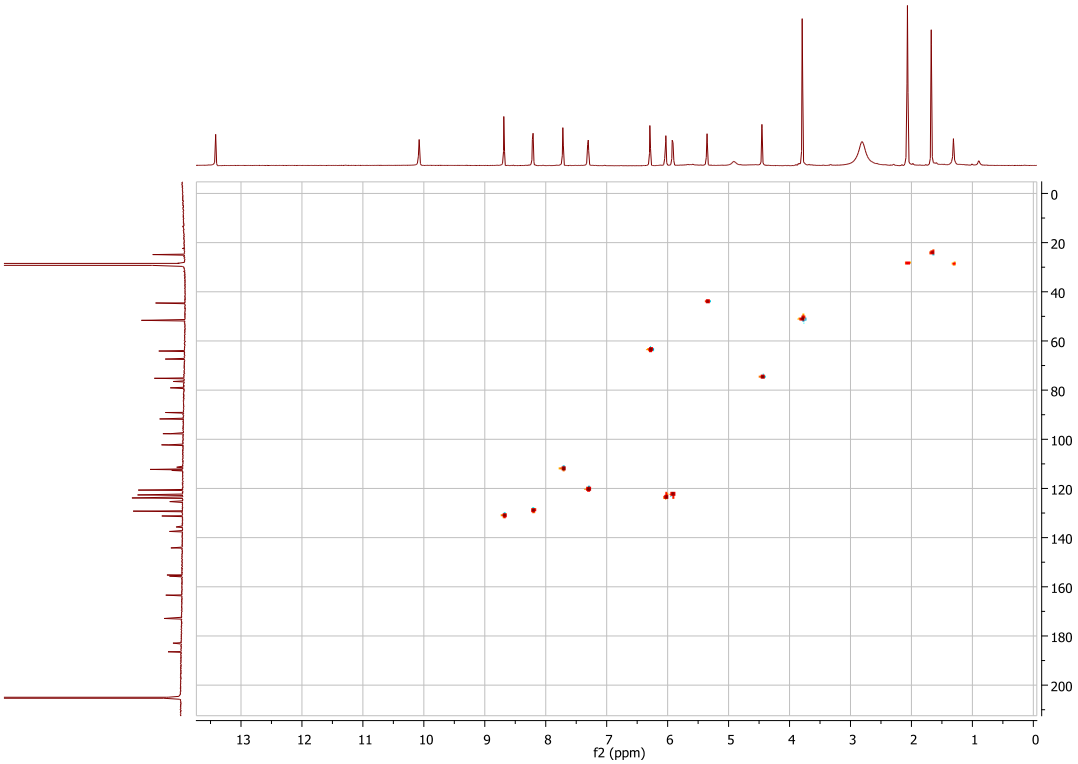

Figure S120. $^{1}H–^{13}C$ HMBC spectrum of TNM F (**20**) (acetone-d_6)

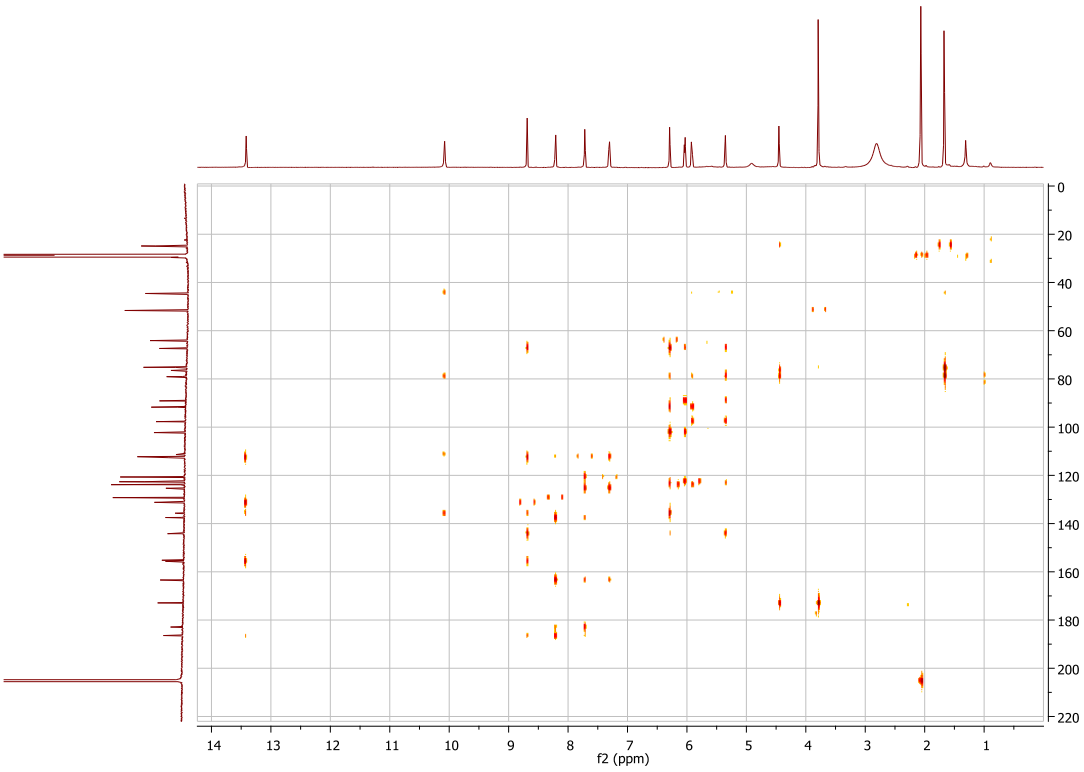

Figure S121. ^{1}H-^{1}H ROESY spectrum of TNM F (**20**) (acetone-d_6)

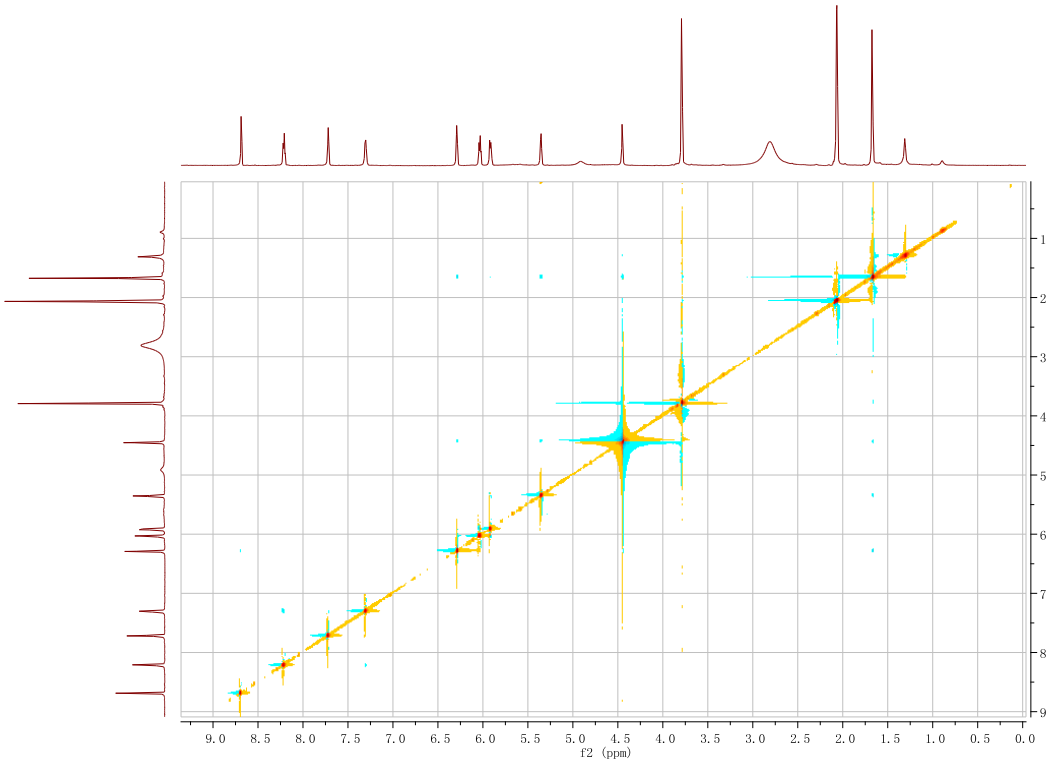

Figure S122. HR-ESI-MS spectrum of **21**

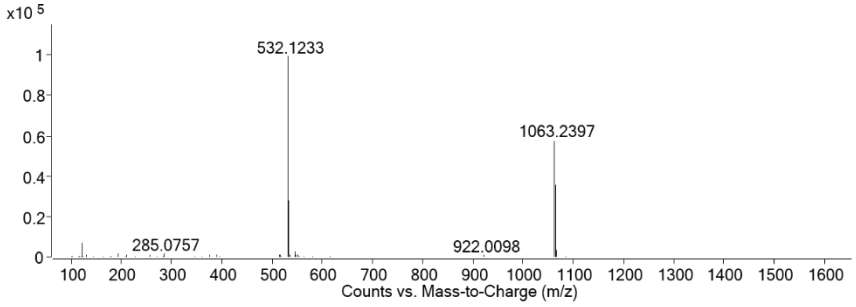

Figure S123. ^{1}H NMR Spectrum of **21** (700 MHz, acetone-d_6)

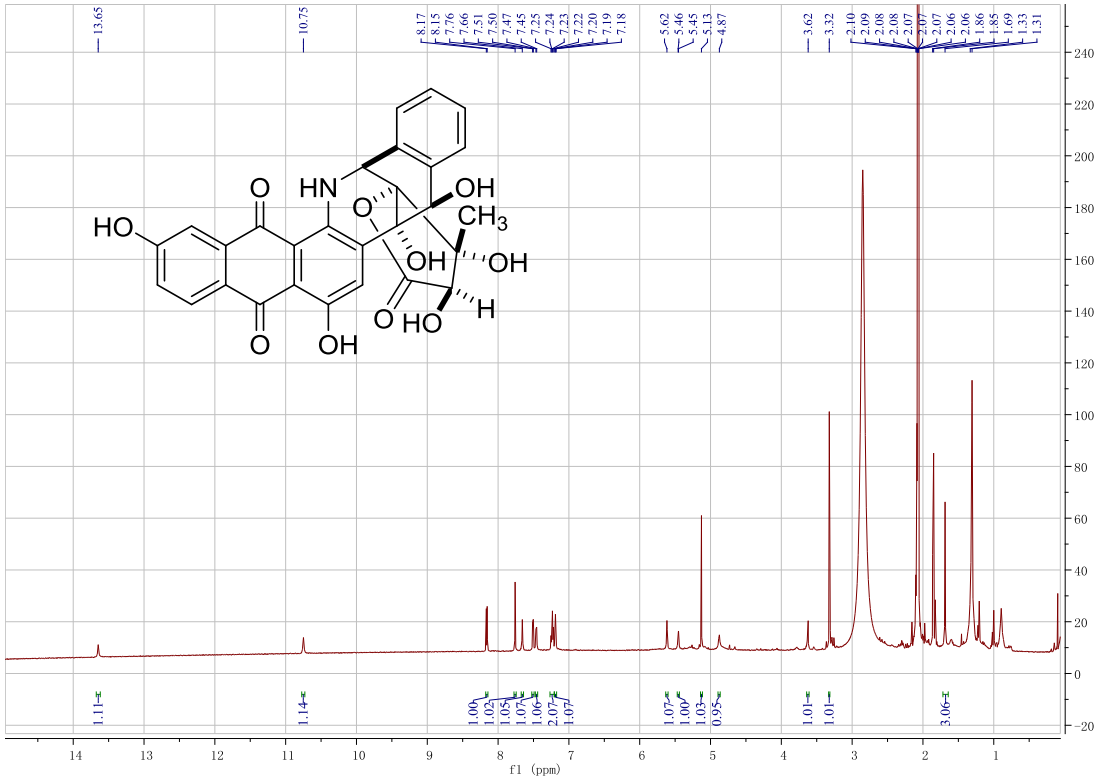

Figure S124. ^{13}C NMR spectrum of **21** (176 MHz, acetone-d_6)

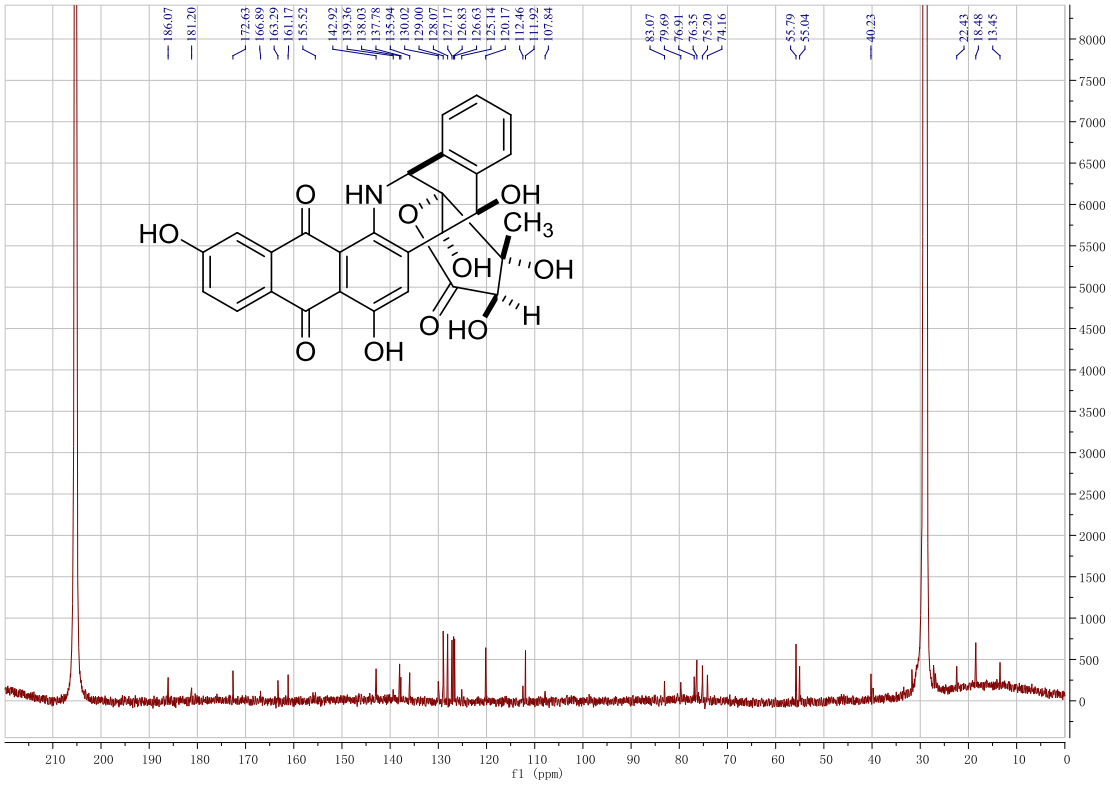

Figure S125. ^{1}H-^{1}H COSY spectrum of **21** (acetone-d_6)

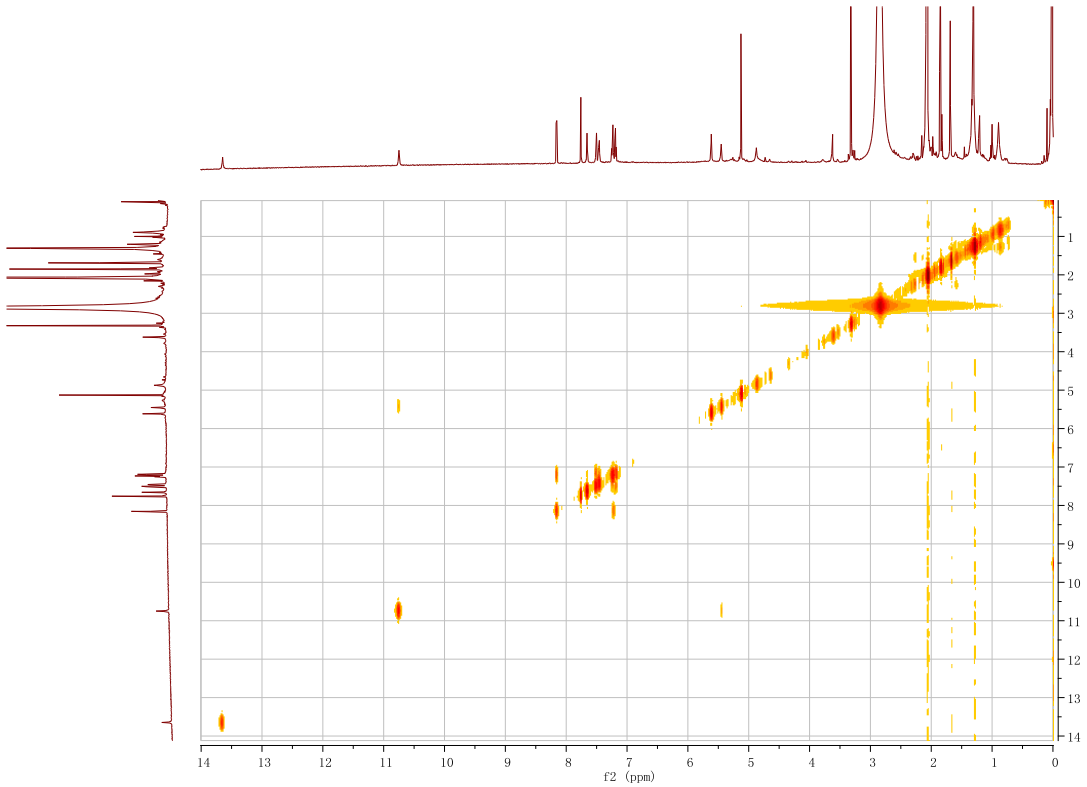

Figure S126. ^{1}H–^{13}C HSQC spectrum of **21** (acetone-d_6)

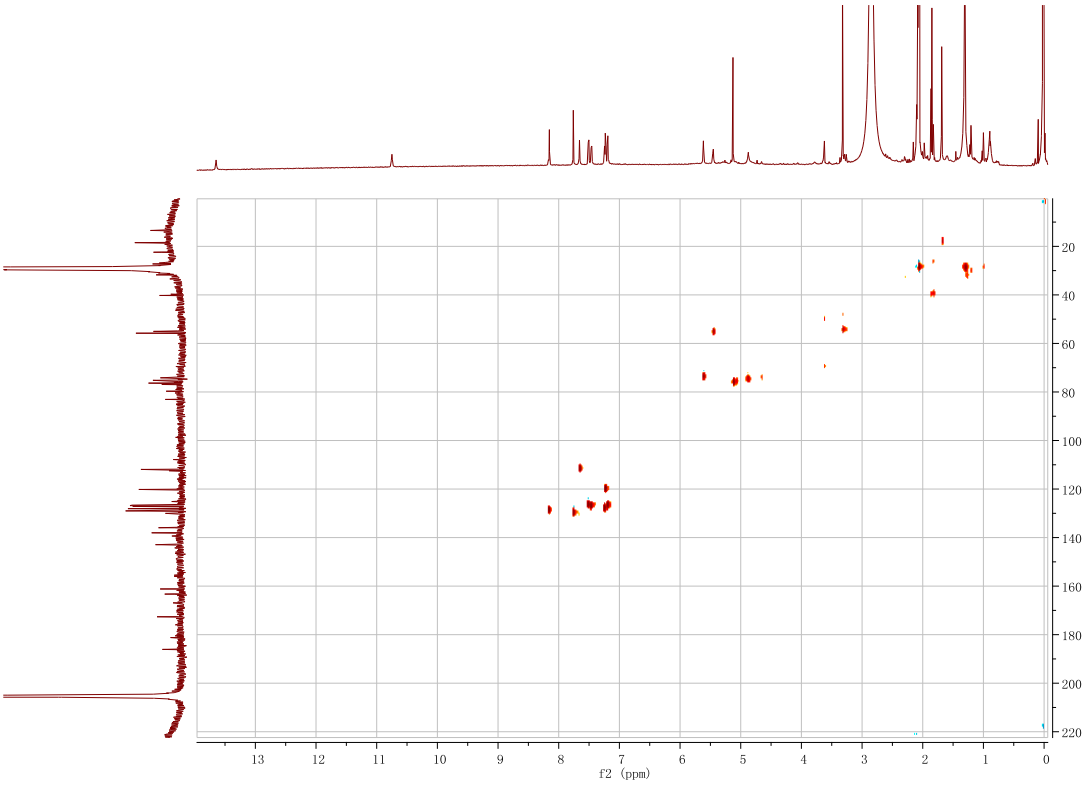

Figure S127. $^{1}H–^{13}C$ HMBC spectrum of **21** (acetone-d_6)

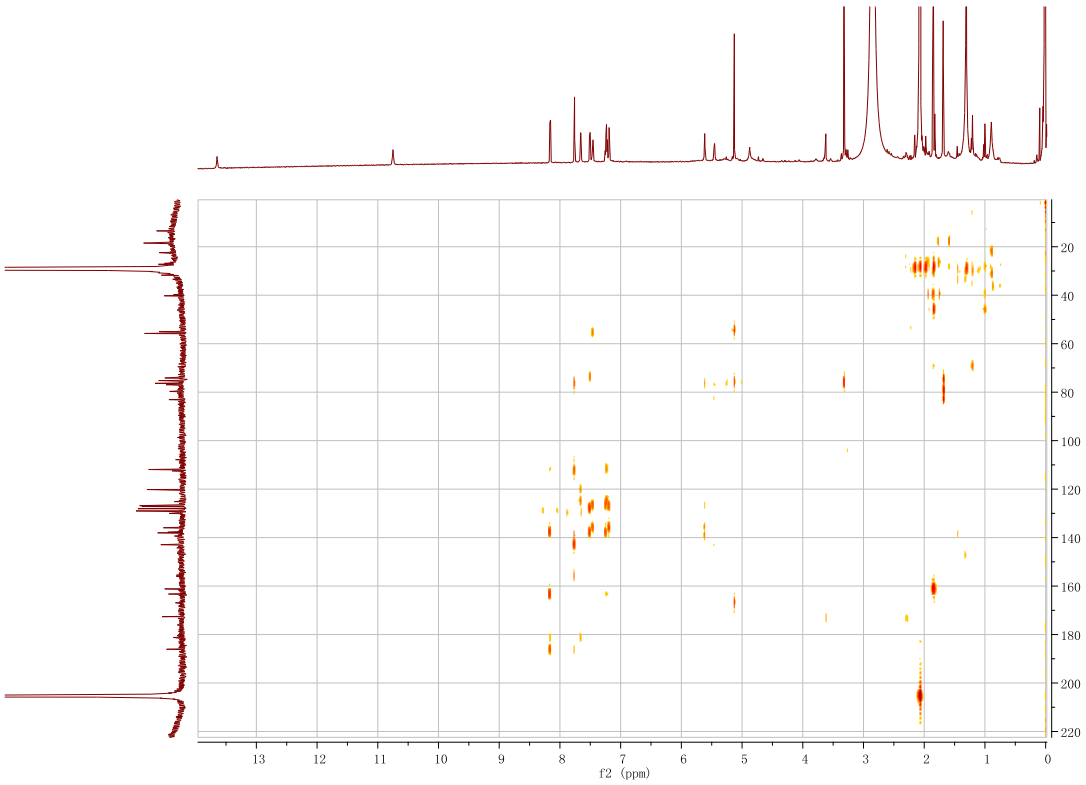

Figure S128. ROESY spectrum of **21** (acetone-d_6)

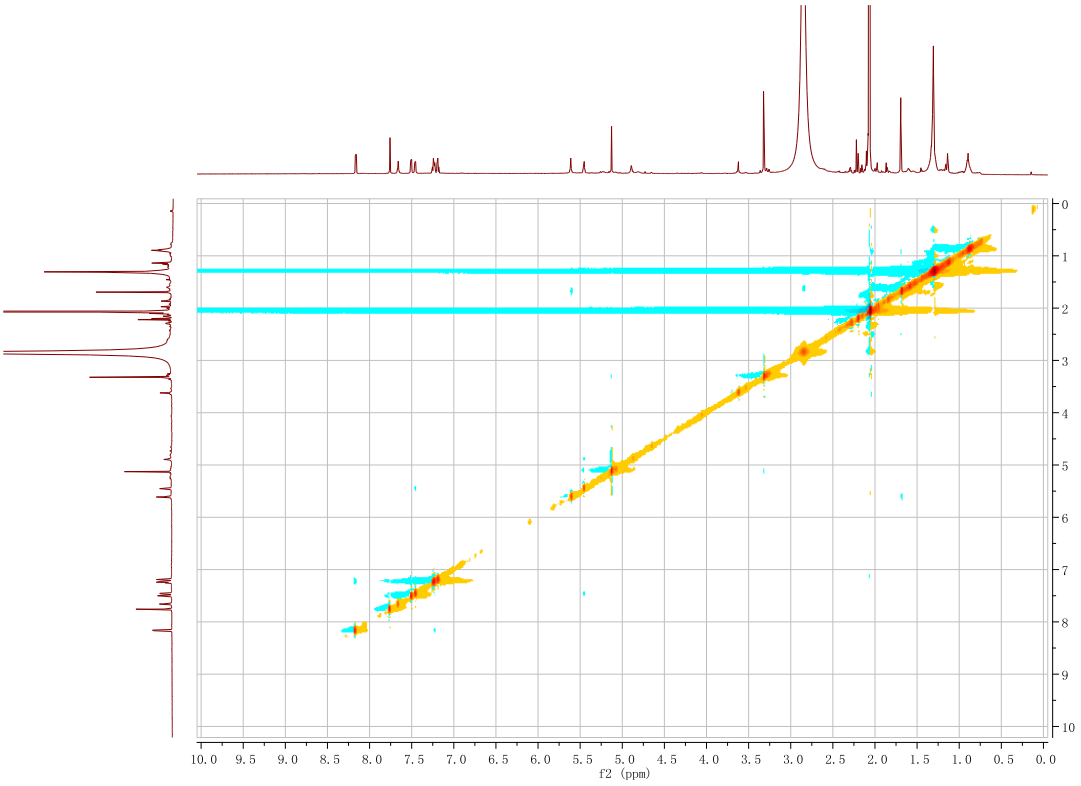

Figure S129. HR-ESI-MS spectrum of **22**

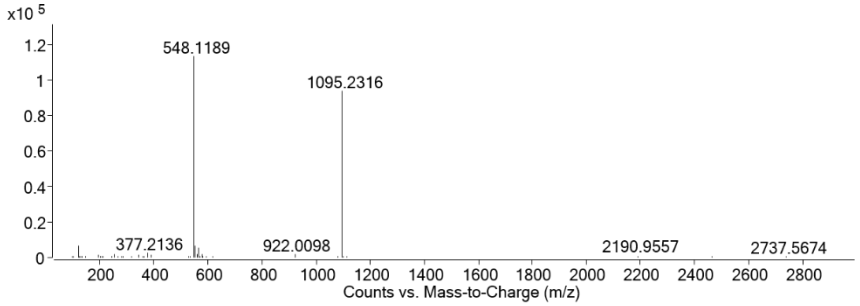

Figure S130. ^{1}H NMR Spectrum of **22** (700 MHz, acetone-d_6)

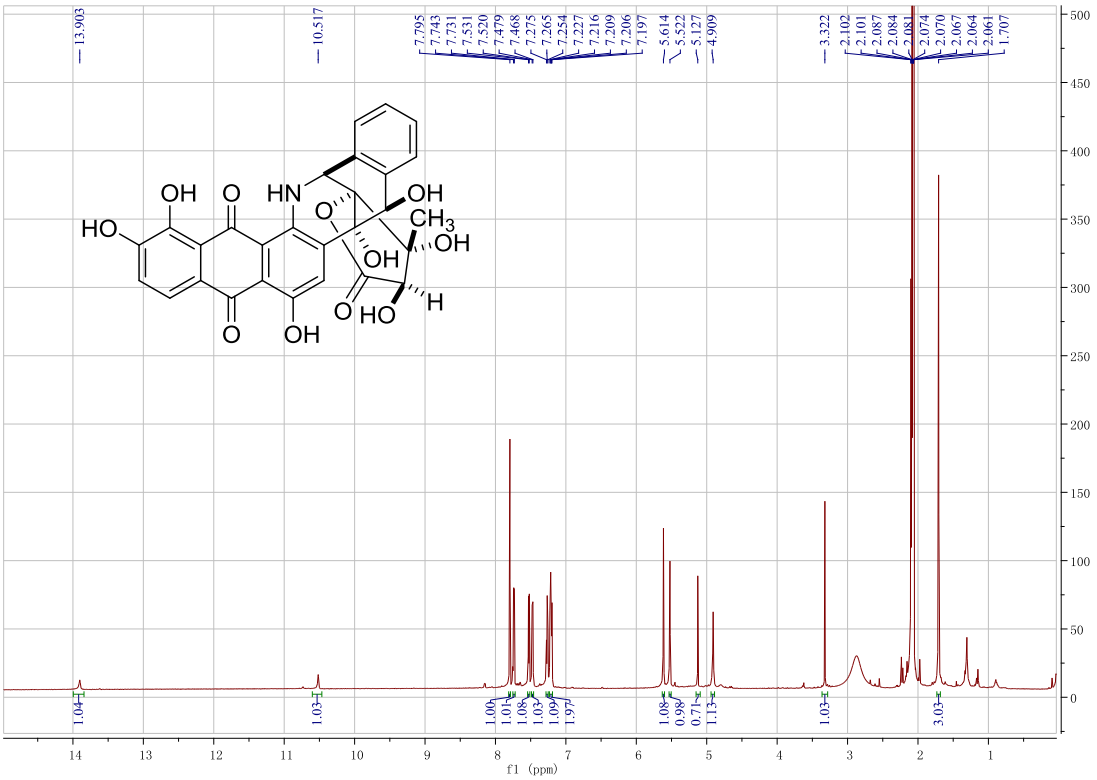

Figure S131. ^{13}C NMR spectrum of **22** (176 MHz, acetone-d_6)

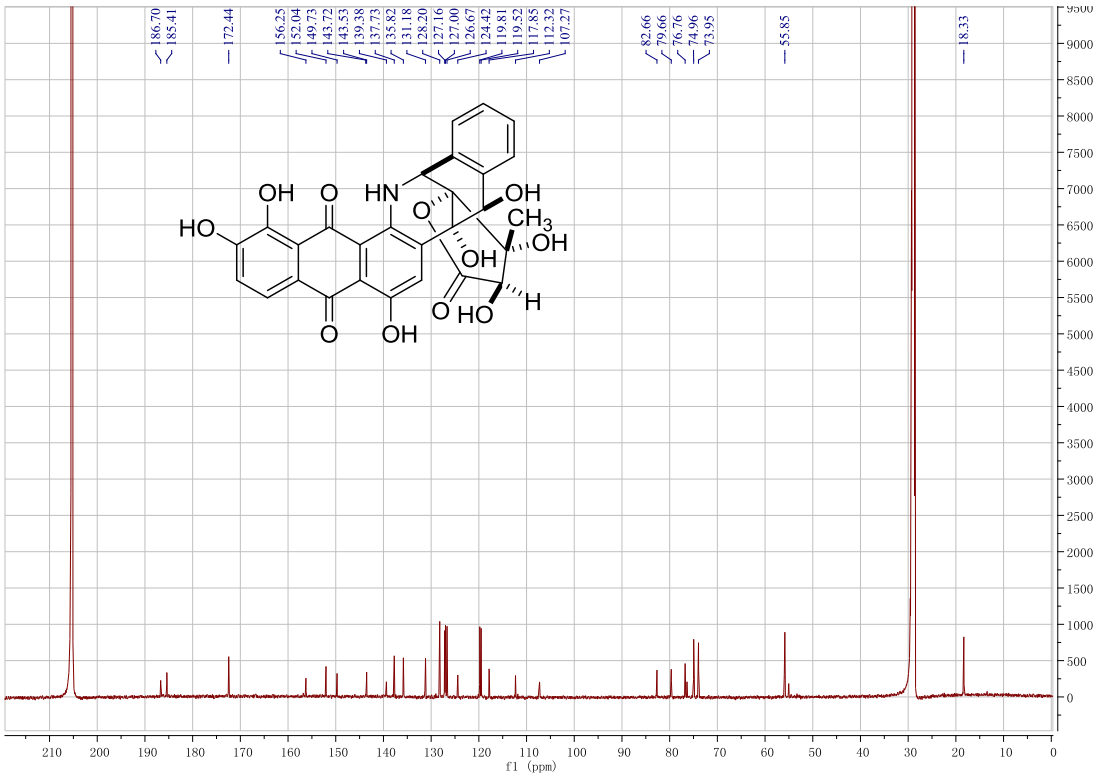

Figure S132. ^{1}H-^{1}H COSY spectrum of **22** (acetone-d_6)

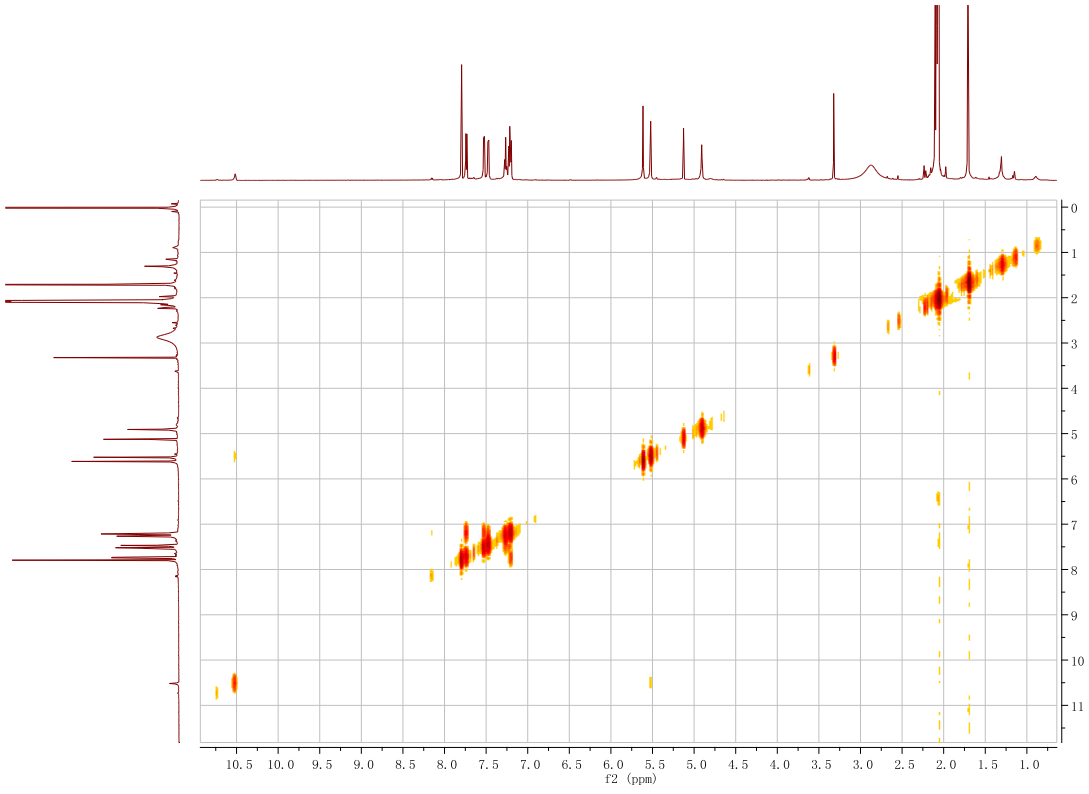

Figure S133. $^{1}H–^{13}C$ HSQC spectrum of **22** (acetone-d_6)

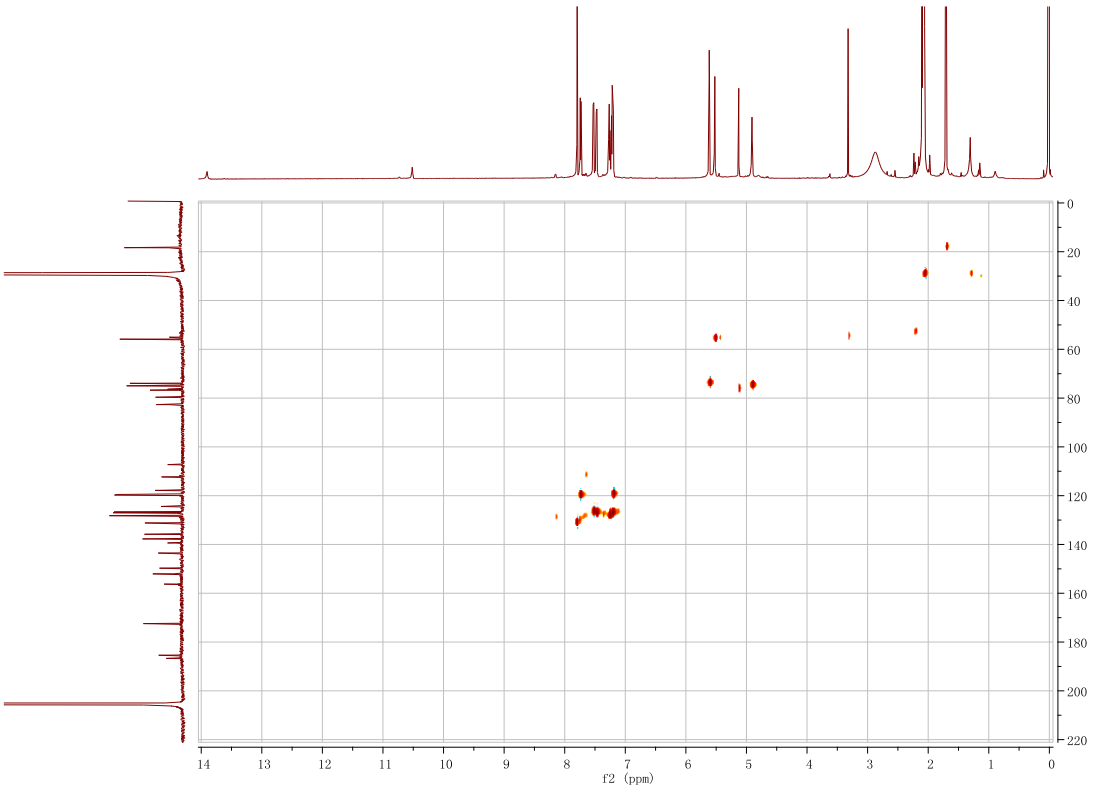

Figure S134. $^{1}H–^{13}C$ HMBC spectrum of **22** (acetone-d_6)

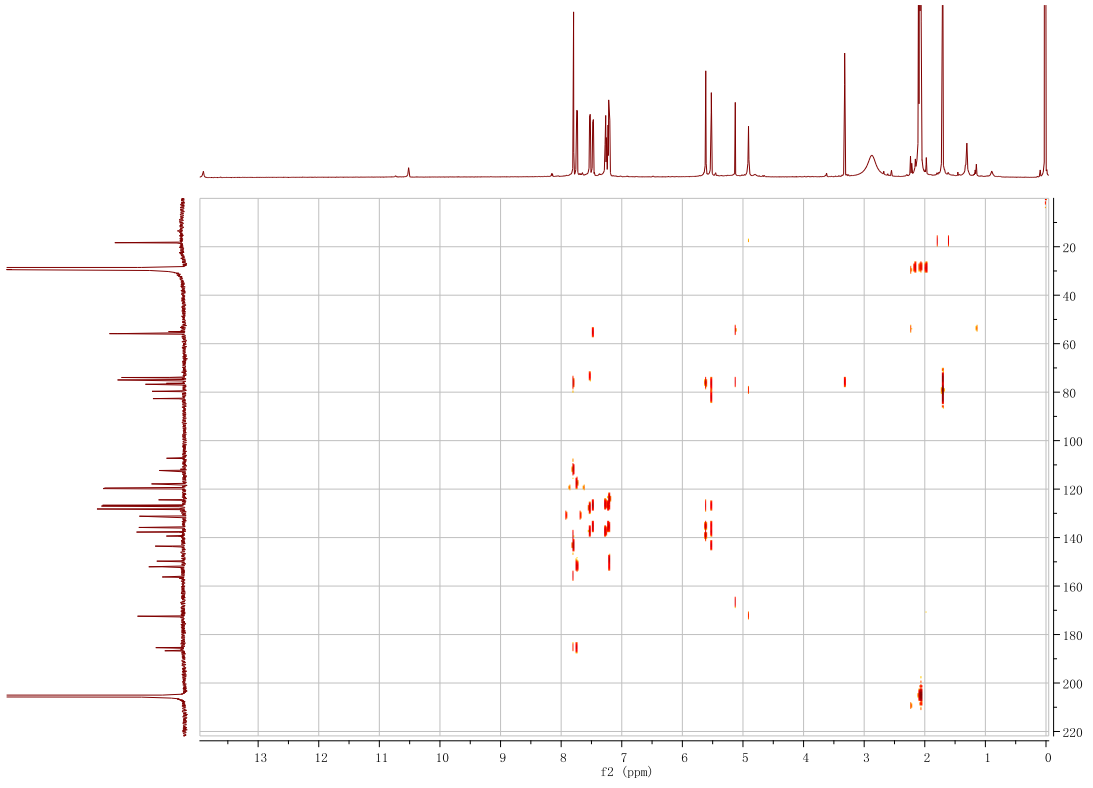

Figure S135. ^{1}H-^{1}H ROESY spectrum of **22** (acetone-d_6)

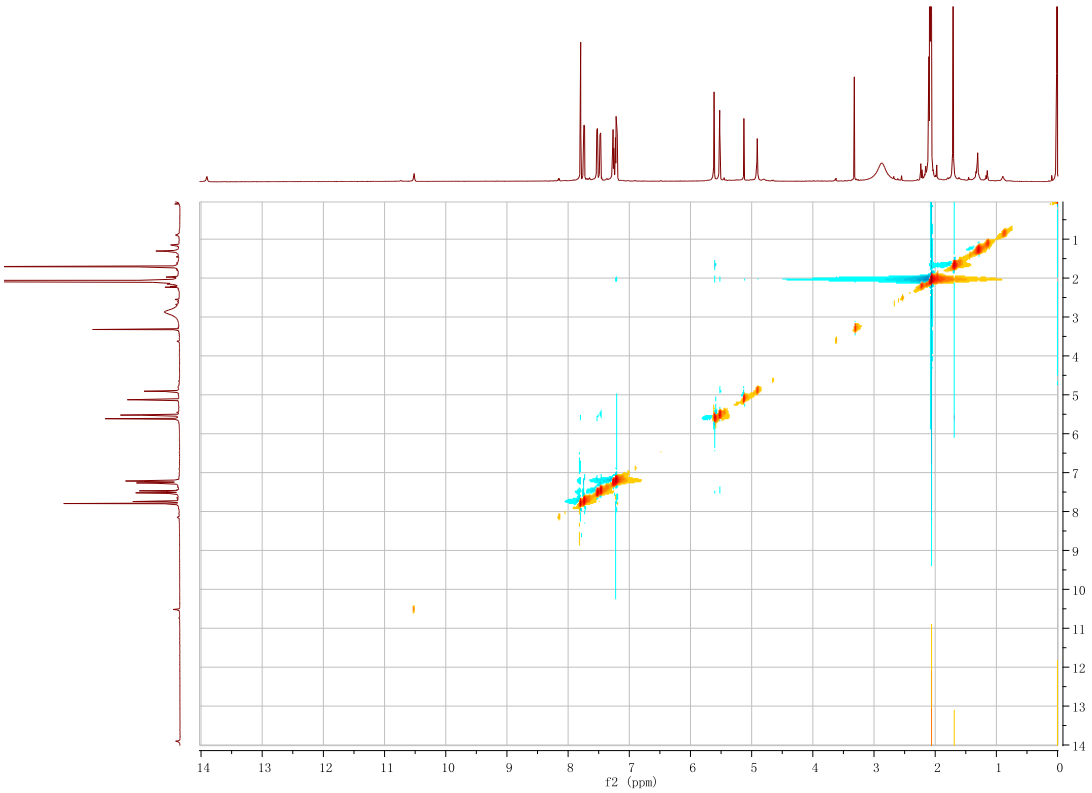

Figure S136. HR-ESI-MS spectrum of **23**

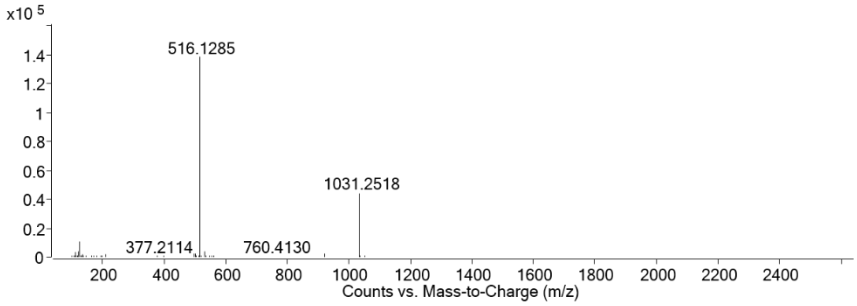

Figure S137. ^{1}H NMR Spectrum of **23** (700 MHz, acetone-d_6)

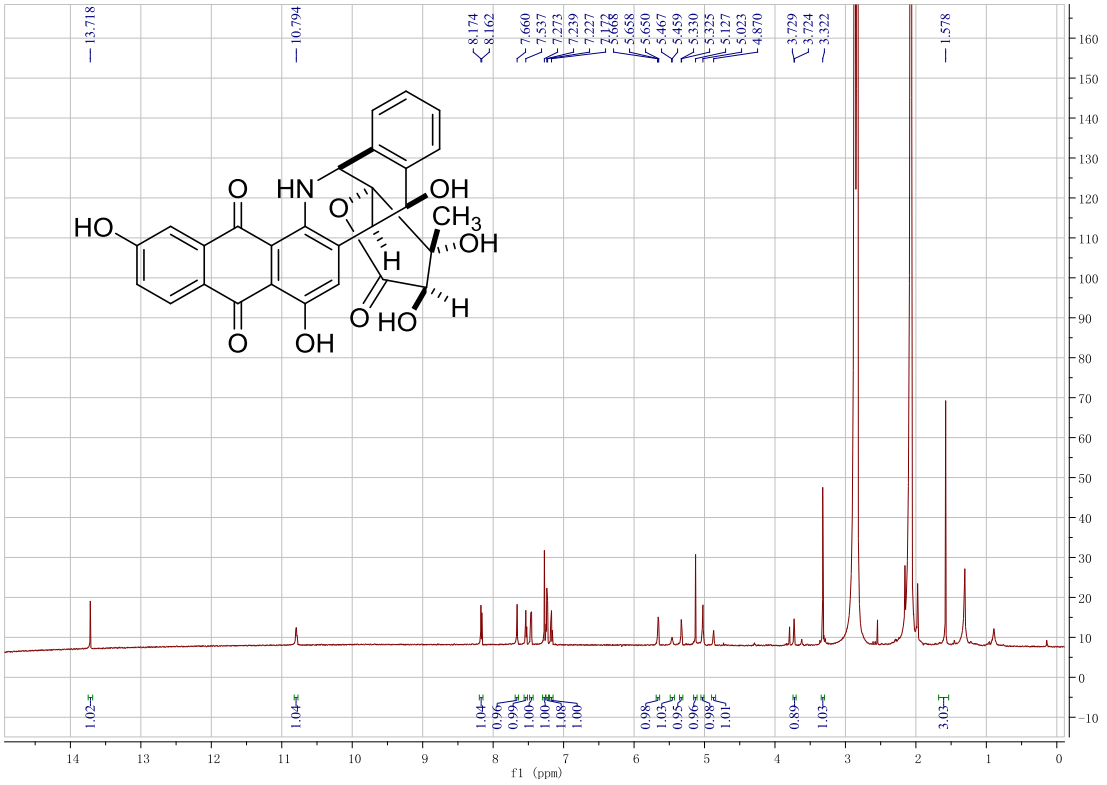

Figure S138. ^{13}C NMR spectrum of **23** (176 MHz, acetone-d_6)

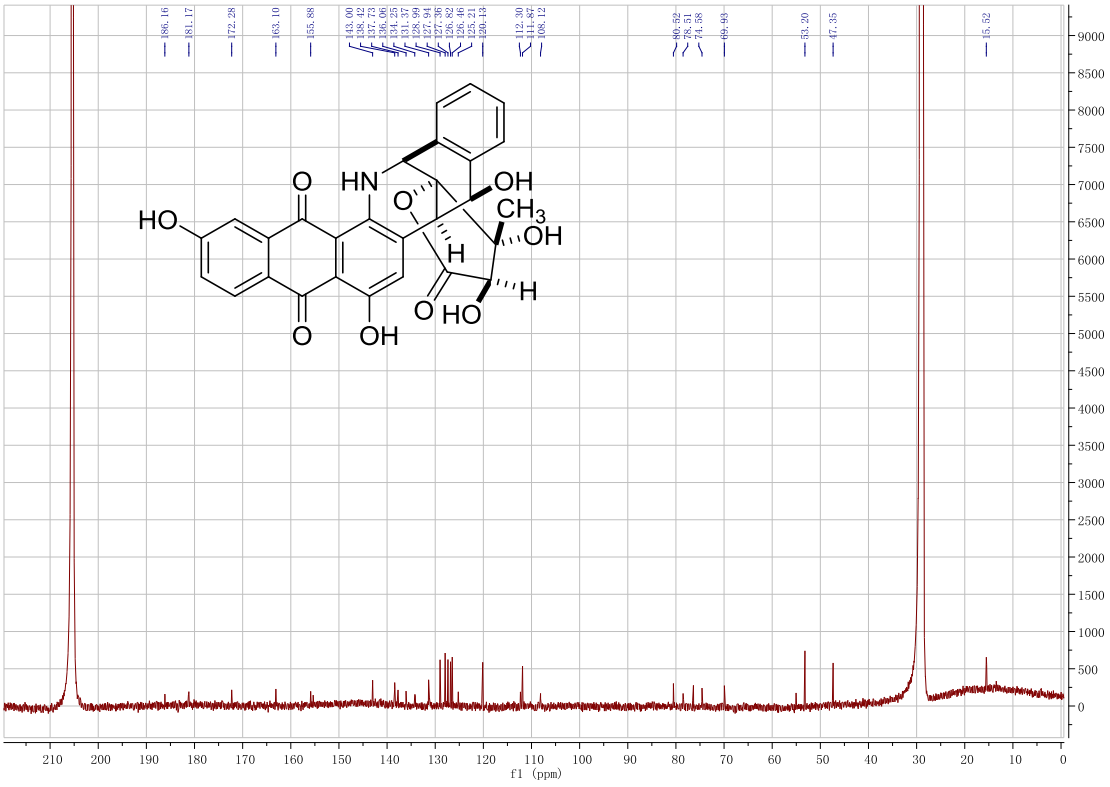

Figure S139. ^{1}H-^{1}H COSY spectrum of **23** (acetone-d_6)

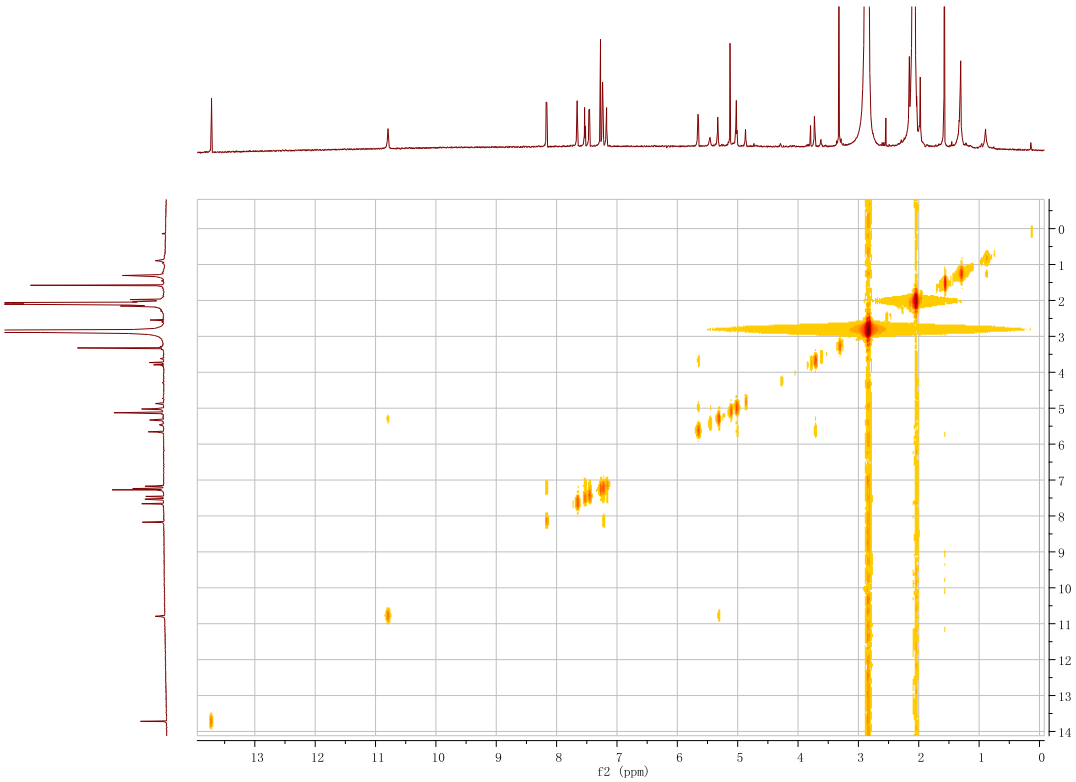

Figure S140. ^{1}H–^{13}C HSQC spectrum of **23** (acetone-d_6)

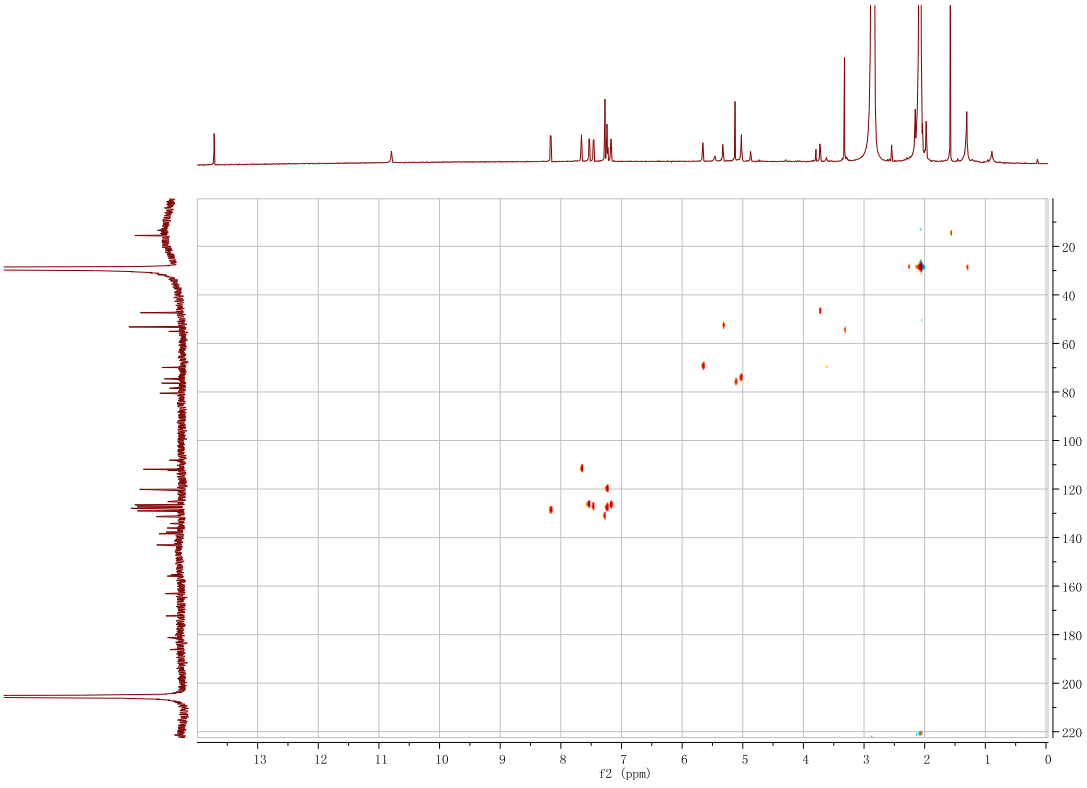

Figure S141. ^{1}H–^{13}C HMBC spectrum of **23** (acetone-d_6)

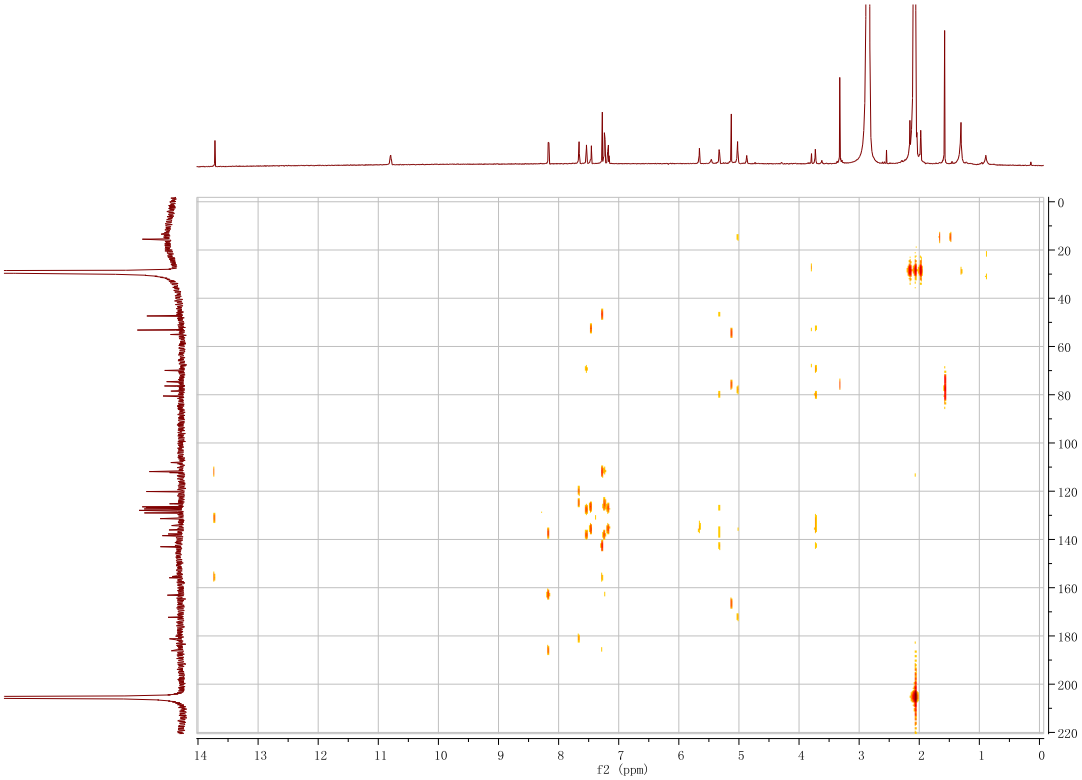

Figure S142. ^{1}H-^{1}H ROESY spectrum of **23** (acetone-d_6)

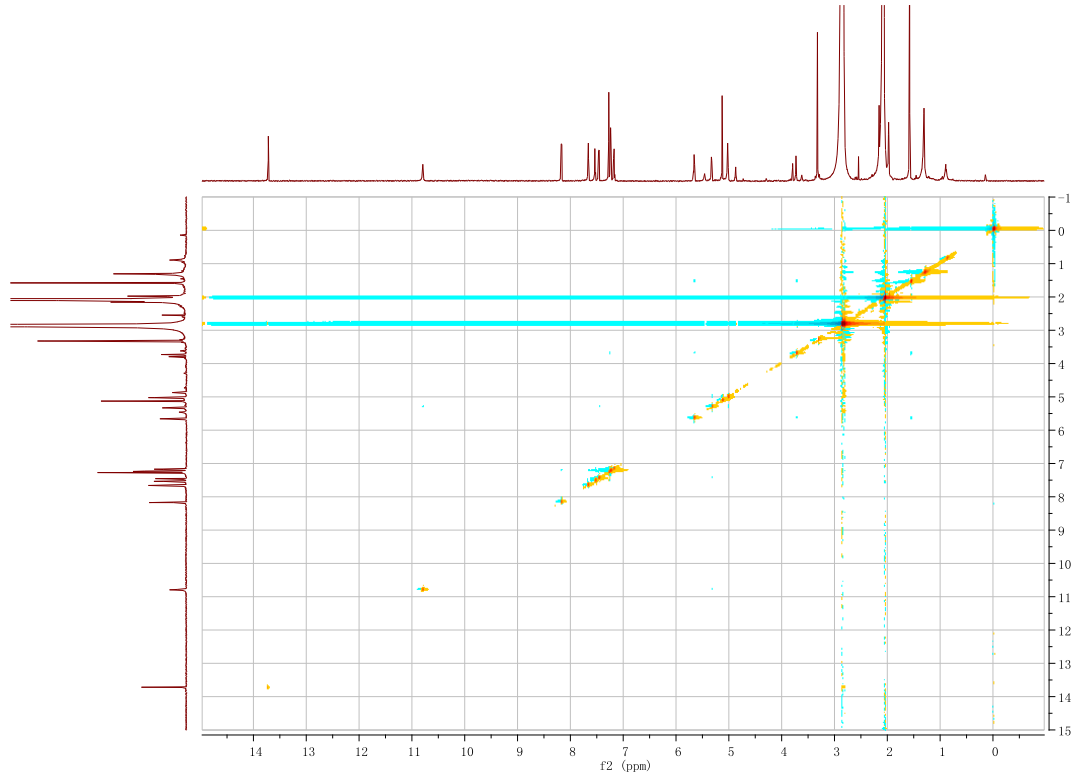

Figure S143. HR-ESI-MS spectrum of **24**

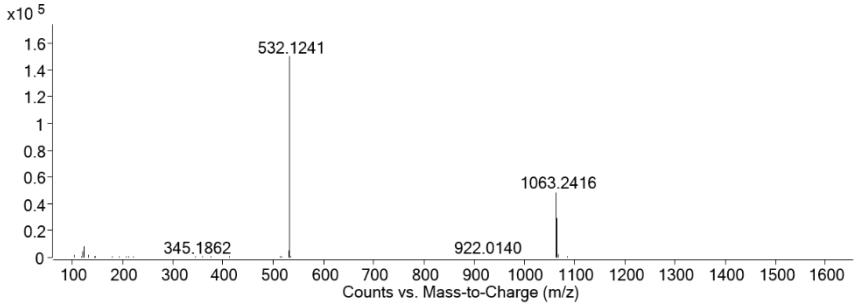

Figure S144. ^{1}H NMR Spectrum of **24** (700 MHz, acetone-d_6)

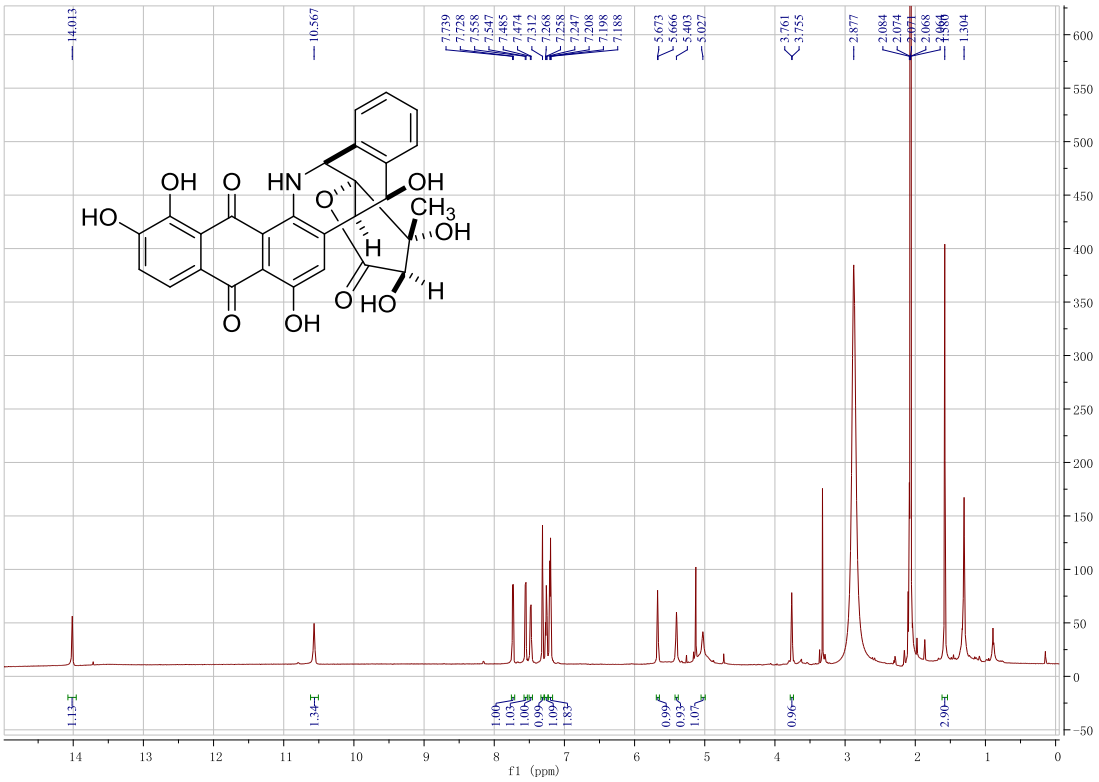

Figure S145. ^{13}C NMR spectrum of **24** (176 MHz, acetone-d_6)

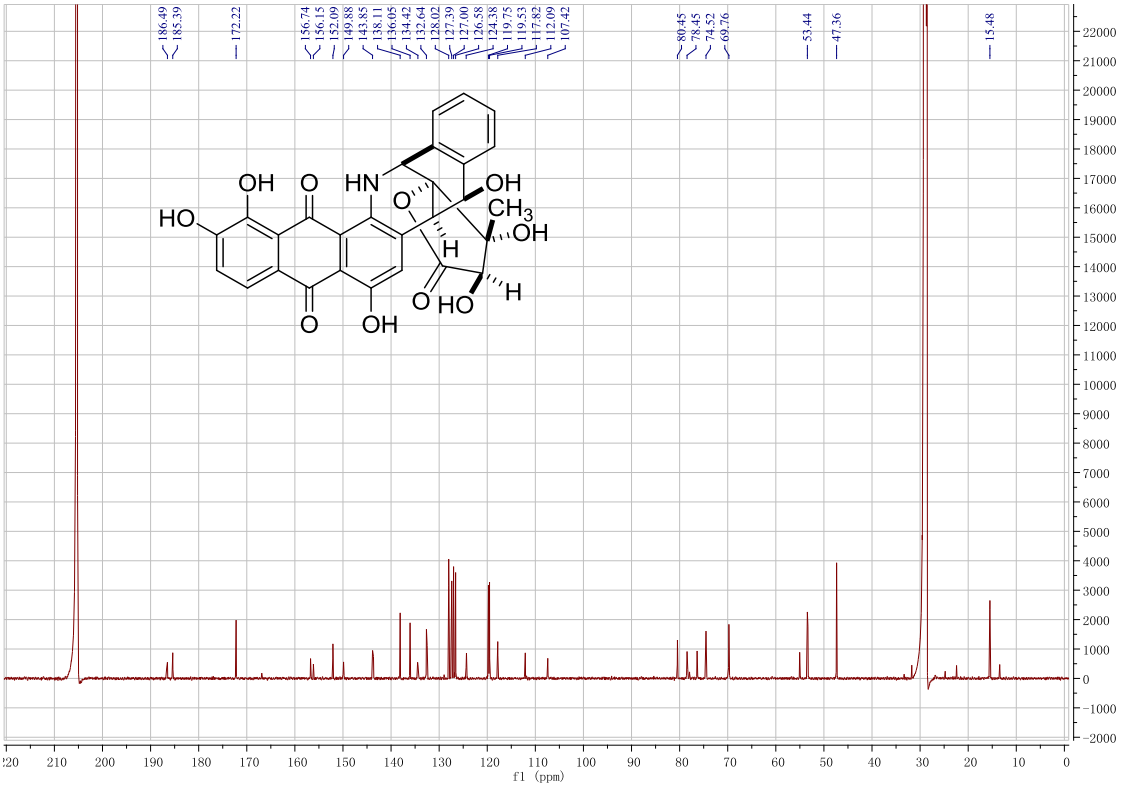

Figure S146. ^{1}H-^{1}H COSY spectrum of **24** (acetone-d_6)

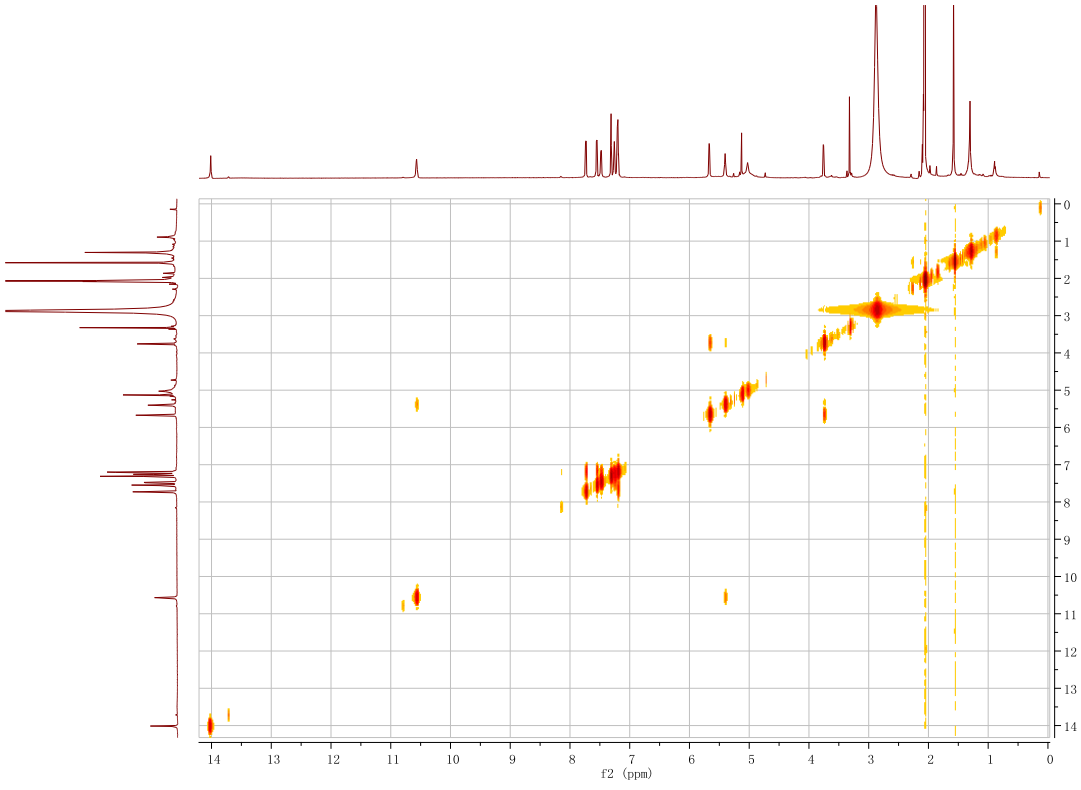

Figure S147. $^{1}H–^{13}C$ HSQC spectrum of **24** (acetone-d_6)

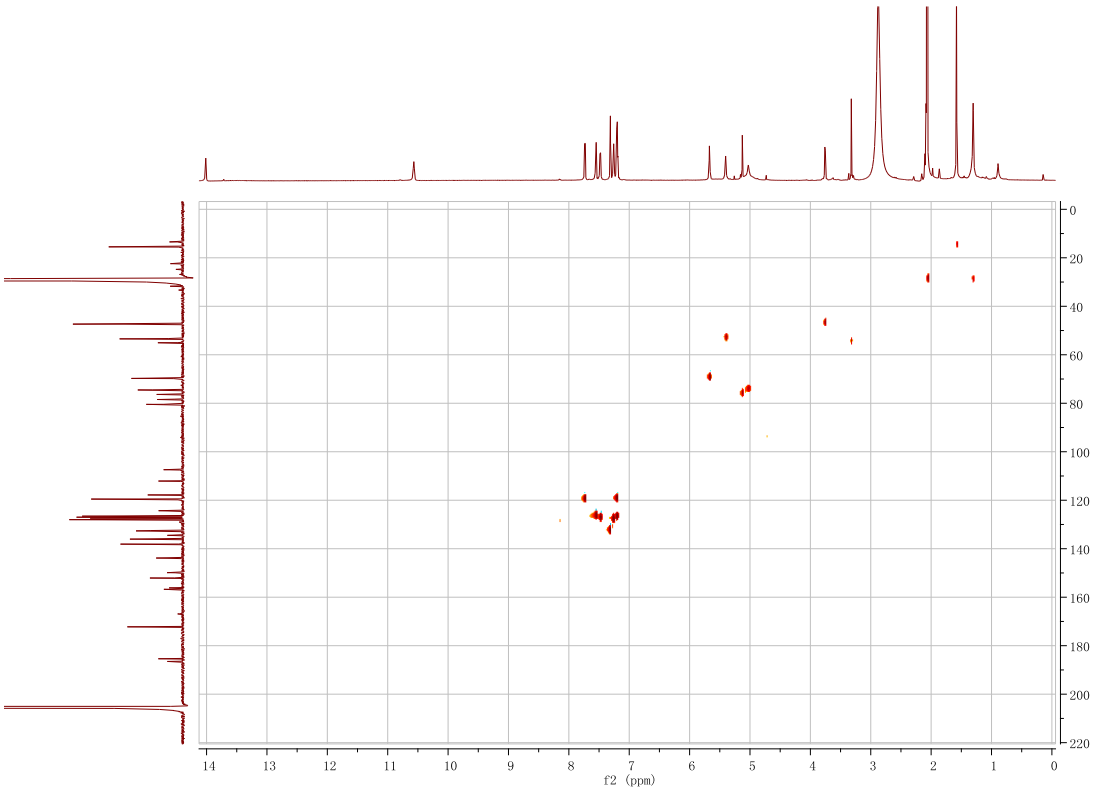

Figure S148. $^{1}H–^{13}C$ HMBC spectrum of **24** (acetone-d_6)

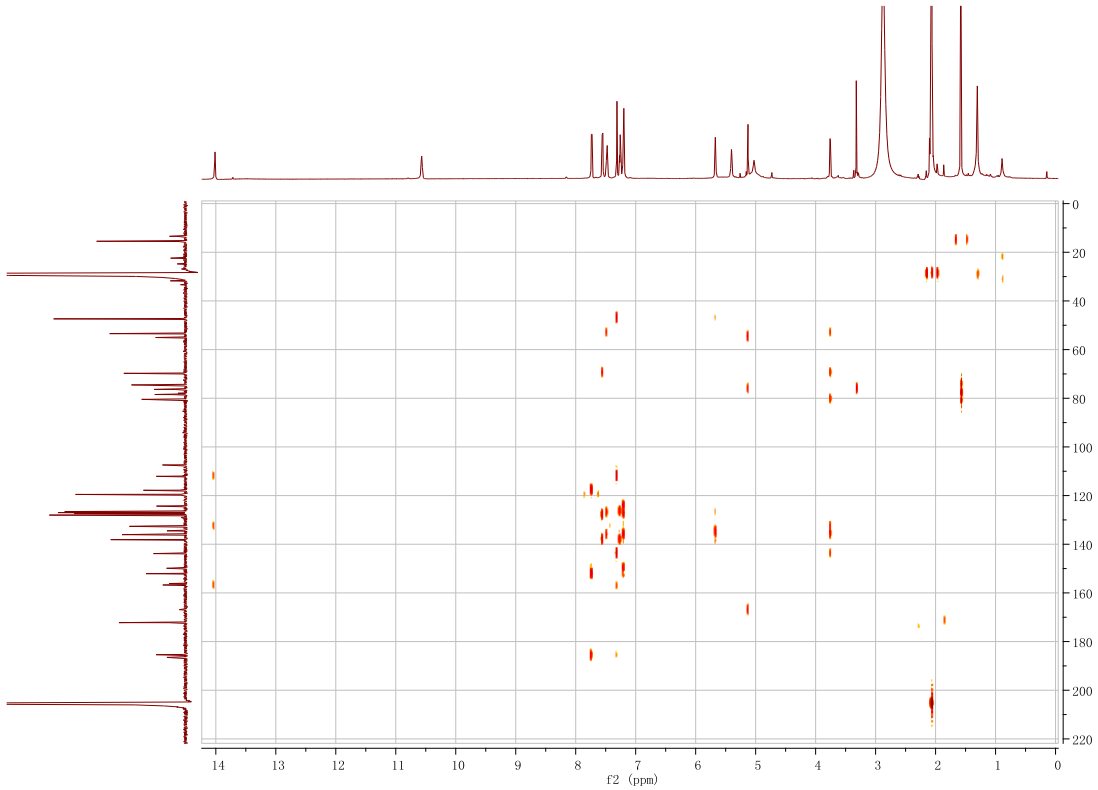

Figure S149. ^{1}H-^{1}H ROESY spectrum of **24** (acetone-d_6)

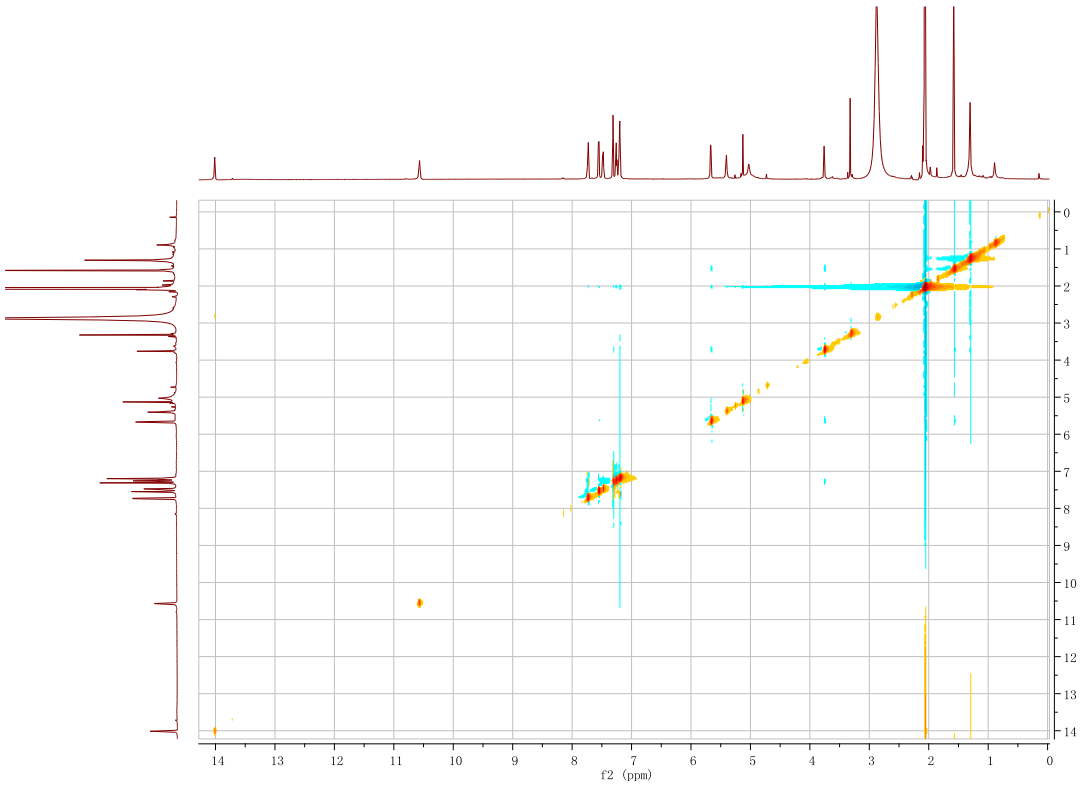

Figure S150. HR-ESI-MS spectrum of **25**

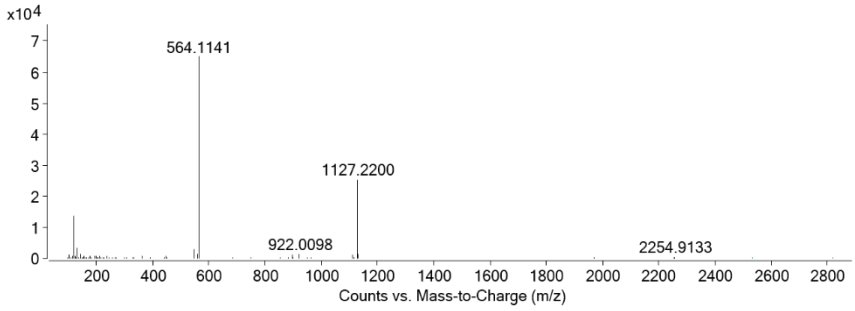

Figure S151. ^{1}H NMR Spectrum of **25** (700 MHz, acetone-d_6)

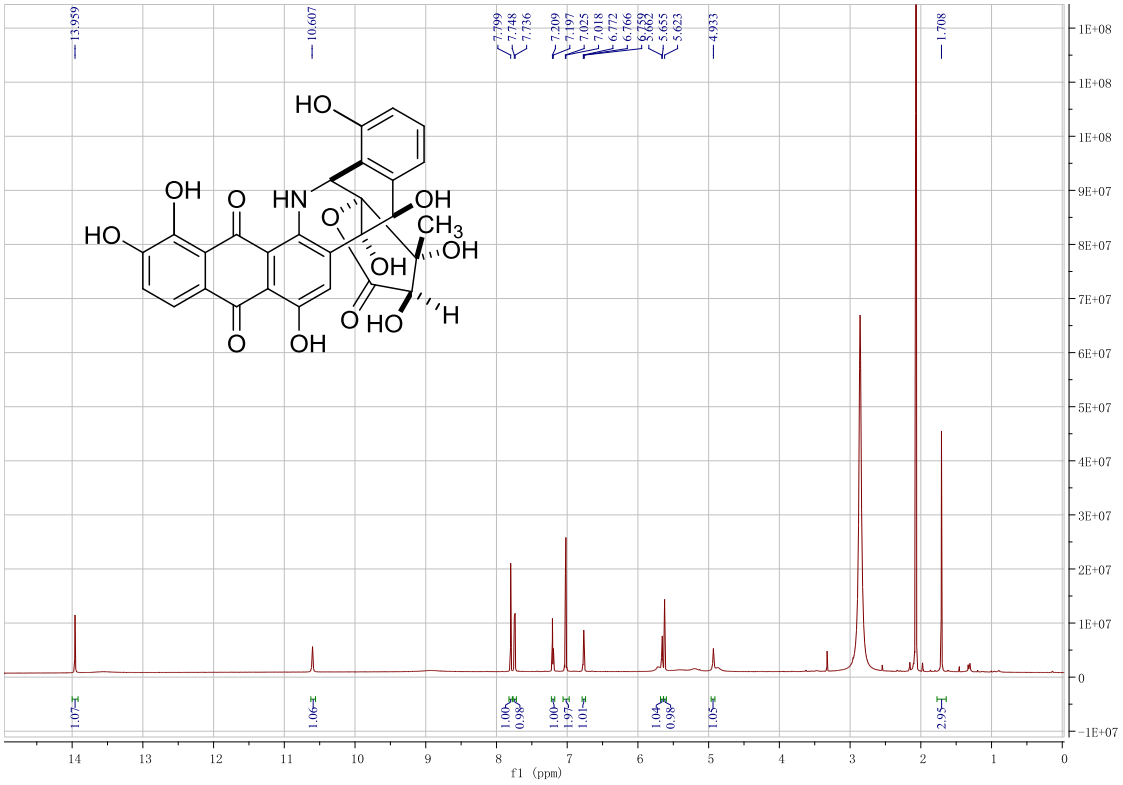

Figure S152. ^{13}C NMR spectrum of **25** (176 MHz, acetone-d_6)

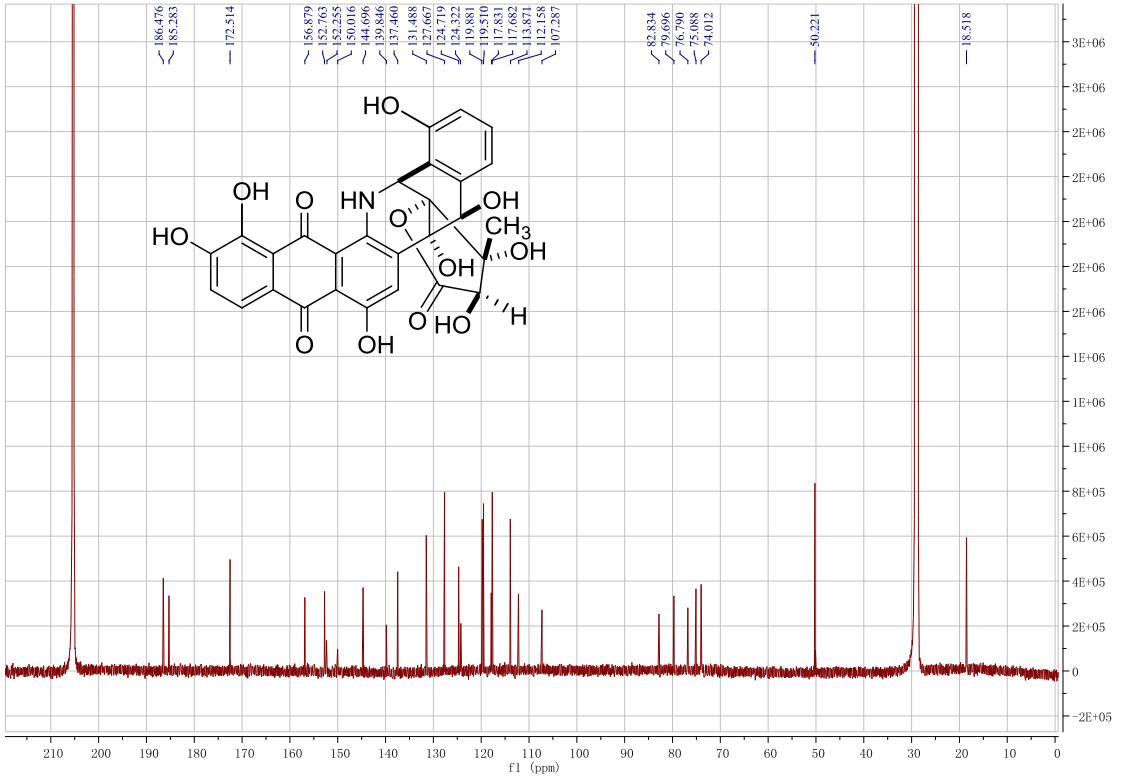

Figure S153. ^{1}H-^{1}H COSY spectrum of **25** (acetone-d_6)

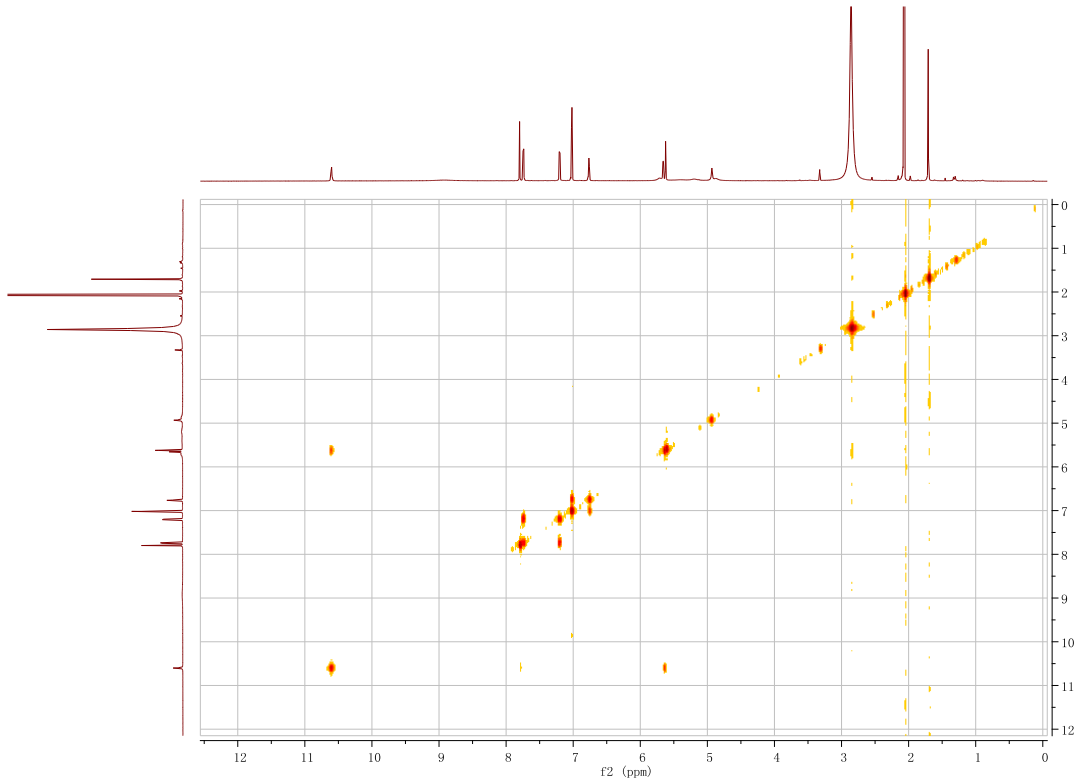

Figure S154. ^{1}H–^{13}C HSQC spectrum of **25** (acetone-d_6)

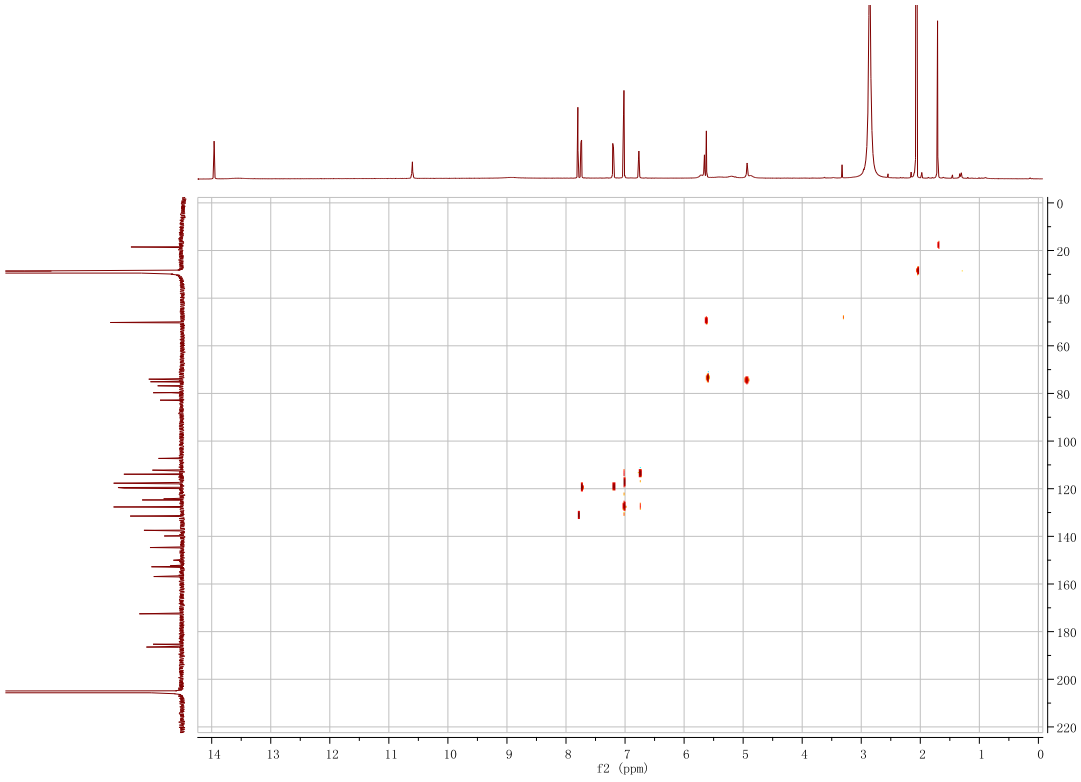

Figure S155. ^{1}H–^{13}C HMBC spectrum of **25** (acetone-d_6)

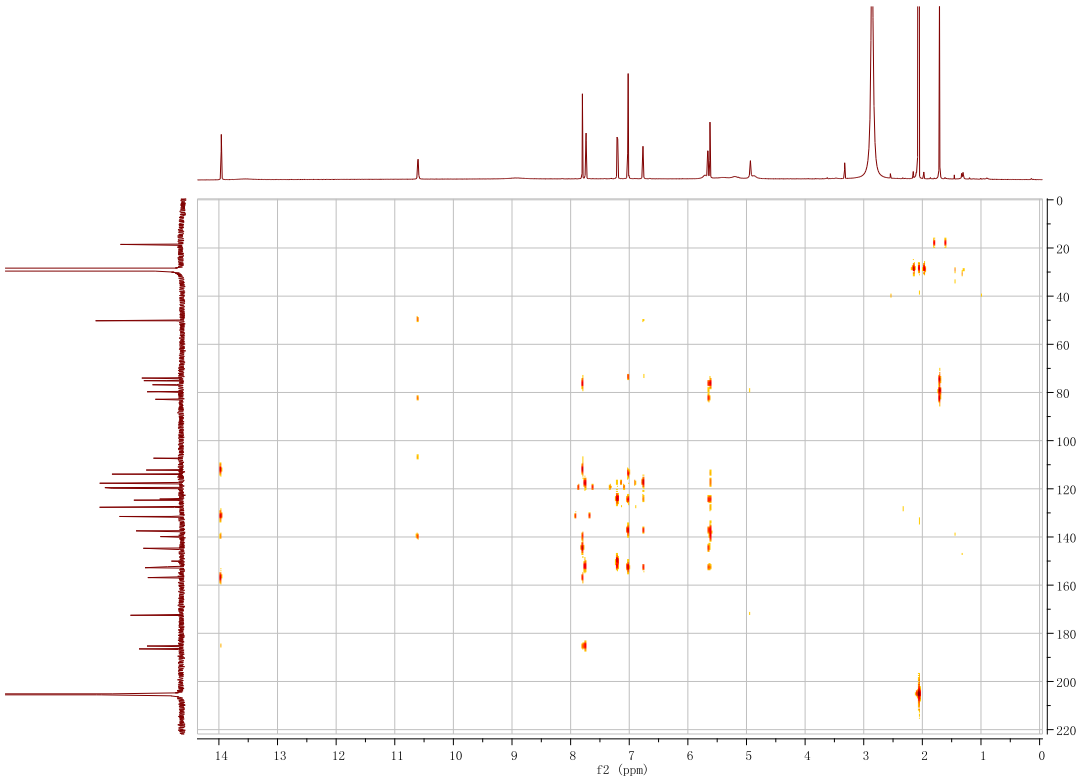

Figure S156. ^{1}H-^{1}H ROESY spectrum of **25** (acetone-d_6)

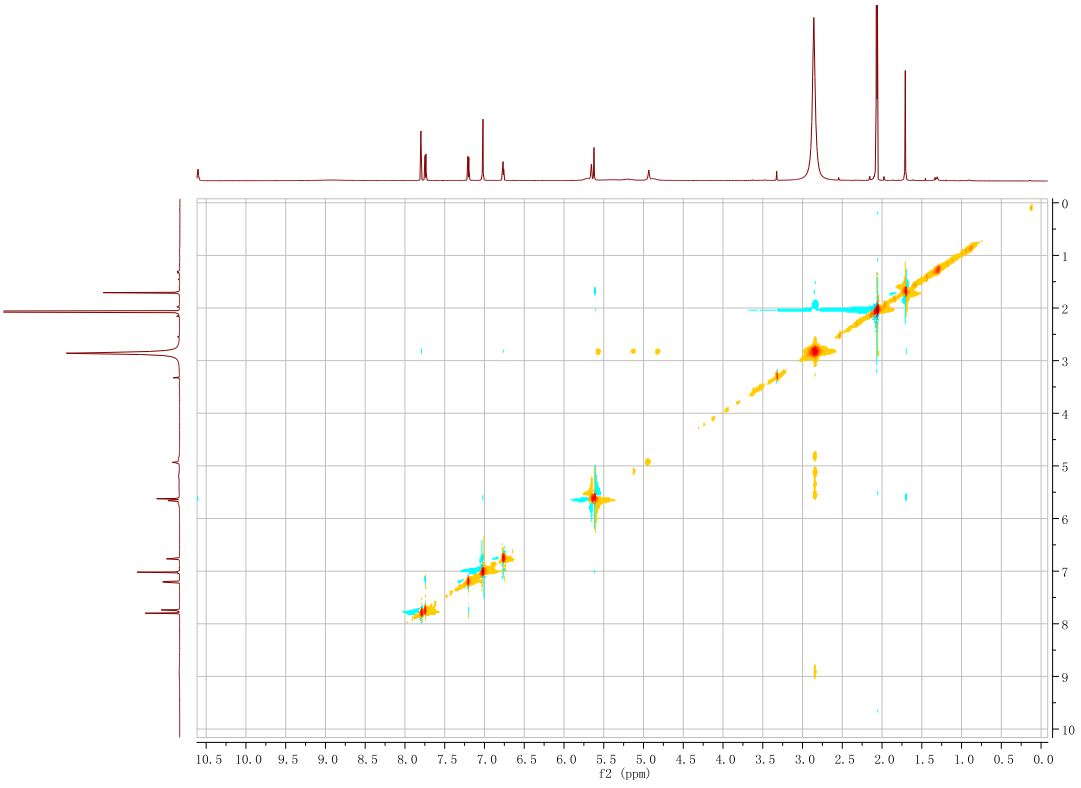

Supporting References

(S1) Sambrook, J.; Russel, D. *Molecular Cloning: A Laboratory Manual*, 3rd ed.; Cold Spring Harbor Laboratory Press: Cold Spring Harbor, NY, 2001.

(S2) Kieser, T.; Bibb, M. J.; Buttner, M. J.; Chater, K. F.; Hopwood, D. A. *Practical Streptomyces Genetics*; The John Innes Foundation: Norwich, U. K., 2000.

(S3) Yan, X.; Ge, H.; Huang, T.; Hindra; Yang, D.; Teng, Q.; Crnovčić, I.; Li, X.; Rudolf, J. D.; Lohman, J. R.; Gansemans, Y.; Zhu, X.; Huang, Y.; Zhao, L.-X.; Jiang, Y.; Van Nieuwerburgh, F.; Rader, C.; Duan, Y.; Shen, B. *mBio* **2016**, *7*, e02104-16.

(S4) Gust, B.; Challis, G. L.; Fowler, K.; Kieser, T.; Chater, K. F. *Proc. Natl. Acad. Sci. U.S.A.* **2003**, *100*, 1541–1546.

(S5) Huang, T.; Chang, C.-Y.; Lohman, J. R.; Rudolf, J. D.; Kim, Y.; Chang, C.; Yang, D.; Ma, M.; Yan, X.; Crnovčić, I.; Bigelow, L.; Clancy, S.; Bingman, C. A.; Yennamalli, R. M.; Babnigg, G.; Joachimiak, A.; Phillips, G. N., Jr.; Shen, B. *J. Antibiot.* **2016**, *69*, 731–740.

(S6) Pan, G.; Xu, Z.; Guo, Z.; Hindra; Ma, M.; Yang, D.; Zhou, H.; Gansemans, Y.; Zhu, X.; Huang, Y.; Zhao, L.-X.; Jiang, Y.; Cheng, J.; Nieuwerburgh, F. V.; Suh, J.-W.; Duan, Y.; Shen, B. *Proc. Natl. Acad. Sci. U.S.A.* **2017**, *114*, E11131–E11140.

(S7) MacNeil, D. J.; Gewain, K. M.; Ruby, C. L.; Dezeny, G.; Gibbons, P. H.; MacNeil, T. *Gene* **1992**, *111*, 61–68.

(S8) Yan, X.; Chen, J. J.; Adhikari, A.; Yang, D.; Crnovcic, I.; Wang, N.; Chang, C.-Y.; Rader, C.; Shen, B. *Org. Lett.* **2017**, *19*, 6192-6195.

(S9) Gao, Q.; Thorson, J. S. *FEMS Microbiol. Lett.* **2008**, *282*, 105-114.

(S10) Nicolaou, K. C.; Dai, W.-M. *Angew. Chem. Int. Ed.* **1991**, *30*, 1387-1530.

(S11) Smith, A. L.; Nicolaou, K. C. *J. Med. Chem.* **1996**, *39*, 2103-2117.

(S12) Nicolaou, K. C.; Wang, Y.; Lu, M.; Mandal, D.; Pattanayak, M. R.; Yu, R.; Shah, A. A.; Chen, J. S.; Zhang, H.; Crawford, J. J.; Pasunoori, L.; Poudel, Y. B.; Chowdari, N. S.; Pan, C.; Nazeer, A.; Gangwar, S. Vite, G.; Pitsinos, E. N. *J. Am. Chem. Soc.* **2016**, *138*, 8235-8246.